



Oklahoma Geological Survey  
G. Randy Keller, *Interim Director*

**Circular 112B**  
ISSN 0078-4397

# **Stratigraphic and Structural Evolution of the Ouachita Mountains and Arkoma Basin, Southeastern Oklahoma and West-Central Arkansas: Applications to Petroleum Exploration: 2004 Field Symposium**

## **Technical Papers**

NEIL H. SUNESON, İBRAHİM ÇEMEN, AND ROGER M. SLATT, *Editors*



Proceedings of a field symposium held October 21-23, 2004, in Poteau, Oklahoma

Co-sponsored by:  
Oklahoma Geological Survey  
and  
ConocoPhillips School of Geology and Geophysics



The Mewbourne College of Earth and Energy  
The University of Oklahoma  
Norman

2008

# OKLAHOMA GEOLOGICAL SURVEY

G. Randy Keller, *Interim Director*

## Survey Staff

**James H. Anderson**, *Manager of Cartography*

**Richard D. Andrews**, *Geologist IV*

**Betty D. Bellis**, *Staff Assistant III*

**Shanika L. Bivines**, *Financial Administrator and Office  
Manager*

**Dan T. Boyd**, *Geologist IV*

**Raymon L. Brown**, *Geophysicist III*

**Brian J. Cardott**, *Geologist IV*

**James R. Chaplin**, *Geologist IV*

**Janise L. Coleman**, *Budget and Account Representative III*

**Tammie K. Creel-Williams**, *Administrative Assistant I*

**Sue B. Crites**, *Editor, Oklahoma Geology Notes*

**Charles R. Dyer III**, *Equipment Operations Maintenance  
Person IV*

**Robert O. Fay**, *Geologist IV*

**Amie R. Gibson**, *Lab/Research Technician III*

**Stanley T. Krukowski**, *Geologist IV*

**Eugene V. Kullmann**, *Manager, OPIC*

**James E. Lawson, Jr.**, *Chief Geophysicist*

**Laurie A. Lollis**, *Graphics Presentations Technician*

**Kenneth V. Luza**, *Engineering Geologist IV*

**Richard G. Murray**, *Copy Center Operator*

**Sue M. Palmer**, *Staff Assistant I*

**David O. Pennington**, *Facilities Attendant II*

**Tom H. Sanders**, *Facilities Attendant II*

**Connie G. Smith**, *Marketing, Public Relations Specialist II*

**Paul E. Smith**, *Supervisor, Copy Center*

**G. Russell Standridge**, *GIS Specialist*

**Thomas M. Stanley**, *Geologist IV*

**Joyce A. Stiehler**, *Shipping and Receiving Technician III*

**Michelle J. Summers**, *Technical Project Coordinator*

**Neil H. Suneson**, *Geologist IV*

**Jennifer L. Veal**, *Staff Assistant II*

**Jane L. Weber**, *Database Coordinator*

## Cover Image

Cemented and fractured sandstones in the Wildhorse Mountain Formation, Jackfork Group (Morrowan), exposed on the north flank of the Lynn Mountain Syncline. The distribution and nature of the orthogonal fracture sets and their relation to the thickness of the sandstone beds in which they occur have potential implications for natural-gas exploration and development in these deep-water strata (Smart and others, this volume). Photograph by Roger M. Slatt.

This publication, printed by the Oklahoma Geological Survey, Norman, Oklahoma is issued by the Oklahoma Geological Survey as authorized by Title 70, Oklahoma Statutes 1981, Section 3310, and Title 74, Oklahoma Statutes 1981, Sections 231-238. 1,500 copies have been prepared at the cost of \$28,928.50 to the taxpayers of the State of Oklahoma. Copies have been deposited with the Publications Clearinghouse of the Oklahoma Department of Libraries.

## PREFACE

Neil H. Suneson  
Oklahoma Geological Survey

In October 2004, the Oklahoma Geological Survey (OGS) held a field symposium in Poteau, Oklahoma on the geology and resources of the Ouachita Mountains and Arkoma Basin in Arkansas and Oklahoma. The three-day meeting consisted of two half-day field trips and a full-day field trip to key outcrops in both states. In addition, researchers active in Arkoma Basin and Ouachita Mountains geology presented papers and posters on a wide variety of topics pertinent to resource evaluation in this part of the southern Midcontinent. This volume is a compilation of many of those papers. It also includes some that were not presented at the 2004 field symposium but are important nonetheless. This volume is a companion to the guidebook that was published for the meeting (Suneson and others, 2005) and a recently published OGS circular (Suneson, 2008) that contains two papers – one presented at the 2004 symposium by J. Kaspar Arbenz on the structural evolution of the tectonic belt, and a “historical” paper written in 1956 for Union Oil Company of California by Peter Misch and Keith Oles on that company’s stratigraphic and structural investigations in the Ouachita Mountains in Oklahoma and Arkansas.

A number of individuals were instrumental in organizing the field symposium and deserve credit for the field trips and presentations. Mike Roberts (Palmer Petroleum) and Charlie Stone (Arkansas Geological Commission [AGC]) were the leaders of the Arkansas part of the field trip; they relied on Ed Ratchford (AGC) for his insight into coalbed methane and Kim Butler (Southwestern Energy) for his knowledge of thrust-faulted Atokan reservoirs. The field trip on the second day of the symposium focused on the geology just west of the Oklahoma – Arkansas state line and was led by Roger Slatt (University of Oklahoma) and Ibrahim Çemen (Oklahoma State University). Their work on the transition zone (Çemen) and Jackfork Group sandstones (Slatt) was a collaborative effort with students and faculty colleagues. The final day of the symposium was a day-long field trip led by Çemen, Dennis Kerr (University of Tulsa), and Neil Suneson (OGS). Çemen and his students have interpreted the structural geology of the transition zone; Kerr described marker beds in the basal part of the Atoka Formation in the hanging wall of the Ti Valley Thrust Fault; and Suneson discussed the Johns Valley Formation and Spiro sandstone. They were assisted by Galen Miller (OGS) and Kevin Smart (Southwest Research Institute) who had mapped and reinterpreted the structural geology of the Potato Hills in light of recent gas discoveries there.

Roger Slatt organized the oral and poster presentations. In addition to the papers contained in this volume, the following presentations were given at the meeting:

- “South Vergence Revisited” by J. Kaspar Arbenz;
- “Structural Geology of the Frontal Ouachitas – Arkoma Basin Transition Zone in Southeastern Oklahoma: Implications for Gas Exploration” by Ibrahim Çemen, Steve Hadaway, Ata Sagnak, Justin Evans, Marline Collins, Osman Kaldirim, Kris McPhail, Gultekin Kaya, Syed Mehdi, and Saleem Akthar;
- “Sequence Stratigraphy of the Atoka Formation (Middle Pennsylvanian), Arkoma Basin, Central Arkansas: Eustatic and Tectonic Signals” by Jamie A. Woolsey and Walter L. Manger;
- “Arkoma Basin Northern-Sourced Atoka Facies Analysis: Incised Valleys and Deltas” by Roderick W. Tillman;
- “Identification of Turbidite Architectural Elements and Porosity Types, Jackfork Group, Potato Hills, Eastern Oklahoma” by Gloria A. Romero and Roger M. Slatt;
- “Natural Gas Production from the Wedington Sandstone (Chesterian, Mississippian) Shallow Gas Province: Brentwood Field, Washington County, Northwestern Arkansas” by Walter L. Manger and Phillip R. Shelby;
- “Geometry of Late Paleozoic Thrusting, Hartshorne Southwest Quadrangle, Arkoma Basin, Southeast Oklahoma: Implications for Gas Exploration” by Steve Hadaway and Ibrahim Çemen;
- “Potential Reservoir Types in the Jackfork Group, Eastern Oklahoma” by Roger M. Slatt, Tosan Omatsola, Alison Garich-Faust, and Gloria Romero;
- “Structural Relationship Between the Potato Hills and the Wilburton Triangle Zone of the Ouachita Mountains, Southeastern Oklahoma” by Gultekin Kaya and Ibrahim Çemen;
- “Characterization of Slope and Basin Facies Tracts, Jackfork Group, Arkansas, with Applications to Deepwater (Turbidite) Reservoir Management” by Roger M. Slatt, Charles G. Stone, and Paul Weimer; and
- “Outcrop Characterization, 3D Geological Modeling, “Reservoir” Simulation, and Upscaling of Jackfork Group Turbidites in Hollywood Quarry, Arkansas” by Camilo Goyeneche and Roger M. Slatt.

The symposium could not have been a success without the logistical support of OGS staff member Michelle Summers, meeting coordinator, and OU School of Geology and Geophysics staff member Terry Brady, registration coordinator.

## References Cited

Suneson, N.H.; Çemen, Ibrahim; Kerr, D. R.; Roberts, M.T.; Slatt, R.M.; and Stone, C.G., 2005, Stratigraphic and structural evolution of the Ouachita Mountains and Arkoma Basin, southeastern Oklahoma and west-central Arkansas: applications to petroleum exploration: Oklahoma Geological Survey Guidebook 34, 128p.

Suneson, N.H. (ed.), 2008, Stratigraphic and structural evolution of the Ouachita Mountains and Arkoma Basin, southeastern Oklahoma and west-central Arkansas: applications to petroleum exploration: 2004 field symposium – the Arbenz – Misch/Oles volume: Oklahoma Geological Survey Circular 112A, 86 p.



# Contents

Preface	iii
<b>Petroleum Systems of the Ouachita Thrust Belt and Foreland Basins (With Emphasis on the Arkoma Basin)</b> James L. Coleman, Jr.	1
<b>Geologic Profiles Derived from Seismic Data West and East of the Arkansas – Oklahoma State Line, Arkoma Basin and Frontal Ouachita Mountains</b> Michael T. Roberts	17
<b>Enhanced Structural Interpretation in the Arkoma Basin with Seismic Attributes</b> Surinder Sahai and Ibrahim Çemen	25
<b>Panola Field – Multiple Atoka Sandstone Gas Reservoirs in T. 5 N., RS. 19-20 E., Latimer County, Oklahoma</b> Richard D. Andrews	31
<b>Restoration of Thrusted Middle Atoka Reservoir Trends, Waveland Field, Arkansas</b> Kim R. Butler	51
<b>Outcrop Fracture Characterization of Pennsylvanian Jackfork Group Sandstones, Ouachita Mountains, Southeastern Oklahoma</b> Kevin J. Smart, Kimberly Scott, and Roger M. Slatt	63
<b>Lower Atoka Highstand Systems Tract: Delineating the Lower Atoka in the Arkoma Basin, Oklahoma</b> Azzeldeen A. Saleh	73
<b>Middle Atoka Lowstand Systems Tract: Delineating the Middle Atoka in the Arkoma Basin, Oklahoma</b> Azzeldeen A. Saleh	99
<b>Upper Atoka Transgressive and Highstand Systems Tracts: Delineating the Upper Atoka in the Arkoma Basin, Oklahoma</b> Azzeldeen A. Saleh	131
<b>Exploration Discipline Matrix: A Key to Reestablishing a Vibrant Exploration Industry in the Midcontinent and Other Mature Provinces</b> Lyle F. Baie and John J. Gallagher, Jr.	157

# Petroleum Systems of the Ouachita Thrust Belt and Foreland Basins (With Emphasis on the Arkoma Basin)

*James L. Coleman, Jr.*  
U. S. Geological Survey  
Reston, Virginia

**ABSTRACT.**—The late Paleozoic Ouachita Thrust Belt and foreland basins extend from its junction with the Appalachian Thrust Belt and foreland basin in eastern Mississippi through Arkansas, Oklahoma, and Texas into northeastern Mexico, where the trend is overrun by Mesozoic tectonic elements of the Sierra Madre Oriental. The Ouachita structural trend is composed of the Black Warrior, Arkoma, Sherman, Fort Worth, Kerr, Val Verde, Marathon, and Marfa Basins, and the uplifted areas of the Ouachita and Marathon Mountains and their subsurface extensions. Strata within the trend are primarily Cambrian-to-Pennsylvanian deep-water siliciclastics, carbonates, and cherts thrust over/against normal-faulted, Cambrian-to-Pennsylvanian shallow-water carbonates and siliciclastics.

Most of the petroleum within the Ouachita trend has probably been derived from four kerogen-rich intervals: Middle–Upper Ordovician, Upper Devonian–Lower Mississippian, Upper Mississippian, and Lower–Middle Pennsylvanian, although these intervals are not uniformly distributed throughout the trend. The Ordovician Womble Shale (and equivalents) is thought to be the source for the now solid hydrocarbons in the Ouachita Mountains. The Devonian Woodford Shale (including the Lower Mississippian Caney Shale and other equivalents) is potentially the most significant source rock within the Ouachita system. It probably sourced the majority of the hydrocarbons in the Arkoma, Val Verde, and Marathon Basins. The Mississippian Barnett and Lewis (Floyd) Shales sourced local oil and gas accumulations in the Fort Worth and Black Warrior Basins, and the Fayetteville Shale sourced gas in the Arkoma Basin. The generally equivalent Stanley Shale has intervals of high organic carbon in the Ouachita Fold Belt. Pennsylvanian coals and kerogen-rich shales sourced known and potentially attributable large volumes of gas in the Black Warrior, Arkoma, Fort Worth, Val Verde, and Marathon Basins. Other potential, but unsubstantiated, source intervals may exist in Precambrian, Cambrian, and Silurian shales and basinal carbonates.

The maturation of source intervals and hydrocarbon generation appear to have occurred from the Silurian to the Triassic eras, with substantial peak generation during the Permo–Pennsylvanian. Reservoir and sealing intervals are present throughout most of the stratigraphic section, with the majority of hydrocarbons produced from the younger Paleozoic section. Production has been most prolific from natural gas reservoirs in the Arkoma and Black Warrior Basins.

## INTRODUCTION

This report is a general review of the hydrocarbon-sourcing intervals and associated petroleum systems of the Ouachita Thrust Belt and foreland basins of Oklahoma, Arkansas, Mississippi, and Alabama. The Ouachita trend, which is one of six thrust belts and foreland basins in North America (Fig. 1), contains Paleozoic strata ranging in age from Cambrian to Pennsylvanian. Details of the stratigraphy and structure are well summarized in Flawn and others (1961); Gatewood

and Fay (1991); Hatcher and others (1989); Lillie and others (1983); Roberts (1994); Viele (1979); and Zimmerman and others (1982) to mention a few. Oil and gas production characteristics and data are summarized by Suneson and Campbell (1990); Perry (1996); and Ryder and others (1996).

The Ouachita structural trend is the westward extension of the Paleozoic Appalachian Thrust and Fold Belt system of eastern North America (Fig. 1). The trend is composed of the Black Warrior (Alabama and Mississippi), Arkoma (Arkansas and Oklahoma), Sherman, Fort Worth, Kerr, Val Verde (Tex-



Basins. Coals and terrestrial organic shales within the Pennsylvanian Pottsville, Atoka, and equivalent units source large volumes of known, and potentially attributable gas in the Black Warrior, Arkoma, Fort Worth, Val Verde, and Marathon Basins. Based on occurrences of stratigraphic equivalents in the Midcontinent and the Appalachian Basin, other potential source intervals may exist in Precambrian, Cambrian, and Silurian shales and basinal carbonates.

To date, the Arkoma Basin is the most structurally deformed, hydrocarbon-bearing area of the Ouachita trend, with production from combination stratigraphic and structural traps, normal-fault blocks, and several productive, thrust-cored anticlines and sets of stacked imbricates. Downdip of the Arkoma Basin fields is a zone of solid hydrocarbons composed of grahamite and imponite (Fig. 3) (Cardott and others, 1993). In contrast with the Arkoma Basin, the Black Warrior Basin, to date, is productive only from normal, antithetic and down-to-the-basin fault traps and combination stratigraphic-structural traps. A large belt of tar sands is developed updip of the Black Warrior Basin fields in both quartz and lime carbonate sandstone beds of Mississippian age (Fig. 3). Both ba-

sins are capped by intervals of Pennsylvanian bituminous and sub-bituminous coal, with well-established, coal-gas methane production.

## BASIN CONFIGURATION

The Ouachita trend is bounded on the east by the Kemper County (Mississippi) Shear Zone (Carboniferous age), which cuts off the Appalachian structural trend on its southeastern end; on the north (and northwest in Texas) by the North American craton and platform strata (Precambrian to Permo-Carboniferous); on the south (and southeast in Texas) by a Mesozoic normal-fault zone, which developed during the opening of the Gulf of Mexico; and on the west by a high-angle reverse-fault zone of Laramide (Mesozoic) age. The Ouachita trend is interrupted by several, regional, high-angle, reverse-fault zones in eastern Mississippi (Kemper County Fault Zone); western Tennessee-eastern Arkansas (Reelfoot Rift); southeastern Oklahoma (Southern Oklahoma fault system); southwestern Texas (Val Verde fault system); and northeastern Mexico-southwestern Texas (Mojave-Sonora megashear).

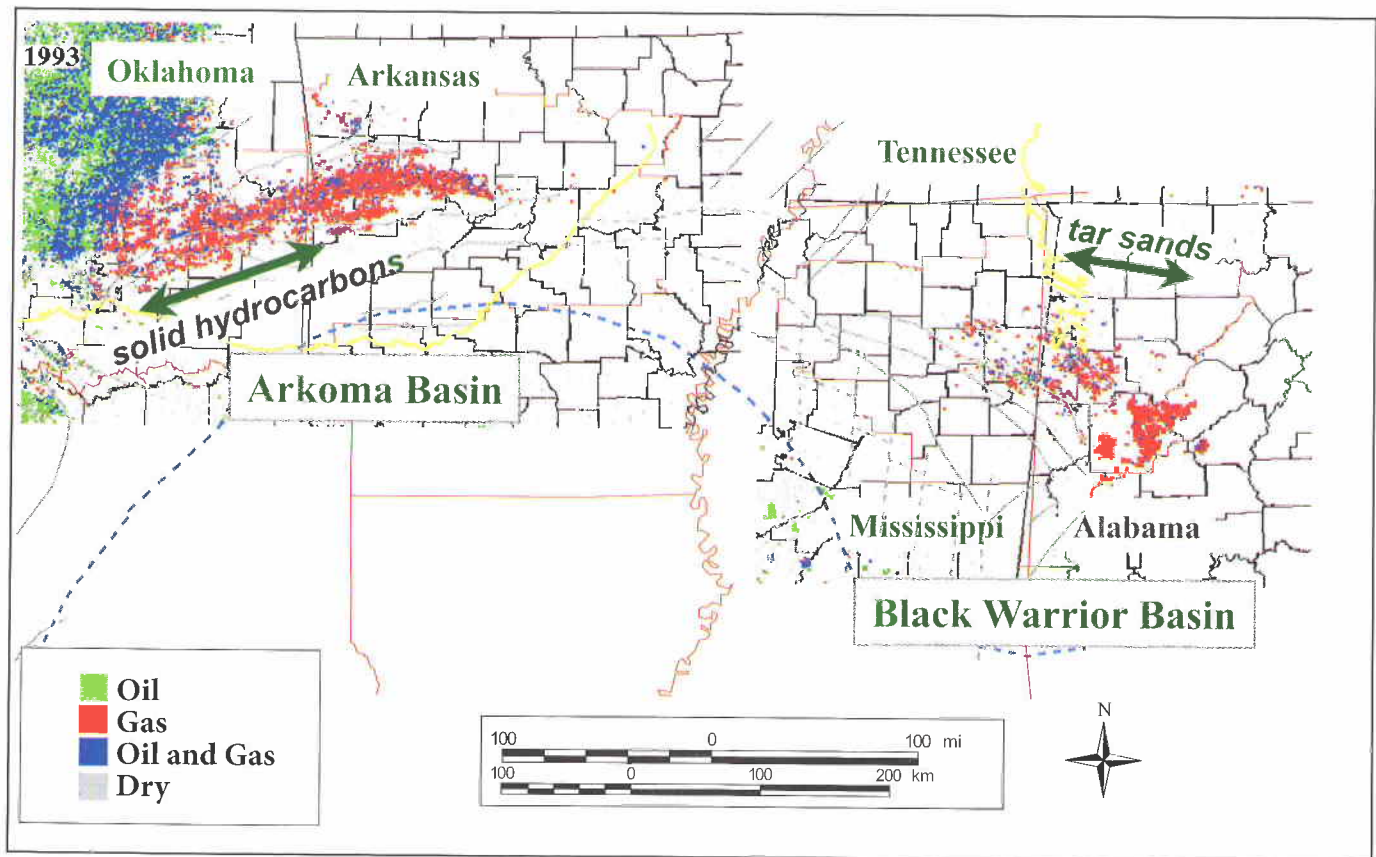


**Figure 3.** Production trends of the Arkoma and Black Warrior Basins (base map adapted from Gautier and others, 1995). Solid and dashed gray lines are faults (solid = outcrop and well-established, subsurface fault traces; dashed = less well-established and inferred, subsurface fault traces).



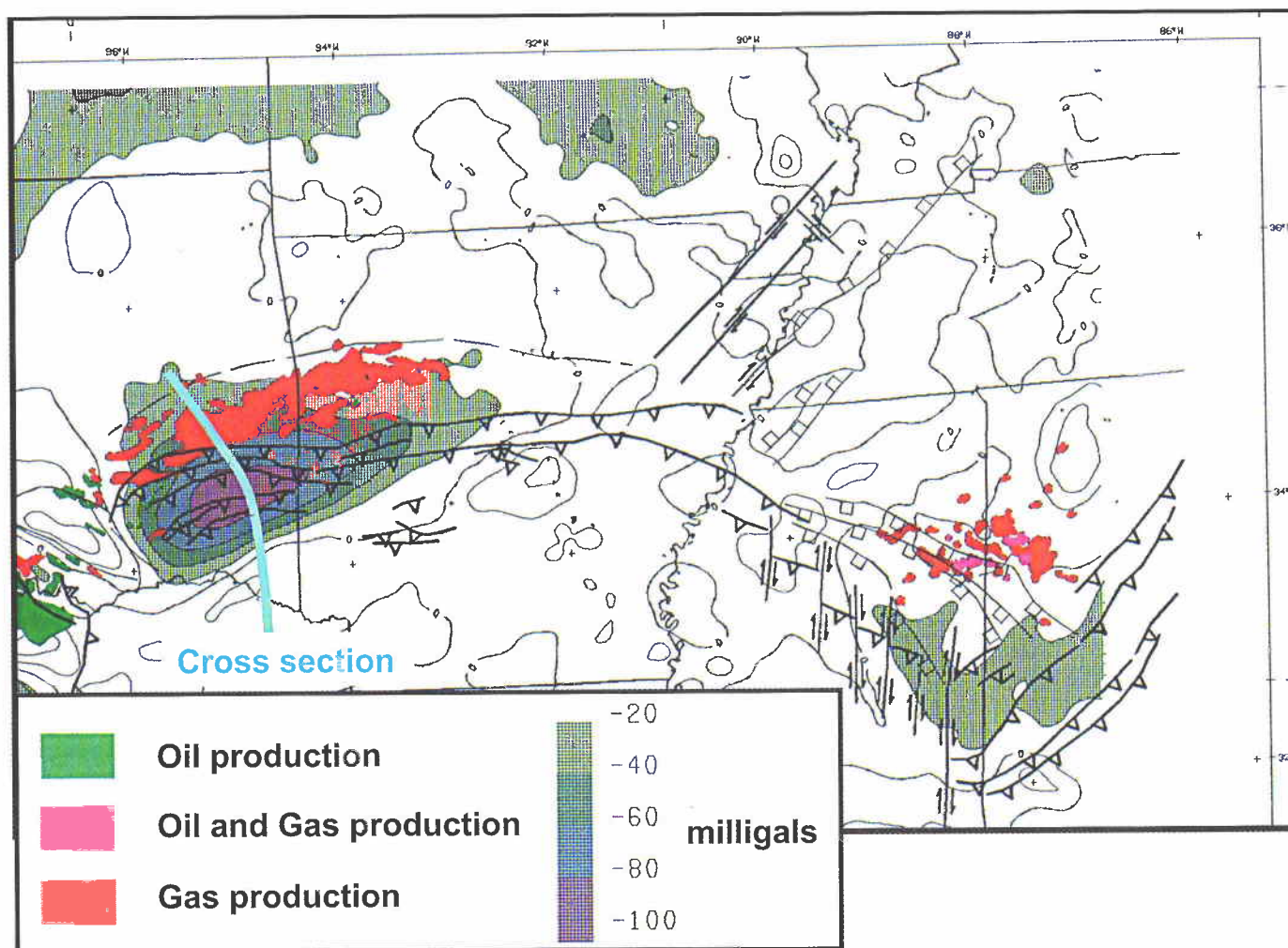


**Figure 4.** Isostatic gravity map with production overlay (adapted from Coleman and others, 2001). Red = gas; green = oil.

The Arkoma Basin extends from the vicinity of the Mississippi River and the southern extension of the Reelfoot Rift Fault Zone on the east to the vicinity of the Ardmore–Anadarko Basin complex in southeastern Oklahoma. The Arkoma Basin is characterized by numerous high-angle, syndepositional normal faults and low-angle décollement-style thrust faults. Based on data from deep wells, seismic profiles, and gravity mapping, the Arkoma Basin ranges from less than 2 km to greater than 10 km deep, with the deepest portion in southeastern Oklahoma and west-central Arkansas (Figs. 4, 5, and 6).

The Black Warrior Basin extends eastward from the vicinity of the Mississippi River to the southwestern end of the Appalachian Orogenic Belt near the border of Mississippi and Alabama. This basin is also characterized by numerous high-angle, normal faults and low-angle décollement-style thrust faults, although the throw on the normal faults is significantly less than those in the Arkoma Basin. Based on data from deep wells, seismic profiles,

and gravity mapping, the Black Warrior Basin ranges from less than 2 km to less than 10 km deep (Fig. 6).

The proximity of both oil and gas production to the deeper portions of these basins suggests that the main area for oil and gas generation and preservation is in and near the deeper parts of the basins (Fig. 4). The gravity anomaly is potentially caused by the increased sedimentary thickness, but may also be a result of reduced lithologic densities from less tectonostratigraphic loading and compaction, as compared with areas along trend to the east.

### THERMAL MATURITY MAPS

Source intervals are most effective when they are at peak thermal maturity for generation of hydrocarbons from kerogen-rich strata. It is common to consider oil-prone source intervals as most effective when they are at “peak oil” levels of thermal maturity, between vitrinite reflectance levels of 0.6% and 1.20%  $R_o$ . It is also common to consider gas-prone source intervals

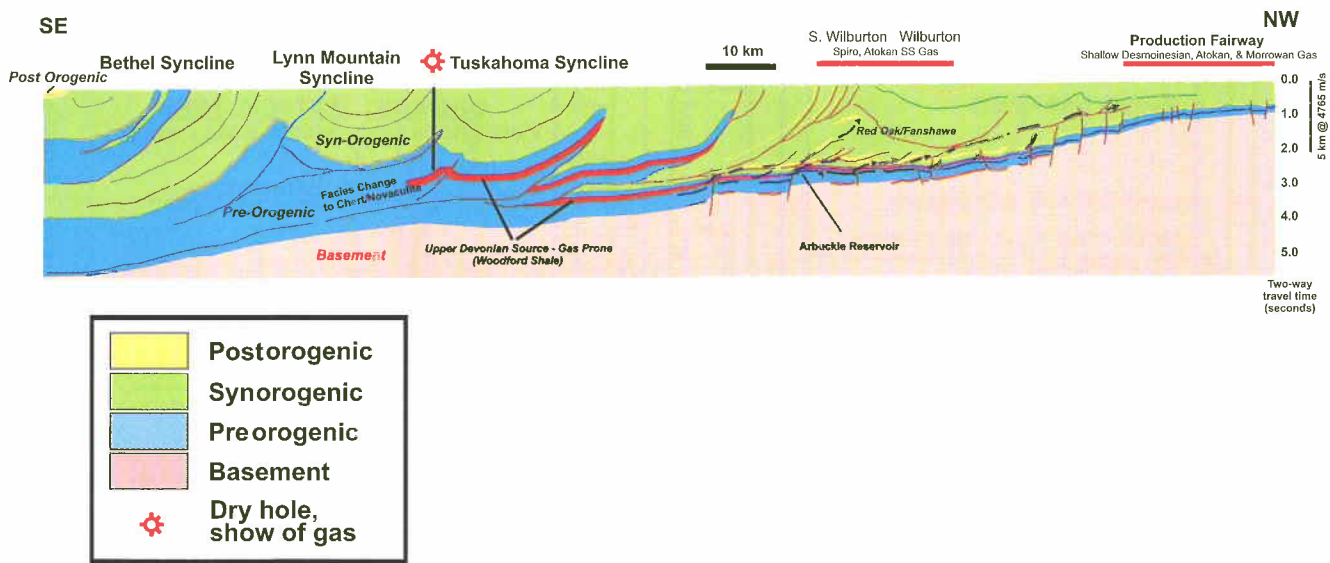


**Figure 5.** Generalized cross section of Arkoma Basin, eastern Oklahoma. Line of section shown on Figure 4 (adapted from Coleman and others, 2001).

as most effective when they are at “peak gas” levels of thermal maturity, between vitrinite reflectance levels of 1.20 and 2.5%  $R_o$ . These considerations may be true for some kerogens, but certainly not for all. Both oil and gas may be generated early (i.e., at pre-peak and peak oil levels of thermal maturity) if catalytic components (such as sulfur) are present or if the majority of the kerogen present in the source interval is plant-derived kerogen. Gas can also be generated from oils and oil-prone kerogen at advanced thermal levels. Both oil-prone and gas-prone kerogens tend to go through maximum generation in the peak oil zone of thermal maturity (Fig. 7).

In this study, four categories were used to illustrate the degree of thermal maturity on the potential source rock intervals: (1) pre-peak oil (0.25–0.6%  $R_o$ ); (2) peak oil (0.6–1.20%  $R_o$ ); (3) peak gas (1.20–2.5%  $R_o$ ); and (4) past-peak gas (>2.5%  $R_o$ ; Fig. 7). The upper thermal limit for oil occurs at approximately 1.35%  $R_o$ . Although methane is a very stable molecule and can endure high thermal maturity levels, its effective upper limit is usually considered to be roughly 3.2%  $R_o$  (Dow, 1977; Perry and others, 1983). Deep Cambro–Ordovician Arbuckle reservoirs within the Arkoma Basin are a notable exception to this rule, with equivalent values (extrapolated from conodont color alteration indices, CAI) in

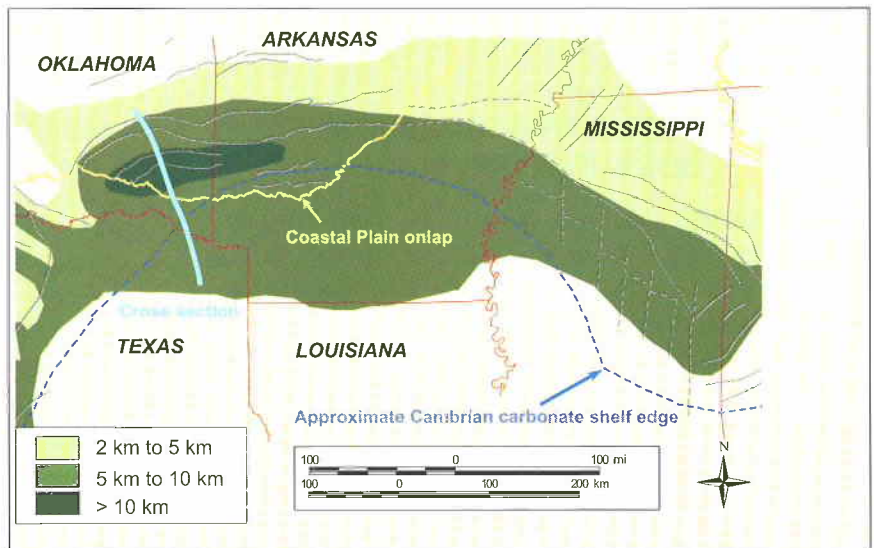


**Figure 6.** Present-day general depth-to-basement map, Arkoma and Black Warrior Basins. Solid and dashed gray lines are faults (solid = outcrop and well-established, subsurface fault traces; dashed = less well-established and inferred, subsurface fault traces). Adapted from Coleman and others, 2001; approximate Cambrian carbonate shelf margin from Hale-Erlich and Coleman, 1991.

excess of 3.2%  $R_o$  (Hendrick, 1992). Reservoir properties tend to degrade below conventional levels of productivity at peak gas thermal maturity. Significant fracture networks are usually required for effective hydrocarbon production in strata that have undergone past-peak gas levels of thermal maturity.

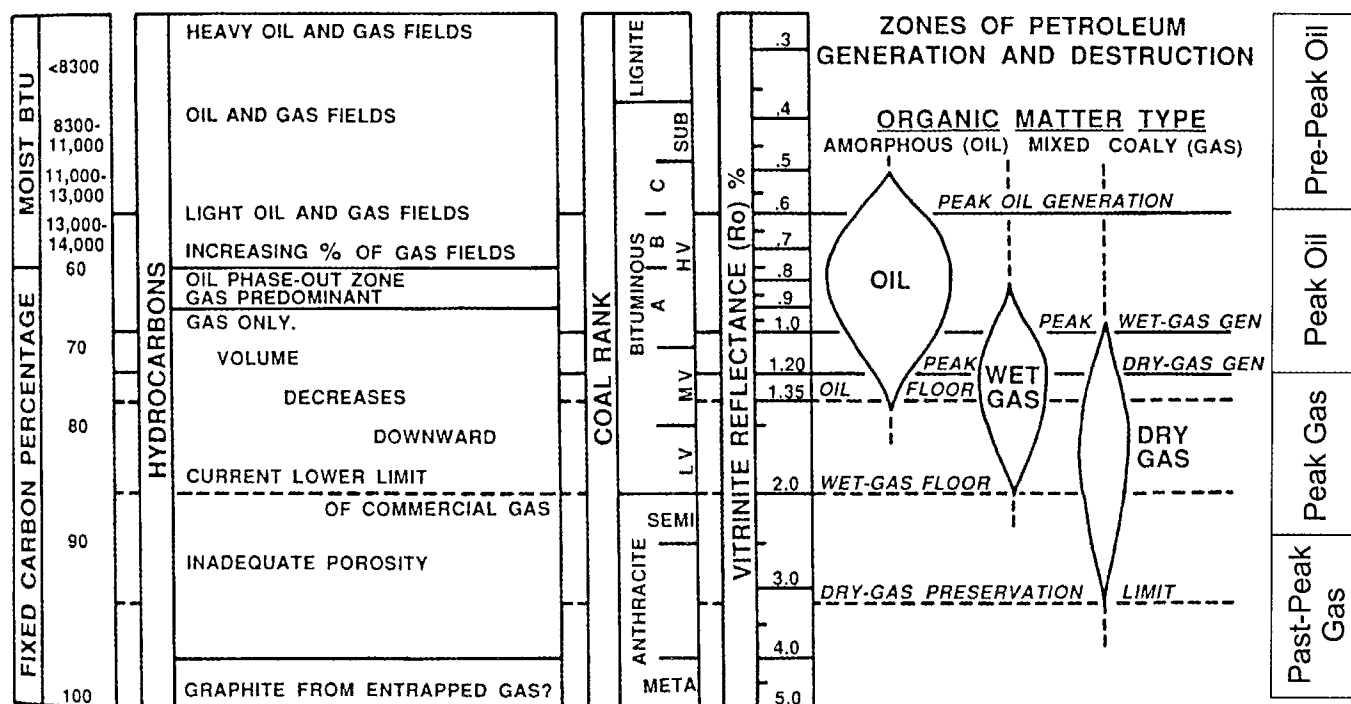


**Figure 7.** Diagram relating thermal maturity mapping levels to vitrinite reflectance, petroleum generation and destruction, and reservoir porosity destruction (modified from Houseknecht and others, 1992, reprinted by permission).

## POTENTIAL HYDROCARBON SOURCE INTERVALS

Curiale (1981, 1983) and Weber (1990, 1992, 1994) reviewed the hydrocarbon sourcing potential for strata in the Oklahoma portion of the Ouachita trend. Carroll and others (1993) discussed source rock characteristics of the Black Warrior Basin of Alabama. As part of a global study of thrust belts and foreland basins, the author and his colleagues examined additional data from the Arkansas portion of the Ouachita trend and the buried strata of the Black Warrior Basin in Mississippi.

Four potential regional hydrocarbon source intervals are recognized in the Arkoma and/or Black Warrior Basins: (1) Middle–Upper Ordovician Sylvan–Polk Creek–Womble Shale; (2) Upper Devonian–Lower Mississippian Woodford–Chattanooga Shale; (3) Lower Carboniferous (Upper Mississippian) Fayetteville–Stanley–Caney–Lewis (Floyd) Shale; and (4) coal beds and coaly shales within the Upper Carboniferous (Lower–Middle Pennsylvanian) Hartshorne, Atoka, and Pottsville Formations. The Silurian Missouri Mountain Shale probably has limited hydrocarbon source potential; however, the kerogen-rich intervals within this unit do not appear to extend across the basin. Even though no direct evidence exists to confirm that additional source intervals within Lower Ordovician and Upper Cambrian strata are regionally effective in sourcing petroleum systems, they have been hypothesized in the study area.

For this study, maps were constructed showing the current thermal maturity of these four potential hydrocarbon source intervals (Figs. 8A–D), based primarily on data from references cited at the end of this report, as well as unpublished data from the U.S. Geological Survey (USGS; Repetski, personal communication, 2004) and Amoco Production Company. Three of these source intervals, Middle–Upper Ordovician (Fig. 8A), Upper Devonian (Fig. 8B), and Upper Mississippian (Fig. 8C), are relatively thin and are thought to have undergone fairly uniform thermal alteration during their burial history. The fourth interval, Lower–Middle Pennsylvanian (Fig. 8D), is extremely thick in the deepest portions of the Arkoma and Black Warrior Basins. The thermal maturity map for the fourth interval displays the current thermal conditions for the Pennsylvanian Pottsville and Atoka Formations. In many places, the Upper–Middle Pennsylvanian Hartshorne Formation has a lower thermal maturity level than that shown on the map.

### Middle–Upper Ordovician

In the Arkoma Basin, the Middle- to Upper-Ordovician Sylvan–Polk Creek–Womble Shales have been confirmed as oil-prone source rocks with total organic carbon (TOC) contents ranging between 0.29 and 6.1% (Figs. 2, 8A; Table 1) (Curiale, 1983; Weber, 1990; Johnson and Cardott, 1992; Titus and Cole, 1996). Throughout most of their extent in the Arkoma



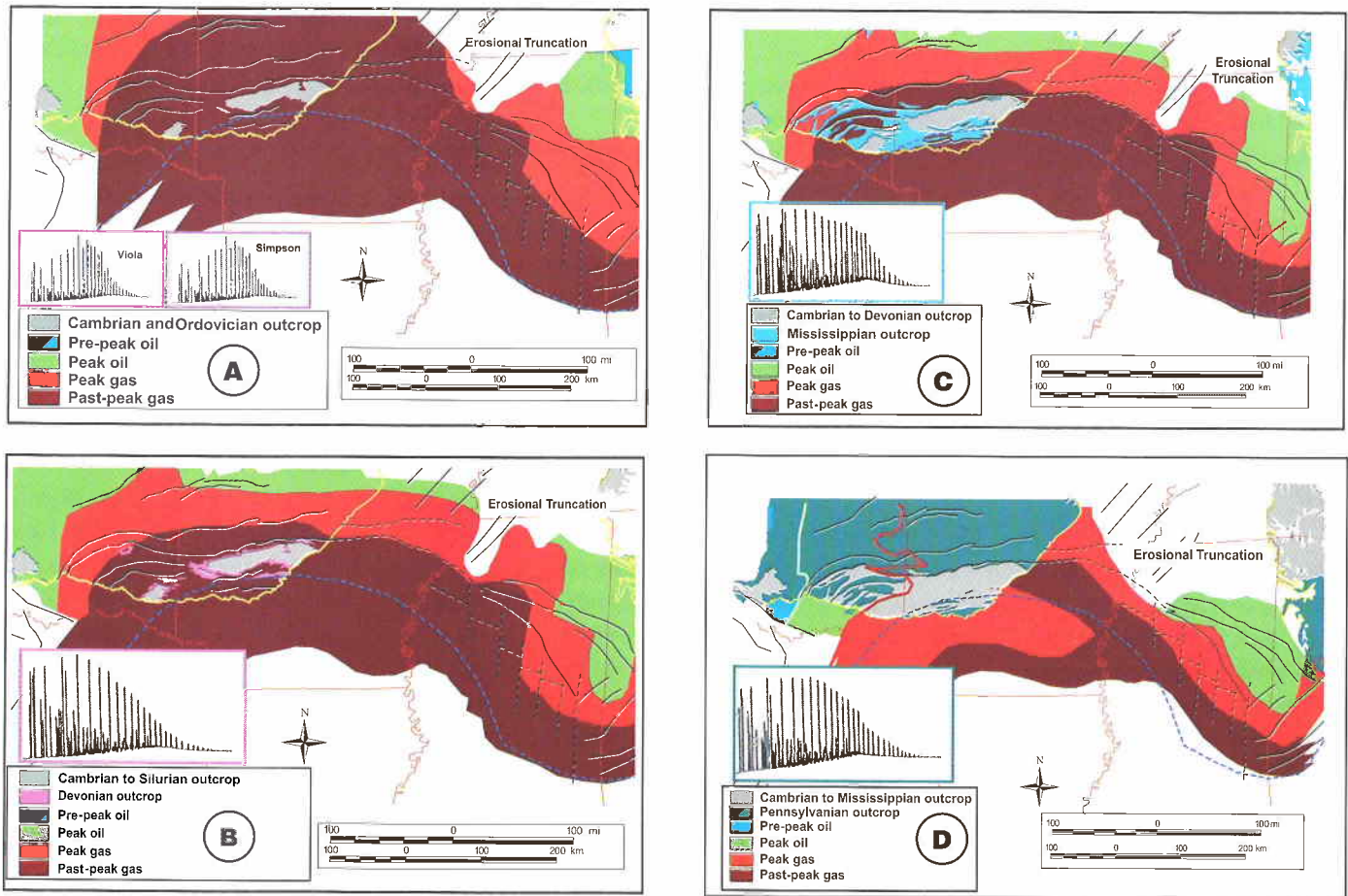


**Figure 8.** Present-day thermal maturity maps of key source intervals in the Arkoma and Black Warrior Basins (same area as Fig. 6). (A) Upper Ordovician; (B) Upper Devonian (also, includes some Lower Mississippian strata); (C) Upper Mississippian; (D) Middle Pennsylvanian. (Modified from Coleman and others, 2001; gas chromatography–flame ionization detector chromatographs from Wavrek, 1992; outcrops from King and Beikman, 1974)

Basin, they are at the past-peak gas level of thermal maturity. Facies equivalents of these shales are not recognized in the Black Warrior Basin, but may be present in the phyllite-grade metamorphic rocks encountered by wells drilled in the thrust-faulted portion of the basin (Flawn and others, 1961).

In the western Ouachita Mountains, Curiale (1983) correlated the heavy oils and solid hydrocarbons with kerogen-rich intervals in the Sylvan–Polk Creek–Womble Shales, with a possible contribution from the Silurian Missouri Mountain Formation (Curiale, 1992). These heavy hydrocarbons have been found in various Paleozoic strata ranging from the Upper Ordovician Bigfork Chert to the Lower Pennsylvanian Jackfork Group sandstone, and they appear to have experienced limited biodegradation, water washing, and devolatilization in conjunction with significant thermal alteration at the basin scale (Ruble and Philp, 1992; Cardott and others, 1993). In Oklahoma, oils generated from Middle–Upper Ordovician strata within the Ouachita trend are produced from Ordovician, Silurian, and Mississippian reservoirs (Campbell and Northcutt, 2001).

### Upper Devonian

The Upper Devonian–Lower Mississippian Woodford–Chattanooga Shale (and equivalents) is probably the most important, continent-wide hydrocarbon source interval in onshore central North America, as these kerogen-rich strata stretch from the Rocky Mountain basins to the Appalachian Basin. It is found throughout the Arkoma and to a lesser extent in the Black Warrior Basin (because of sedimentary thinning and erosional truncation; Comer, 1992; Comer and Hinch, 1987; Johnson and Cardott, 1992). In the study area, these strata have an organic richness that ranges from 2.0% to 12.5% TOC (Table 1). Throughout much of the Ouachita trend, this interval is at a peak gas to past-peak gas level of thermal maturity (Fig. 8B). In the main portion of the Arkoma Basin, the Woodford Shale contains primarily Type II kerogen and is an excellent oil source interval. Along the northern flank of the Arkoma Basin (Ozark Uplift) and Black Warrior Basin, however, it is diluted with terrigenous material and has a mixture of Type II and Type III kerogen; here it generated gaseous and



liquid hydrocarbons (Johnson and Cardott, 1992; Carroll and others, 1993).

The Woodford–Chattanooga source interval has been correlated with oils in the Arkoma Shelf reservoirs and with condensates in the Arkoma Basin (Comer, 1992; Amoco Production Company internal report, 1994). The Chattanooga Shale is also a potential source interval in parts of the Black Warrior Basin, but it has not been definitively correlated with the oils produced there. Oil and gas generated from these Upper Devonian intervals within the Ouachita trend are produced from Ordovician, Devonian, Mississippian, and Pennsylvanian reservoirs in Oklahoma (Wavrek, 1992; Campbell and Northcutt, 2001).

### Upper Mississippian

The Upper Mississippian Fayetteville–Caney–Lewis (Floyd) Shales have been recognized as a potential hydrocarbon source interval in the Ouachita trend for many years (Curiale, 1983; Weber, 1994; Carroll and others, 1993). The interval is predominantly gas-prone in the Arkoma Basin, but has a more oil-prone character in the Black Warrior Basin to the east and the Fort Worth Basin to the west. Within the study area, it ranges in richness from 0.17 to 9.5% TOC and extends across the spectrum from peak oil to past-peak gas in the Arkoma and Black Warrior Basins (Table 1; Fig. 8C).

The Upper Mississippian shales have been correlated with the oils produced from Mississippian reservoirs in the Black Warrior Basin, and they may be the source of the heavy oils in the tar sands of northern Alabama (Robertson Research, 1985; Carroll and others, 1993). This interval is generally equivalent to the Barnett Shale, which hosts a significant fractured shale gas play in the Fort Worth Basin. Gas production from pre-

sumed fractured Fayetteville Shale has recently been established in the northern Arkoma Basin of Arkansas (Korell and others, 2004; Southwestern Energy Company, 2004)

### Lower–Middle Pennsylvanian

The Lower and Middle Pennsylvanian Pottsville, Atoka, and Hartshorne Formations contain coal beds and kerogen-rich shales, which are dominantly gas-prone across the Ouachita trend. The shales in this interval vary in organic richness from 0.22 to 3.0% TOC (Table 1) and in thermal maturity from pre-peak oil to past-peak gas (Fig. 8D).

The slightly older Pottsville Formation, which includes the Mary Lee/Blue Creek and Pratt coal beds, hosts a prolific coalbed methane (CBM) industry in the Black Warrior Basin of Alabama. To the west, gas-prone shales in the slightly younger Jackfork, Johns Valley, and Atoka Formations have been recognized from geochemical sampling of outcrop exposures, but none of these shales has been clearly tied to gas production from Pennsylvanian strata. In the Arkoma Basin, coal beds in the Hartshorne Formation have been successfully developed as gas reservoirs. Additional potential has been recognized in younger coal beds of the McAlester, Savanna, and Boggy Formations.

## TIMING OF HYDROCARBON GENERATION

Byrnes and Lawyer (1999) have reviewed and modeled the hydrocarbon generation history of the Arkoma Basin and Ouachita Fold Belt in Oklahoma and Arkansas. Carroll and others (1993, 1995) have presented similar work on the Black Warrior Basin of Alabama. Repetski (personal communication, 2004) provided access to unpublished USGS data for

**TABLE 1.— Table of Known and Hypothetical Hydrocarbon Source Intervals in the Arkoma and Black Warrior Basins with TOC values**

Age	Formations	Minimum TOC (%)	Maximum TOC* (%)	Average TOC* (%)
Pennsylvanian	Hartshorne, Atoka, Johns Valley, Jackfork	0.22	3.0	1.95
Mississippian	Fayetteville, Caney, Stanley, Lewis (Floyd)	0.17	9.5	2.2
Devonian	Woodford, Chattanooga, Upper Arkansas Novaculite	2.0	12.5	8.5
Silurian	Missouri Mountain	<1.0	1.4	—
Ordovician	Sylvan–Viola, Womble, Polk Creek	0.29	6.1	3.2
Cambrian	Collier	—	—	—

\*Excluding coal sample analysis.

Source: data from Curiale, 1983; Weber, 1990; Johnson and Cardott, 1992; Korell and others, 2004.

Mississippi to update earlier modeling work by Hines (1988). These and other workers have shown that the maturation of the Paleozoic sedimentary pile was driven primarily by depositional burial within the larger Ouachita Basin. At first, burial was relatively slow, with deposition of low-volume, passive-margin, carbonate slope and shelf sediments, interspersed with deposition of basinal turbidite-debrite and chert during the early Paleozoic. During the late Paleozoic, burial became rapid, with high-volume siliciclastic, deltaic, and basin-fan sedimentation, interspersed with carbonate and chert deposition. Maximum foreland basin burial, both from sedimentary deposition and structural thickening caused by advancing thrust sheets during the Pennsylvanian and Early Permian, caused the main hydrocarbon source intervals previously discussed to evolve rapidly from pre-peak oil levels of thermal maturity to levels as high as past-peak gas in the deepest parts of the basin (Figs. 8A–D).

Houseknecht and Matthews (1985) interpreted a significant component of local thermal alteration to Mesozoic intrusion within the Mississippi Embayment. Their work, as well as that of others, clearly shows an increase in thermal maturity of all Paleozoic stratigraphic intervals from west to east along the outcrop and within the subsurface. Substantially less data are available from the subsurface of eastern Arkansas and western Mississippi, but the available data also indicate an increase in thermal maturity toward the area of Mesozoic intrusions (Fig. 9). The suggestion that a local increase in thermal maturity was caused by Mesozoic intrusions was rejected by Byrnes and Lawyer (1999) based on work by Desborough and others (1985) and Arne (1992), who

indicated from zircon and apatite-fission track analysis that maximum thermal maturity in Ouachita Paleozoic rocks were reached prior to the onset of Mesozoic plutonic intrusions. The work by Desborough and others (1985) and Arne (1992) was apparently restricted to outcrop samples, which were taken from the western edge of the intrusion area. Similar zircon and apatite-fission track analyses apparently have not been performed on samples from equivalent subsurface strata in Arkansas and Mississippi to see if these findings are pertinent across the entire Arkoma–Black Warrior Basin transition.

## PETROLEUM SYSTEMS

The Arkoma and Black Warrior Basins are primarily gas-productive (Table 2). Condensates are produced from some wells in Oklahoma, and crude oil is produced from some fields in Oklahoma, Arkansas, and Mississippi. Solid and low-gravity crude oil has been found in both basins. Because of these conditions, clear correlation of liquid hydrocarbons to source interval has been difficult and not without some debate. Where crude oils are present, however, it has been possible to correlate source interval to reservoir fluid.

Because of the relatively high degree of faulting and fracturing in the Ouachita trend, hydrocarbons from older strata have migrated upward into younger formations. This migration has been demonstrated by oil–source rock correlations of solid and liquid hydrocarbons; a similar migration path can also be assumed for natural gas.

In the Arkoma Basin and Ouachita Fold Belt, hydrocarbons sourced from Ordovician strata have been identified in

Ordovician, Silurian, and Mississippian reservoir rocks. The heavy oil in Mississippian and Pennsylvanian sandstones is related to oils originally derived from Ordovician strata. Hydrocarbons sourced from Devonian strata (including Lower Mississippian intervals) have been identified in Ordovician, Devonian, Mississippian, and Pennsylvanian reservoir rocks. Hydrocarbons derived from Mississippian units have been inferred to be that found in fractured Mississippian Fayetteville Shale reservoirs. Hydrocarbons from Pennsylvanian source intervals are inferred in Hartshorne coal reservoirs in the CBM fields and less so in at least some of the Pennsylvanian shallow-water and deep-water sandstone reservoirs (Petroleum Information Corporation, 1989; Car-

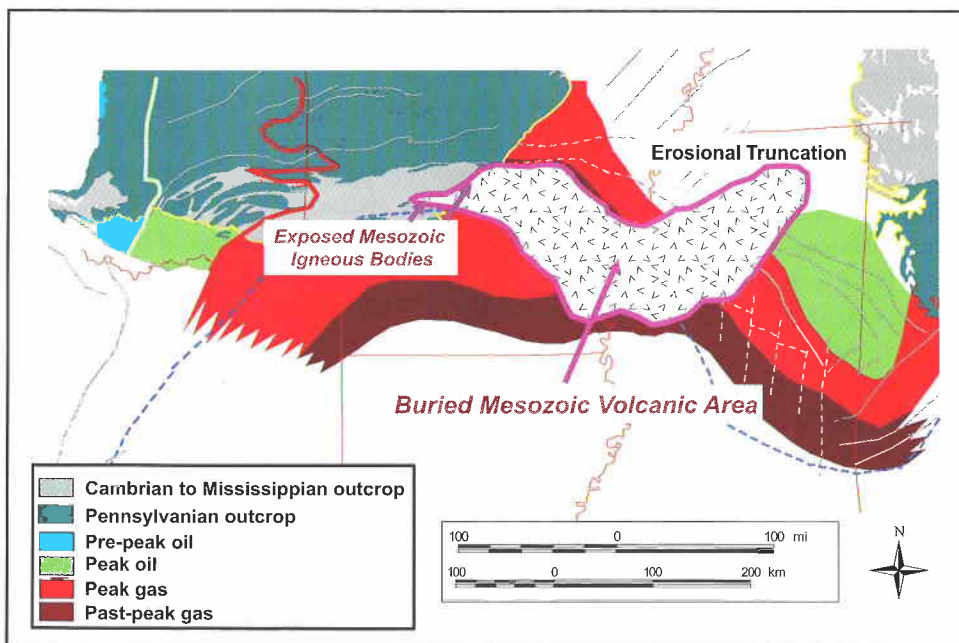


**Figure 9.** Mesozoic igneous areas in the Arkoma and Black Warrior Basins (modified from Coleman, 1991; superimposed on Figure 8D).

**TABLE 2.—Table of Known and Hypothetical Hydrocarbon Source Intervals in the Arkoma and Black Warrior Basins with Kerogen Type and Generated Hydrocarbon Product Type Age**

Gas	Formations	Kerogen Type	Product
Pennsylvanian	Hartshorne, Atoka, Johns Valley, Jackfork	III	Gas
Mississippian	Fayetteville, Caney, Stanley, Lewis (Floyd)	II, III	Oil, gas
Devonian	Woodford, Chattanooga, Upper Arkansas Novaculite	II, III	Oil, gas
Silurian	Missouri Mountain	II (?)	Oil (?)
Ordovician	Sylvan–Viola, Womble, Polk Creek	II	Oil
Cambrian	Collier	II (?)	Oil (?)

Source: Modified from Curiale, 1983; Weber, 1990; Johnson and Cardott, 1992; Comer, 1992; Carroll and others, 1993, 1995; Korell and others, 2004.

dott, 1998; Campbell and Northcutt, 2001; Korell and others, 2004).

In the Arkoma Basin, the preponderance of vertical hydrocarbon migration paths in a system of both high-angle normal faults and low-angle thrust faults has led to a highly efficient discovery process, wherein the largest fields were found first (Fig. 10A). The first fields were drilled on surface anticlines, which, fortuitously, hinted at structural and stratigraphic closure on older reservoirs at depth.

In the Black Warrior Basin, oil derived from Mississippian source intervals has been identified in Mississippian reservoir rocks, and natural gas sourced from Pennsylvanian strata is inferred in Pottsville coal reservoirs. Natural gas produced from Ordovician, Mississippian, and Pennsylvanian reservoirs has not been clearly tied to any of the source intervals discussed. It is assumed that the high organic content strata within the Mississippian and Pennsylvanian rocks sourced reservoir intervals of these ages. Source intervals in the Ordovician and/or Devonian strata in the deep Black Warrior Basin may have produced the gas extracted from Middle Ordovician dolomite reservoirs deeper in the basin.

The historical development of hydrocarbon production in the Black Warrior Basin has been somewhat enigmatic and certainly inefficient, as there has been an almost random discovery history in the basin (Fig. 10B). Prior to the discovery and development of CBM reservoirs, the main producing trends of the Black Warrior Basin were buried beneath sediments of the Gulf Coastal Plain, which only faintly mimic the underlying structural grain. Hence, large surface anticlines were not available to guide early explorers. With the development of reflection seismic profiling, normal fault-bounded

structures were identified, drilled, and in some cases, natural gas production established. Oil shows were not uncommon; in fact, large tar sand deposits were known from the outcrop area of Mississippian strata in northwest Alabama and northeast Mississippi. Even so, no crude oil production was established until 1982, when drilling at Coal Fire Creek Field found oil in what was thought to be a gas productive trend. Two years before, large-scale CBM production was initiated at Oak Grove Field (Fig. 10B).

## RESOURCE ASSESSMENT

Teams from the USGS have assessed the remaining resources of the various sub-basins of the Ouachita trend (Gautier and others, 1995; Hatch and others, 2003; Pollastro and others, 2004). By combining the work of these three teams, it is possible to develop an understanding of the remaining hydrocarbon potential within the Ouachita trend (Fig. 11). It is clear that the residual potential in both the Arkoma and Black Warrior Basins will be probably be dominated by natural gas or natural gas liquids. It is also apparent that the potential of these two basins is minor when compared to the remaining potential for the Texas Ouachita basins, which have assessed volumes of hydrocarbons as much as 100 times that of the Arkoma and Black Warrior Basins (Table 3).

## BASIN-SCALE, GEOTECHNICAL EXPLORATION RISKS

Future oil and natural gas exploration in the Arkoma and Black Warrior Basins will take place with some distinct advantages and disadvantages. A number of petroleum systems

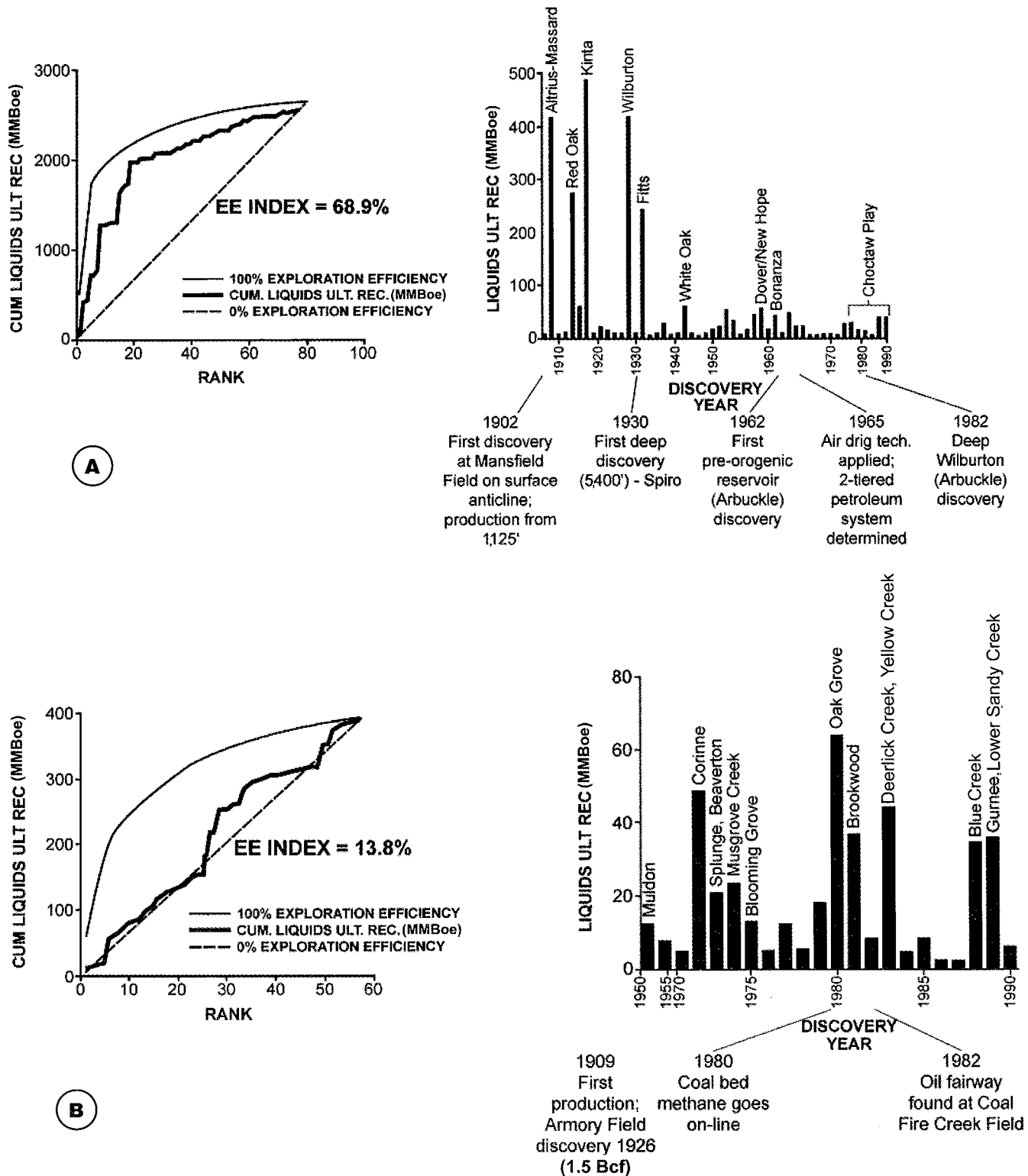


**Figure 10.** Charts depicting exploration efficiency index (EE) of fields within the Arkoma and Black Warrior Basins, with attributed ultimate recoverable (ULT REC) volume by year and descriptions of significant technology applications and/or new play types. (A) Arkoma Basin; (B) Black Warrior Basin (from Coleman and Tasker, 1994). MMBoe= million barrels of oil equivalent (6 trillion cubic feet of gas  $\approx$  1 MMBoe). EE is a calculation of the relative efficiency of exploration within a set of fields. An EE of 100% indicates that the largest field was found first, followed by the next largest, and so forth. An EE of 0% occurs when there is no chronological order of field finding by field size (i.e., a purely random set of events). Rank is the order of fields by size, with 1 being the largest field, 2 the next largest, and so forth.

**Table 3.— Compilation of Resource Assessment (F50 Values)**

Basin	Oil (MMBo)*	Natural Gas (Tcfg)†	Natural Gas Liquids (MMBngl)‡
Black Warrior Basin	5.9	8.5	7.6
Arkoma Basin	3.4	4.7	74.5
Texas Ouachita basins (Fort Worth, Val Verde, Marathon)	114.7	26.7	1,080.1
Total	124.0	39.9	1,162.2

\* Million barrels of oil.

† Trillion cubic feet of natural gas.

‡ Million barrels of natural gas liquids.

Source: USGS National Oil and Gas Assessment teams: Gautier and others, 1995; Hatch and others, 2003; Pollastro and others, 2004.

have been identified, ranging in age from Ordovician to Pennsylvanian. Generation and initial migration of hydrocarbons from most source intervals took place about the same time in all source intervals (during the Late Pennsylvanian) as a result of foreland basin sedimentation, tectonic loading, and deep burial. Mississippian oil-prone source intervals are still within or near the oil window of thermal maturity in portions of the trend. Gas-prone coal beds are present at shallow to deep depths.

Unfortunately, with these advantages come several disadvantages. Most areas with favorable reservoir and source interval characteristics have been heavily drilled, leaving few (or possibly no) areas for low-risk opportunities. For the most part, the yet-to-be-found carbonate and siliciclastic reservoirs probably will have poor reservoir characteristics (i.e., low porosity and permeability). High thermal maturity due to synorogenic depositional and tectonic loading has probably adversely affected reservoir properties over much of the remaining areas to be drilled. Remaining hydrocarbon trap sizes will probably be small at shallow depths, but potentially large at greater depths. Thrust faulting and normal faulting may have created fragmented structures and disconnected compartments of high structural complexity. Whereas this highly fragmented condition may contribute to increased gas production potential (rate and accessible cumulative volume per well), it also may increase the risk for seal failure, potentially preventing any production at all. This fragmented reservoir

condition may also increase the difficulty in obtaining clear seismic images of potential hydrocarbon traps.

The discovery and development of new fields in the Arkoma and Black Warrior Basins will require patience and strong reservoir characterization skills to maximize production and exploitation efficiency. The development in 2003 of deep Ordovician reservoirs within the Black Warrior Basin, based on a 1971 discovery (Champlin, 2003), may presage a new round of drilling and field development. Applications of horizontal drilling technology, following enhanced seismic imaging and processing, may also enhance growth potential in existing fields.

## SUMMARY

The distribution and effectiveness of the petroleum systems in the Arkoma and Black Warrior Basins are a function of Pennsylvanian sedimentation (burial), subsidence, and tectonics. The effects of Mesozoic igneous activity in the eastern Arkoma and western Black Warrior Basins and fold belts are uncertain, but may be detrimental to both hydrocarbon source and reservoir intervals. Thermal maturity in the Arkoma and Black Warrior Basins has apparently restricted the optimum area for future oil and gas development. The discovery of significant, new, potential source intervals will probably not have a substantial effect on development history of either the Arkoma or Black Warrior Basins. Effective reservoir performance (over most of the area) will probably require a significant tectonic component in the form of pervasive fracturing



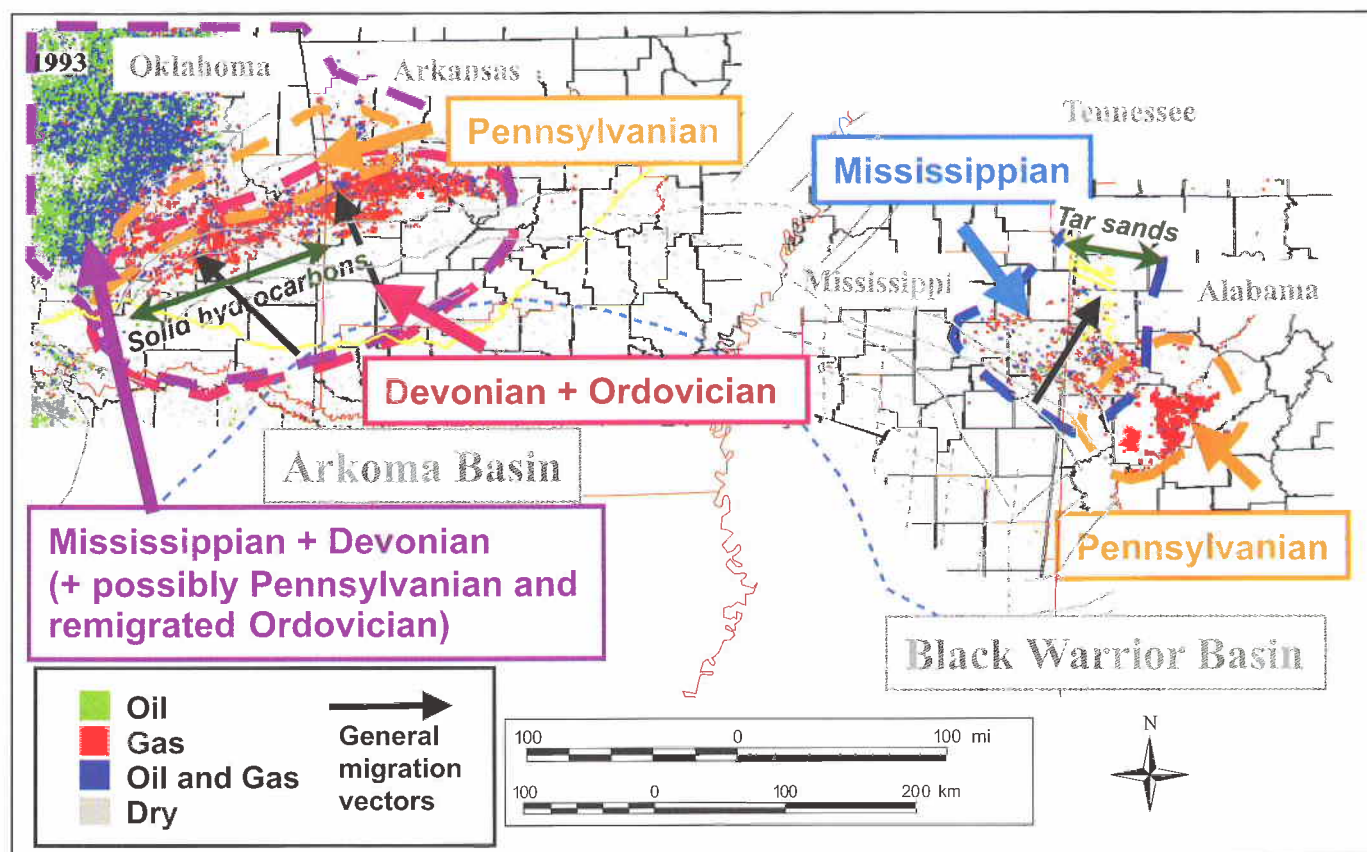


**Figure 11.** Generalized map showing hypothetical distribution of petroleum systems and general hydrocarbon migration vectors. Solid and dashed gray lines are faults (solid = outcrop and well-established, subsurface fault traces; dashed = less well-established and inferred, subsurface fault traces). (Production base map from Gautier and others, 1995)

to overcome adverse reservoir conditions caused by geologic age, original burial depth, diagenetic gradient, and grain- and pore-throat sizes. The Arkoma Basin has a highly efficient discovery history and profile, suggesting that new play concepts will be required there for the “next big discovery.” The Black Warrior Basin, on the other hand, has a highly inefficient discovery history. Although it is likely that significant new fields will not be found with existing play concepts, the projected history of the basin does not rule out that possibility.

### ACKNOWLEDGMENTS

This study is updated and expanded from work originally done at Amoco Production Company as part of a global study of the petroleum system potential of thrust belts and foreland basins. It was originally presented in summary form at the 2001 American Association of Petroleum Geologists’ annual convention (Coleman and others, 2001). Colleagues in that effort were Milford Davis, Jeff Cook, and Lance Eggers. For this updated version, John Repetski (USGS) shared unpublished conodont CAI data from the Arkoma and Black Warrior Basins. Appreciation

is extended to USGS colleagues David Houseknecht, Christopher Swezey, and Robert Milici for their reviews.

### REFERENCES CITED

- Arne, D. C., 1992, Evidence from apatite fission track analysis for regional Cretaceous cooling in the Ouachita Mountain Fold Belt and Arkoma Basin of Arkansas: *American Association of Petroleum Geologists Bulletin*, v. 76, p. 392–402.
- Byrnes, A. P.; and Lawyer, Gary, 1999, Burial, maturation, and petroleum generation history of the Arkoma Basin and Ouachita Fold Belt, Oklahoma and Arkansas: *Natural Resources Research*, v. 8, p. 3–26.
- Campbell, J. A.; and Northcutt, R. A., 2001, Petroleum systems of sedimentary basins in Oklahoma, in Johnson, K. S.; and Merriam, D. F. (eds.), *Petroleum systems of sedimentary basins in the southern Midcontinent, 2000 symposium*: Oklahoma Geological Survey Circular 106, p. 1–5.

- Cardott, B. J., 1998, Coal as gas-source rock and reservoir, Hartshorne Formation, Oklahoma: Oklahoma Geological Survey Special Publication 98-7, p. 41–62.
- Cardott, B. J.; Ruble, T. E.; and Suneson, N. H., 1993, Nature of migrabitumen and their relation to regional thermal maturity, Ouachita Mountains, Oklahoma: *Energy Sources*, v. 15, p. 239–267.
- Carroll, R. E.; Pashin, J. C.; and Kugler, R. L., 1993, Burial history and source-rock characteristics of Mississippian and Pennsylvanian strata, Black Warrior Basin, Alabama, *in* Pashin, J. C. (ed.), *New perspective on the Mississippian System of Alabama*: Alabama Geological Society 30th annual field trip guidebook, p. 79–88.
- \_\_\_\_\_, 1995, Burial history and source-rock characteristics of Upper Devonian through Pennsylvanian strata, Black Warrior Basin, Alabama: Geological Survey of Alabama Circular 187, 29 p.
- Champlin, S. D., 2003, Underexplored oil and gas trends of Mississippi: *Transactions Gulf Coast Association of Geological Societies*, v. 53, p. 123–134.
- Coleman, J. L., Jr., 1991, Seismic stratigraphic confirmation of a buried Late Proterozoic terrane, Sunflower County, Mississippi: *Mississippi Geology*, v. 12, no. 3–4, p. 32–42.
- Coleman, J. L., Jr.; and Tasker, D. R., 1994, Exploration risks in thrust belts and foreland basins [abstract]: *European Association of Exploration Geophysicists/European Association of Petroleum Geologists Workshop on Petroleum Exploration and Production in Thrust Belts and Foreland Basins*, June 6, 1994, Vienna, Austria, p. 3.
- Coleman, J.; Davis, M.; Cook, J.; and Eggers, L., 2001, Comparative analysis of the exploration potential of the thrust belts and foreland basins of North America [abstract]: *American Association of Petroleum Geologists Annual Convention Abstracts CD*, 2 p.
- Comer, J. B., 1992, Organic geochemistry and paleogeography of Upper Devonian formations in Oklahoma and northwestern Arkansas: Oklahoma Geological Survey Circular 93, p. 70–93.
- Comer, J. B.; and Hinch, H. H., 1987, Recognizing and quantifying expulsion of oil from the Woodford Formation and age-equivalent rocks in Oklahoma and Arkansas: *American Association of Petroleum Geologists Bulletin*, v. 71, p. 844–858.
- Curiale, J. A., 1981, Source rock geochemistry and liquid and solid petroleum occurrences of the Ouachita Mountains, Oklahoma: University of Oklahoma, Norman, unpublished Ph.D. dissertation, 286 p.
- \_\_\_\_\_, 1983, Petroleum occurrences and source-rock potential of the Ouachita Mountains southeastern Oklahoma: *Oklahoma Geological Survey Bulletin* 135, 65 p.
- \_\_\_\_\_, 1992, Petroleum geochemistry of Texas and Oklahoma oils along the Marathon–Ouachita fold–thrust belt, south-central U.S.A.: *Chemical Geology*, v. 98, p. 151–173.
- Desborough, G. A.; Zimmerman, R. A.; Elrick, M. B.; and Stone, C. G., 1985, Early Permian thermal alteration of Carboniferous strata in the Ouachita Region and Arkansas River Valley, Arkansas [abstract]: *Geological Society of America, Abstracts with Programs*, v. 17, no. 3, p. 155.
- Dow, W. G., 1977, Kerogen studies and geological interpretations: *Journal of Geochemical Exploration*, v. 7, p. 79–99.
- Flawn, P. T.; Goldstein, A., Jr.; King, P. B.; and Weaver, C. E., 1961, *The Ouachita System*: University of Texas Publication 6120, 401 p.
- Gatewood, L. E.; and Fay, R. O., 1991, The Arbuckle/Ouachita facies boundary in Oklahoma: Oklahoma Geological Survey Circular 92, p. 171–180.
- Gautier, D. L.; Dolton, G. L.; Takahasi, K. I.; and Varnes, K. L., 1995, National assessment of United States oil and gas resources—results, methodology, and supporting data: U.S. Geological Survey Digital Data Series DDS-30, 1 disk.
- Hale-Erlich, W. S.; and Coleman, J. L., Jr., 1991, The Ouachita–Appalachian juncture: a Paleozoic transpressional zone in the southeastern U.S.A.: *American Association of Petroleum Geologists Bulletin*, v. 77, p. 552–568.
- Hatch, J. R.; Pawlezewicz, M. J.; Charpentier, R. R.; Cook, T. A.; Crovelli, R. A.; Klett, T. R.; Pollastro, R. M.; and Schenk, C. J., 2003, Assessment of undiscovered oil and gas resources of the Black Warrior Basin province, 2002: U.S. Geological Survey Fact Sheet FS-038-03, 2 p.
- Hatcher, R. D., Jr.; Thomas, W. A.; and Viele, G. W. (eds.), 1989, *The Appalachian–Ouachita orogen in the United States: Geology of North America, Geological Society of America Decade of North American Geology (DNAG)*, v. F-2, 767 p.
- Hendrick, S. J., 1992, Vitrinite reflectance and deep Arbuckle maturation at Wilberton Field, Latimer County, Oklahoma: Oklahoma Geological Survey Circular 93, p. 176–184.
- Hines, R. A., 1988, Carboniferous evolution of the Black Warrior foreland basin, Alabama and Mississippi: University of Alabama, Tuscaloosa, unpublished Ph.D. dissertation, 231 p.
- Houseknecht, D. W.; Hathon, L. A.; and McGilvery, T. A., 1992, Thermal maturity of Paleozoic strata in the Arkoma Basin: Oklahoma Geological Survey Circular 93, p. 122–132.
- Houseknecht, D. W.; and Matthews, S. M., 1985, Thermal maturity of Carboniferous strata, Ouachita Mountains: *American Association of Petroleum Geologists Bulletin*, v. 66, p. 923–930.

- Johnson, K. S.; and Cardott, B. J., 1992, Geologic framework and hydrocarbon source rocks of Oklahoma: Oklahoma Geological Survey Circular 93, p. 21–37.
- King, P. B.; and Beikman, H. M., 1974, Geologic map of the United States (exclusive of Alaska and Hawaii): U.S. Geological Survey, 3 sheets, scale 1:2,500,000: Digital file available at <http://pubs.usgs.gov/dds/dds11>
- Korell, Harold; Lane, Richard; and Kerley, Greg, 2004, Southwestern Energy Company announces Fayetteville Shale play in Arkoma Basin teleconference: [http://www.swn.com/investor\\_relations/press/08-18-2004.pdf](http://www.swn.com/investor_relations/press/08-18-2004.pdf) [accessed 12/15/2004]
- Lillie, R. J.; Nelson, K. D.; deVoogd, Beatrice; Brewer, J. A.; Oliver, J. E.; Brown, L. D.; Kaufman, Sidney; and Viele, G. W., 1983, Crustal structures of Ouachita Mountains, Arkansas: a model based on integration of COCORP reflection profiles and regional geophysical data: American Association of Petroleum Geologists Bulletin, v. 67, p. 907–931.
- Perry, W. J., 1996, Arkoma Basin Province (062), in Charpentier, R. R.; Klett, T. R.; Obuch, R. C.; and Brewton, J. D., (compilers), Tabular data, text, and graphical images in support of the 1995 national assessment of United States oil and gas resources: U.S. Geological Survey Digital Data Series DDS-36, PROV62.RTF, 16 p.
- Perry, W. J.; Wardlaw, B. R.; Bostick, N. H.; and Maughan, E. K.; 1983, Structure, burial history, and petroleum potential of frontal thrust belt and adjacent foreland, southwest Montana: American Association of Petroleum Geologists Bulletin, v. 67, p. 725–743.
- Petroleum Information Corporation, 1989, Drilling the deep Arkoma Part 2: Structures and source rocks: Petroleum Frontiers, v. 6, n. 3, 41 p.
- Pollastro, R. M.; Hill, R. J.; Ahlbrandt, T. A.; Charpentier, R. R.; Cook, T. A.; Klett, T. R.; Henry, M. E.; and Schenk, C. J., 2004, Assessment of undiscovered oil and gas resources of the Bend Arch–Fort Worth Basin province of north-central Texas and southwestern Oklahoma, 2003: U.S. Geological Survey Fact Sheet 2004-3022, 2 p.
- Roberts, M. T., 1994, Geologic relations along a regional cross section from Spavinaw to Broken Bow, eastern Oklahoma, in Suneson, N. H., and Hemish, L. A. (eds.), Geology and resources of the eastern Ouachita Mountains frontal belt and southeastern Arkoma Basin, Oklahoma: Oklahoma Geological Survey Guidebook 29, p. 137–160.
- Robertson Research, 1985, Oil generation in Black Warrior Basin, Alabama: a geochemical study: Robertston Research (U.S.), Inc., Kingwood, Texas, 328 p.
- Ruble, T. E.; and Philp, R. P., 1992, A reevaluation of the geochemical characteristics of solid bitumens from the Ouachita Mountains, Oklahoma: Oklahoma Geological Survey Circular 93, p. 337–342.
- Ryder, R. T.; Rice, D. D.; and Flinn, T. M., 1996, Black Warrior Basin Province (065), in Charpentier, R. R.; Klett, T. R.; Obuch, R. C.; and Brewton, J. D., (compilers), Tabular data, text, and graphical images in support of the 1995 national assessment of United States oil and gas resources: U.S. Geological Survey Digital Data Series DDS-36, PROV65.RTF, 22 p.
- Southwestern Energy Company, 2004, Southwestern Energy announces capital program and guidance for 2005 and provides update of Fayetteville Shale play: Southwestern Energy Company press release, Thursday, December 9, 2004 [http://biz.yahoo.com/prnews/041209/dath013\\_1.html](http://biz.yahoo.com/prnews/041209/dath013_1.html) [accessed 12/15/2004]
- Suneson, N. H.; and Campbell, J. A., 1990, Oil and gas exploration in the western Ouachita region, Oklahoma: Oklahoma Geological Survey reprint, 12 p. (originally published as Ouachitas need more exploratory drilling, Oil & Gas Journal, v. 88, no. 15, p. 65–69 and no. 16, p. 85–87).
- Titus, C. A. O.; and Cole, G. A., 1996, Source rock potential and sediment thermal maturity trends in the Ouachita overthrust of southeast Oklahoma and southwest Arkansas: Oklahoma Geological Survey Open-File Report 5-96, 64 p. (originally completed as Sohio Petroleum Company Report GE [CD] 01 in 1986).
- Viele, G. W., 1979, Geologic map and cross section, eastern Ouachita Mountains, Arkansas: Geological Society of America Map and Chart Series MC-28F, Geological Society of America, Boulder, Colorado.
- Wavrek, D. A., 1992, Characterization of oil types in the Ardmore and Marietta Basins, southern Oklahoma aulacogen: Oklahoma Geological Survey Circular 93, p. 185–195.
- Weber, J. L., 1990, Comparative study of crude-oil compositions in the frontal and central Ouachita Mountains: Oklahoma Geological Survey Special Publication. 90-1, p. 101–117.
- , 1992, Organic matter content of outcrop samples from the Ouachita Mountains, Oklahoma: Oklahoma Geological Survey Circular 93, p. 347–352.
- , 1994, A geochemical study of crude oils and possible source rocks in the Ouachita tectonic province and nearby areas, southeast Oklahoma: Oklahoma Geological Survey Special Publication 94-2, 32 p.
- Zimmerman, Jay; Roeder, D. H.; Morris, R. C.; and Evansin, D. P., 1982, Geologic section across the Ouachita Mountains, western Arkansas: Geological Society of America Map and Chart Series MC-28-Q, scale 1:250,000, Geological Society of America, Boulder, Colorado.





# Geologic Profiles Derived From Seismic Data West and East of the Arkansas–Oklahoma State Line, Arkoma Basin and Frontal Ouachita Mountains

*Michael T. Roberts*

Palmer Petroleum, Inc., Shreveport, Louisiana

## INTRODUCTION

The geology of the southern Arkoma Basin and frontal zone of the Ouachita Mountains is complex and not completely understood. Several cross-sectional studies have been published focusing on this zone of Pennsylvanian–Permian deformation (e.g., Briggs and Roeder, 1975; Wickham, 1977; Viele, 1979; Arbenz, 1984, 1989; Zimmerman and others, 1982; Lillie and others, 1983; Roberts, 1994). These sections differ from each other in interpreted styles of deformation and in the handling of basic questions regarding the structural relationship between major tectonic elements. I do not propose to answer all of these questions. Instead, I will present two additional profiles derived from multichannel seismic lines located in western Arkansas (Fig. 1) and compare the geology revealed by these data to that of the seismic lines I used for a cross section west of the Arkansas–Oklahoma state line (Roberts, 1994). The seismic data for the present study were provided by Compagnie Generale de Geophysique (CGG). The previously published cross section used seismic data that started near Big Cedar, Oklahoma, and trended north to near Brushy, Oklahoma. It included the Mulberry Fault on the north side of the Arkoma Basin, the Backbone and Heavener Anticlines and intervening Cavanal Syncline of the Arkoma Basin, the frontal thrust fan south of the Choctaw Fault, and the Ti Valley, Briery, and Windingstair Faults of the Ouachita system. The section was carried north and south using outcrop data.

Cross section A (Fig. 2) trends due south from near Greenwood, Arkansas, to a point just north of Shut-In Mountain, all of which is covered by CGG line 606. The cross section continues southward based on outcrop data from the COGEOMAP of Haley and Stone (1995) through west Mena, Arkansas, and the first ridges of Arkansas Novaculite south of Mena. This section is approximately 21 mi east of the Oklahoma section in Roberts (1994). Section A begins with the Washburn Anticline, en echelon with the Backbone Anticline, and a major gas-producing structure in Arkansas (dominantly from Atokan sandstone

reservoirs). It passes southward in the Arkoma Basin through an anticline near Mansfield, the site of the first commercial gas well in Arkansas in 1902, and then across the Poteau Syncline. Farther south, the section crosses a major anticline at Walker Mountain, then the Ross Creek and Johnson Creek Faults of the frontal Ouachitas. The seismic data terminate in a complex area of faulted lower Atokan strata 1 mi east of Horseshoe Mountain. To the south, outcrops are of thrustured Ouachita facies strata of the Jackfork Group, Johns Valley Formation, and Stanley Group north of Mena, and complexly deformed Stanley shales, Arkansas Novaculite, and older units south of Mena. The cross section terminates at the south end of the Potter Quadrangle.

Cross section B (Fig. 3) begins nearly 11 mi east of A, and follows CGG seismic lines 6 and 1 south across the Washburn Anticline and Poteau Syncline to near Waldron, Arkansas, where it bends toward the southeast, crosses the Ross Creek Fault and the Y City Fault, 3.5 mi south of which the seismic data terminate. The cross section is offset to the west approximately 8 mi along the Y City Fault to near Y City, where it continues south through the Board Camp Quadrangle using the surface geology of Haley and Stone (1995). South of Y City are thrustured Ouachita facies of Jackfork–Johns Valley and Stanley strata. A major fault, 2.5 mi north of the Y City Fault, carried Ouachita facies (Johns Valley at the surface) over the middle Atoka. It must somehow connect with the major Oklahoma Ti Valley Fault system, which is also interpreted as bringing Ouachita facies far to the north over the Atokan foredeep units. This fault is called the Ti Valley Fault in this paper (and by C. Stone, personal communication, 2004). South of Irons Fork Mountain, the cross section passes through complexly deformed Stanley shales, Arkansas Novaculite, and older units of the “core zone” anticlinorium or Benton Uplift.

The area of these three cross sections is where the geologic structures and nomenclatures of the Oklahoma Ouachitas somehow merge into those of the Arkansas side of the thrust belt.

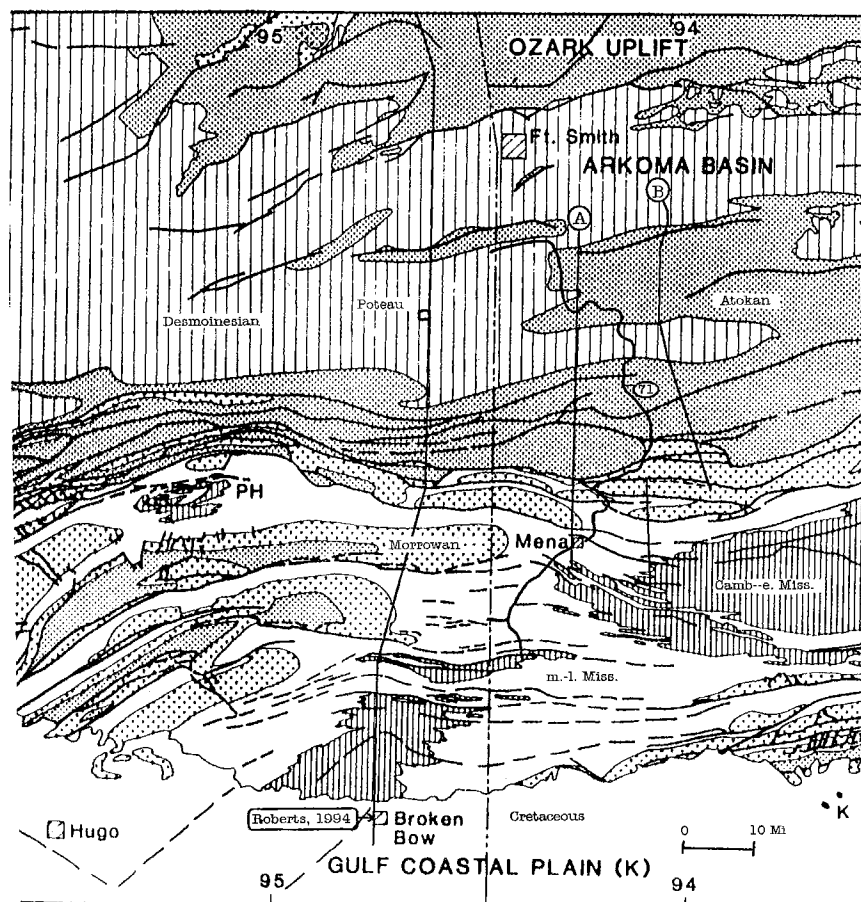


**Figure 1.** Location map for cross sections A and B discussed in this report (geologic base from Arbenz, 1989). Also shown is location of Roberts' (1994) cross section.

The exact ties of the structures across the state line are still being worked on—for example, what do the Choctaw, Ti Valley, and other major Oklahoma thrusts correlate to in west Arkansas? As previously stated, the fault north of Y City that carries the frontal Ouachita facies should tie with the Ti Valley Fault, but its connection is not clear from surface mapping as the intervening Horseshoe Mountain Syncline–Atoka complex cuts off the fault west of Boles, Arkansas. The area of these sections is also the place where the frontal Ouachita belt widens dramatically from the Mena region into southeastern Oklahoma and a bend occurs in the so-called core zone of the Benton–Broken Bow Uplift. Cover structures revealed by the seismic tool, as well as surface geology, change along strike through this area and some of these changes may be related to lateral ramps in the cover strata and basement fault complexes at depth. Duplex structures are present in both the Arkoma Basin cover and in the Ouachita facies.

### CROSS SECTION A

The cross sections are presented as seismic-line drawings interpreted with the help of the surface outcrops (Haley and

Stone, 1995). The horizontal scale is in miles (Fig. 2) but the vertical scale is in seconds. The unit boundaries are interpreted by projection from the surface to depth (time) and the faults and other features are interpreted from the seismic data. The display is approximately 1:1, assuming an average velocity of 12,000 feet per second (fps) (which is probably too slow; some areas are possibly closer to 13,500 fps). The section extension south of the seismic data was done from surface data and approximate known thickness of units but was drawn to match the seismic scale. This is not strictly proper but serves to illustrate a model for the continuation of the geology revealed by the seismic line.

The seismic data from near Greenwood, Arkansas, south to the Ross Creek Fault (Fig. 2) show that the Atoka is detached from underlying lower Atoka and older strata by a low-angle thrust fault that comes to the surface in a fan of thrusts in the core of the Washburn Anticline. South of the Poteau Syncline this detachment steepens southward and merges with a regional décollement surface that lies in Mississippian shales above the older carbonate platform strata of the Ozark facies. The underlying Ozark facies strata are block faulted but form a south-dipping ramp overall. Listric normal faults formed in Mississippian–Morrowan and lowest Atokan clastics lie between the platform blocks and the intra-Atoka detachment. Above

the detachment ride broad synclines and cusped anticlines in Atokan and Desmoinesian clastics and coals. Some thrusts may be reactivated listric normal faults. Some listric normal faults can still be seen under the detachment. Much recent development drilling has taken place along the Washburn Anticline for gas reserves (e.g., Gragg, Booneville, and Chismville Fields) in Atoka sandstones. Under the Washburn Anticline, the Ozark facies are nearly 9,000 ft deep, but under the Ross Creek Fault they may rest at 27,000 ft or more below the surface, buried by thrust sheets and increased thickness of lower Atokan, Morrowan, and Mississippian clastics.

In this area, large thrusts also lie north of the Ross Creek Fault, bringing lower Atoka over middle Atoka strata. Some studies have correlated these faults with the Choctaw Fault system of Oklahoma. Immediately south of the Ross Creek Fault, the Johnson Creek Fault defines the northern edge of an enigmatic, thrust synformal complex of lower and middle Atoka. The seismic data end within this Atoka complex and are not easily interpreted within and beneath it. The data, however, along

with the pattern of surface geology mapped by Haley and Stone (1995), are interpreted to show a flat, shallow detachment fault separating the Atokan synform from deeper thrustured Ouachita basinal facies and Atokan foredeep facies.

The relationships near Boles and Y City indicate that either the Ti Valley thrust sheet plunges beneath a detached Atoka synform or that the Atoka strata overlie it erosionally. I have chosen the first possibility for this cross section and show the Ti Valley Fault beneath the detached Atoka units, itself thrust far over foredeep clastics of lower Atokan age and underlying older units, including the Ozark platform facies. Under the Ti Valley area, the platform facies may be more than 28,000 ft below the surface. Possible basal Atoka units such as the Spiro may be only 12,000–13,000 ft deep in stacked thrust sheets. A basal Atoka sandstone correlated with the Spiro by C. Stone (personal communication, 2004) occurs in the overlying synform north and west of Shut-In Mountain.

The geology at, and south of, Shut-In Mountain is highly simplified and based on surface mapping, with the idea that a core of reactivated, thrustured basement rocks and Ozark facies strata underlie thrustured, far-traveled, coeval basinal strata of the Ouachita facies. Shut-In Mountain itself may be a structural window of the core of a duplex under the Horseshoe Mountain Synform. It is composed of Jackfork Group strata flanked by Johns Valley Formation and lower Atoka strata. Arbenz (personal communication, 2003) considers this area to be a partially exhumed triangle zone. Fourche and Rich Mountains are masses of Jackfork Group sandstones carried northward on thrusts in the Stanley Group. Complexly faulted, steep-dipping Stanley Group units northeast of Mena are truncated by a low-angle fault that bounds the Rich Mountain Syncline. The cross section shows an interpretation of the low-angle fault as roof to a duplex of Stanley and older units at depth. Around Mena, major thrusts bring Stanley and older core-zone basinal facies to the north. At the south end, the section shows the Arkansas Novaculite thrust to the surface—the southern facies of the Novaculite, out of place, apparently thrust over the northern facies not exposed in this location (C. Stone, personal communication, 2004). Geologic map patterns in the Mena area and south are suggestive of folded thrusts and duplexes in the cover rocks.

### COMPARISON WITH OKLAHOMA CROSS SECTION

The Oklahoma cross section (Roberts, 1994) traverses the area where the frontal Ouachita belt widens north–south. In the Arkoma Basin portion, this cross section and section A (Fig. 2) are similar. Under the south flank of the Backbone Anticline (en echelon to Washburn), the platform facies are 9,000 ft deep. The core of the Backbone Anticline is a thrust that flattens into a detachment in the lower Atoka, which underlies all of the Arkoma

Basin to the south along this line. Under the Choctaw Fault, the platform facies are nearly 20,000 ft deep—somewhat shallower than in the Arkansas section A. Duplexes in the lower Atokan, Morrowan, and Mississippian clastics underlie the detachment in the Heavener Anticline and Choctaw Fault areas. The intra-basement décollement shown by seismic data in eastern Oklahoma was not imaged on the western Arkansas data used in this study, but was seen on other Arkansas data. Presence of the décollement is indicated by the apparent reactivation of a basement normal fault to a reverse fault under the Mansfield area (section A) and another under the Poteau–Pilot Knob Syncline (Fig. 3).

Unlike the Arkansas seismic data, the Oklahoma data carried and could be interpreted far south of the frontal Choctaw and Ti Valley Faults. The data indicated that the detachment in the lower Atoka seen under the Arkoma Basin continues under the Choctaw, Ti Valley, Briery, and Windingstair Faults almost as far as Big Cedar (where the data end). It appears to form a roof fault for duplexes of lower Atoka and older units, as is seen under the Choctaw Thrust fan. This detachment rests nearly 16,000 ft under the Briery Fault trace, where the platform facies strata lie approximately 26,000 ft below the surface. South of the Choctaw Fault fan, the Ti Valley sheet carries thrustured and folded Jackfork–Johns Valley and lower Atoka rocks; the Briery and Windingstair Faults bring Stanley and Jackfork rocks to the north. For more than 15 mi south of the seismic line, the surface geology reveals thrustured Stanley Group and broad synclines of Jackfork Group. Regional map relationships indicate that these synclines are underlain by detachments separating them from duplexes of Stanley and older Ouachita basinal facies. These detachments were omitted from an earlier published cross section (Roberts, 1994), but a deeper detachment was shown that carried the basinal facies northward over the coeval platform. The south end of section A, however, is in the core duplex region that appears to plunge westward under the more gently deformed Stanley–Jackfork units of eastern Oklahoma.

### CROSS SECTION B

Section B (Fig. 3) is drawn, as described for section A (Fig. 2), as a representation in time of the geology along CGG lines 6 and 1, with an offset southward continuation using the surface information of Haley and Stone (1995). This cross section (Fig. 3) also begins at the Washburn Anticline, but between Greenwood and Booneville, Arkansas. In this location the anticline is a little broader but exhibits similar core thrusts, which merge into a detachment surface in the lower Atoka. A second, shallower detachment—also in the lower Atoka—is interpreted to the surface on the south limb of the anticline. A large, mainly synclinal area lies between that fault and the Ross Creek Fault, and is detached from the deeper section by the upper detachment fault in the lower Atoka, which dips gently south then rises to be cut off

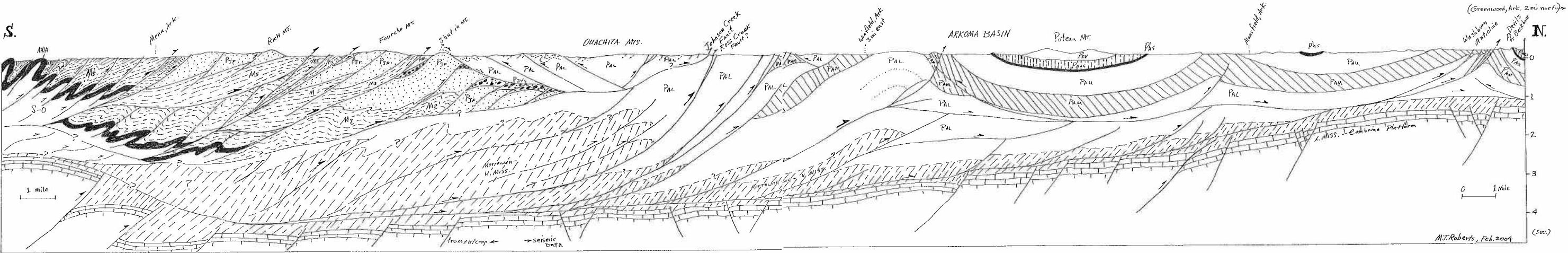


**Figure 2.** Cross section A along CGG seismic line 606 in western Arkansas, with extension south of Mena, Arkansas. I used the COGEOMAP surface geology of Haley and Stone (1995). Abbreviations: S–O = Silurian–Ordovician units; MDa = Arkansas Novaculite;

Ms = Stanley Group; Pjf = Jackfork Group; Pjv = Johns Valley Formation; Pal, Pam, Pau = lower, middle, and upper Atoka Formation; Phs = Hartshorne Sandstone; Pmac = McAlester Formation; Psv = Savanna Formation.

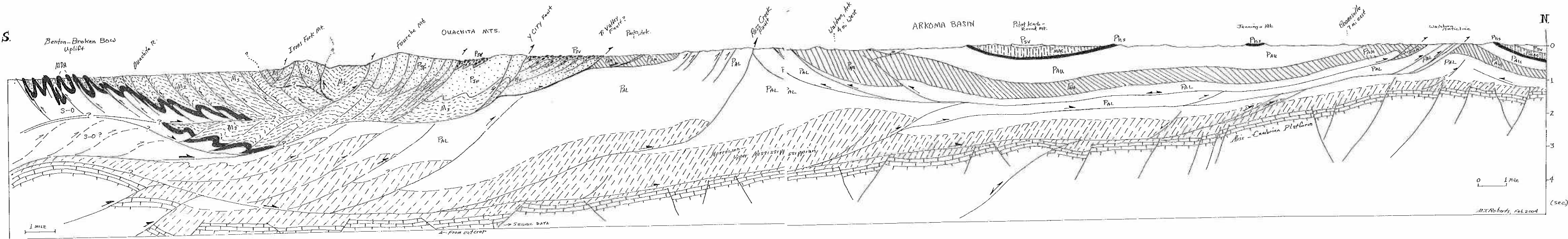


**Figure 3.** Cross section B, along CGG seismic lines 1 and 6 in western Arkansas, with extension south of Y City, Arkansas. I used the

COGEOMAP surface geology of Haley and Stone (1995). Abbreviations same as Figure 2.



by the Ross Creek Fault. An anticline of lower Atoka, Morrowan, and Mississippian strata lies beneath this detachment under the south limb of the Poteau Syncline. As seen in section B (Fig. 3) and in Roberts (1994), the underlying Ozark platform strata are block-faulted and detached from shallower units by a detachment surface in the Mississippian shales. The platform facies appear to be at the same depth (time) under the Ross Creek Fault in both sections A and B (estimated at 27,000 ft).

The structure between the Ross Creek and Ti Valley Faults is much simpler and less compressed in section B than in section A. These sections are nearly 15 mi apart at the Ross Creek trace. To account for the considerable differences between the two requires a tear fault or lateral ramp. At the Ti Valley Fault on section B, the platform is estimated to be 29,000 ft below the surface. The Ti Valley Fault dives to 11,500–12,000 ft on the south end of the seismic line, roughly 3 mi south of its surface trace (approximately a 37° fault-plane dip). The platform facies strata lie 32,000–33,000 ft below the surface at the south end of the seismic line. Thrusted lower Atokan, Morrowan, and Mississippian clastics appear to lie between the Ti Valley sheet and the platform sequence. The seismic data on the south end of this line are more easily interpreted than that of section A.

Using surface geology, section B continues south, offset along the Y City Fault about 8 mi west to the vicinity of Y

City. The section crosses the Mill Creek Anticline and Fourche Mountain, which are north-thrusted masses of Jackfork Group–Johns Valley Formation strata. Stanley strata are thrust northward over the Jackfork on the south flank of Fourche Mountain. Irons Fork Mountain to the south is another block of Jackfork, overthrust by Stanley on its south flank. The relationship between the Irons Fork–Jackfork body and the Stanley strata on its north flank are not as clear (Fig. 4). The contact there may be a folded thrust, an old normal (“growth”) fault carried along by later thrusts, or Irons Fork Mountain may be a window in a folded thrust that connects around it. Section B shows Irons Fork Mountain as a block detached from deeper Stanley units by a folded fault. The structures in the Stanley and older basinal facies rocks south of Irons Fork Mountain are south-verging, small-scale features interpreted as carried along by a large north-directed thrust. Note that this same general region to the west (south end of section A) exhibits north-verging, small-scale structures. A major structural discontinuity must separate these two areas (Fig. 5). Complexly faulted and folded Arkansas Novaculite and older units crop out in the southern part of the Board Camp Quadrangle at the south end of section B. These units are interpreted to overlies duplexes in the early Paleozoic basinal facies, which themselves overlies basement–platform facies duplexes. For more discussion of these relationships, refer

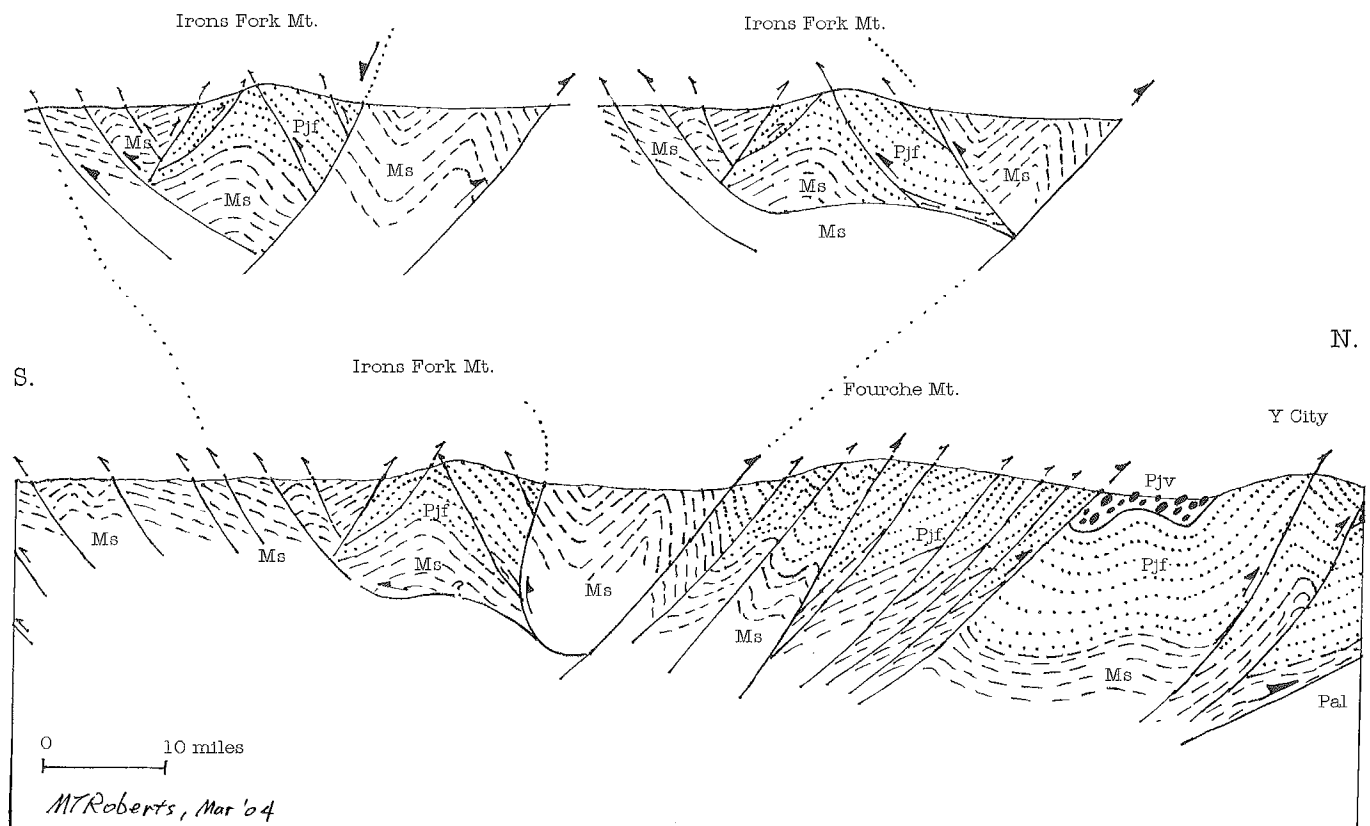


**Figure 4.** Near surface geology in vicinity of Irons Fork Mountain, south of Y City, Arkansas, based on the COGEOMAPS of Haley and Stone (1995). Alternate interpretations of Irons Fork Mountain are shown, and others exist. Abbreviations same as Figure 2.

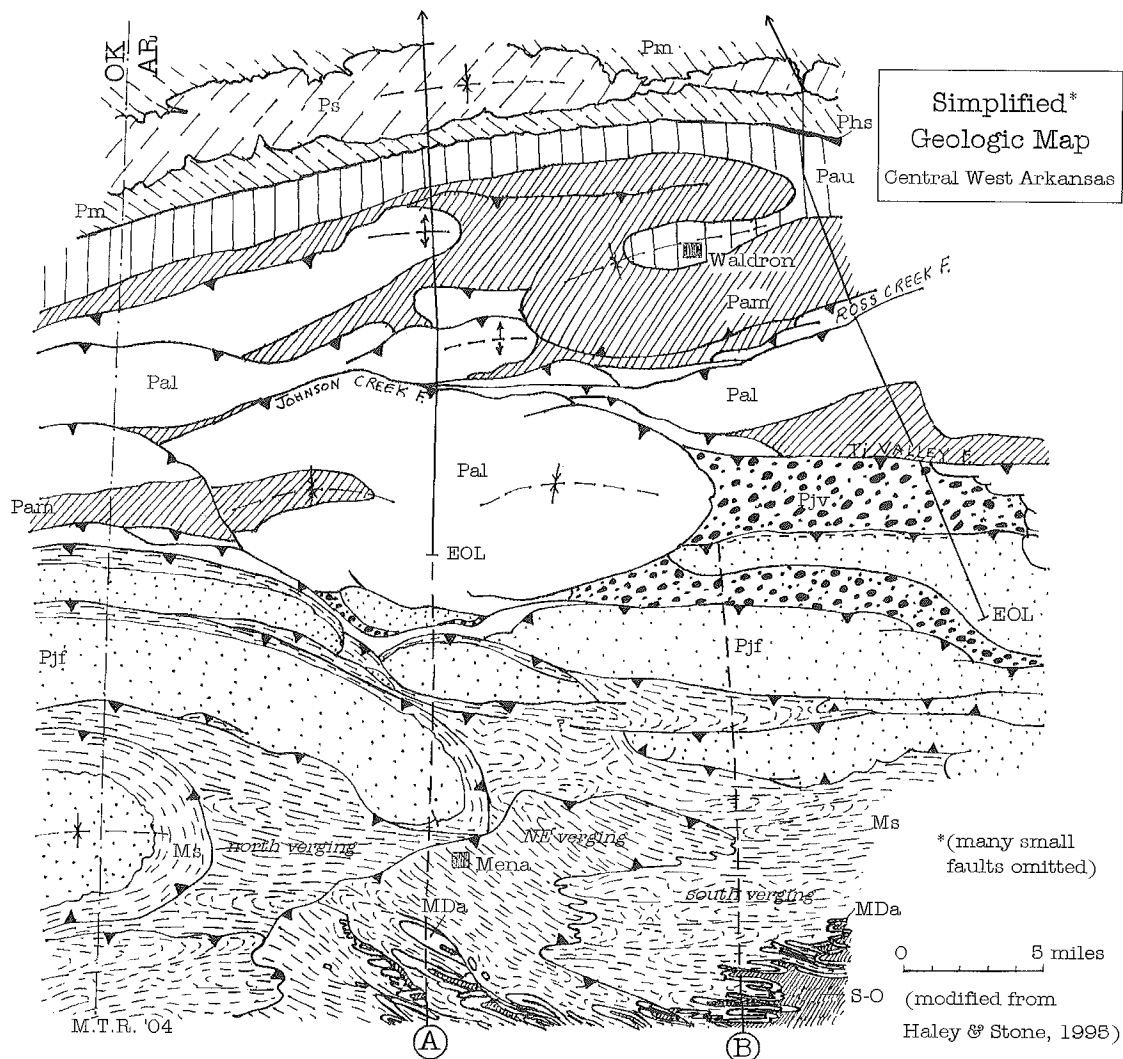


**Figure 5.** Simplified geologic map of central western Arkansas, showing south ends of seismic lines (EOL) used in cross sections A and B. Dashed lines are extensions of cross sections based on surface geology. Abbreviations same as Figure 2 except Pm = McAlester Formation; Ps = Savanna Formation.

to Roberts (1994). The depth to the basement duplexes in this location would only be a wild guess; however, near Broken Bow a well penetrated the basal décollement at nearly 11,700 ft depth and went into shelf facies beneath the overthrust, coeval basinal Ouachita facies rocks. Sections A and B were drawn to mimic that depth relationship.

### MANY UNANSWERED QUESTIONS

The cross sections presented here are not meant to be final products. They illustrate the geologic relationships in the Arkoma Basin and frontal Ouachita Mountains of western Arkansas, as revealed by the interpretation of two regional, multichannel seismic data traverses coupled with the surface geology of Haley and Stone (1995). Many questions remain unanswered. They fall into, but cannot be completely separated by these two

categories: stratigraphic and structural problems. On the stratigraphic list are issues such as

1. The origins of the Johns Valley Formation olistostromal units;
2. The relationship between the Morrowan–Mississippian units under the lower Atoka in the southern Arkoma Basin and the Jackfork–Stanley Groups of the Ouachita Thrust Belt;
3. Palinspastic restorations of the various facies of the Ouachita system;
4. The nature of some contacts in the Ouachitas—faults or unconformities? This question applies to relationships between units above and below the Devonian section, to units above and below the upper Stanley, and to units above and below the lower Atoka. These boundaries

have been traditionally considered to be conformable but tectonized;

5. Details of the paleogeography–depositional environments of the major Ouachita facies.

The structural list identifies issues such as

1. The continuation (or explanation for discontinuities) of the major Oklahoma faults into Arkansas;
2. The nature of relationships around the broad surface synclines of eastern Oklahoma and western Arkansas, which seem to be surrounded by low-angle faults that cut off higher-angle faults (related to #4 on the stratigraphic list);
3. The nature of deep structures in the Benton–Broken Bow Uplift core zone;
4. The stacking pattern of the major thrust sheets to include any possible duplexes or continuation of surface geology to depth;
5. The travel distance of major thrust sheets and original (restored) positions (relates to #3 on the stratigraphic list);
6. The structure of the basement–platform surface in the inner parts of the thrust belt and core zone.

Although these lists are incomplete, they include many key questions. Some of these can be answered by careful construction of balanced sections using computer programs and accurate surface and subsurface (well-log) data. Wells do not exist, however, in many areas important to our understanding, and the interpreter's selection of models still biases one's construction of deep relations.

I am still impressed by the evidence for far travel of the Ti Valley Fault system (e.g., Roberts, 1994) and the need for a regional décollement that separates the Ouachita deep-water facies strata in the thrust belt from the coeval Ozark platform facies strata structurally beneath them. Some workers, however, consider the Oklahoma Ti Valley Fault, per se, to not be as far traveled (N. Suneson, personal communication, 2004). The seismic data also can be interpreted to show a considerable amount of lower Atoka, Morrowan, and Mississippian foredeep-fill clastic strata tucked under the frontal thrusts and Ti Valley sheet, which are not far traveled from their sites of deposition. These lower Atoka through Chesterian clastics were deposited on top of an earlier Mississippian–Cambrian platform sequence that was broken by block faulting, subsided, and was later depressed by foredeep loading of the thrust sheets from the south. These Carboniferous clastic strata are not far traveled, but are the same age as the Stanley–Jackfork–lower Atoka carried far north by the Ti Valley system above them. The thrust sheets that carry

the basal Devonian and older strata over the coeval platform strata are the most far-traveled thrust sheets. Refer to Arbenz (1989) and Roberts (1994) for a more detailed discussion of the geologic history of the area.

## REFERENCES CITED

- Arbenz, J. K., 1984, A structural cross section through the Ouachita Mountains of western Arkansas, *in* Stone, C. G.; and Haley, B. R. (eds.), A guidebook to the geology of the central and southern Ouachita Mountains, Arkansas: Arkansas Geological Commission Guidebook 84-2, p. 76–84.
- , 1989, The Ouachita System, *in* Bally, A. W.; and Palmer, A. R. (eds.), The geology of North America—an overview: Geological Society of America, Boulder, Colorado, The Geology of North America, v. A., p. 371–396.
- Briggs, Garrett; and Roeder, D. H., 1975, Sedimentation and plate tectonics, Ouachita Mountains and Arkoma Basin, *in* Briggs, Garrett; McBride, E. F.; and Miola, R. J. (eds.), Sedimentology of Paleozoic flysch and associated deposits, Ouachita Mountains–Arkoma Basin, Oklahoma: Dallas Geological Society, p. 1–22.
- Haley, B. R.; and Stone, C. G., 1995, COGEOMAPs, Ouachita Mountains and Arkoma Basin, Arkansas: Arkansas Geological Commission, 178 7.5' (1:24,000) open-file sheets.
- Lillie, R. J.; Nelson, K. D.; deVoogd, Beatrice; Brewer, J. A.; Oliver, J. E.; Brown, L. D.; Kaufman, Sidney; and Viele, G. W., 1983, Crustal structures of Ouachita Mountains, Arkansas: a model based on integration of COCORP reflection profiles and regional geophysical data: American Association of Petroleum Geologists Bulletin, v. 67, p. 907–931.
- Roberts, M. T., 1994, Geologic relations along a regional cross section from Spavinaw to Broken Bow, eastern Oklahoma, *in* Suneson, N. H.; and Hemish, L. A. (eds.), Geology and resources of the eastern Ouachita Mountains frontal belt and southeastern Arkoma Basin, Oklahoma: Oklahoma Geological Survey Guidebook 29, p. 137–160.
- Viele, G. W., 1979, Geologic map and cross section, eastern Ouachita Mountains, Arkansas: Geological Society of America Map and Chart Series MC-28F.
- Wickham, John, 1977, Interpretation of the Ouachita Mountains, Oklahoma, *in* 29th annual field conference guidebook: Wyoming Geological Association, Casper, Wyoming, p. 523–530.
- Zimmerman, Jay; Roeder, D. H.; Morris, R. C.; and Evansin, D. P., 1982, Geologic section across the Ouachita Mountains, western Arkansas: Geological Society of America Map and Chart Series MC-28-Q.



## Enhanced Structural Interpretation in the Arkoma Basin with Seismic Attributes

*Surinder Sahai*

Hess Corporation  
Houston, Texas

*Ibrahim Çemen*

Oklahoma State University  
Stillwater, Oklahoma

**ABSTRACT**—The Ouachita Mountains in southeastern Oklahoma and western Arkansas have been the subject of intense geological work for the past two decades primarily because of their hydrocarbon potential, as well as that of the Arkoma Basin. In addition to petrophysical work, several structural studies have been conducted to generate balanced cross sections from available surface geological maps and from subsurface data such as well logs and seismic.

The seismic data used in previously published studies was acquired in the 1970s and 1980s and is of marginal quality. The technical advances achieved in seismic acquisition and processing in the last two decades now make it possible to acquire better data in complex areas. An analysis of a recently acquired seismic line in the Wilburton Gas Field of the Arkoma Basin clearly shows the thrusting of the Spiro sandstone that has been used as a key-bed in past estimates of structural shortening in the area. Seismic attributes, such as instantaneous amplitude, add another dimension to the interpretation by providing glimpses of subtle faulting previously unseen in seismic data from the Arkoma Basin.

We used seismic attributes of the Spiro sandstone to determine shortening in the footwall of the Choctaw Fault as a result of Pennsylvanian thrust faulting. We found that the Spiro has shortened about 21%. This is much lower than the shortening determined along the structural cross sections traversing the hanging wall of the Choctaw Fault zone. Therefore, we suggest that much of the shortening in the frontal Ouachitas–Arkoma Basin transition zone must have occurred along the Choctaw Fault zone.

### INTRODUCTION

The Arkoma Basin in southeastern Oklahoma and western Arkansas is a foreland basin formed as a result of the Ouachita orogeny during the Pennsylvanian (Fig. 1). The Arkoma Basin has been the subject of intense geological work for the past two decades. The intensity of exploration and production activity in the basin has recently accelerated as a result high gas and oil prices. The Wilburton and Hartshorne Gas Fields of the central Arkoma Basin (Fig. 2) produce gas mostly from sandstones of the Atokan and Desmoinesian age. Figure 3 shows the general stratigraphy of Atokan and Desmoinesian strata. The lower Atokan Spiro sandstone is one of the most prolific reservoirs in the two fields. It has a distinct log signature and is a strong reflector in the seismic data.

As in all fold–thrust belts, such as the Canadian Rockies, the Alps, and the Himalayas, deformation in the Ouachita Mountains grades from the strongly deformed frontal belt into mildly deformed foreland within an area usually referred to as the “transition zone.” The Choctaw Fault is the leading-edge thrust of the frontal Ouachitas and is the structural boundary between the Ouachita Mountains and the Arkoma Basin in Oklahoma. Therefore, the Choctaw Fault and associated structures define the transition zone in the Ouachita Mountains.

The geometry of thrust faulting in the frontal Ouachitas–Arkoma Basin transition zone has been controversial. Suneson (1995) summarized several structural interpretations dealing with this geometry. Several of the studies proposed the presence of a triangle zone with a backthrust (Hardie, 1988; Camp and Ratliff, 1989; Reeves and others, 1990; Milliken, 1988; Perry and Sune-

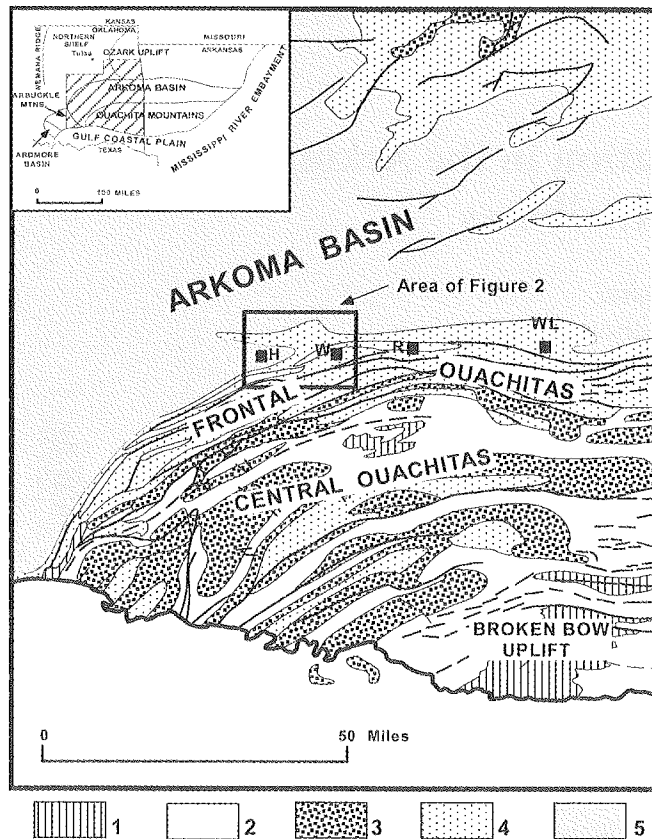


**Figure 1.** Simplified geologic map of the Ouachita Mountains in southeastern Oklahoma. The insert on the top left shows the major geologic provinces of eastern Oklahoma and western Arkansas. Explanation: (1) Early and middle Paleozoic (Cambrian through Early Mississippian); (2) Middle and late Mississippian (Stanley Group of Ouachita facies); (3) Morrowan (Jackfork Group and Johns Valley Formation of Ouachita facies); (4) Atokan (Spiro–Wapanucka, and Atoka Formations of the frontal Ouachitas and Arkoma Basin); (5) Desmoinesian (Hartshorne, McAlester, Savanna, and Boggy Formations of the Krebs Group of the Arkoma Basin). Abbreviations: H = Hartshorne; W = Wilburton; and WL = Wister Lake (modified from Johnson, 1988; Arbenz, 1989; and Çemen and others, 2001a).

son, 1990; Wilkerson and Wellman, 1993; Valderrama and others, 1994). Some workers have suggested that all the thrust faults in the transition zone are south-dipping (Bertagne and Leising, 1989; Tilford, 1990) and therefore there is no triangle zone.

During the mid to late 1990s, the sedimentology of the Spiro sandstone and the structural geology of the Wilburton Gas Field area were studied by a group at Oklahoma State University's School of Geology. By using available surface and subsurface data, the group constructed many balanced structural cross sections and concluded that a well-developed triangle zone and a duplex

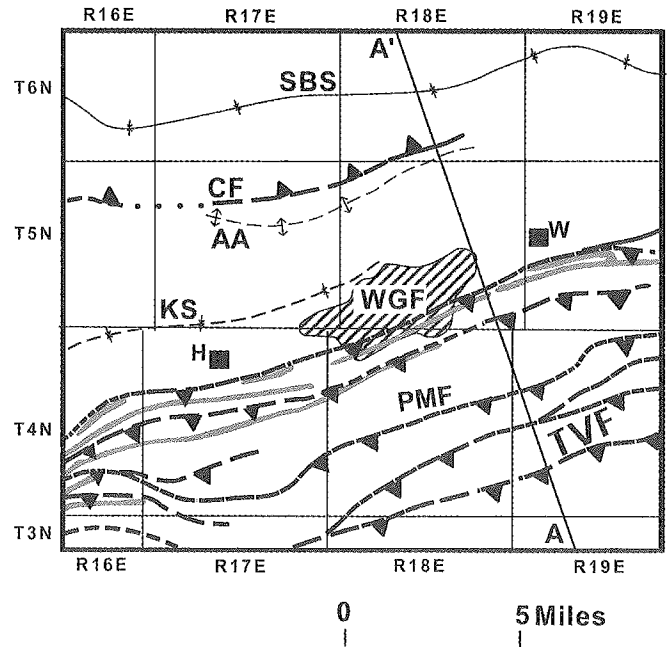


**Figure 2.** Simplified map of the Wilburton Gas Field and surrounding areas, showing major structural features, the outcrops of the Spiro sandstone (dotted pattern), and the line of cross section A–A'. Abbreviations: H = Hartshorne; W = Wilburton; AA = Adamson Anticline; CF = Carbon Fault; KS = Kiowa Syncline; PMF = Pine Mountain Fault; SBS = San Bois Syncline; TVF = Ti Valley Fault; WGF = Wilburton Gas Field (modified from Çemen and others, 2001b).

structure exists in the Wilburton Gas Field area (Çemen and others, 2001a, b). One such cross section is shown in Figure 4.

Recently acquired seismic data in the Arkoma Basin is of much better quality than the data previously available for structural interpretation. The improvement in acquisition and processing technology is primarily responsible for better quality data. Figure 5 shows a seismic line oriented approximately perpendicular to the major thrust faults in the frontal Ouachitas. This line was extracted from a 3-D volume and clearly shows major seismic reflectors, including the Spiro sandstone, which was previously used by Çemen and others (2001a, b) and Hadaway and Çemen (2005) as the key bed in their structural restorations.

In this paper, we show that seismic attributes can further enhance the utility of available seismic data for structural interpretation in the Arkoma Basin. We use seismic-attribute data to better understand the structural geometry of the duplex structure in the footwall of the Choctaw Fault zone in the Wilburton Gas Field area. We also restore the seismic line to the “time” of the Spiro deposition to calculate a shortening in the footwall of the Choctaw Fault zone following the Spiro deposition in the Early Pennsylvanian.

PENNSYLVANIAN	DESMOINESIAN	Marmaton Group Cabiness Group	
		Krebs Gp.	Boggy Fm. Savanna Fm. McAlester Fm. Hartshorne Fm.
	ATOKAN	Atoka Fm. Red Oak ss. Panola ss. Cecil ss. Spiro ss.	
	MOR.	Wapanucka Ls. Springer Fm.	

Figure 3. Pennsylvanian stratigraphy of Oklahoma portion of the Arkoma Basin (modified from Çemen and others, 2001a).

### SEISMIC ATTRIBUTES

A seismic attribute is a property of recorded seismic data that leads to a better understanding of subsurface geology. For example, one of the basic attributes of seismic data is the seismic amplitude. From the early history of seismic interpretation, geophysicists have mapped the amplitude of seismic data for geological interpretation. In the past two decades, the amplitude attribute and its variations have been used in innovative ways to extract better information about the lithology, fluid content, and other physical properties of rocks. The well-known amplitude-versus-offset (AVO) analysis is one example of an application that relies on amplitude-derived attributes of intercept and gradient. In general, the use of seismic attributes in the petroleum industry has increased considerably in the last few years. Brown (2001) lists over 70 attributes related to seismic data. As pointed out by Brown (2001), however, many of these attributes are not independent but derived from the basic seismic attributes of amplitude, frequency, phase, and attenuation. An understanding of the derivation of a seismic attribute is essential for determining whether it makes sense for a particular application (Sheline, 2005).

In the 1970s and early 1980s, the attributes of amplitude, frequency, and phase were used for stratigraphic and structural interpretation. These attributes are collectively referred to as “instantaneous attributes” (White, 1991) because, mathematically speaking, they can be calculated at any time-sample point in the seismic data from the complex trace representation of a seismic

trace. For example, the complex trace representation  $F(t)$  of a real time-series  $f(t)$  is given by,

$$F(t) = A(t) e^{i\gamma(t)}$$

where  $A(t)$  is the instantaneous amplitude and  $\gamma(t)$  is the instantaneous phase (Sheriff, 2002). The instantaneous frequency can be calculated from the time-derivative of  $\gamma(t)$ .

The instantaneous amplitude is also known as the envelope of the seismic trace and can be thought of as the low-frequency representation of the trace (Fig. 6). Taner and Sheriff (1977) provide examples of how the instantaneous amplitude and other basic attributes can be used to enhance interpretation of seismic data. Brown (1999) shows an example of the use of instantaneous amplitude in interpreting seismic data when the phase of the data is unknown.

### SEISMIC DATA FROM ARKOMA BASIN

Figure 5 shows an arbitrary seismic line pulled from a three-dimensional migrated volume of data acquired in the Arkoma Basin. The line is oriented approximately perpendicular to the main faults such as the Choctaw Fault in the frontal Ouachitas and is located in Latimer County (Oklahoma) west of the Wilburton Gas Field. The southeast end of the line barely crosses the south-dipping Choctaw Fault; hence, the fault is not fully visible in the seismic data. The northwest end of the seismic line is close to the Carbon Fault but does not cross it. The continuity of reflectors in the shallow section is quite good except toward the southeast portion of the line where the reflectors are chaotic. This could be the result of the lateral velocity variations in the vicinity of the high-angle Choctaw Fault where the older rocks in the hanging wall of the fault are in contact with the lower-velocity strata in the footwall of the fault. Therefore, proper migration of the shallow section is difficult to achieve without high-effort static corrections and a good velocity model.

The section between 0.8 sec and 1.6 sec shows good reflectors throughout the length of the line but the effect of the thrust from the southeast is quite evident. This time interval contains the middle Atokan Red Oak and Brazil sandstones which are good producers of hydrocarbons in the Arkoma Basin. The section below this interval is the lower Atokan shale and is devoid of good reflectors. This is because the sands within the lower Atokan shale are thin (Çemen and others, 2001b) and thus below the detection limit of the seismic data. The thickening and thinning of the shale is probably the result of deformation because of thrusting.

The lower Atokan Spiro sandstone is a very strong reflector and is at a depth of 1.6 sec and 2.2 sec in the seismic data shown in Figure 5. This is the result of its sharp seismic impedance contrasting with the overlying shale. The Spiro has been used as a key bed for calculating percent shortening in the Ouachitas (Çemen and others, 2001a, b; Hadaway and Çemen, 2005). Because of structural complexity resulting from thrusting, however, the

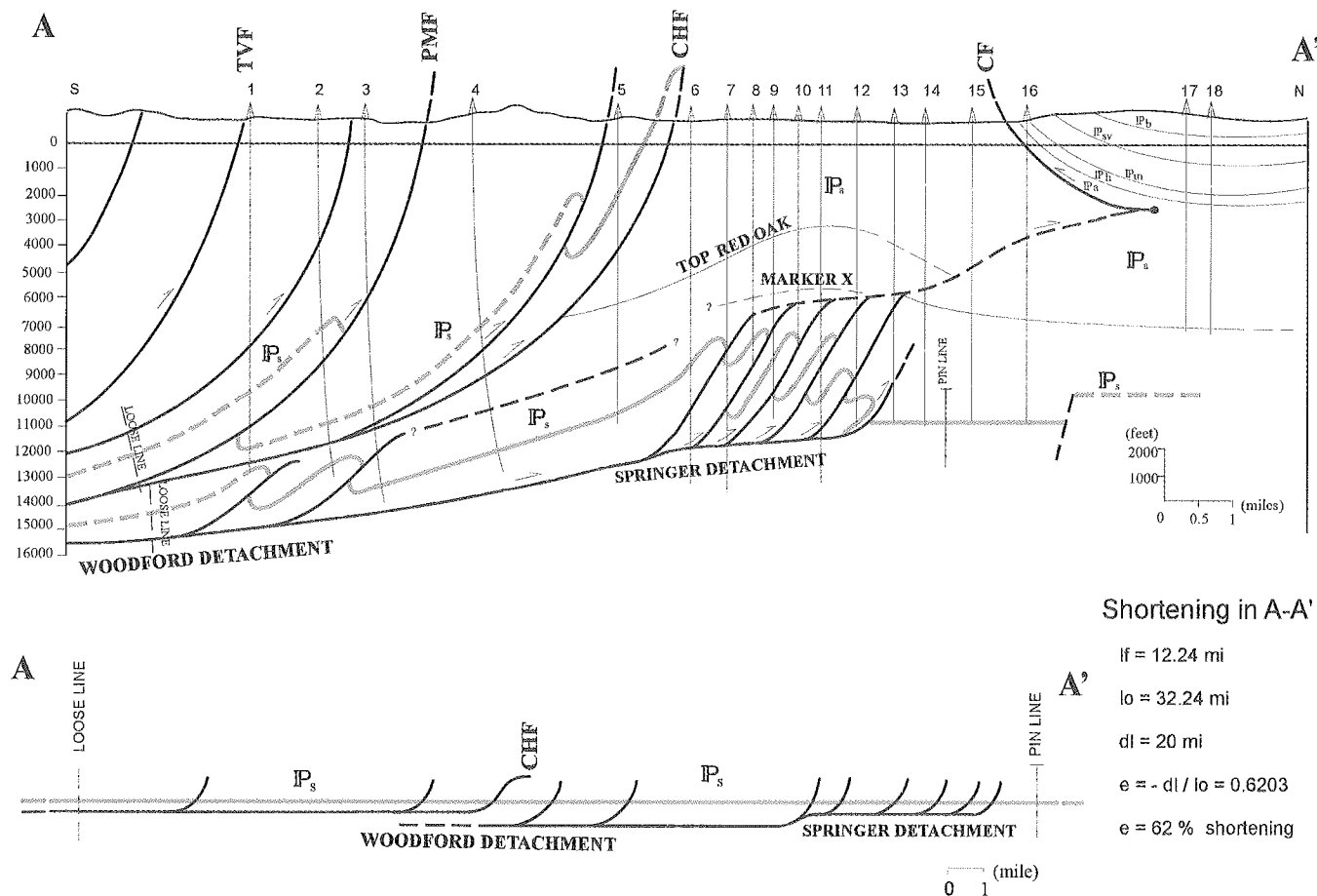


**Figure 4.** Cross section A-A' and its restoration. The cross section shows the presence of the Wilburton triangle zone, duplex structure, and other structural features in the Wilburton area. Line of cross section is located on Figure 2. The restored cross section suggests 62.03% shortening along the original length of the Spiro sandstone due to Pennsylvanian thrusting in the area. See text for explanation. Abbreviations: If = final length; lo = original length; dl = difference between original and final lengths; e = extension; CF = Carbon Fault; CHF = Choctaw Fault; LAD = Lower Atokan Detachment; PMF = Pine Mountain Fault; Pa = Atoka Formation; Ph = Hartshorne Sandstone; Pm = McAlester Formation; Ps = Spiro sandstone; Psv = Savanna Sandstone; TVF = Ti Valley Fault (from Çemen and others, 2001b).

extent of the Spiro sandstone is not easy to see in the seismic data shown in Figure 7. In order to improve interpretation of the lower Atokan section, some of the basic seismic attributes were examined using the Kingdom Suite® software (Seismic Micro-Technology Inc., Houston, Texas). The instantaneous amplitude, or envelope, of the seismic trace seemed to work best in providing enhanced structural detail not only in the lower Atokan section, but throughout the seismic section (Fig. 7). For example, in the shallow section consisting of the Brazil and Red Oak sandstones, the clarity of the faults is much improved, giving a better picture of the structural development of the upper and middle Atokan strata than when using the previously available seismic data (Çemen and others, 1994).

## STRUCTURAL GEOLOGY

Based on the available surface and subsurface data of the mid to late 1990s, Çemen and others (2001a,b) determined that the Wilburton Gas Field area contains a well-developed triangle zone between the mildly compressed Arkoma Basin and frontal Ouachita fold-thrust belt (Fig. 4). The triangle zone is located in the footwall of the Choctaw Fault and is flanked by that fault to the south and the Carbon Fault to the north. The hanging wall of the Choctaw Fault contains several south-dipping, imbricate fan thrust faults. A duplex structure is present in the footwall of the Choctaw Fault zone. It contains hinterland-dipping imbricate thrust faults splaying, in a break-forward sequence of thrusting, from the Springer Detachment (Fig. 4). The imbricate thrusts join a detachment surface in the Atoka Formation (Fig. 4) named the Lower Atokan Detachment (LAD) by Çemen and others (2001b). The

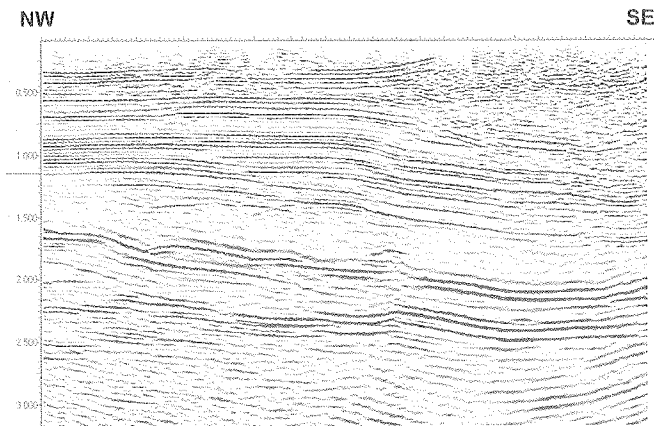


**Figure 5.** A seismic line taken from the 3-D volume of seismic data. The line is oriented approximately 20° west of north. The vertical scale is two-way time in seconds. The Spiro sandstone is a strong reflector imaged at about 1.6 sec. in the northwest corner of the line.

detachment displaces the middle Atokan Red Oak sandstone before reaching a shallower depth and forming the Carbon Fault as a north-dipping backthrust below the San Bois Syncline (Figs. 2, 4).

The cross sections by Çemen and others (2001a, b) were restored by using the key-bed restoration method in order to find the percentage of shortening that was experienced as a result of Pennsylvanian thrusting. When restored to their position at the time of the Spiro sandstone deposition, the cross sections suggested about 60% shortening in the area extending from the Ti Valley Fault to the south and the Carbon Fault to the north (Fig. 4).

In this paper, we have restored a seismic line by using seismic attributes of the Spiro sandstone in the footwall of the Choctaw Fault zone. The section suggests a 21% shortening based on the seismic line studied. This is a much smaller shortening than reported in the Ouachita Thrust Belt system by many previous studies, including Çemen and others (2001a, b) and Hadaway and Çemen (2005) along the cross sections that extended from the San Bois Syncline southward to the hanging wall of the Ti Valley Fault zone (Fig. 4). Recently, Collins (2006) has restored the cross sec-

tions in the footwall of the Choctaw Fault zone in the area east of the town of Wilburton. She found that the shortening in the footwall of the Choctaw Fault zone ranges from 26% to 30% along her cross sections. Our study, together with Collins (2006), suggests that much of the shortening in the Ouachita Fold-Thrust Belt occurs south of the Choctaw Fault where the Spiro strata have been thrust up to the surface and are exposed in outcrops.

## SUMMARY AND CONCLUSIONS

The instantaneous amplitude attribute of the seismic data is a powerful tool for mapping the key-bed Spiro sandstone. Thus, the amount of shortening in the Arkoma Basin can be easily calculated directly from the seismic section. The shortening of 21% obtained from newly acquired seismic data in the basin is much less than the previously reported shortening in the Ouachita Thrust Belt region. The cross sections reported in previous studies, however, extended southward to the Ti Valley Fault zone. Therefore, much of the shortening as a result of thrusting in the Ouachitas occurred to the south of the hanging wall of the Choctaw Fault.

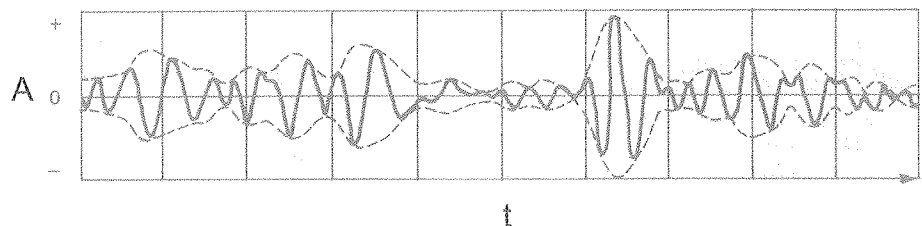


**Figure 6.** A seismic trace and its envelope. The solid line is the seismic trace; the dashed line is the envelope (modified from Sheriff, 2002). Abbreviations: A = amplitude; t = time.

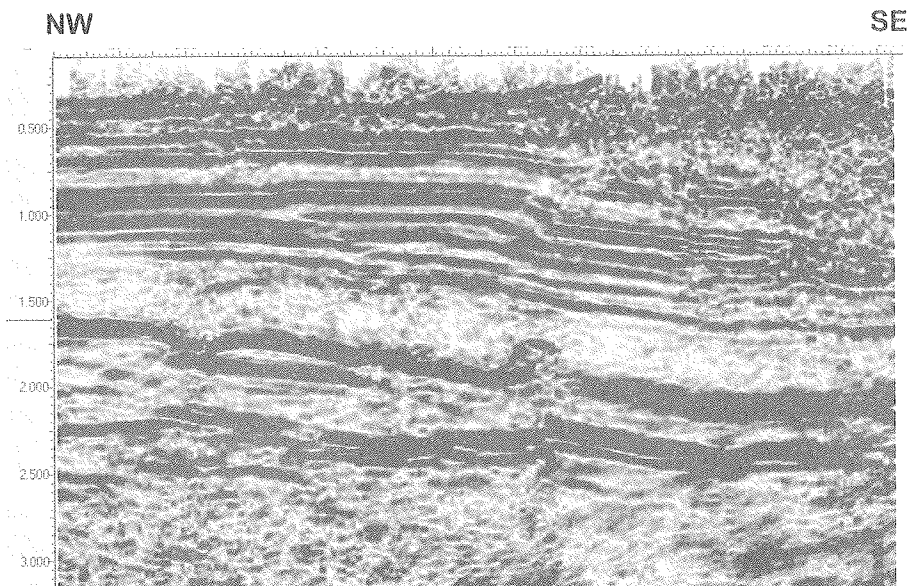


**Figure 7.** The instantaneous amplitude (envelope) of the seismic data shown in Figure 5. The vertical scale is two-way time in seconds.

## ACKNOWLEDGMENTS

Devon Energy supplied the seismic data used in this study, as well as a grant supporting the work. The authors are grateful for Devon's support and their permission to publish the data. We are thankful to Seismic Micro-Technology Inc. for providing the Kingdom Suite® software used in the study. Steve Hadaway assisted us with the illustrations.

## REFERENCES CITED

- Arbenz, J.K., 1989, The Ouachita System, *in* Bally, A.W., and Palmer, A.R. (eds.), *The geology of North America—an overview*: Geological Society of America, Boulder, Colorado, p. 371–396.
- Bertagne, A.J.; and Leising, T.C., 1989, Seismic exploration of Ouachita frontal fairway, southeastern Oklahoma: *Oil & Gas Journal*, v. 87, no. 4, p. 88–90.
- Brown, A.R., 1999, Interpretation of three-dimensional seismic data: *American Association of Petroleum Geologists Memoir* 42, 514p.
- Brown, A.R., 2001, Understanding seismic attributes: *Geophysics*, v. 66, p. 47–48.
- Camp, W.K.; and Ratliff, R.A., 1989, Balanced cross-section through Wilburton Gas Field, Latimer County, Oklahoma: implications for Ouachita deformation and Arbuckle (Cambro-Ordovician) exploration in Arkoma Basin (abstract): *American Association of Petroleum Geologists Bulletin*, v. 73, p. 1044.
- Çemen, Ibrahim; Al-Shaieb, Zuhair; Feller, Rodney; and Akthar, Saleem, 1994, Preliminary interpretation of a seismic profile and the Spiro reservoir pressure data in the vicinity of the Wilburton Gas Field: *Oklahoma Geological Survey Guidebook* 29, p. 249–251.
- Çemen, Ibrahim; Evans, Justin; and Sagnak, Ata, 2001a, Eastern continuation of the Wilburton triangle zone in the Red Oak Gas Field area, frontal Ouachitas–Arkoma Basin transition zone, southeastern Oklahoma, *in* Johnson, K.S., and Merriam, D.F. (eds.), *Petroleum systems of sedimentary basins in the southern Midcontinent*, 2000 symposium: *Oklahoma Geological Survey Circular* 106, p. 81–95.
- Çemen, Ibrahim; Sagnak, Ata; and Akthar, Saleem, 2001b, Geometry of the triangle zone and duplex structure in the Wilburton Gas Field area of the Arkoma Basin, southeastern Oklahoma: *Oklahoma Geological Survey Circular* 104, p. 87–98.
- Collins, M.R.H., 2006, Geometry of late Paleozoic thrusting, Wilburton and Damon quadrangles, Arkoma Basin, southeast Oklahoma: *Oklahoma State University*, unpublished M.S. thesis, 84p.
- Hadaway, Steve; and Çemen, Ibrahim, 2005, Tear faulting and compartmentation for gas production in Southwest Hartshorne Gas Field, Arkoma Basin, southeast Oklahoma: *Shale Shaker*, v. 55, p. 101–111.
- Hardie, W.E., 1988, Structural styles of the frontal thrust belt of the Ouachita Mountains, southern Pittsburg County, Oklahoma: *Oklahoma Geology Notes*, v. 48, p. 232–246.
- Johnson, K.S., 1988, General geologic framework of the field-trip area, *in* Johnson, K.S. (ed.), *Shelf-to-basin geology and resources of Pennsylvanian strata in the Arkoma Basin and frontal Ouachita Mountains of Oklahoma*: *Oklahoma Geological Survey Guidebook* 25, p. 1–5.
- Milliken, J.V., 1988, Late Paleozoic and early Mesozoic geologic evolution of the Arklatex area: *Rice University*, unpublished M.S. thesis, 259p.
- Perry, W.J., Jr.; and Suneson, N.H., 1990, Preliminary interpretation of a seismic profile across the Ouachita frontal zone near Hartshorne, Oklahoma: *Oklahoma Geological Survey Special Publication* 90-1, p. 145–148.
- Reeves, D.L.; Schreiner, W.P.; and Sheffield, T.M., 1990, Stop 6–New State Mountain (Amoco 1-5 Rosso Unit): *Oklahoma Geological Survey Special Publication* 90-1, p. 37–40.
- Sheline, Hans, 2005, Don't abuse seismic attributes: *American Association of Petroleum Geologists Explorer*, v. 26, p. 22–23.
- Sheriff, R.E., 2002, *Encyclopedic dictionary of applied geophysics*, 4th edition: *Society of Exploration Geophysicists*, 429p.
- Suneson, N.H., 1995, Structural interpretations of the Arkoma Basin - Ouachita Mountains transition zone, southeastern Oklahoma: a review, *in* Johnson, K.S. (ed.), *Structural styles in the southern Midcontinent*, 1992 symposium: *Oklahoma Geological Survey Circular* 97, p. 259–263.
- Taner, M.T.; and Sheriff, R.E., 1977, Application of amplitude, frequency and other attributes to stratigraphic and hydrocarbon determination, *in* Payton, C.E. (ed.), *Seismic stratigraphy—applications to hydrocarbon exploration*: *American Association of Petroleum Geologists Memoir* 26, p. 301–327.
- Tilford, M.J., 1990, Geological review of the Ouachita Mountains Thrust Belt play, western Arkoma Basin, Oklahoma: *Oklahoma Geological Survey Special Publication* 90-1, p. 169–196.
- Valderrama, M.H.; Nielsen, K.C.; McMechan, G.A.; and Hunter, Holly, 1994, Three-dimensional seismic interpretation of the triangle zone of the frontal Ouachita Mountains and Arkoma Basin, Pittsburg County, Oklahoma: *Oklahoma Geological Survey Guidebook* 29, p. 225–241.
- White, R.E., 1991, Properties of instantaneous seismic attributes: *The Leading Edge*, v. 10, no. 7, p. 26–32.
- Wilkerson, M.S.; and Wellman, P.C., 1993, Three dimensional geometry and kinematics of the Gale-Buckeye thrust system, Ouachita fold and thrust belt, Latimer and Pittsburg Counties, Oklahoma: *American Association of Petroleum Geologists Bulletin*, v. 77, p. 1082–1100.

# Panola Field

## Multiple Atoka Sandstone Gas Reservoirs in T. 5 N., RS. 19–20 E. Latimer County, Oklahoma

*Richard D. Andrews*  
Oklahoma Geological Survey  
Norman, Oklahoma

**ABSTRACT**—The purpose of this paper is to interpret the nature of faulting and to identify sandstone distribution patterns, depositional environments, and hydrocarbon trapping mechanisms of Atoka sandstones in Panola Field. The study offers general information but is more detailed than a typical regional study. In this respect, the paper should be valuable for delineating reservoir trends, thicknesses, production characteristics, hydrocarbon trapping mechanisms, structural styles, and fault displacements.

The study encompasses the entire areal extent of producing Atoka reservoirs in Panola Field. All subsurface interpretations, thickness determinations, bedding profiles, and reservoir data originate solely from well logs. First, I identified and correlated sandstone intervals in order to recognize fault zones and repeated sections and to compile isopach thickness data. Next, I determined gross and net sandstone thickness values within each sandstone interval using a 50% sand/shale cutoff and 6% porosity cutoff, respectively. I made no attempt to map individual sandstone packages or beds within the major sandstone intervals. Detailed mapping of this nature is possible, however, and is recommended to further enhance the understanding of the reservoirs.

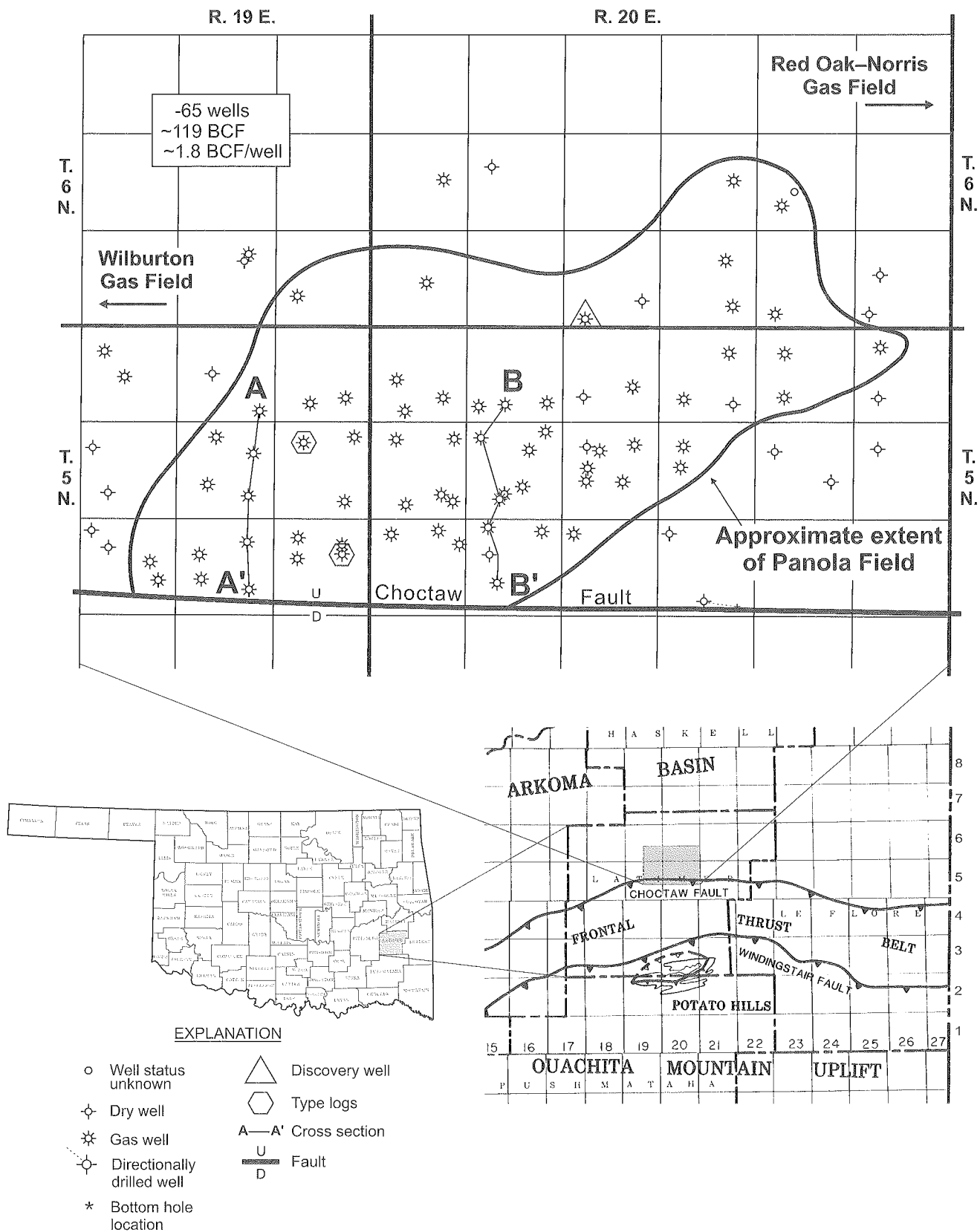
Cumulative gas production is currently ~119 billion cubic feet (BCF) from 65 wells. Gas reservoirs consist of Atokan sandstones that are structurally complex because of folding and high-angle reverse faulting. Gas production is best when sandstones have >6–8% porosity, measure more than 100 ohm-meters ( $\Omega\cdot m$ ) resistivity, and occur in the upper reaches of structural closures. Structurally low areas often have high calculated water saturation. Depleted zones are also encountered because of the proximity of competing wells. Pockets of gas may be extremely small as a result of intense faulting. In plan view, the distribution pattern of sandstone contained in most of the mapped intervals appears sheetlike, elongated, or both. This implies multiple depositional environments. Because of diagnostic bedding characteristics exemplified by a “ratty” or blocky log profile, an interbedded relationship between hundreds or even thousands of feet of low-resistivity shale ( $<\sim 5 \Omega\cdot m$ ), and a lack of terrestrial or shallow-water strata (or both, as interpreted from well logs and basin-rim outcrops), these sandstones probably represent turbidite packages comprised of channel and sheet lobe deposits. Although the thickness of gross sandstone (regardless of porosity) may be many tens or even hundreds of feet, the actual producing reservoir thickness (having a porosity >6–8%) is considerably thinner.

### INTRODUCTION

Panola Field is located along the downthrown northern side of the Choctaw Fault in north-central Latimer County (Fig. 1). The field produces dry gas from several middle and lower Atoka sandstone reservoirs in a structurally complex setting. North-directed high-angle reverse faults result in repetitive beds, increased stratigraphic thicknesses, locally high dip angles, and crustal shortening. The 54-section study area

lies in the south-central part of the Arkoma Basin between the large Red Oak–Norris Field to the east and Wilburton Field to the west.

Cumulative gas production from Panola Field is currently ~119 BCF from 65 wells for an average of ~1.8 BCF per well. Most wells produce from a single reservoir but many wells also have commingled production from two to four different sandstones, repeated sections, or both. From well-log interpretations, many sandstone beds that are not completed appear to have additional gas potential.





Log patterns depicting textural profiles of Atoka sandstone intervals in Panola Field vary considerably. Some have distinct coarsening-upward textural profiles, whereas others

## HISTORY OF EXPLORATION IN PANOLA FIELD

In this study area, the first known well drilled to the Atoka was made by Mobil Oil Company in sec. 33, T. 6 N., R. 20 E. Drilled in 1964, this gas well was completed in the lower Atokan Spiro sandstone. Only a handful of other wells were drilled

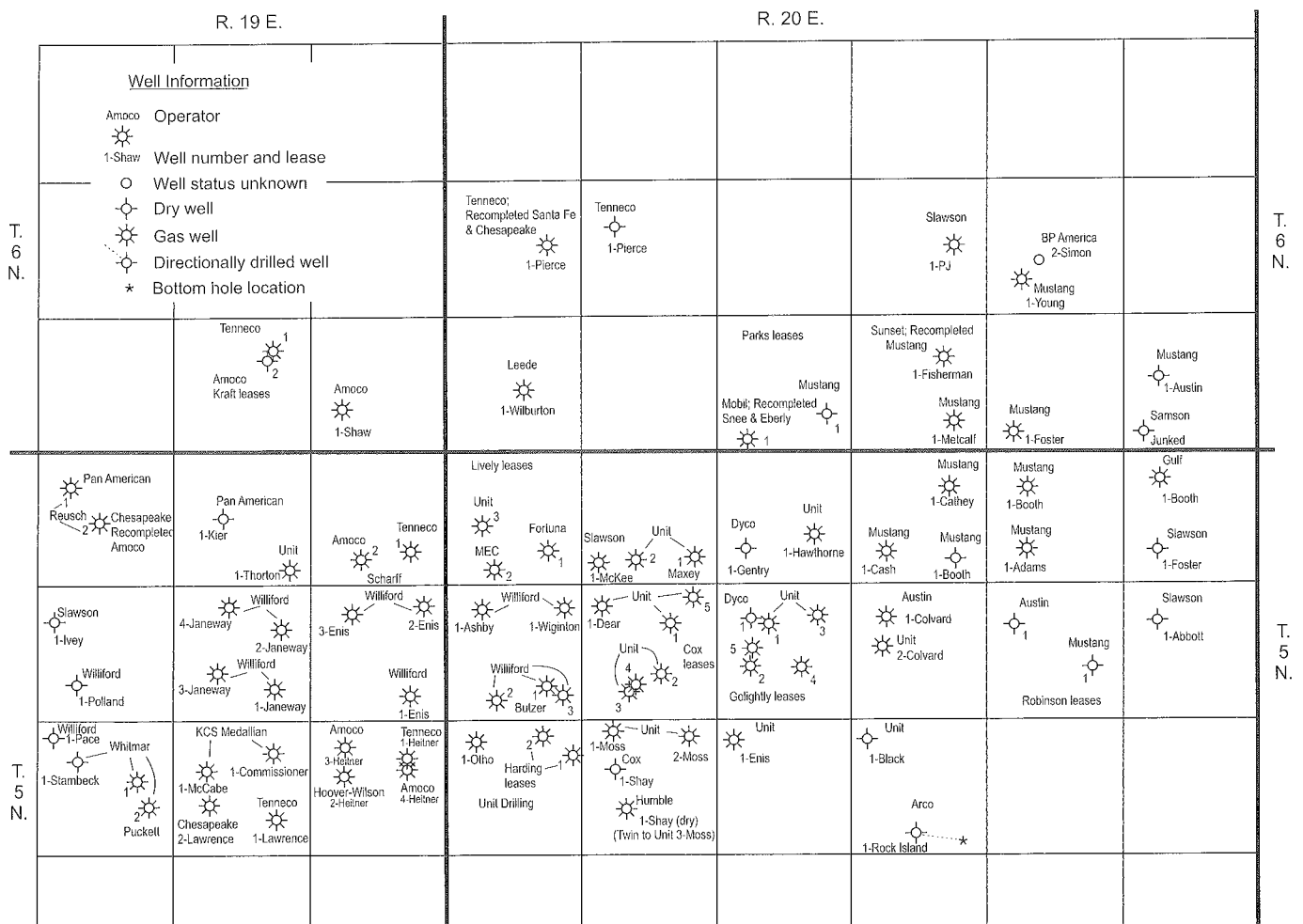


**Figure 2.** Well information map showing operators, well numbers, and lease names in Panola Field, north-central Latimer County, Oklahoma.

to the Atoka in the 1960s. Some wells found additional gas potential in the Spiro but little else in the Atoka. For most of two decades, Panola Field remained essentially undiscovered until the completion of several additional Atoka wells during the 1970s. The main development of this area occurred in the late 1990s and thereafter. Although several companies were active in this field, Unit Petroleum and Williford are currently the principal operators.

## STRATIGRAPHY

Several discrete sandstone intervals are identified in this area of investigation by Suneson and Hemish (1994). The principal reservoirs occur in the middle and lower Atoka and are identified with a ☼ symbol following their names (Fig. 3). These reservoirs are widespread throughout much of the area, yet are not correlative to the surface (the Spiro sandstone being an exception). Therefore, subsurface names with respect to stratigraphic nomenclature are strictly informal.

On a regional scale, identifying the lithologic boundary of the Atoka Formation in the southern part of the Arkoma Basin is theoretically simple—the upper contact lies beneath the Hartshorne Sandstone and the lower contact lies above the Morrowan Wapanucka Limestone. In places this is easy to determine; in others it is not. In deeper parts of the basin, the Atoka is more than 10,000–12,000 ft thick but thins rapidly northward. Most of the formation consists of dark gray to black marine shale with about a dozen discrete sandstone intervals occurring largely in the lower half of the formation (Fig. 3). In this paper, I specifically discuss only those of the middle Atoka. Of note is the fact that some interpretations (as noted on completion reports) alternatively call the Diamond sandstone (of this study) the Red Oak sandstone.

With respect to regional sandstone distribution patterns, the middle Atoka in Panola Field contains relatively thick sandstone sequences as compared to elsewhere in the basin. This includes more than 150 ft of sandstone in both the Bullard and Cecil zones, nearly 100 ft in the Diamond zone, and more than 50 ft in the Panola zone. Much of this sandstone occurs in numerous, relatively thin tabular beds, each separated by shale of approximately the same thickness. Individual sandstone intervals are separated by thick shale sequences several hundreds or thousands of feet thick. The relatively uniform gamma-ray (GR) log signature; consistent, very low resistivity ( $<5 \Omega\cdot\text{m}$ ); and absence of distinctive shallow-marine or terrestrial strata (delta-front sandstone and/or coal) is evidence of deeper marine deposition.

Few wells in the study area penetrate the entire Atoka Formation (i.e., to the Wapanucka Limestone). Consequently, isopach map patterns and reservoir characteristics are less well known for the deepest middle Atoka sandstones.

PENN SYLVANIAN					SYSTEM
MIDDLE		DESMOINESIAN			SERIES
		Hartshorne	McAlester	FORMATION	
		(Keota Sandstone) (Tamaha Sandstone) (Cameron Sandstone) Booch (Warner) sandstone			
		Hartshorne & (Hartshorne) sandstone			
		upper	(Webbers Falls Sandstone) Gilcrease sandstone Fanshawe sandstone		
		middle	Red Oak sandstone Panola sandstone ☼ Diamond sandstone—also called Red Oak ☼ Brazil sandstone ☼ Bullard sandstone ☼ Cecil sandstone ☼ Shay sandstone ☼		
		lower	Spiro sandstone ☼ Foster sandstone		
LOWER					
MORROWAN		(Wapanucka Limestone) ☼ Limestone Gap shale			
Union Valley		(Union Valley Limestone) (Cromwell Sandstone)			

☼ Denotes gas reservoirs in Panola Field (modified from Suneson and Hemish, 1994)

**Figure 3.** Stratigraphic chart of part of the Lower and Middle Pennsylvanian stratigraphy showing gas producing sandstones (denoted by a ☼ symbol) in the south-central part of the Arkoma Basin, Oklahoma. Names in parentheses denote formal (surface) nomenclature. Modified from Suneson and Hemish (1994).

## CROSS SECTIONS

The stratigraphy and structural configuration of various Atoka sandstone units is best shown by two detailed north-south cross sections (Plates 1, 2) (in pocket). These are constructed across the west and east ends of Panola Field so that their traces are about 2.5 mi apart. Both sections are structurally controlled and incorporate GR and resistivity (Res) logs across roughly 6,000 ft of Atoka strata for five wells. In both cross sections, the vertical and horizontal scales are the same, which reduces exaggeration. Nevertheless, the width of the log on the section greatly distorts this scale, particularly in regard to fault angles. Figure 4 shows how these cross sections tie-in with a regional interpretation by Çemen and others (2001).

Each sandstone interval has unique log characteristics, making identification and correlation within each well and between wells relatively easy. Recognition of repeated sections

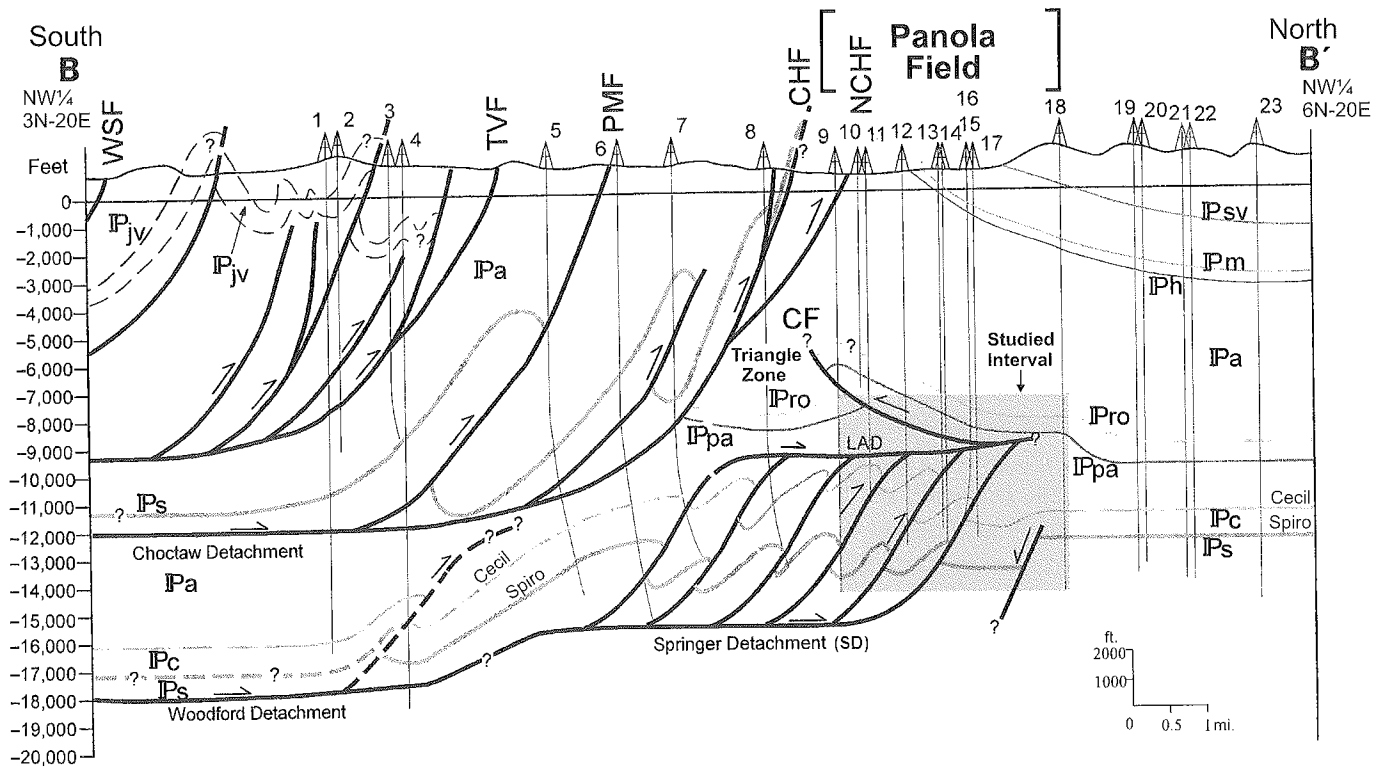


**Figure 4.** Structural cross section B-B' showing the eastern continuation of the Wilburton Triangle Zone and other structural features through area of T. 4-6 N., along the western half of R. 20 E. Notes: CF = Carbon Fault; CHF = Choctaw Fault; NCHF = Northern Choctaw Fault; LAD = Lower Atokan Detachment; PMF = Pine Mountain Fault; IPc = Cecil sandstone; IPro = Red Oak sandstone; IPa = Panola sandstone; IPps = Spiro sandstone; IPsv = Savanna Formation; TVF = Ti Valley Fault; WSF = Windingstair Fault. Modified from Çemen and others (2001, p. 86).

within the Atoka interval permits precise identification of fault planes. Reconstructing the prestructural configuration of the area, however, was extremely difficult, especially when balancing cross sections. It became apparent that the structural complexity is much more severe than illustrated and that incorporating new or additional well data will most likely change interpretations. Therefore, these sections are intended to represent the basic fault geometry. Plausible fault displacement was interpreted by comparing log traces of repeated sections with logs of the whole Atoka interval. The final cross sections were hand-drawn, taking into consideration interval thickness and structural distortion caused in reconstructing vertical and lateral displacement.

#### Cross Section A-A' (Plate 1) (in pocket)

This section preferentially shows wells that are productive from the middle Atoka Bullard and Cecil sandstones in the western half of Panola Field. In this area, faulting seems to be less severe with fewer repeated sections as compared to the middle Atoka in the eastern half of the field.

At Location 1 (farthest north), the Unit #1 Thornton well has the most complicated structure represented in this cross section. Here, the middle Atoka Brazil sandstone is repeated three times and the Diamond sandstone twice. Three high-angle reverse faults are mapped to accommodate this unusual stratigraphic sequence. In the Thornton well, all middle Atoka sandstones (except for the Cecil) are poorly developed and consist largely of shale and thin sandstone beds. The Cecil, however, has more than 100 ft gross sandstone and is the only zone completed in the well. Here, the Cecil sandstone produced more than 0.7 BCF gas since August 2000.

Only 2,200 ft to the south, at Location 2, the Williford #2 Janeway well has one major reverse fault, causing the Panola and Diamond sandstone sequences to be repeated. Thickening of the Bullard and underlying Cecil sandstones at Location 2 made them attractive completion targets and both zones were perforated. Commingled gas production from both reservoirs of slightly more than 0.9 BCF is surprisingly small considering the thickness and quality of these two sandstone reservoirs. One explanation for this relatively low production volume

could be that the reservoirs occur in relatively small fault slices, thus diminishing their areal extent.

At Location 3, about 0.5 mi south of Location 2, the Wilford #1 Janeway is the only well in this section that does not appear to be faulted above the lower Atoka to any large extent. Five of the principal middle Atoka sandstones are present yet none are repeated. The Shay sandstone is not developed in this part of Panola Field. As shown in Plate 1 (in pocket), the Bullard is the only sandstone having significant porosity, yet cumulative production is only slightly more than 0.25 BCF gas. Again, this reservoir must be limited in areal extent by additional faulting not represented in this cross section.

The KCS Medallion #1 Commissioner well at Location 4 is approximately 0.5 mi south of Location 3 and has a repeated section consisting of the Panola, Diamond, and Brazil sandstone units. Because of additional faulting just to the north, the previously mentioned overthrust Atoka units are structurally high to most others in the western part of the field. Despite this, and even with the presence of good reservoir properties in the subthrust Diamond sandstone, this well is productive only in the much lower subthrust Bullard sandstone. Cumulative gas production from the Medallion well is considerably higher than the field average and has produced ~5.8 BCF.

The final well presented in this cross section, the Tenneco #1–14 Lawrence, is located less than 0.25 mi north of the Choctaw Fault. Here, the Panola through Brazil sediments are repeated by a high-angle reverse fault that probably extends beneath the Choctaw Fault. In the Tenneco well, only the Diamond sandstone is well developed; the Bullard and Cecil have thinned and are shaly. The Diamond sandstone is perforated and this zone produced almost 0.4 BCF gas.

#### Cross Section B–B' (Plate 2) (in pocket)

This is a dip section in the eastern half of Panola Field. Repetitive high-angle faults are closely spaced, causing Atoka sandstones to be repeated in a complex manner in all five wells presented. The severity of faulting seems to diminish northward—the inferred direction of fault displacement. Unsubstantiated is the relationship of high-angle reverse faults depicted in both A–A' and B–B' (Pls. 1, 2) (in pocket), with the Springer Detachment (SD) of Çemen and others (2001).

In Well #1 (farthest north), the Panola sandstone is repeated, leaving the lower part of the middle Atoka essentially undisturbed. Most of the studied sandstone units are well developed in this part of the field except the Bullard, which is absent. Only the Cecil sandstone is completed and has a cumulative production of more than 0.6 BCF gas. As usual, the Brazil interval displays its “feathery” log appearance owing to the interbedded nature of sandstone and shale.

At Location 2, roughly 0.34 mi south, the Unit #1 Dear well has a repeated Brazil section (Brazil overlying Brazil). The

lowest of the middle Atoka sandstone units in this well becomes abnormally thick, yet only the Shay sandstone is perforated. The single-zone completion of the Shay produced ~6.4 BCF gas, making it one of the best wells in the field. Other sandstone intervals such as the Panola, Diamond, and Bullard also seem to have gas potential but are not completed.

Between wells 2 and 3—a distance of more than 0.5 mi—at least two major reverse faults are interpreted to account for the complicated repeated Atoka section depicted in the Unit #3 Cox well. Here, the Cecil is repeated three times and the Shay and Brazil each twice. Completed zones included over- and subthrust Shay, subthrust Cecil, and the lower Atokan Spiro sandstones. Despite all of the apparent reservoirs, this well produced only about 1 BCF gas. Obviously, reservoirs in this well constitute fault slivers of relatively small proportion. Otherwise, cumulative production might have been immense.

Only about 0.25 mi to the south, at Location 4, the Unit #1 Moss well has several Atoka sandstone units repeated, as shown in the cross section. The intensity of faulting has made the normal Atoka stratigraphic interval practically unrecognizable. This trend extends southward to the Humble well at Location 5. Here, the stratigraphic interval is greatly expanded because of repeated sections in the middle Atoka. At the very bottom of the log, the Spiro and Morrowan Wapanucka are present in their normal stratigraphic positions, indicating that faulting has not appreciably affected the lower Atoka in this immediate area. Immediately south of the Humble well is the Choctaw Fault; presumably all or most of the high-angle reverse faults interpreted in this cross section dip beneath it to the south.

## STRUCTURE

Panola Field is located in the very south-central part of the Arkoma Basin and just north of the Choctaw Fault (Fig. 5). The study area appears to be a westerly extension of the Brazil Anticline, which trends to the east–northeast. Structural adjustments in Panola Field, however, are much more severe than the simple anticlinal folding depicted on this map. Numerous high-angle reverse faults trend roughly east–west and have hundreds of feet of throw (to the north).

Çemen and others (2001) depicted the Panola area as an easterly extension of the Wilburton Triangle Zone—a structural configuration bounded by the Choctaw Fault on the south, a backthrusting fault to the north (the Carbon Fault), and a horizontal detachment plane within the Atoka (lower Atokan Detachment or LAD). This structural interpretation (Fig. 4) therefore incorporates north-directed thrusting along both the Springer Detachment (SD) and LAD with southern movement (backthrusting) along the Carbon Fault. These structural elements are not entirely supported this study's findings.

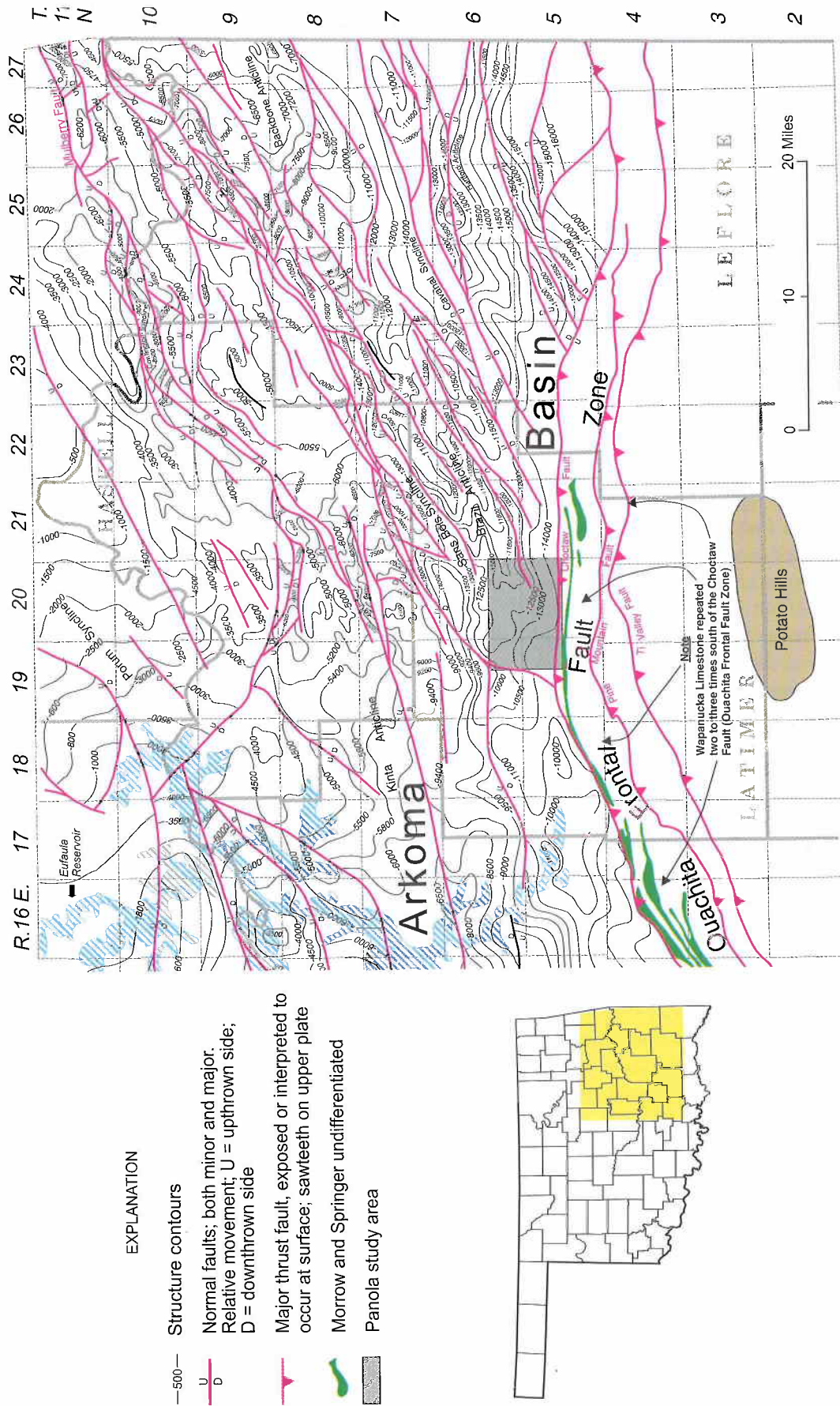


**Figure 5.** Structure map depicting the top of the Wapanucka Limestone, south-central Arkoma Basin. The Wapanucka Limestone directly underlies the Atoka Formation.



All faults within the field are presumed to have a common lower detachment beneath the Atoka (i.e., the SD) similar to that portrayed by Çemen and others (2001). The paucity of deep well penetrations in the study area is not sufficient to verify this. Additionally, faults extending upward from the SD do not always coalesce along a common detachment in the LAD also as interpreted by Çemen and others (2001). Using the same well data, reverse faults appear to penetrate the entire lower and middle Atoka, including sandstone units from the Panola through the Shay. If present, a detachment seems more likely to occur above the Panola in the upper Atoka. Backthrusting along the Carbon Fault in the triangle could not be verified using only well data. This displacement may be hard to envision because of the field's close proximity to the Choctaw Fault. Structural interpretations and fault displacement are shown on field cross sections A–A' and B–B' (Pls. 1, 2) (in pocket).

Based entirely on well control, the principal displacements affecting the middle and lower Atoka in Panola Field are interpreted to consist of high-angle reverse faults with displacement to the north. Because fault planes are interpreted to be very high-angle, the corresponding horizontal movement of sandstone intervals is believed to be relatively small, perhaps less than several hundred feet. This is evident by noting similarities of well-log characteristics of repeated (overthrust) sandstone zones to the same section in the subthrust (Fig. 6). Nevertheless, because of the sheer number of reverse (thrust) faults, significant crustal shortening took place, perhaps more than 30–50% locally. Conversely, stratigraphic thickening in the lower and middle Atoka probably is more conspicuous. Locally, certain Atoka intervals may be twice their normal thickness as a result of reverse faulting.

## SANDSTONE DISTRIBUTION AND DEPOSITIONAL ENVIRONMENTS

The principal sandstone reservoirs in Panola Field (in descending stratigraphic order) include the Panola, Diamond (or possibly Red Oak), Bullard, Cecil, and Shay (Fig. 3). Not included is the Brazil sandstone that occurs throughout the study area but is not productive in the field. The lower Atokan Spiro sandstone is also widespread and is productive northeast of Panola Field.

Two types of sandstone thicknesses are used in quantifying and qualifying these Atoka sandstones. Gross sandstone is determined from the 50% sandstone–shale line on GR logs and does not include shale breaks or shaly sandstone, whereas net sandstone has a minimum density-neutron cross-plot porosity (based on limestone matrix) of 6%. Where sandstone intervals are repeated or truncated by faulting, only the thickest and most complete interval is selected to represent the estimated net or gross thickness for a particular well.

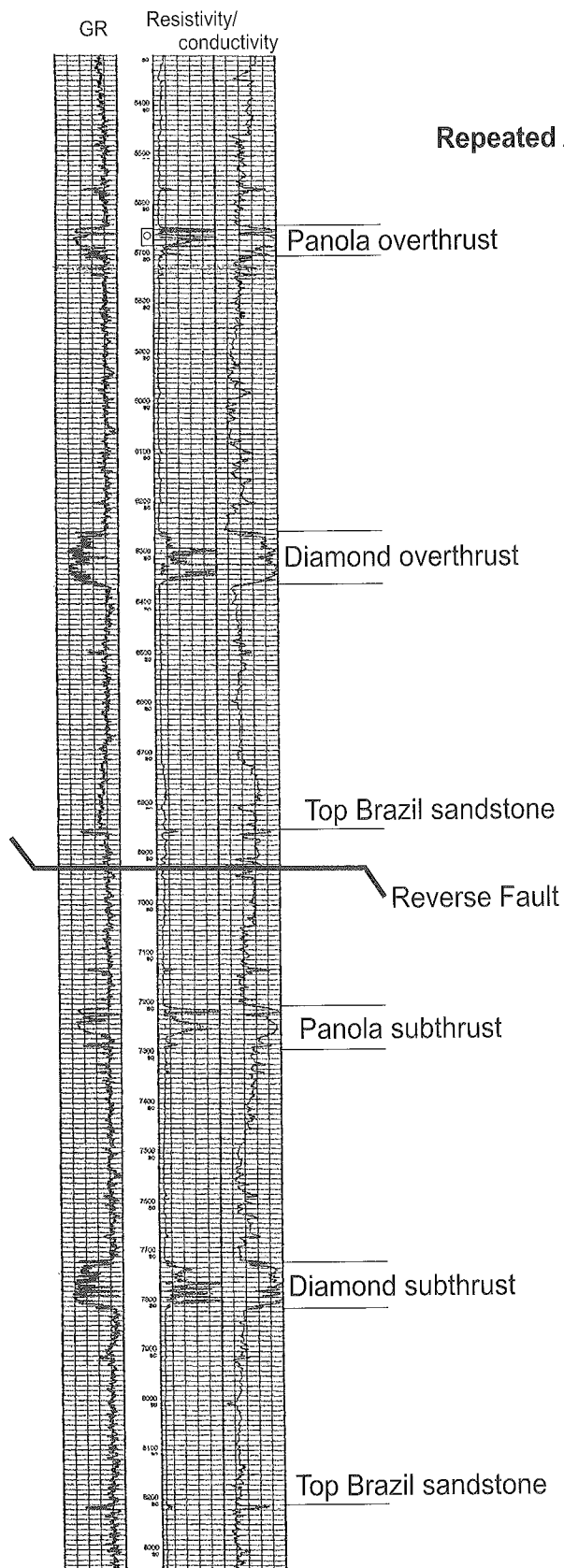
### Panola Sandstone (Figs. 7, 8, 9, 10)

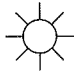
The Panola sandstone occurs throughout the study area but is best developed within the northern half of T. 5 N., R. 20 E. The maximum gross sandstone thickness is ~80 ft but is typically 25–30 ft (Fig. 7). The thickest Panola sandstone occurs in north–south trends that thicken to the south. The Panola sandstone interval almost always contains numerous shale interbeds, particularly at the base. Log patterns indicate a consistently upward-coarsening (cleaning) textural pattern with a well-developed upper sandstone zone that constitutes the reservoir. This log character persists across very large areas and throughout most of this study region but is not diagnostic of any specific marine depositional environment. Furthermore, the Panola sandstone interval is bounded both above and below by hundreds of feet of relatively uniform shale presumably of open-marine origin. There are no continental, deltaic, or carbonate strata either above or beneath this interval that would suggest a shallow or terrestrial origin. Therefore, the Panola sandstone was probably deposited in a relatively deep (marine) ocean or continental slope environment that often host turbidite deposits. The latter interpretation seems more likely when examining sandstone distribution trends (Fig. 7). The facies components of the Panola sandstone are likely that of channel deposits grading southward into fan-sheet lobes, as illustrated by Bouma (2000) in Figure 8.

The Panola sandstone becomes reservoir quality when density-neutron cross-plot porosity (based on limestone matrix) exceeds ~6%. The distribution of such sandstone is portrayed on the net sandstone isopach map (Fig. 9). The net sandstone usually has porosity in the range of 5–10% but is locally higher. Using a 6% porosity cut-off, the thickness of net Panola sandstone is mostly <15 ft, which is considerably thinner than the gross sandstone depicted in Figure 7. Overall, net sandstone thickens to the south and “zeros out” to the north. Wells producing from the Panola sandstone are shaded to show their location relative to the thickness of net sandstone. Log traces depicting textural, porosity, and bedding characteristics of the Panola sandstone are represented in Figure 10. The Panola sandstone is commonly repeated; higher porosity zones tend to occur in the shallower, overthrust part of the structure.

### Diamond Sandstone (Figs. 11, 12, 13)

Figure 11 shows the gross thickness of Diamond sandstone. In the subsurface, this sandstone interval occurs throughout much of the southern Arkoma Basin. Some operators in Panola Field correlate it with the Red Oak sandstone that is a significant reservoir farther to the northeast. The Diamond sandstone thickens southward to more than 70–90 ft whereas the sandstone shales-out northward in the southern



  
 Vastar Resources  
 #4-13 Heitner  
 SW $\frac{1}{4}$  NE $\frac{1}{4}$  sec. 13, T. 5 N., R. 19 E.  
 KB 612'  
 Perforated 5,648'–5,681' (Panola)  
 10,041'–10,095' (Bullard)  
 10,264'–10,313' (Cecil)  
 Completed 6-2001  
 Cum Gas 945 MMCF

**Figure 6.** Well log of the Vastar Resources #4-13 Heitner well (SW $\frac{1}{4}$ NE $\frac{1}{4}$  sec. 13, T. 5 N., R. 19 E.) showing part of the middle Atoka repeated section.



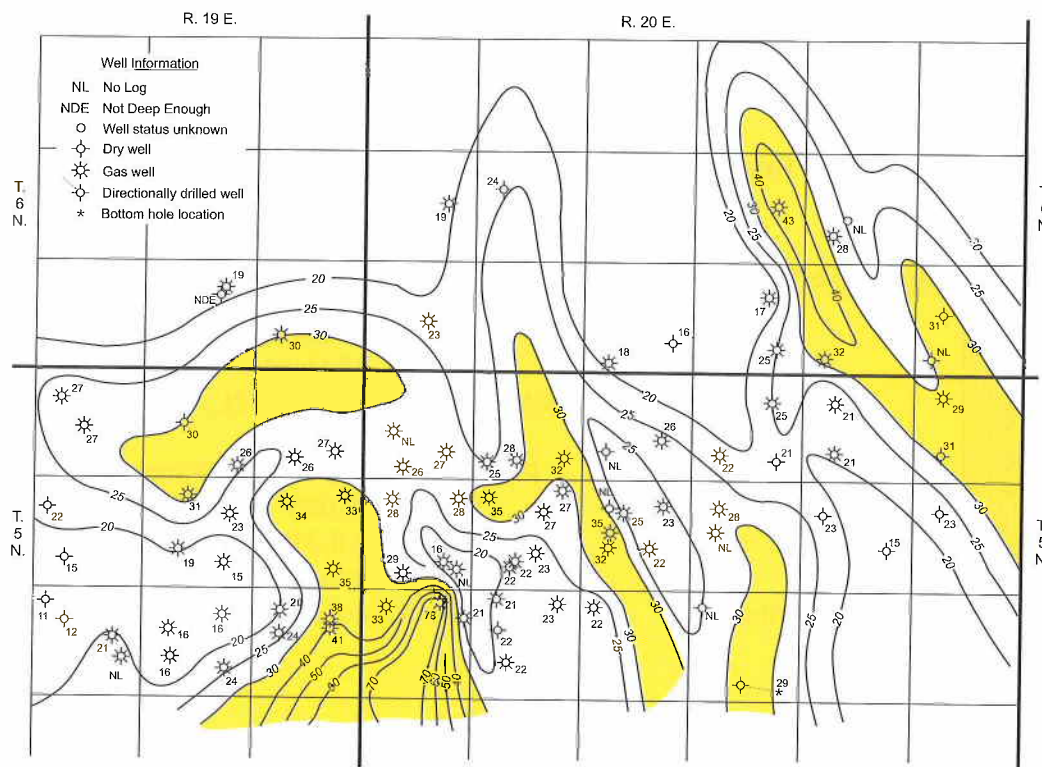


**Figure 7.** Gross isopach map of the Panola sandstone in Panola Field, north-central Latimer County, Oklahoma. Contour interval is either 5 ft or 10 ft (as indicated). See Figure 2 for well names.

half of T. 6 N. Most areas in Panola Field have more than 40 ft gross sandstone but thicknesses vary considerably over very short distances. A distinct north-south trend is very evident for this sandstone but major channeling, as indicated by significant downcutting (erosion of key marker beds), is not apparent in surrounding well logs.

Using a 6% porosity cut-off, the thickness of net Diamond sandstone (Fig. 12) is reduced considerably. Individual sandstone zones seldom have more than 40 ft net sandstone and there is essentially no porous sandstone north of T. 5 N. Therefore, producing wells, as indicated by a shaded pattern, are located in the central area where reverse faults position the reservoir in the structurally highest position within the field. Porosity logs indicate a cross-plot porosity (limestone matrix) of ~5–10% and locally higher.

Log patterns of the Diamond sandstone are generally unique; on small-scale resistivity logs (Fig. 6, or in cross sections A–A' and B–B' shown in Pls. 1, 2; in pocket), the sandstone interval has textural profiles that appear relatively blocky. Detail logs,

however, reveal an overall coarsening-upward textural profile in the lower part and a fining-upward textural profile in the upper part. By and large, the Diamond sandstone interval is composed of numerous thin sandstone beds separated by thin shale beds. The former usually have relatively sharp upper and lower bed boundaries though both contacts may be gradational. These bedding characteristics are shown in Figure 13.

The ratty log character of the Diamond sandstone as exemplified in Figure 13 confirms how severely partitioned individual sandstone beds are in a vertical sense. Laterally, however, individual sandstone beds are

very persistent for hundreds of feet or more. This consistent log pattern (i.e., thin tabular sandstone beds having extensive lateral continuity), and clustering of thin sandstone beds in zones separated by hundreds of feet of low-resistivity marine shale, are the principal lines of evidence supporting a deep-

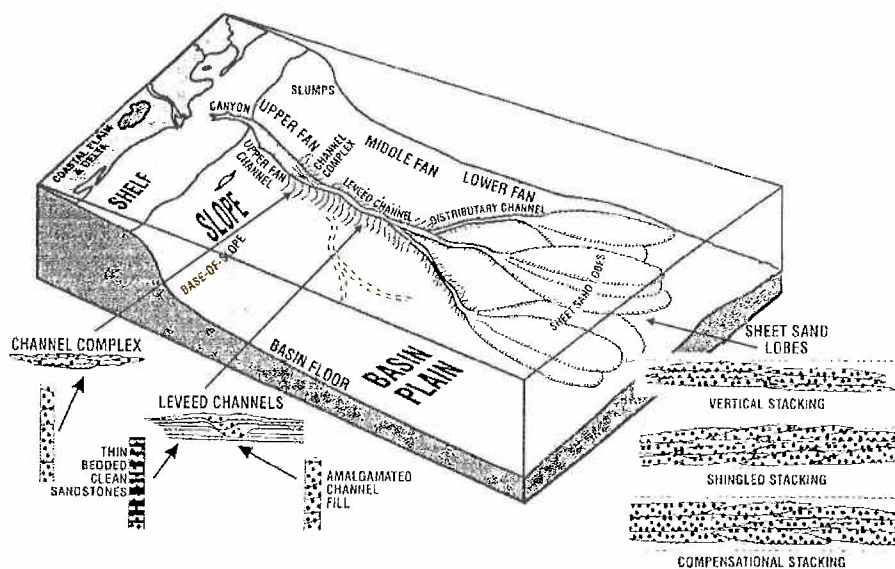


**Figure 8.** Block diagram showing facies components of a fine-grained turbidite system. Modified from Bouma (2000).

marine (turbidite) depositional environment. Using the facies model of Bouma (2000), the Diamond sandstone was probably deposited in sheet sand lobes within the lower and middle turbidite fan. Within sand lobes, small channels up to several feet thick may also be present.

### Bullard Sandstone (Figs. 14, 15)

The Bullard is the most areally restricted sandstone interval in this study since it occurs only in the west-central part of Panola Field. Nevertheless, it is one of the thickest and best Atoka reservoirs in Panola Field. The maximum gross sandstone thickness is slightly more than 150 ft in the NE¼ T. 5 N., R. 19 E. (Fig. 14). The distribution of sandstone is elongate west-to-east and its areal extent mimics the depocenter of the Arkoma Basin during Atokan time. Well logs of this interval (see cross sections A–A' and B–B', Pls. 1, 2; in pocket) are probably the blockiest of the Atoka sandstones although numerous thin shale beds are also evident on more detailed well logs. Isopach map patterns and textural profiles of this sandstone are not suggestive of any specific depositional environment or transport direction although the rather sharp upper and lower contacts of many of the sandstone packages indicate rapid and sudden deposition and abandonment. Its stratigraphic position within the Atoka sequence, areal confinement in the deep basin, and bounding deep-marine shale strata again point to a deep-marine origin. The Bullard sandstone was probably deposited in a valley-slope or basin-center setting. Sediment likely originated from the marine shelf located farther to the east-northeast and transported deeper into the basin during mass-movement (turbidite) depositional processes.

The distribution of net Bullard sandstone (Fig. 15) is much the same as the gross sandstone (Fig. 14). Although there is a relatively small reduction in the thickness of net sandstone, the thicker-bedded nature of this sandstone member seems to preserve a secondary porosity that is commonly 6–10% and greater locally. Virtually every well containing >10 ft net Bullard sandstone (shaded wells) was completed in this reservoir.

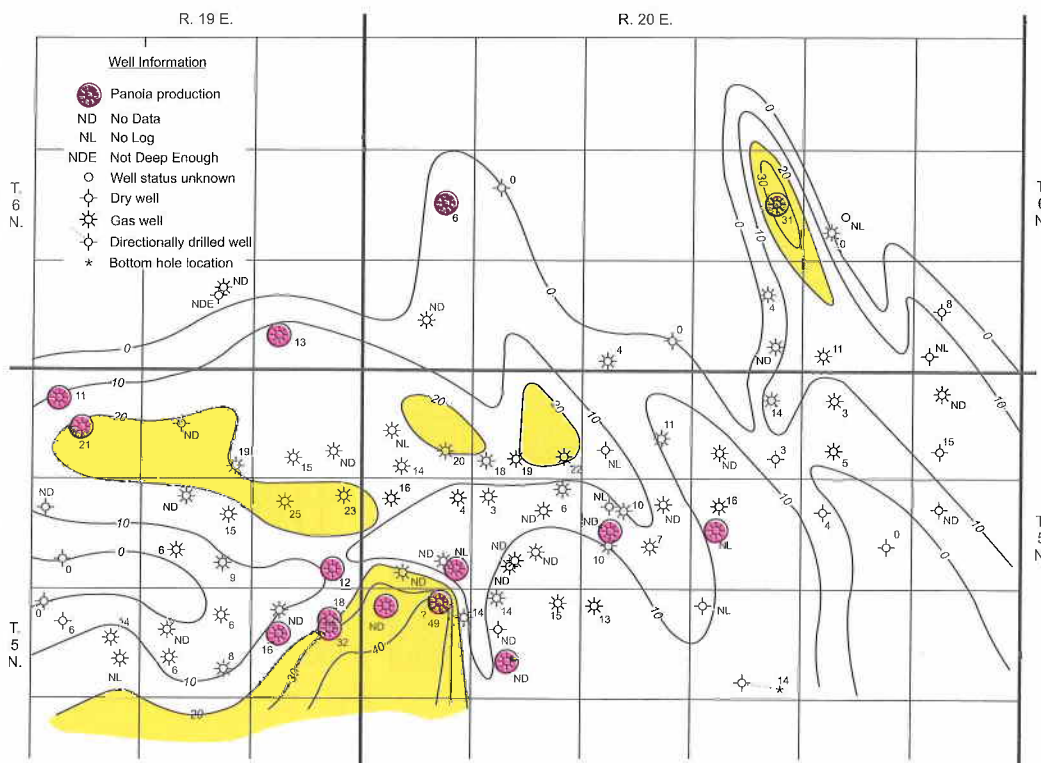


**Figure 9.** Net isopach map of the Panola sandstone in Panola Field, north-central Latimer County, Oklahoma. Net sandstone has cross-plot log porosity  $\geq 6\%$ . Contour interval is 10 ft. See Figure 2 for well names.

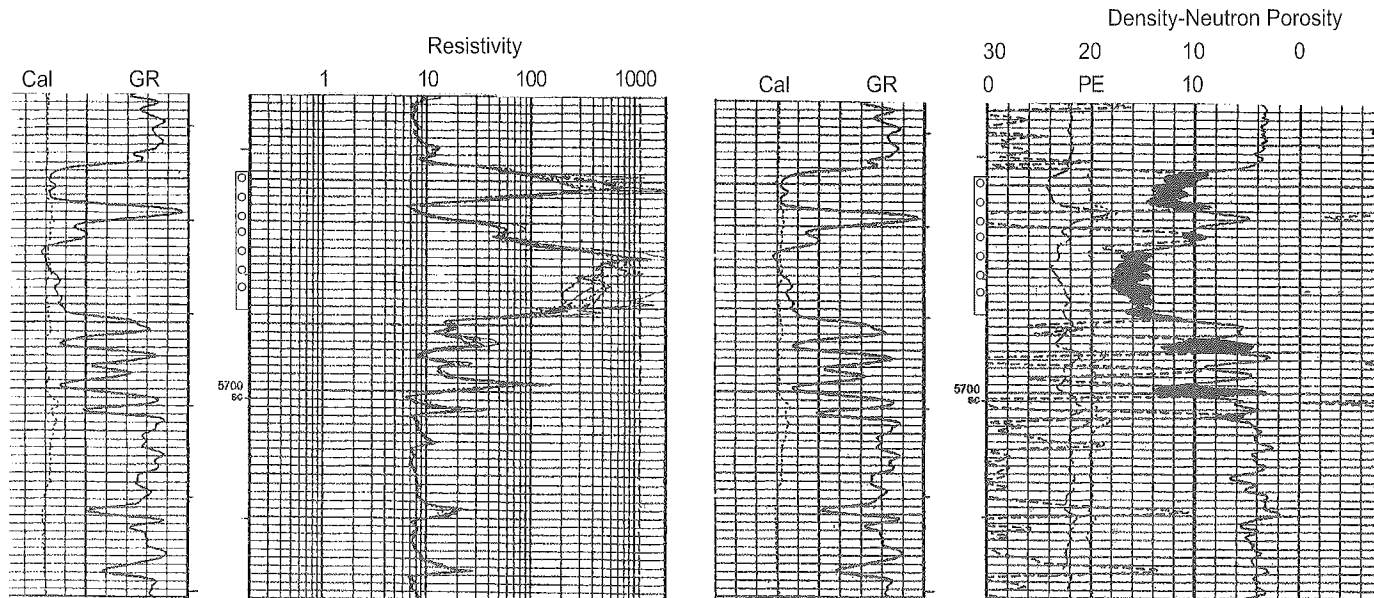
### Cecil Sandstone (Figs. 16, 17, 18)

Within Panola Field, the Cecil sandstone is the thickest reservoir unit in the Atoka Formation. In the NW¼ T. 5 N., R. 20 E. it is >150 ft thick (Fig. 16). As with the Bullard, the areal distribution of the Cecil sandstone is oval-shaped east-to-west along the northern half of T. 5 N. This distribution pattern is also suggestive of basin-center or valley-slope deposition.

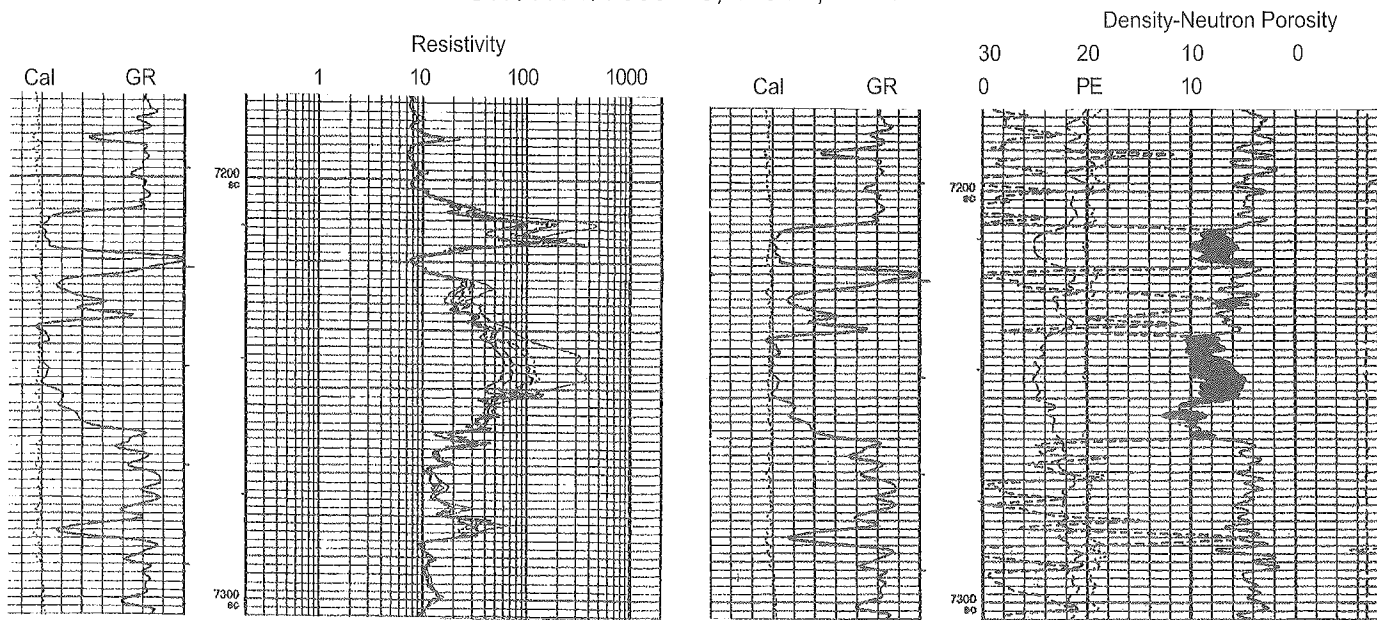
The Cecil sandstone interval is unique for the Atoka because of the extremely thick, “ratty” log signature (Fig. 17). This is portrayed on all log traces but is most striking on the GR and resistivity logs. Individual sandstone beds have relatively sharp upper and lower contacts with shale and are generally only a few to several feet thick. Their interbedded relationship with shale obviously impedes vertical permeability between individual sandstone beds which by themselves can be laterally persistent. As with all lower and middle Atoka sandstones in this area, the Cecil is bounded above and below by hundreds of feet of monotonous marine shale.

The net Cecil sandstone (Fig. 18) is considerably thinner than that of the gross thickness (Fig. 16). Individual bed sets can be relatively clean, but the accompanying PE log trace (Fig. 17) clearly indicates that much of the sandstone is shaly. This, along with pervasive shale interbeds reduces hydrocarbon mobility greatly. Where net sandstone thicknesses reach ~20 ft or more, production is almost always established as indicated

### Panola sandstone-overthrust



Vastar Resources  
#4-13 Heitner  
SW $\frac{1}{4}$  NE $\frac{1}{4}$  sec. 13, T. 5 N., R. 19 E.



### Panola sandstone-subthrust

**Figure 10.** Detail well logs of the Panola sandstone in the Vastar Resources #4-13 Heitner well (SW $\frac{1}{4}$ NE $\frac{1}{4}$  sec. 13, T. 5 N., R. 19 E.). The figure shows gamma ray (GR), resistivity, caliper (CAL), photo-electric (PE), and density-neutron porosity. Overthrust (upper) and subthrust (lower) sections of the Panola sandstone are shown for comparison.



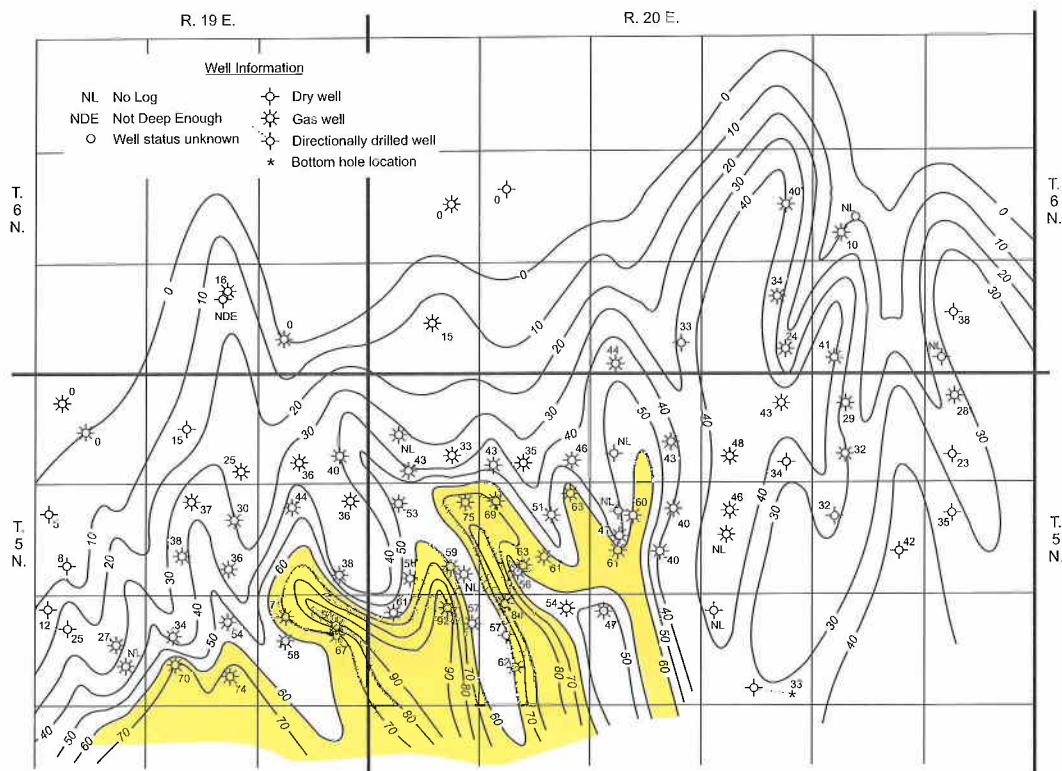


**Figure 11.** Gross isopach map of the Diamond sandstone in Panola Field, north-central Latimer County, Oklahoma. Contour interval is 10 ft. See Figure 2 for well names.

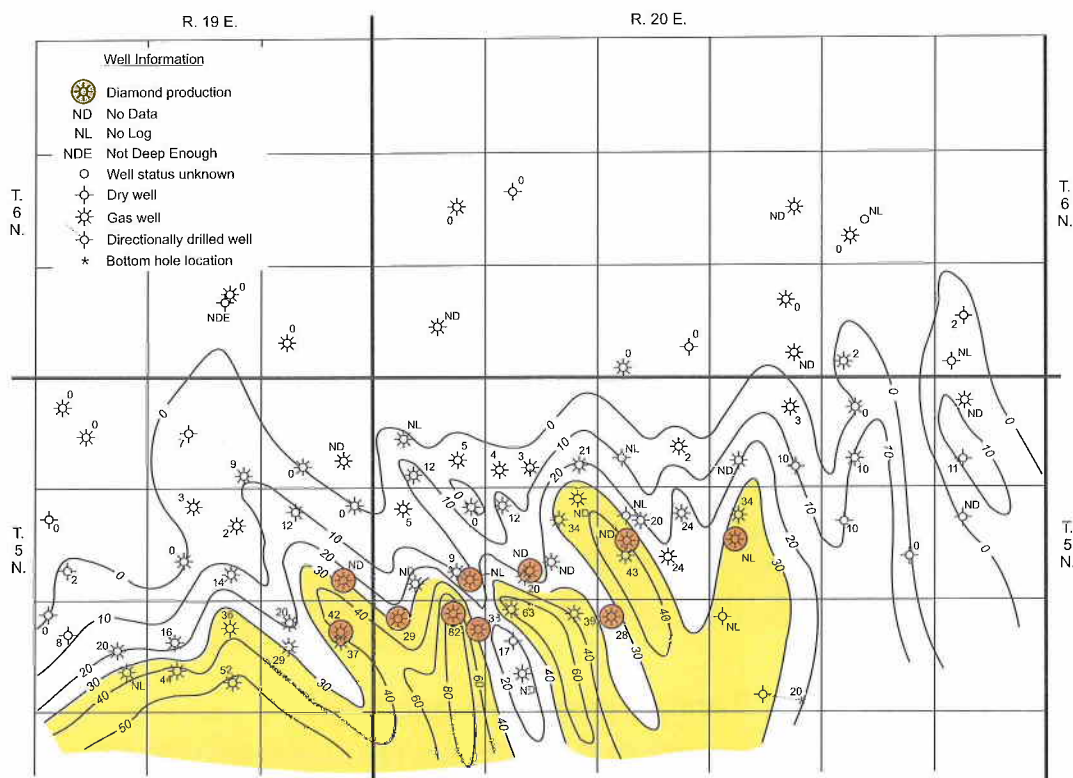
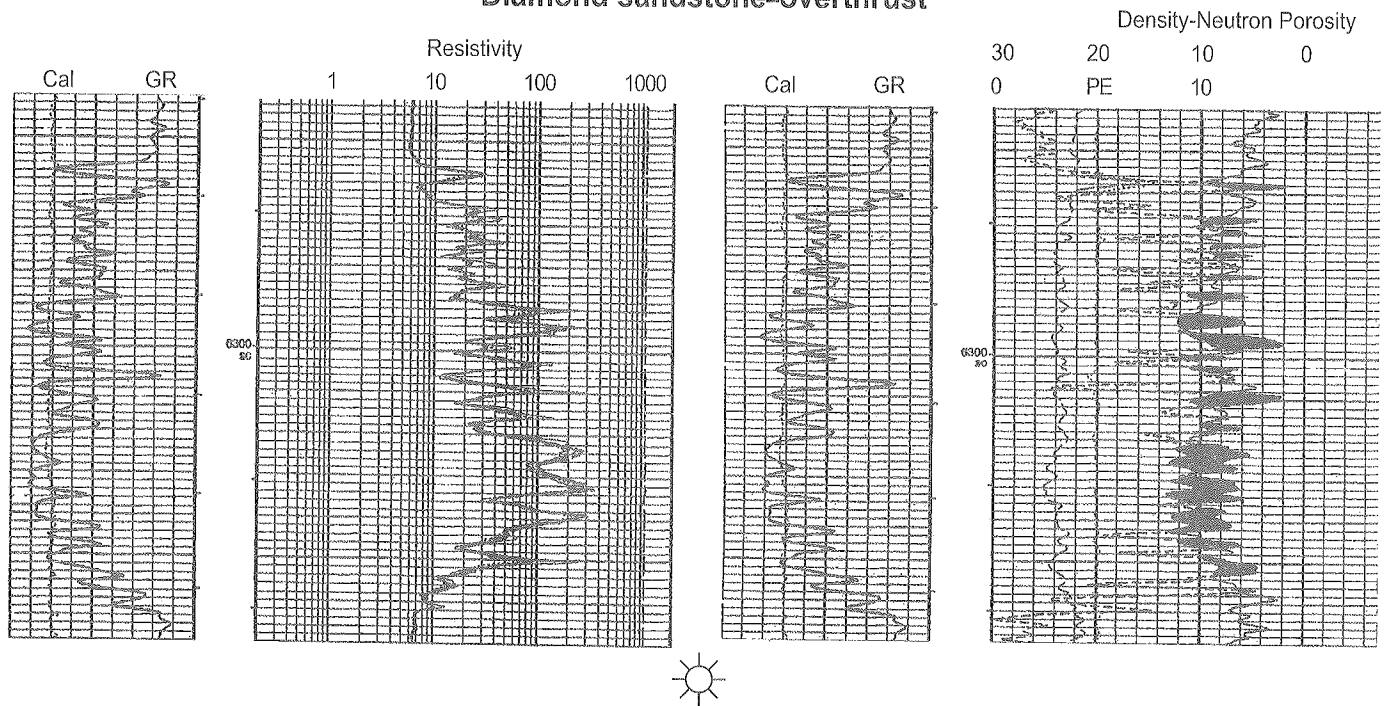
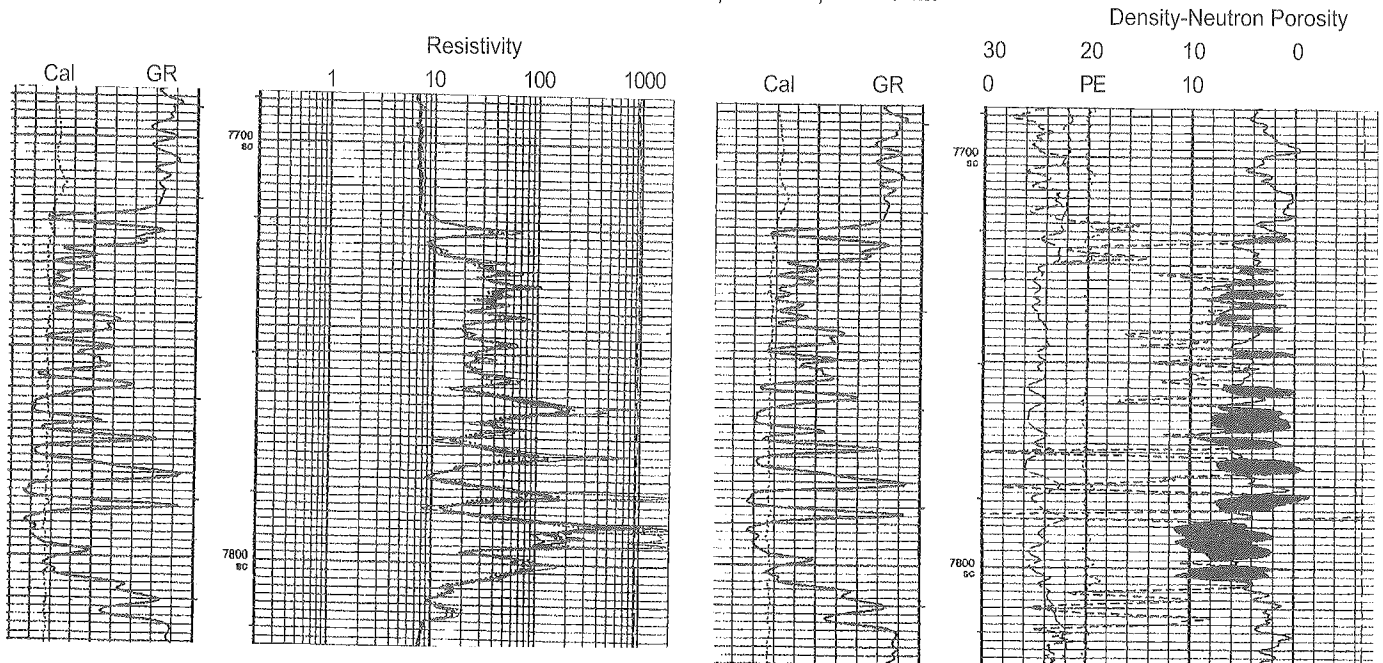


**Figure 12.** Net isopach map of the Diamond sandstone in Panola Field, north-central Latimer County, Oklahoma. Net sandstone has cross-plot log porosity  $\geq 6\%$ . Contour interval is 10 ft or as indicated. See Figure 2 for well names.

### Diamond sandstone-overthrust



Vastar Resources  
#4-13 Heitner  
SW $\frac{1}{4}$  NE $\frac{1}{4}$  sec. 13, T. 5 N., R. 19 E.



### Diamond sandstone-subthrust

**Figure 13.** Detail well logs of the Diamond sandstone in the Vastar Resources #4-13 Heitner well (SW $\frac{1}{4}$ NE $\frac{1}{4}$  sec. 13, T. 5 N., R. 19 E.). The figure shows gamma ray (GR), resistivity, caliper (CAL), photo-electric (PE), and density-neutron porosity. Overthrust (upper) and subthrust (lower) sections of the Diamond sandstone are shown for comparison.

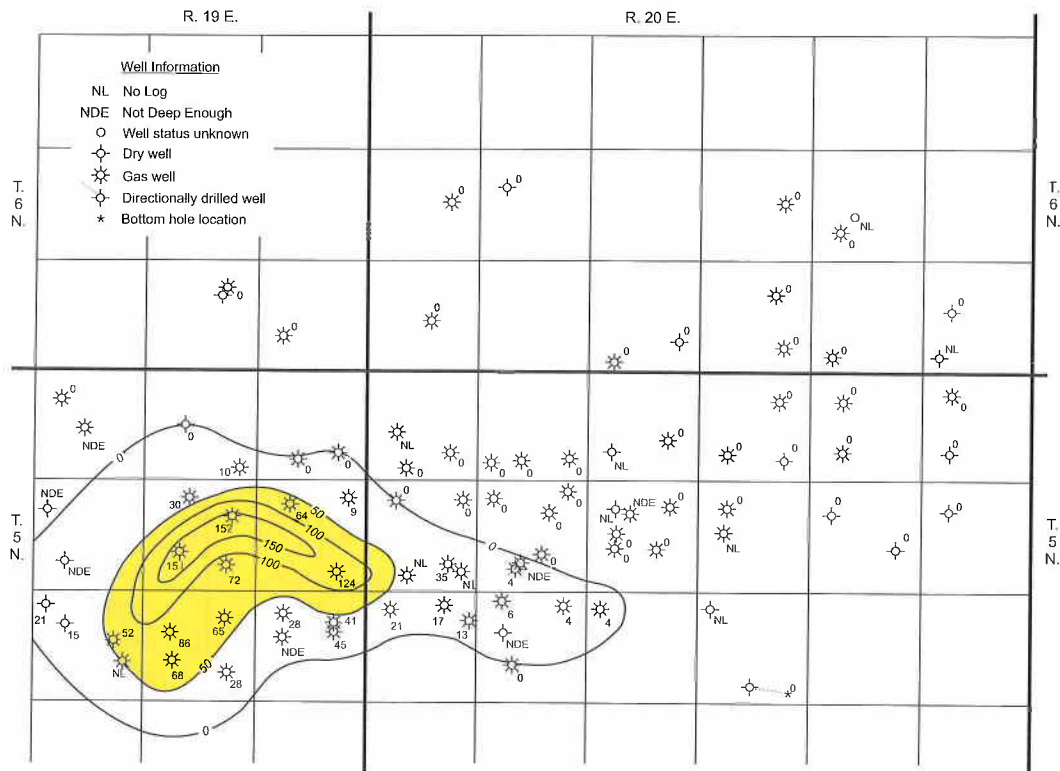


**Figure 14.** Gross isopach map of the Bullard sandstone in Panola Field, north-central Latimer County, Oklahoma. Contour interval is 50 ft. See Figure 2 for well names.

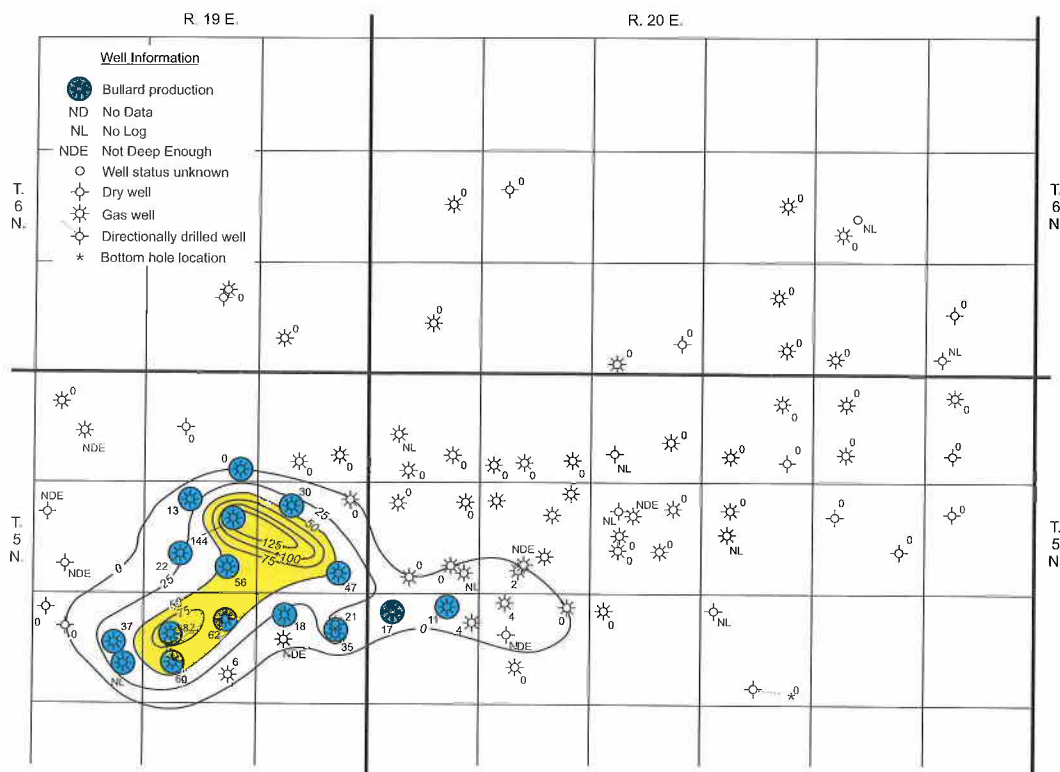


**Figure 15.** Net isopach map of the Bullard sandstone in Panola Field, north-central Latimer County, Oklahoma. Net sandstone has cross-plot log porosity  $\geq 6\%$ . Contour interval is 25 ft. See Figure 2 for well names.





## Multiple Atoka Sandstone Gas Reservoirs in T. 5 N., RS. 19–20 E.

47

Producing Formation Code: P=Panola; D=Diamond; B=Bullard; C=Cecil; S=Shay; Sp=Sprio; Cr=Cromwell														
Abbreviations used: BHP = bottom hole pressure; IBHP = initial bottom hole pressure; MCF = thousand cubic feet; MCFGPD = thousand cubic feet gas per day; IP = initial production; YTD = year to date														
Location	Lease Name	Well Num	Well Status	Producing Formation	Operator Name	Pressure IBHP/BHP (PSI)	IP (MCFGPD)	Gas Cum (MCF)	Gas YTD Prod	First Prod Date	Last Prod Date	TD	U Perf	L Perf
T. 5 N., R. 19 E.														
1 NE SE SW	SCHARFF	2	Gas, active	C	BP AMERICA	5255/?	900	732,120	25,161	1999/10	2004/03	11,890		
1 C SE	SCHARFF	1-1	Gas, active	C	BP AMERICA	5402/?	885	3,437,056	6,603	1987/01	2004/02	12,470	11,536	11,736
2 N2 SE SE	THORNTON	1	Gas, active	C	UNIT PETROLEUM	3153/?	1,564	694,314	14,808	2000/06	2004/02	12,302	11,693	11,842
3 C NW	REUSCH	1	InactiveGas		CHESAPEAKE			272,748		1965/12	1990/08	12,300	6,956	7,025
3 C NW	REUSCH C NW	1	Gas, active	P, Sp	CHESAPEAKE			21,165,938	8,004	1965/12	2004/02	12,300		
3	REUSCH UNIT #2	2	Gas, active	Sp?	BP AMERICA			6,117,467	934,233	1996/04	2004/02	11,600		
3 E2 E2 W2	REUSCH	2	InactiveGas	P	BP AMERICA		478	33,181		1996/01	1999/12	7,150	6,584	6,614
11 C SE	JANEWAY	1-11	Gas, active	B	WILLIFORD ENERGY	2449/1629	175	271,074	3,236	1993/08	2004/02	12,510	11,012	11,086
11 NW SE NE	JANEWAY	2	Gas, active	B, C	WILLIFORD ENERGY		5,240	916,497	27,306	2000/03	2004/02	12,400	11,440	11,924
11 E2 NE NW	JANEWAY	4	Gas, active	B, C	WILLIFORD ENERGY	2220/?	990	63,455	5,970	2003/02	2004/02	12,100	11,535	11,920
11 SW NE SW	JANEWAY	3	Gas, active	B	WILLIFORD ENERGY		523	174,753	7,751	2001/11	2004/02	11,964	11,330	11,522
12 SW NE NW	ENIS	3	Gas, active	B, C	WILLIFORD ENERGY		1,570	202,853	6,006	2001/02	2004/02	12,250	11,514	12,076
12 N2 S2 SE	ENIS OTHO	1-12	Gas, active	P, D, B	WILLIFORD ENERGY		168	305,488	3,816	1997/10	2004/02	12,350		
12 N2 S2 SE	OTHO ENIS	1-12	InactiveGas		WILLIFORD ENERGY			211,142		1990/11	2001/05			
12 SE NW NE	ENIS	2	Gas, active	C	WILLIFORD ENERGY	5423/?	2,100	932,593	10,059	1998/05	2004/02	12,725		
13 NE SW NE	HEITNER	1-13U	InactiveGas		BP AMERICA	985/760		1,708,760		1992/07	2000/05	13,023	6,314	7,660
13 NE SW NE	HEITNER	1-13L	InactiveGas		BP AMERICA			2,947,769		1992/07	1999/10	13,000		
13 NE SW NE	HEITNER	1-13	Gas, active	P, D, B	BP AMERICA	5285/1102	1,650	1,190,510	54,203	1999/08	2004/03	13,000		
13 S2 N2 NW	HEITNER	3-13	Gas, active		BP AMERICA	2701/2248	4,100	2,777,646	90,079	1999/04	2004/03	10,340	10,016	10,056
13 NE SW NE	HEITNER	4-13	Gas, active	P, B, C	BP AMERICA		3,400	945,318	58,191	2001/08	2004/03	10,600	5,645	10,330
13 NE SW NE	HEITNER	1	InactiveGas	P, B	BP AMERICA			7,843,081		1986/10	1998/05	13,023		
13 N2 S2 NW	HEITNER	2	Gas, active	P	WILLIFORD ENERGY		300	317,479	11,140	1998/05	2004/02	7,750	5,350	5,380
14 C NE	COMMISSIONER	1-14	Gas, active	B	KCS RESOURCES	3781/1442	3,700	5,802,667	80,927	1998/06	2004/02	10,350	10,138	10,212
14 S2 N2 SE	LAWRENCE	1-14	Gas, active	D	CHESAPEAKE	1529/397	142	358,751	3,328	1990/08	2004/03	11,900	7,201	7,277
14 NW NE SW	LAWRENCE	2-14	Gas, active	B	CHESAPEAKE		1,484	255,818	142,972	2002/10	2003/08	10,500		
14 C S2 NW	MCCABE	1	Gas, active	B	KCS RESOURCES	4369/2924	18,207	5,730,574	212,496	1999/10	2004/02	10,720	10,214	10,266
15 S2 N2 SE	PUCKETT	2-15	Gas, active	B	WHITMAR EXPLORATION		1,200	162,924	25,200	2003/04	2004/02	10,777		
15 S2 S2 NE	PUCKETT	1-15	Gas, active	B	WHITMAR EXPLORATION	4428/1630	8,874	4,671,193	72,418	1999/01	2004/02	10,620	10,404	10,644
T. 5 N., R. 20 E.														
3 C SW	CASH-MITCHELL	1-3	Gas, active	S	MUSTANG FUEL	6144/670	3,000	5,999,857	24,290	1984/02	2004/03	11,577	11,404	11,455
3 NE NE SW NE	CATHEY	1-3	InactiveGas	Sp	MUSTANG FUEL	4872/273	1,200	2,048,144		1979/09	1989/06	14,343	12,646	12,704
4 E2 E2 NW SE	HAWTHORNE	1-4	Gas, active	S	UNIT PETROLEUM	6827/1241	2,350	7,818,065	31,646	1982/09	2004/03	11,644	11,564	11,644
5 N2 SW SW	MCKEE	1-5	Gas, active	S	UNIT PETROLEUM	7253/1894	6,027	4,306,880	4,526	1987/10	2004/02	12,416	12,224	12,270
5 E2 SE SW	MAXEY	2	Gas, active	C	UNIT PETROLEUM		750	618,109	40,315	2000/12	2004/03	12,250	11,763	11,836
5 NE NW SE SE	MAXEY	1-5	Gas, active	C	UNIT PETROLEUM	4787/1758	1,215	1,613,300	11,910	1983/09	2004/03	12,283	11,504	11,614
6 NW NE SW	LIVELY	3	Gas, active	C	UNIT PETROLEUM		1,052	232,552	54,257	2003/06	2004/02	12,196	11,604	11,634
6 C SE SW	LIVELY 2-6	2-6	Gas, active	C	UNIT PETROLEUM	6982/2505	1,283	3,253,784	47,692	1990/09	2004/02	12,600	11,952	12,146
6 C SE	LIVELY	1-6	Gas, active	C, S	UNIT PETROLEUM	7162/1932	2,990	4,476,985	26,072	1985/11	2004/02	12,881	11,643	12,197
7 NE SE SW	BUTZER	182	Gas, active	C, S	WILLIFORD ENERGY		3,000	896,215	76,642	2002/04	2004/02	12,890	10,954	12,267
7 NW SE SE	BUTZER	3	Gas, active	P, D	WILLIFORD ENERGY		1,550	39,322	39,322	2004/01	2004/02	6,716		
7 C SE	BUTZER	1-7	InactiveGas	C, S	WILLIFORD ENERGY	4338/661	2,252	1,489,760		1984/12	2002/07	12,890	11,341	12,382
7 SW NE NE	WIGINGTON	1-7	InactiveGas	C, S	WILLIFORD ENERGY		1,491	1,150,998		1990/02	1998/10	12,891	12,698	12,754
7 S2 N2 NW	ASHBY	1T	Gas, active	C, S	WILLIFORD ENERGY	3998/?	1,220	117,572	13,297	1998/10	2003/12	13,183		
7 SW NE NE	WIGINGTON	1-7	Gas, active	C, S	WILLIFORD ENERGY	3195/903		787,620	22,015	1998/08	2004/03	12,891		
7 S2 N2 NW	ASHBY	1	Gas, active	C, S	WILLIFORD ENERGY	5055/?		703,910	14,467	1998/09	2004/02	13,183		
8 NW SE SW	COX	3	Gas, active	C, S, Sp	UNIT PETROLEUM			73,534	2,852	2001/12	2004/02	14,119	10,430	13,933
8 NE SW NE	COX	1	Gas, active	C, S	UNIT PETROLEUM	4608/?	1,647	182,479	3,673	1998/06	2004/02	12,400	11,682	11,846
8 NE SW NE	COX	1-8	Gas, active		UNIT PETROLEUM	7355/1485		873,659	4,121	1983/11	2003/08	12,400	12,122	12,187
8 SE NW NW	DEAR	1	Gas, active	S	UNIT PETROLEUM	6636/615	1,600	6,368,540	34,700	1988/11	2004/03	12,720	12,510	12,570
8 SW NW SE	COX	2	Gas, active	S	UNIT PETROLEUM		260	1,873,229	16,114	1996/03	2004/02	12,490	10,244	10,277
8 NW SE SW	COX	3	Gas, active	C, S, Sp	UNIT PETROLEUM	5122/?	4,257	894,626	30,430	2001/06	2004/02	14,119	10,430	10,514
8 E2 E2 SW	COX	4	Gas, active	D	UNIT PETROLEUM		1,925	461,317	30,398	2002/06	2004/02	6,600	6,326	6,370
8 NW NE NE	COX	5	Gas, active	S	UNIT PETROLEUM		150	33,653	5,904	2002/10	2004/03	12,373	12,117	12,178
9 NW SE NW	GOLIGHTLY	5	Gas, active	P, D	UNIT PETROLEUM		100	106,284	25,927	2003/03	2004/02	7,241		
9 N2 N2 SW	GOLIGHTLY	2	Gas, active	C	UNIT PETROLEUM	4339/826	1,502	1,774,947	41,908	2000/09	2004/03	11,100	10,214	10,264
9 NE NW NE	GOLIGHTLY	3	Gas, active	S	UNIT PETROLEUM	1384/584	912	998,804	55,559	2000/10	2004/03	11,892	11,650	11,690
9 N2 SE NW	GOLIGHTLY	1	Gas, active	S	UNIT PETROLEUM	5967/348	3,192	2,003,827	27,908	1983/06	2004/03	12,870	11,870	11,926
9 NW NW SE	GOLIGHTLY	4	Gas, active	C	UNIT PETROLEUM		2,998	1,069,039	85,246	2002/04	2004/03	10,839	9,941	9,972
10 SW SE NW	COLVARD	2	Gas, active	P, D	UNIT PETROLEUM		375	64,528	16,854	2003/08	2004/03	11,500	5,917	6,480
10 C NW	COLVARD	1	Gas, active	S	UNIT PETROLEUM	7544/1745	3,699	3,863,137	4,796	1984/02	2004/03	12,000	11,345	11,371
16 S2 NW NW	ENIS	1	Gas, active	D, S	UNIT PETROLEUM		1,000	108,245	2,614	2001/12	2004/02	11,234	10,584	11,076
17 SW NE SW	MOSS	3	Gas, active	P	UNIT PETROLEUM		850	103,011	7,471	2003/02	2004/02	11,200	6,582	6,629
17 NE NW NW	MOSS	1	Gas, active	C	UNIT PETROLEUM		982	1,175,542	18,225	2000/02	2004/02	11,532	10,070	11,420
17 NE NW NE	MOSS	2	Gas, active	C	UNIT PETROLEUM		527	500,639	12,720	2001/09	2004/02	11,602	9,962	11,017
18 C E2 NE	HARDING	1	Gas, active	D, C	UNIT PETROLEUM		696	539,496	10,048	1998/04	2004/02	13,550		
18 S2 N2 NE	HARDING	2	Gas, active	P, D, B	UNIT PETROLEUM		200	956,695	30,961	2000/12	2004/02	10,335	5,480	10,212
18 SE NW NW	OTHO	1	InactiveGas	P, D, B	UNIT PETROLEUM			631,108		1989/06	2002/08	11,007	5,988	7,816
18 SE NW NW	OTHO #1	1	InactiveGas		UNIT PETROLEUM	1899/1603		225,545		1988/07	1989/04	11,007		
18 SE NW NW	OTHO	1	Gas, active		UNIT PETROLEUM		4,073	1,018,439	24,664	1997/10	2004/02	11,019	5,420	5,456
18 C E2 NE	HARDING	1	InactiveGas	D, C	UNIT PETROLEUM	1566/462		649,860		1986/02	1998/08	13,550	7,336	7,394
T. 6 N., R. 19 E.														
36 SE NW SW	SHAW #1-36	1	Gas	Sp	CHESAPEAKE			1,052,589	8,915	1986/08	2004/03	14,374	14,112	14,153
36 SE NW SW	SHAW	1	InactiveGas	P	CHESAPEAKE		145	39,635		1996/04	1997/09	14,574	9,054	

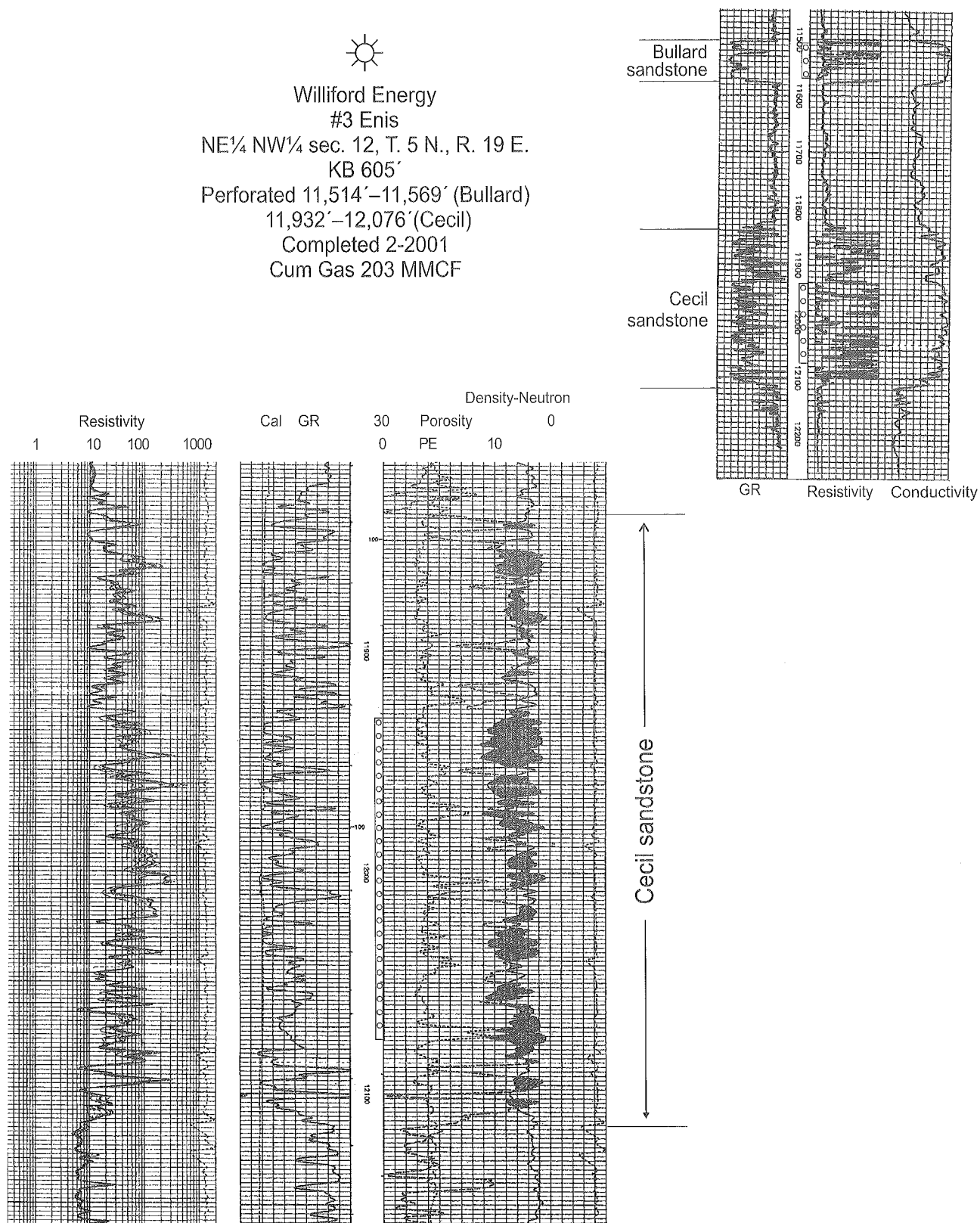


**Figure 17.** Detail well logs of the Cecil sandstone in the Williford Energy #3 Enis well (NE¼NW¼ sec. 12, T. 5 N., R. 19 E.). The figure shows gamma ray (GR), resistivity, caliper (CAL), photo-electric (PE), and density-neutron porosity. The small-scale inset log lacks reservoir detail but is useful for basic identification of sandstone intervals. Also shown is the thick shale sequence separating the Cecil and Bullard sandstone intervals.

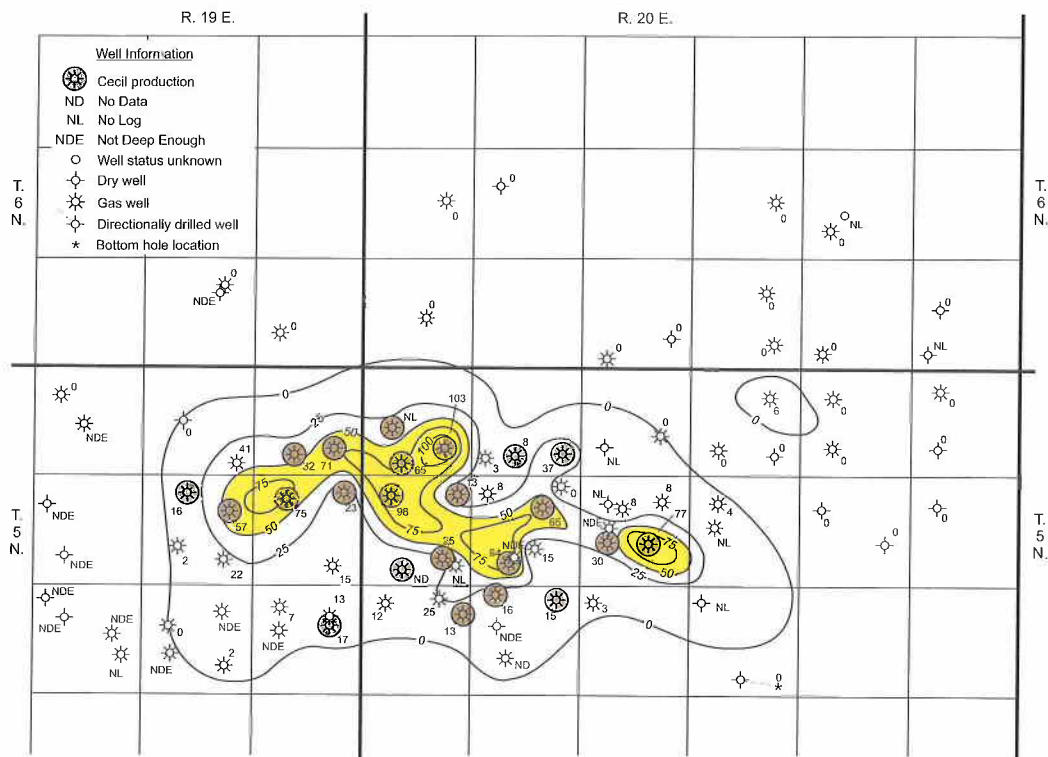


**Figure 18.** Net isopach map of the Cecil sandstone in Panola Field, north-central Latimer County, Oklahoma. Net sandstone has cross-plot log porosity  $\geq 6\%$ . Contour interval is 25 ft. See Figure 2 for well names.

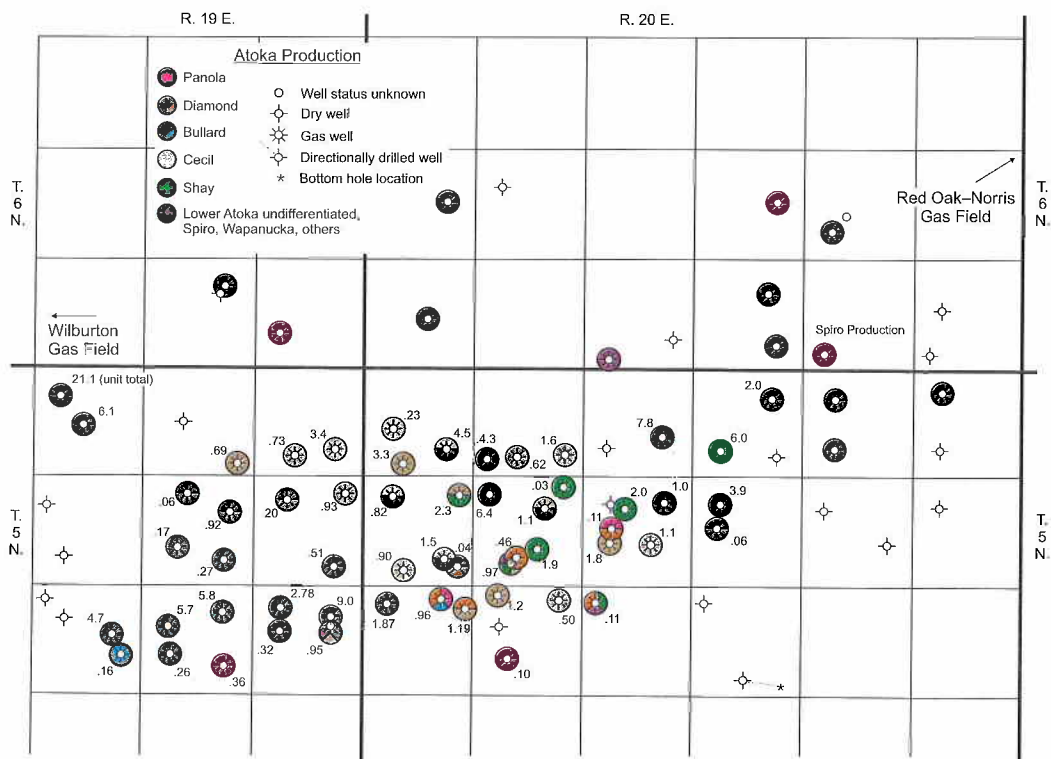


**Figure 19.** Production map of wells in Panola Field, north-central Latimer County, Oklahoma. Color-coding of producing wells identifies the various Atoka reservoirs. Production values are in BCF. Data are from IHS Energy Data and are current through February 2004.

tion (IP), supplements Figure 19. Data are from IHS Energy Data and are current through February 2004.

The better wells in Panola Field produce from the Bulard, Cecil, and Shay (the latter is not studied). Each of these sandstones are capable of producing 1–5 BCF gas per well. The stratigraphically higher reservoirs, including the Panola and Diamond, generally produce <1 BCF gas per well only in that these reservoirs are much thinner.

The initial gas production potential for Atoka wells varies from ~1–5 million cubic ft gas per day (MMCF). Thin, depleted, or tight reservoirs will come on for less. The initial bottom-hole pressure (IBHP) varies widely because of structural compartmentalization and ranges from ~4,000 to 7,500 psi (see Table 1 for specific data). This indicates that the Atoka reservoirs are slightly over-pressurized (>0.43 psi/ft) as compared to the overlying reservoirs of the Hartshorne and Booch sandstones, which are underpressurized.

## REFERENCES CITED

- Andrews, R.D., 2003, Cromwell play in southeastern Oklahoma: Oklahoma Geological Survey Special Publication 2003-2, 87 p.
- Bouma, A.H., 2000, Fine-grained, mud-rich turbidite systems: model and comparison with coarse-grained, sand-rich systems, *in* Bouma, A.H.; and Stone, C.G. (eds.), *Fine-grained turbidite systems: American Association of Petroleum Geologists Memoir 72/SEPM Special Publication 68*, p. 9-20.
- Çemen, Ibrahim; Evans, Justin; and Sagnak, Ata, 2001, Eastern continuation of the Wilburton triangle zone in the Red Oak Gas Field area, frontal Ouachitas–Arkoma Basin transition zone, southeastern Oklahoma, *in* Johnson, K.S.; and Merriam, D.E. (eds.), *Petroleum systems of sedimentary basins in the southern Midcontinent, 2000 symposium: Oklahoma Geological Survey Circular 106*, p. 81–95.
- Suneson, N.H.; and Hemish, L.A., 1994, Geology and resources of the eastern Ouachita Mountains frontal belt and southeastern Arkoma Basin, Oklahoma: Oklahoma Geological Survey Guidebook 29, p. 3-133.

## Restoration of Thrusted Middle Atoka Reservoir Trends, Waveland Field, Arkansas

*Kim R. Butler*

Southwestern Energy Company  
Fayetteville, Arkansas

**ABSTRACT**—The Waveland Field is a gas development project along the Ranger Anticline. The field is being developed on less than 80-acre well spacing. This drill spacing is regulated based on the structural complexities and limited drainage of gas from the tight middle Atoka reservoirs.

The Ranger Anticline is located in the southern Arkoma Basin between the Poteau and Mount Magazine Synclines. The anticline is cored by antiformal, stacked-duplex thrust sheets, which repeat middle Atokan sandstone reservoirs. These thrust faults have individual offsets of a few hundred to more than 11,500 ft.

The identified middle Atokan sandstones are fine to very fine grained, poorly sorted sublitharenites with a clay matrix >7%. Reservoir permeability ranges from <0.001 to 2.13 millidarcies (mD) across a porosity range from 3% to 17%. Because the effective permeability is not sufficient for economic production, every well is hydraulically fractured to enhance the natural-fracture system.

The middle Atoka–upper Borum formation is the main subject of this study. This formation is more than 600 ft thick and has been subdivided into three parasequences. Main sand bodies in these parasequences range from a few feet to more than 100 ft of net sand. Serialized balanced profiles were utilized to restore the thrust offsets and trend maps for the parasequences were created. The prethrust trend maps indicate each parasequence is a channelized turbidite fan. The restoration of the porosity trends has been a key factor in determining the areal extent of the reservoirs and successfully predicting the offset locations for development in the Waveland Field.

### INTRODUCTION

Exploitation of middle Atokan–age tight gas sands in the Arkansas Arkoma Basin is being accelerated. Since 2001, the Arkansas Oil and Gas Commission (AOGC) has granted de-spacing associated with Booneville, Chismville, Gragg, Mansfield, and Waveland Fields. These fields are located along the southern limit of the Arkoma Basin. These six fields have produced more than 500 Bcf of gas (PI/Dwights, 2004) and in 2004 accounted for more than 30% (151 million cubic feet of gas per day [Mmcfg/d]) of the Arkansas Arkoma Basin's total daily production (478 Mmcfg/d).

The de-spaced fields produce from multiple middle Atokan–age deep-water siliciclastics. These middle Atokan clastics are repetitive and appear to be related by similar genetic deposition. The sands can be correlated to zones between regional shale markers. Amid the regional shales, the sands can amalgamate to greater than 100 ft in net-sand thickness. The areal distribution of these sands has been described as lenticular,

isolated, or occurring in pods. Individual beds, encountered in the well bore, cannot be correlated with any confidence between wells.

During the Ouachita orogeny, the middle Atokan stratigraphic section underwent compression. The Ouachita deformation manifests in low-angle thrusting that utilizes regional and local shale zones as bedding-plane detachments. The deformation has complicated the correlation and palinspastic restoration of the depositional trends. The repetitive nature of the sands causes confusion as to whether similar sands are related to deposition or are thrust repeats.

This paper describes the middle Atoka–upper Borum formation, which is a major productive unit in the Waveland Field. The upper Borum formation has been correlated based on guidelines for sequence stratigraphy. Using the principles of balanced cross sections for low-angle thrust terrains, the Ranger Anticline structure is restored to a pre-deformation stage in order to determine the sand deposition patterns.

## LOCATION

The Waveland Field is located on the crest of the Ranger Anticline (Fig. 1), in Yell and Logan Counties, Arkansas. The towns of Belleville, Havana, Waveland, and Blue Mountain are located proximal to the field.

Immediately north of the area is Mount Magazine — at 2,753 ft elevation, the highest point in Arkansas (Fig. 1). Waveland Field is bisected by the Petit Jean River and Blue Mountain Lake, established by the Army Corps of Engineers in 1947, covers the anticline's core.

As defined by the AOGC, Waveland Field covers 46 one-mile sections of T. 5 N., Rs. 24-26 W. (Arkansas Oil and Gas Commission, 1967a, 1967b, 1968, 2003, 2004).

## WAVELAND FIELD HISTORY

The first well drilled in the Ranger Anticline was the C. B. Shaffer #1-15 (sec. 15, T. 5 N., R. 24 W., TD 3,095 ft) by the Fort Smith Lumber Company. Drilled in 1915, this open-hole well tested approximately 500 Mmcfg/d but was abandoned. Twenty additional wells, eight producing gas, were drilled from 1923 to 1985. As of July 2004, a total of 77 wells have been drilled, 48 have produced gas, and 46 remain active and productive.

Prior to the 2003 field rules changes, 39 wells had been drilled in the Waveland area. Active drilling from 2003–2004 added 23 producing wells (as of July 2004). In-fill drilling continues near producing wells and exploration is expanding the

productive field limits. Since 1970, the field has produced 13.8 Bcfg and daily production is more than 22 Mmcfg/d.

## ATOKA FORMATION SEQUENCE STRATIGRAPHY

Sequence-stratigraphic principles define a sequence boundary as a relatively conformable succession of genetically related strata and their correlative surfaces bounded between unconformities (Van Wagoner and others, 1990).

The base of the Atoka Formation is an unconformity boundary with the Morrowan clastics (Sutherland, 1988; Link and Roberts, 1986; Table 1). The Atoka Formation is a transgressive-to-regressive siliciclastic sequence. The internal correlation of the Atoka Formation is largely interpreted as conformable. The siliciclastic sequence regression continued into the Desmoinesian. There is no upper unconformity boundary preserved in the Arkansas Arkoma Basin, but the Ouachita deformation postdates early Desmoinesian deposition.

Regional correlation separates the Atoka Formation into lower, middle and upper Atoka (Table 1). These separate conformable, genetically-related sand and shale units. Finer subdivisions are local to a region or field-by-field definition.

Deep wells over the Ranger Anticline, such as the Pleas Garner #1-29 (sec. 29, T. 5 N., R. 26 W.), S. M. Bettis #1-14 (sec. 14, T. 5 N., R. 23 W.) and Danville #1-33 (sec. 33, T. 5 N., R. 22 W.), indicate the Atoka Formation is approximately

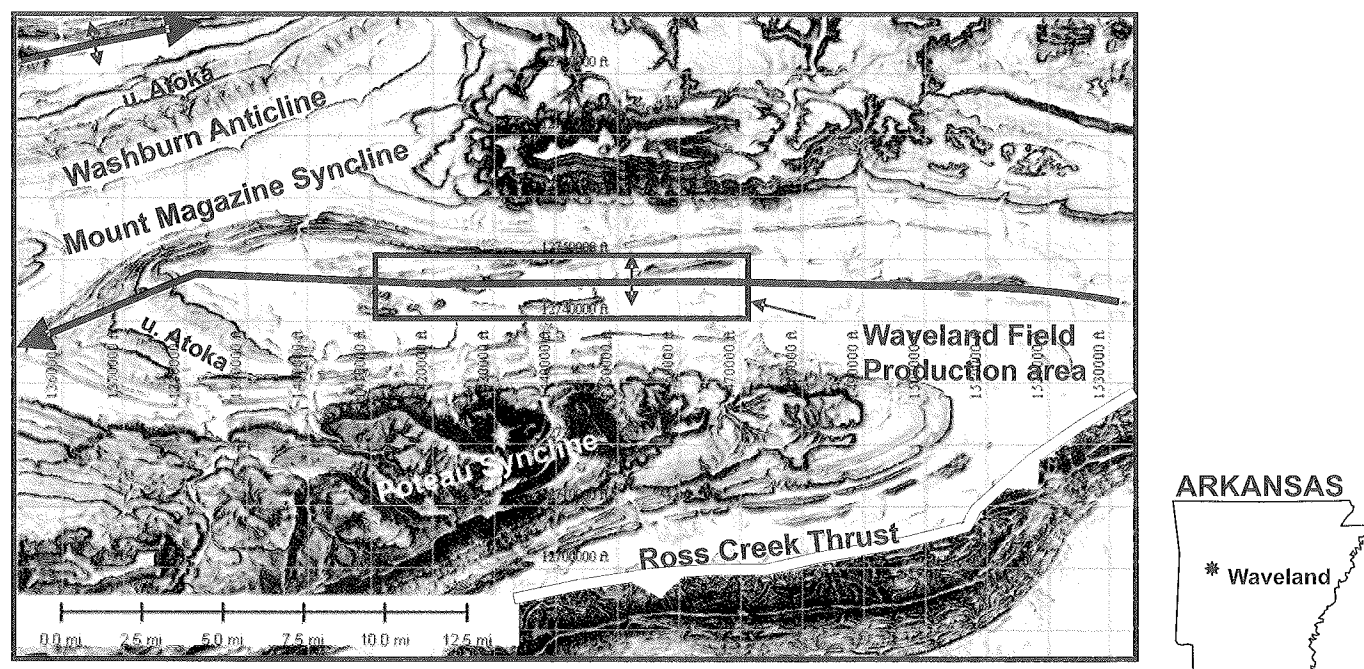


**Figure 1.** Digital elevation terrain map of Ranger Anticline. The Ranger Anticline is an east–west trending, asymmetric, north-verging anticline cored by duplex thrusts that repeat middle Atoka formations. The thrusts do not offset the upper Atoka sand ridges surrounding the field. (Map data source: USGS, Projection: UTM (Ft) NAD 1927).

SOUTH				ESTIMATED UNFAULTED THICKNESS (FEET)		NORTH		
-----14.9 MILES-----								
Ma	PERIOD/STAGE	FORMATION		DANVILLE 1 SECTION 33 T.5N., R.22W.	PLEAS GARNER 1 SECTION 29 T.5N., R.25W.	MOUNT MAGAZINE SYNCLINE	HUCKLEBERRY 1 SECTION 1 T.6N., R.24W.	
306.5	DESMOINESIAN	MARMATON GROUP	HOLDENVILLE		present only in Oklahoma			
			WEOKA WETMAKA CALVIN					
		CABINISS GROUP	SENORA STUART THURMAN					
UNCONFORMITY								
	DESMOINESIAN	KREBS GROUP	BOGGY SAVANNA MCALESTER HARTSHORNE			present 9 mi N		
			2250					
308	ATOKAN	ATOKA	upper			4900	4508	
			middle	Basham Nichols Turner upper Borum Borum shale lower Borum Areci		5795		4903
				lower	Moyer Casey Sells Orr/Sprio		3250	
311.7								
UNCONFORMITY								
318.1	MORROWAN		KESSLER HALE	2380			1405	
UNCONFORMITY								
359.2	MISSISSIPPIAN	FAYETTEVILLE		520			345	
		BOONE		170			253	
UNCONFORMITY								
428.2	DEVONIAN- SILURIAN	PENTERS/HUNTON		220			461	
448.3	ORDOVICIAN	VIOLA		1460			936	
		ARBUCKLE		+ 1061			+ 650	

Age data based on Rohde (2004)

**TABLE 1.**— Stratigraphy of Ranger Anticline and surrounding area

14,900 ft thick. Twelve miles north, the Atoka Formation thins to 11,700 ft (Huckleberry #1–1, sec. 1, T. 6 N., R. 24 W.).

The unfaulted lower Atoka in the Waveland area is approximately 4,900 ft thick (Fig. 1). The same stratigraphic section 12 mi north is at least 3,900 ft thick. The lower Atoka includes informal formations, the Spiro-Orr, Cecil, Sells, Casey, and Moyers formations and their correlative equivalent units. These units are shallow-water, deltaic-shelfal clastics.

The unfaulted middle Atoka in the Waveland area is approximately 3,900 ft thick. The middle Atoka thins 12 mi north to 3,300 ft and includes informal formations, the Areci, lower Borum, upper Borum, Turner, Nichols, and Basham formations and their correlative equivalent rock units. These units are deep-water clastics.

The unfaulted upper Atoka sequence is approximately 6,100 ft thick on the south flank and 5,600 ft thick near the axis of the Mount Magazine Syncline (Fig. 1). Twelve miles north of Waveland, on the north flank of the Mount Magazine Syncline, the upper Atoka is approximately 4,500 ft thick. The upper Atoka includes informal formations, the Alma and upper Carpenter formations and their correlative equivalent units. In the study area, these units are deep-water clastics, but they are the upper part of this deep-water sequence. The upper Atoka grades conformably into the shallow-water Desmoinesian clastics.

The Desmoinesian strata are approximately 2,250 ft in thickness. In the Mount Magazine Syncline, the Hartshorne, McAlester, and Savanna Formations are preserved. The youngest Desmoinesian-age strata preserved in Arkansas is the Boggy Formation. These units are fluvial-deltaic clastics.



Above the Boggy Formation, the Desmoinesian Thurman Formation marks the upper limit to this conformable clastic wedge. The Thurman Formation, preserved only in Oklahoma, is composed of chert conglomerates derived from the Ouachita deformation and deposited northward (Sutherland, 1988; Elmore and others, 1990). The Thurman Formation represents the oldest preserved indication of the Arkoma contractional tectonics caused by the Ouachita orogeny as post-Boggy Formation in the late Desmoinesian (Link and Roberts, 1986; Denison, 1989).

### WAVELAND FIELD MIDDLE ATOKA RESERVOIRS

Regionally, the middle Atoka units squeeze or expand depending on the paleotopography created by accommodation space without unconformities. The middle Atoka units of the Waveland Field are defined as a parasequence set: a succession of genetically related beds or bed sets, which are relatively conformable, that form a distinctive stacking pattern and are commonly bounded by major marine flooding surfaces and their correlative surfaces (Van Wagener and others, 1990).

The type log for the Waveland Field middle Atoka reservoir sands is the Brasher #1-11, sec. 11, T. 5 N., R. 25 W. (Figs. 2A, 2B). This well was drilled to a total depth of 7,500 ft near the crest of the Ranger Anticline. The middle Atoka informal formations, from bottom to top, are the lower Borum, upper Borum, Turner, Nichols, and Basham. These informal formation are recognized by the AOGC as common but separate reservoir units within the Waveland Field.

The lower Borum formation is a sand-prone, parasequence unit overlying thick lower Atoka shale. Based on deep wells flanking the Ranger Anticline, the lower Borum is approximately 600 ft thick. The unit is extensively thrust faulted. Commonly, the top 100 ft is a major reservoir in the Waveland Field.

Above the lower Borum formation is the Borum shale, which

is extensively thrust faulted and is 300–1,100 ft thick. The shale is interpreted as the correlative deep-water equivalent of a marine flooding surface for the top of the lower Borum parasequence. Overlying the Borum shale is the upper Borum formation, which is between 500 and 650 ft. This formation is a major reservoir in the Waveland Field. The Turner formation is a thick regional shale unit with minor sands overlying the upper Borum formation. The Turner formation is approximately 1,100 ft thick. Sandstones occasionally occur in the middle and upper half of the unit. The transition between the Turner formation and the overlying Nichols formation is increasing sands. The Nichols formation is nearly 500 ft thick and its net sand is a maximum of 80 ft. The Nichols is a minor reservoir unit in the Waveland Field. The Basham formation is the top of the middle Atoka. The unit is separated from the Nichols formation by a shale interval. The sands are thickest at the base and beds thin upward into upper Atoka shales. The

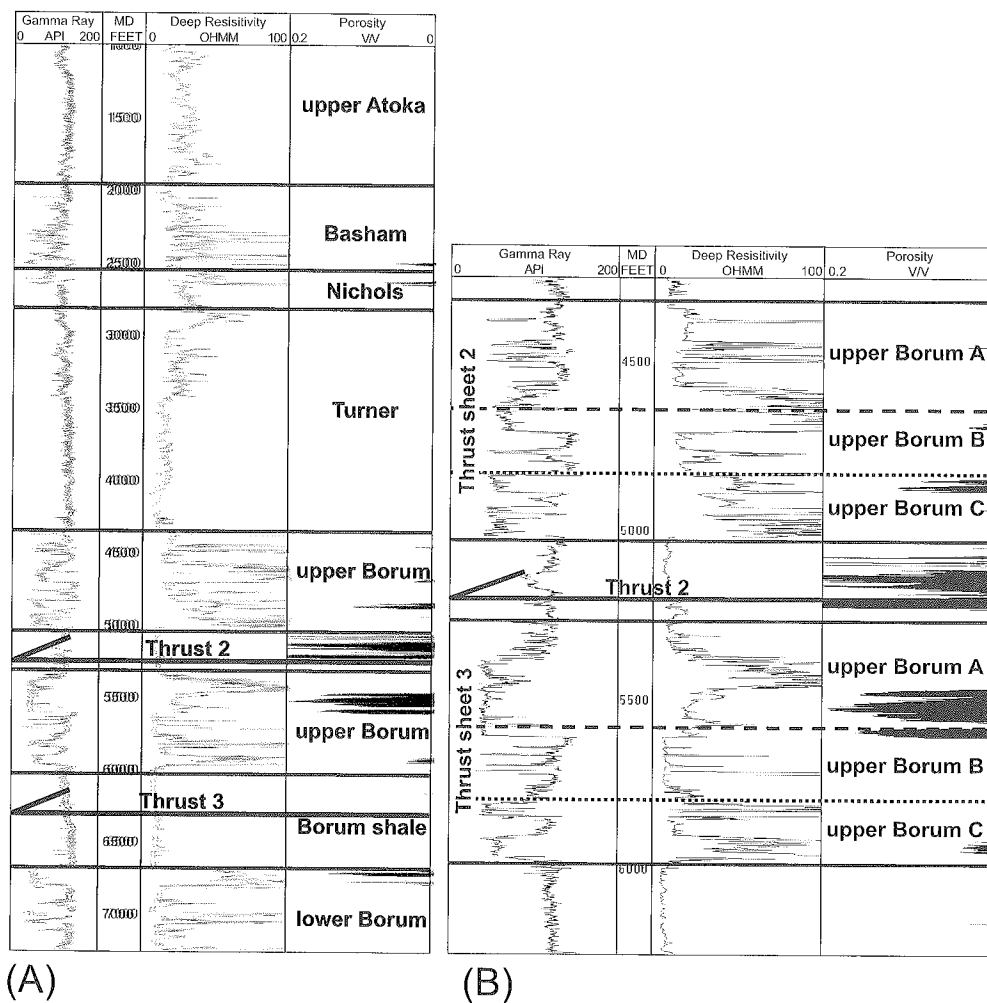


**Figure 2.** Type log, Waveland Field, Brasher #1-11, sec. 11 T. 5 N., R. 25 W. Measured depth (MD) is in feet. Effective porosity (PHIE) is shown in track 4. (A) The log illustrates the middle Atoka stratigraphy and reservoir units. (B) Enlarged view of parasequence subdivisions of upper Borum formation. The upper Borum is duplicated by a low-angle thrust.

unit is a minor producing reservoir in the Waveland Field. The Basham is up to 500 ft in gross thickness. Occasionally, sands amalgamate to approximately 70 ft net thickness.

### MIDDLE ATOKA RESERVOIR CHARACTERISTICS

Within the Waveland Field, Southwestern Energy Company has analyzed 160 sidewall cores in the lower Borum, upper Borum, Nichols, and Basham formations of the middle Atoka Formation. Compositionally, the sands are quartzarenites to sublitharenites and typically are very fine-to-fine grained, sub-angular to subrounded, and poorly sorted (Fig. 3). Matrix and cement consists of up to 15% authigenic chlorite and illite with minor kaolinite, quartz overgrowths, and calcite-dolomite cements.

The porosity versus permeability relationship is exponential (Fig. 4). Increased matrix porosity equates to increased matrix permeability. The porosity reaches a maximum of 18% in sidewall cores. Permeability ranges from 0.001 to 3 millidarcies. The median sidewall core porosity is 9.44% and median permeability is 0.018 millidarcies.

Drilling in the Arkoma Basin is commonly conducted without mud. The drill hole is left open to atmosphere, which

leaves reservoir formation pressure unconfined. Gas flares up to several million cubic feet per day have been recorded. Multi-million-cubic-feet gas flares are related to larger open fractures. It is not uncommon in the Waveland Field to drill productive gas reservoirs without recording a significant open-hole gas flare, but after hydraulic-fracture treatment, the same reservoir can produce several million cubic feet of gas per day.

Based on a few samples, natural fractures have up to 50 millidarcies permeability. Quartz crystal needles up to 12 mm in length, and euhedral terminations have been recovered in well cuttings. Preserved filled fractures have been found up to 500  $\mu$ m in width.

Image logs indicate that individual sand beds are 1 ft to several feet thick, and they may amalgamate to over 100-ft-thick bed sets. Open and closed fractures are seen on the image logs. The middle of the amalgamated sands contained preserved porosity. Open-hole electric logs have been correlated to sidewall cores to calibrate the logs (Fig. 5). The best porosity zones correlate to sands that exhibit blocky gamma-ray (GR) curves which indicate reduced shale intervals.

Fractures enhance permeability more than 100 times the matrix permeability. Fracture orientation across the Waveland Field exhibits a north-northeast – south-southwest to west-northwest – east-southeast strike orientation. The fractures dip more than 50° and the fracture system displays a complex conjugate relationship.

### STRUCTURE

The Waveland Field lies along the crest of the Ranger Anticline, a major east-west trending fold (Fig. 1). Blythe and others (1988) identified the structure as a fault-propagation fold. The north limb dips from 35° N to vertical to overturned. Vertical to overturned dips are closely associated with the structural culmination along the anticlinal axis. The south limb dips 10–20°. The anticline is doubly plunging. Atokan shales and sands, correlated as equivalent to the Basham and Nichols formations, are exposed in the anticline's core (Co-hoon and Vere, 1988).

Blythe and others (1988) indicated that the Ranger Anticline is offset by imbricate thrusts at the surface, but these faults do not offset the upper Atokan sandstones of the anticline's limbs. The Poteau Syncline bounds the anticline on the south and the Mount Magazine Syncline on the north limb. The Mount Magazine Syncline crowds out the western plunge of the Ranger Anticline. The eastern plunge nose of the Ranger Anticline is crowded out by the Petit Jean Syncline and the Ross Creek Thrust. Arbenz (1989) referred to the folds north of the Ross Creek Thrust as a triangle or duplex zone.

Drilling in the core of the Ranger Anticline has encountered multiple north-verging, low-angle thrusts. Middle Atoka

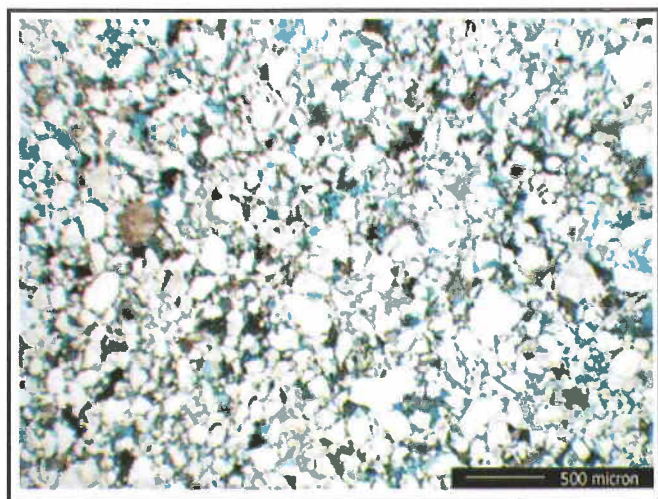


**Figure 3.** Typical thin-section view, Brasher #1-11 upper Borum A sand. Scale bar: 500  $\mu$ m (500 microns is equivalent to 0.5 millimeters or 0.0197 inches). The upper Borum sands are quartzarenites to sublitharenites. Cementation is dominantly clays (chlorite-illite-smectite) with quartz overgrowths and dolomite/calcite. Measured porosity is 13.4%. Air permeability is 0.929 millidarcies. Porosity is dominated by intergranular porosity but includes lesser amounts of microporosity associated with the clay matrix and some intragranular porosity within partially dissolved sand grains. (Thin-section analysis: Geosystems, Houston, Texas for Southwestern Energy, personal communication, 2002.)

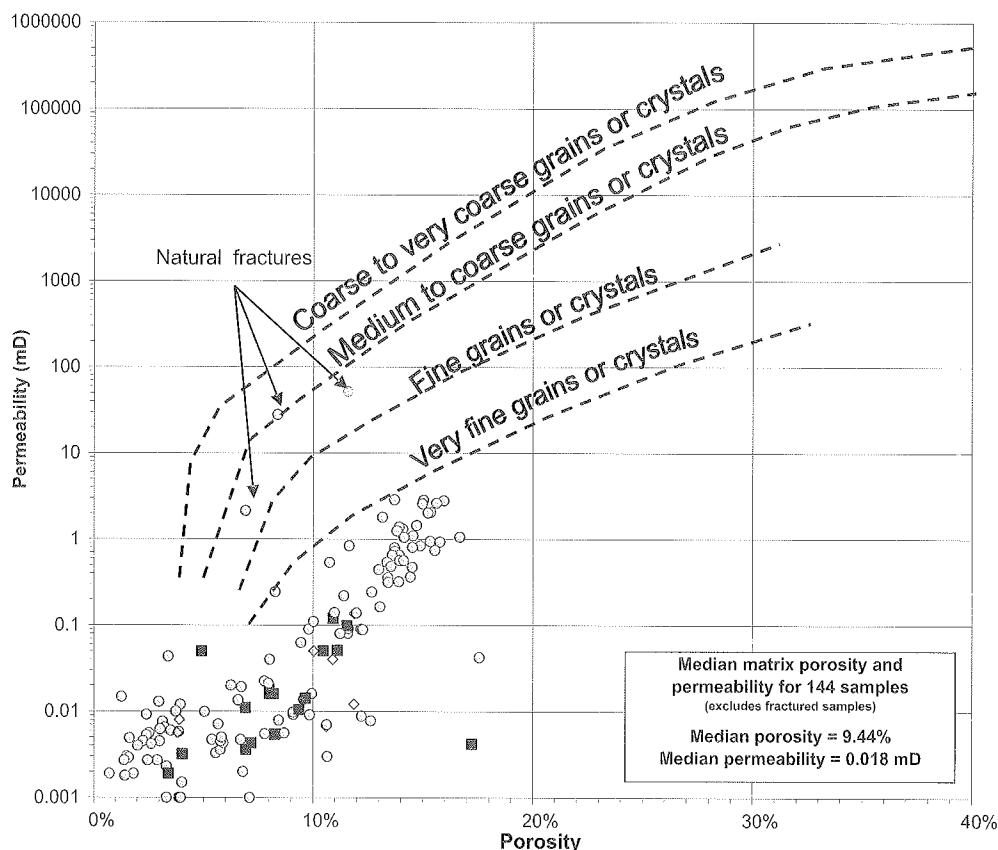


**Figure 4.** Middle Atoka sidewall-core porosity versus permeability, Waveland Field. Open diamonds: Basham–Nichols formations; gray circles: upper Borum formation; black squares: lower Borum formation. Matrix porosity versus permeability shows an exponential trend. Fractured samples show 100-fold increase in permeability versus nonfractured samples. Composite sandstone/dolomite porosity versus permeability trend lines modified after Coalson and others (1990) and Hartman and others (2000). (Sidewall-core analyses: PTS Labs, Houston, Texas for Southwestern Energy, personal communication, 2000–2004.)

shales act as regional and local décollement horizons. The thrust segments of this bedding plane ramp upward through the sandstone units of the lower Borum and upper Borum and the Nichols–Basham formations.

The subsurface exhibits two thrust styles.

1. A large amplitude propagation thrust-fold involving the entire Atokan stratigraphic section. This fold reflects the general surface fold. The main thrust appears to flatten at depth near the base of the Atoka Formation.
2. An anticlinal stack of low-angle thrusts involving only the middle Atokan stratigraphic section overlies the larger fold. The anticlinal thrust stack forms a duplex structure.

All the north-verging thrusts were emplaced in a normal sequence of development: older, structurally higher thrusts are deformed by younger, structurally lower thrusts. The large-amplitude propagation thrust folds the middle Atoka duplex structure.

The propagation thrust ramps up from a basal detachment near the base of the Atoka Formation (Arbenz, 1989). The detachment is recognized on COCORP Ouachita Line 1 (Lillie and others, 1983). The thrust carries a coherent back limb up to 4,000–4,900 ft thick. At the base of the lower Atoka, thrust throw is estimated to be 14,000 ft. The thrust offset diminishes upward as the fold tightens. At the upper detachment, thrust throw is approximately 6,000 ft. The thrust appears to flatten in a detachment horizon within the Turner formation and may climb northward into additional décollement horizons within the upper Atokan shales.

The middle Atoka duplex structure creates an antiformal fold. The amplitude of the duplex stack is 3,500–5,000 ft in height. Pre-thrust thickness for the middle Atoka is approximately 1,500 ft. Thrusts bounded between the lower Borum and the Borum shale repeat the lower Borum sandstone units.

The Borum shale is a detachment zone. The unit thickens from an unfaulted thickness of approximately 300 ft to more than 1,100 ft.

Two upper Borum major thrust sheets have been delineated by well penetrations. The upper two thrusts are major productive zones in the Waveland Field. The restored offset between the hanging wall (upper thrust) and footwall (lower thrust) is a minimum of 11,500 ft. This offset is a minimum because no wells or seismic data have yet defined the southern footwall cutoff for the thrust. On the upper thrust, along the crest of the larger propagation fold, thrust splays delineate the terminal end of the thrust sheet. A smaller, upper Borum triangle zone is created at the terminus of the each thrust as it flattens into a detachment zone in the Turner formation.

Based on well-log correlations and surface outcrops, the Basham and Nichols formations are exposed surrounding Blue Mountain Lake. Cohoon and Vere (1988) identified these outcrops as lower Atoka turbidite-channel sands. The Basham–Nichols sandstone ridges can be seen truncated

south of upper Atoka sandstone on north limb beneath a regional detachment.

Combined shortening estimated by all the thrusts encountered in the Waveland Field is estimated to be between 53,000–66,000 ft. The thrust solely involving the upper Borum duplex zone has approximately 20,000 ft of net horizontal offset. No major imbricate thrusts offset the upper Atoka Formation immediately north of the Ranger Anticline. The transfer of the shortening at Ranger Anticline is interpreted to continue northward and laterally westward toward the Washburn Anticline (Fig. 1).

### UPPER BORUM CORRELATION

In the Waveland Field, many wells have intersected the two productive upper Borum thrust sheets and encountered two complete upper Borum sections. Figures 6A and 6B are two stratigraphic cross sections of the upper Borum formation. The profiles are strike oriented for each thrust sheets. The profiles cover a two-mile horizontal distance. The two sections use the same wells but are split above and below by a major thrust. The sections are interpreted as unfaulted between the major thrusts in the shales at the base and top of the section. Each profile uses the top of the upper Borum as a datum. The closest spacing based on current drilling in the field is approximately 765 ft.

Gamma-ray interpolation is initially used to correlate the internal units of the upper Borum formation and identify the sand-prone units. This method maps the digital values of the gamma-ray log and extrapolates it toward the adjacent wells to distinguish clay content. Gamma-ray units less than 70 API units equate to sands. Shaly sands and silts are approximately 70–100 API units. Shales are more than 100 API units.

The initial interpolation of the upper Borum formation indicates the internal sands and shales expand or contract between the top and base. The base of the upper Borum is consistently the contact between clean Borum shale and the lowermost blocky upper Borum sandstones. The top of the

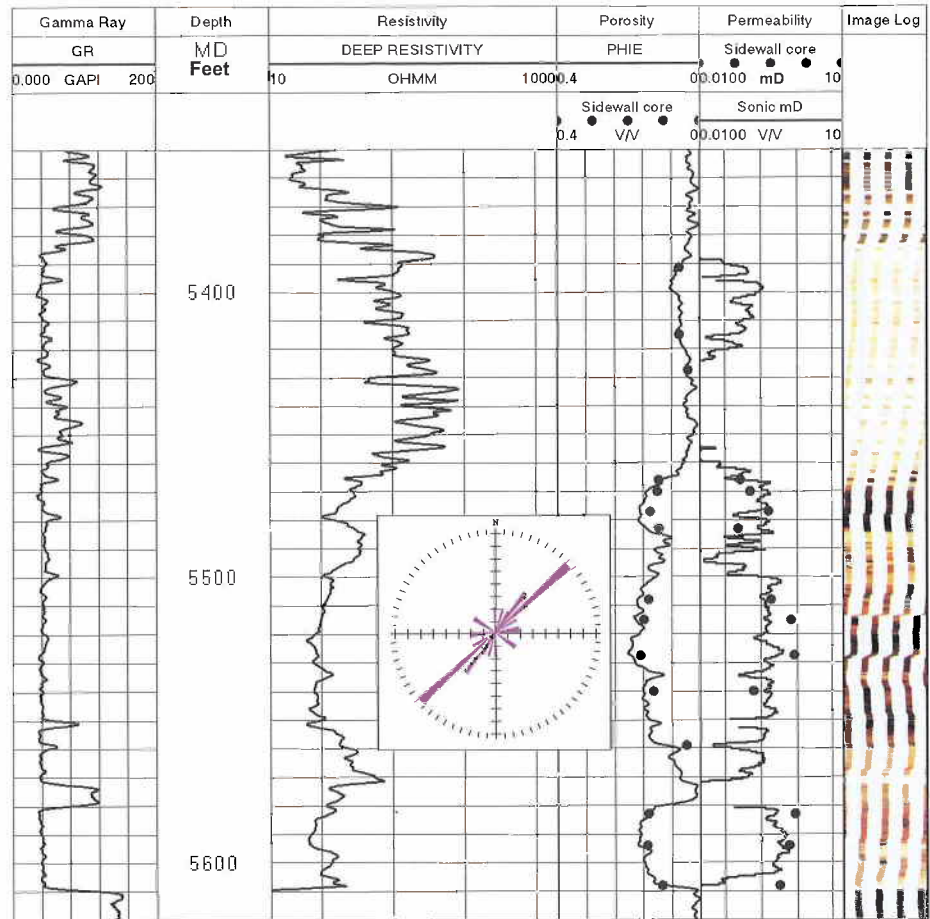


**Figure 5.** Type-log reservoir characteristics, Brasher #1–11 upper Borum A sand. Reservoir sands have a gamma ray value less than 70 API units. Sidewall-core porosity (solid circles) ranges from 3% to 17% (log porosity >8% shown by gray fill). Sidewall-core permeability (solid circles) ranges from <0.001 to 1.09 millidarcies. Dipole sonic (black line in Permeability track) shows estimated log permeability. Schlumberger oil-based mud images (OBMI) delineates 1–2 ft bed sets. Dark OBMI bands reflect lower resistivity and higher porosity zones, not shale. Fracture strike from the image log is represented in the Rose diagram as predominantly northeast–southwest. GAPI=gamma ray in American Petroleum Institute standard units, OHMM=ohm-meters, PHIE=calculated effective porosity V/V = decimal values, mD=millidarcies.

upper Borum is at the peak of an upward-thinning gamma ray profile and the Turner formation shales.

Three internal parasequence units are defined in the upper Borum formation. From base to top, the sequences are the C, B and A sands. The parasequences are based on coherent packages of upward-thinning clastic sequences and overlying conformable shales. The parasequence units can be delineated into thinner units, but for practical hydrocarbon management, reservoir sands are defined as a coherent package in pressure communication. Matrix permeability of juxtaposed sand beds and vertical fractures link bedding across thin shales.



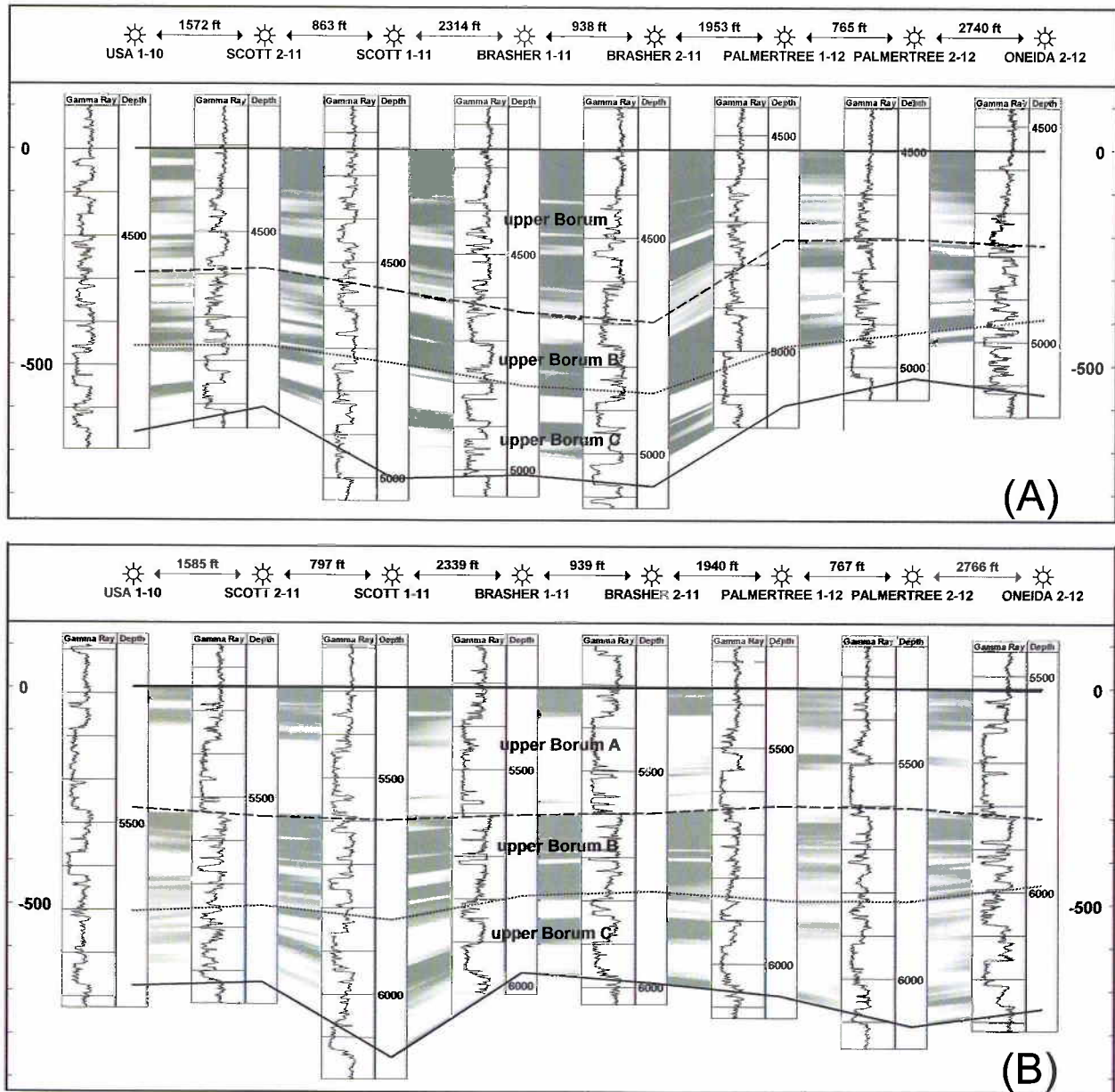


**Figure 6.** Upper Borum stratigraphic correlation (gray = shaly sands to shale; white = sand). Location of sections is shown on Figures 8, 9, and 10. (A) Upper thrust (Thrust #2): the upper Borum formation is characterized by three main upward-thinning gamma-ray profiles. The C sand is the dominant reservoir sand. (B) Lower thrust (Thrust #3): the upper Borum formation is dominated by two main reservoir sands, A and C.

The base C sand–base upper Borum formation is the same base of blocky sands against the underlying Borum shale. The boundary is sharp, but image logs show it is a conformable contact, with no erosional downcutting. The C sand consists of one or two blocky sands and is up to 100 ft in thickness. These blocky sands are found on the upper and lower thrust-sheet profiles with only minimal lateral variations. The top of the C sand is an upward-thinning profile positioned at overlying thicker shale or a sharp shale-break at the top of the

uppermost blocky sand. The base of the next higher upward-thinning profile defines the base of the B sand.

The B sand contains more shale than the C sand, but it has significant sands. If the B sand were solely shale, the top of this unit would be interpreted as the correlative unit to a maximum marine flooding surface, but the upward-thinning bedding profiles indicate the clastics were deposited between or near proximal sand-prone units. The B sand contains multiple upward-thinning shaly sand packages on both thrust sheets.

These shaly sands weakly correlate laterally across the upper and lower thrust cross section.

The A sand basal contact is at the base of blocky sands on the lower thrust and the base of an upward-thinning shaly sand package on the upper thrust. The difference between the two thrusts sheets is extreme when compared to the relative consistency of the blocky C sands or the relatively shale-prone B sands on both thrust sheets. The contrast is even greater given the 100–150 ft net sand for this unit on the lower thrust sheet. The lower thrust A sands are coherent across the strike profile. The A sand in the upper thrust sheet is shaly but exhibits an upward-thinning sequence. If the C sand is a proximal unit and the B sand is a distal unit, the A sand exhibits both characteristics, but this view is based on the areal extent shown in these profiles.

### UPPER BORUM RESTORATION

With the large thrust offset, restoration of the parasequence sets across faults is key to mapping the parasequences. The A and C sands appear to be laterally consistent over a cross-sectional distance, but differences exist across thrusts.

Serialized balanced profiles similar to Figure 7 were used to determine thrust-fault orientations. The upper thrust has a minimum of 11,500 ft of horizontal offset. The well penetrations for the A, B, and C parasequences for the upper thrust sheet were moved 11,500 ft south. The restoration juxtaposes the relative distances of the upper Borum in the upper and lower thrust-sheet penetrations of a single wellbore.

Figures 8, 9, and 10 are restored net-sand-isopach maps for each defined parasequence set. A gamma-ray cutoff of 70 API units is used to define clean sands versus shale, silts, or shaly sands. No bias is used in constructing the contours and all data values are honored. Profile lines from Figures 6A and 6B are indicated on the maps.

The net-sand-isopach map for the C sand (Fig. 8) indicates that the unit is extremely thick, but it is not a blanket unit. The map defines two or more amalgamated sand trends. The unit forms a sand body up to 6 mi wide and 6 mi long, which is the north–south extent of the data

points. Sands are greater than 100 ft thick but are separated by shale units less than 25 ft thick. Reservoir-quality sands are greater than 8% porosity and more than 50 ft thick.

The net-sand-isopach map for the B sand (Fig. 9) indicates that the unit is less extensive than the C sand but has linear sand trends that are 75–100 ft thick across the lower thrust. Reservoir-quality sandstones are greater than 8% porosity and more than 50 ft in thickness. The reservoir-sand trends overlie the thick net-sand trends.

The A sand isopach map (Fig. 10) indicates the sands are extremely thick and oriented east–southwest. The lower-thrust sand body is up to 2 mi wide and at least 5 mi in length. The sands amalgamate to more than 200 ft thick. Several north–south-oriented lobes up to 100 ft thick branch from the main east–south–east sand body. These side channels are less than 0.5 mi wide. Reservoir-quality sands are greater than 8% porosity and more than 50 ft thick. These reservoir-sand trends overlie thick net-sand trends with more than 100 ft thickness on the lower thrust. The reservoir-quality sands occur where sands are blocky.

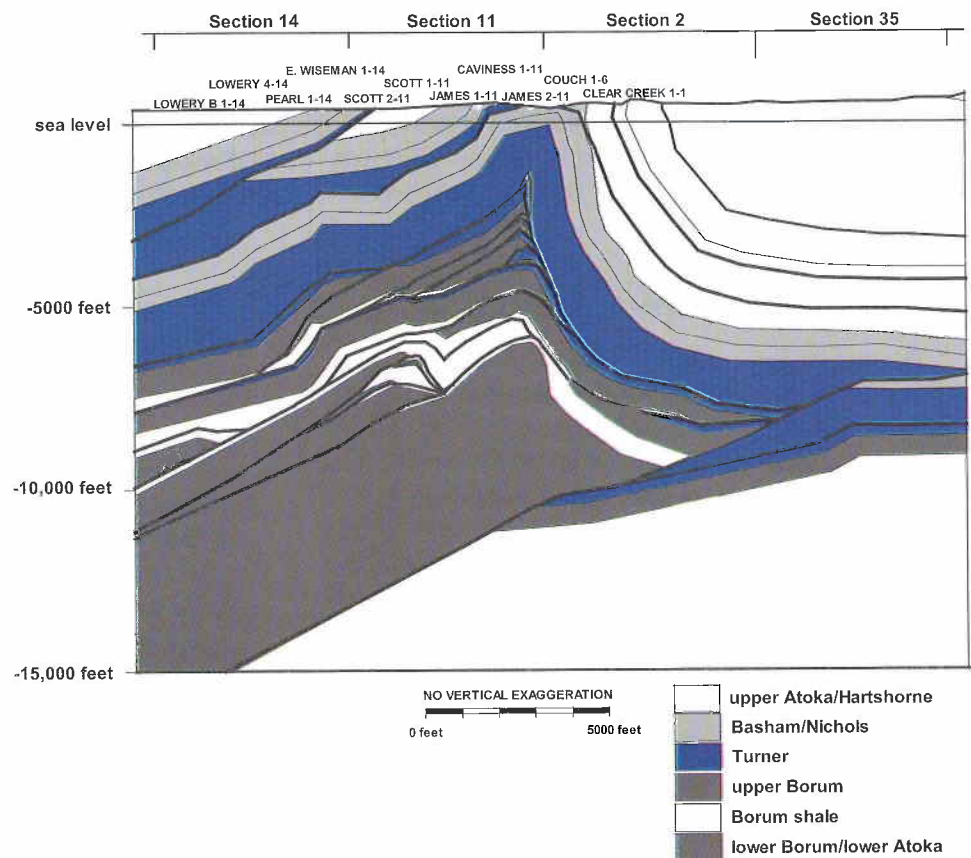


**Figure 7.** North–south structural cross section across the Waveland Field. Productive gas sands are found in the middle Atoka Basham–Nichols, upper Borum, and lower Borum formations. The profile illustrates the two levels of structure: (1) An upper, older, low-angle duplex zone involving the lower Borum to Basham. Regional shales between sand-prone units form detachment horizons; (2) A lower, younger, thrust-propagation fold deforming the duplex zone and involving the lower–upper Atoka strata.



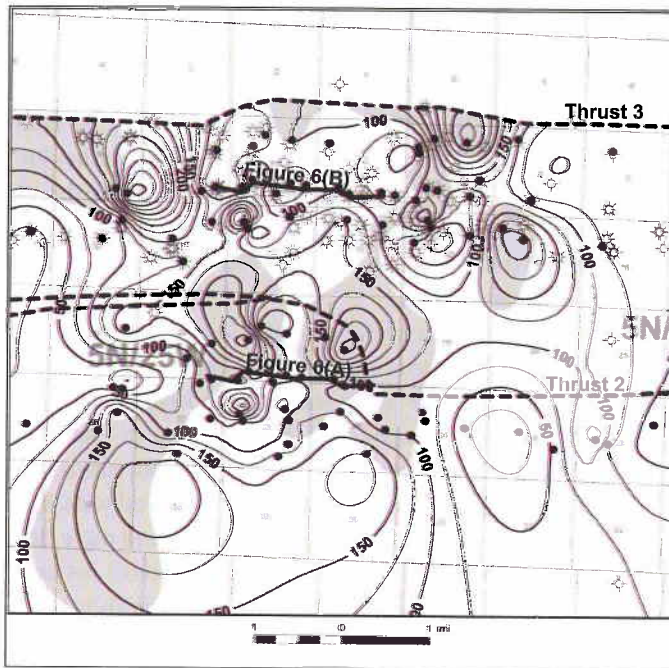


**Figure 8.** Thrust restoration, net-sand isopach, upper Borum C sand. Data points (black circles) restored to relative pre-thrust position (thrusts = dashed lines) indicate thick amalgamated sands greater than 100 ft thick form a 2–5-mi-wide anastomosing pattern. Current well positions are shown by well symbols. Net sand with porosity greater than 8% and more than 50 ft (gray filled polygons) overlies the thicker net-sand trends.

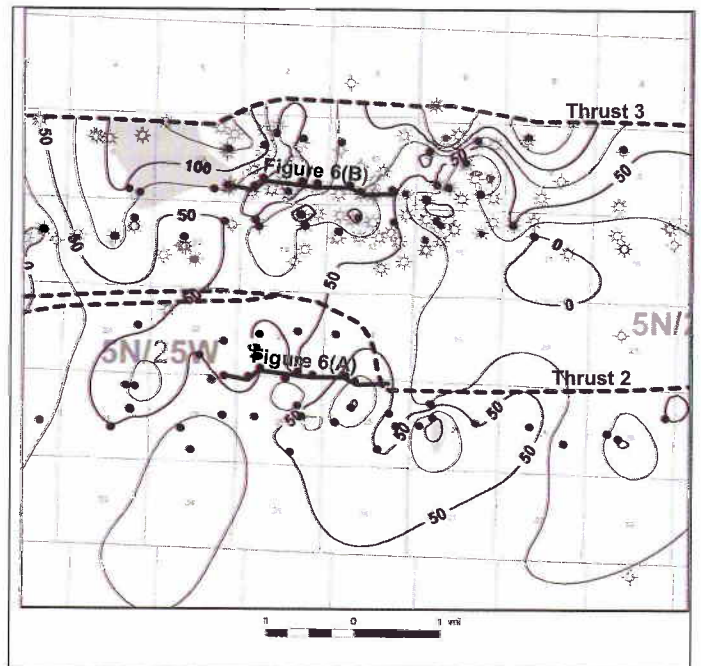


**Figure 9.** Thrust restoration, net-sand isopach, upper Borum B sand. Data points (black circles) restored to relative pre-thrust position (thrusts = dashed lines) indicate thick amalgamated sands more than 50–100 ft thick form trends that are several miles wide. Current well positions are shown by symbols. Net sand with porosity greater than 8% and more than 50 ft (gray filled polygons) overlies the thicker net-sand trends.

## DEPOSITIONAL MODEL

The middle Atoka sands over the Waveland Field are interpreted based on models for deep-water turbidites and low-stand – basin-floor fans (Vail and Wornardt, 1991; Bouma and others, 2002; Delery and Bouma, 2003). This interpretation is based on the external and internal characteristics summarized as follows.

1. The upper Borum sands are poorly sorted, clay-rich, and fine-grained.
2. Bed sets on image logs are 1–2 ft thick. The A and C sands amalgamate in blocky zones with more than 100 ft of net sand. The thick sands have few shale layers.
3. The base of the C and A sand parasequences exhibit sharp, nonerosional, basal contacts. Image logs show laminated to massive sands with convoluted bedding and slumps.
4. In the restored 40 mi<sup>2</sup> study area, the sandstone shows curvilinear trends that combine into 4- to 6-mi-wide composite bodies. The aspect ratio of channel-width – to – thickness is greater than 100:1, typical of the fine-grained, mud-rich fans described by Delery and Bouma (2003).

5. Thick regional Borum and Turner shales encase the upper Borum sands.

## DISCUSSION

The low-stand – basin-floor-fan model seems incompatible because the global sea level during the Atokan was relatively high (Vail, 1977).

What processes could deliver sands into the deep-water Arkoma Basin during the Late Pennsylvanian age?

The Atokan age lasted 3.7 million years, from 311.7 to 308 Ma (Rohde, 2004). The Atoka Formation in the immediate vicinity of the Waveland Field is approximately 14,900 ft thick. If the Atokan age is evenly divided by the Atoka Formation thickness, the 550–650-ft-thick, middle Atoka–upper Borum formation was likely deposited in a span of approximately 100,000–200,000 years. This corresponds to a fourth-order cycle. The internal, upper Borum parasequences are interpreted as fifth-order depositional cycles and each parasequence spans less than 100,000 years.

The Atokan-age sediments occurred during the same time as the Late Mississippian–Pennsylvanian glaciation across southern Gondwanaland. Interglacial (flooding) and glacia-

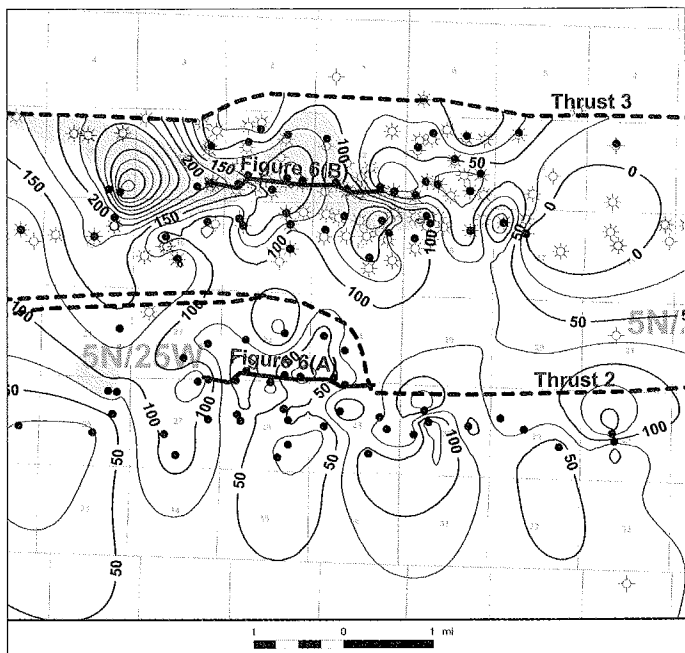


**Figure 10.** Thrust restoration, net-sand isopach, upper Borum A sand. Data points (black circles) restored to relative pre-thrust position (thrusts = dashed lines) indicate thick amalgamated sands more than 100 ft thick form a 2- to 4-mi-wide fan pattern. Current well positions are shown by symbol. Net sand with porosity greater than 8% and more than 50 ft (gray filled polygons) overlies the thicker net-sand trends.

tion (sea-level fall) cycles are being interpreted during the upper Atokan–Desmoinesian age (Smith and Reed, 2000; Scheffler and others, 2003; Saltzman, 2003). These glacial-driven sea-level events are fourth- to fifth-order sea-level cycles.

The Arkoma Basin was the terminal basin for the Atokan clastics derived from the structural highs of the Appalachian Mountains (Link and Roberts, 1986). The Atoka Formation is considered a mud-rich clastic system due to the high clay content within the sands and the net sand-to-shale volume for the entire Atoka Formation. High sea level and distance of source contributed to the fine-grained dominance of these clastic sediments.

The upper Borum parasequences are interpreted here as reflecting periods of bypass of fine-grained sands from the Arkoma Basin shelf into deep water.

## CONCLUSIONS

The characterization of the Waveland Field continues to define aspects of the Arkoma Basin. Thrust faulting is dominant in the field and in the southern part of the basin. The Waveland Field structure is characterized by major duplex structures controlled by the mechanical aspects of the middle

Atoka lithostratigraphic units. The deformation shows a major impact on the natural-fracture characteristics in the reservoirs.

The middle Atoka formations are major parasequence units within the Atoka Formation. Predictive reservoir trends are tested by increased drilling and are actively modified by understanding the upper Borum formation turbidite model. The reservoir data show a clear relationship of porosity and permeability to the middle Atokan sand trends.

The middle Atokan tight gas sands are an underexploited resource in the Arkansas Arkoma Basin. Well logs are the primary data in mapping the subsurface in the basin. Newer field rules allowing tighter well spacing have increased active drilling and gas production.

## ACKNOWLEDGMENTS

I would like to thank Executive Vice President Richard Lane of Southwestern Energy and Vice President John D. Thaler of SEECO, Inc., and my fellow Southwestern Energy teammates for their encouragement and permission to present this paper. I would also like to thank Charlie Stone (Arkansas Geological Commission) for his encouragement and enthusiasm in promoting Arkansas geology. Geosystems (Houston, Texas) conducted the thin-section analyses and PTS Labs (Houston, Texas) carried out the sidewall-core analyses for Southwestern Energy.

## REFERENCES CITED

- Arbenz, J. K., 1989, Ouachita thrust belt and Arkoma Basin, in Hatcher, R. D., Jr.; Thomas, W. A.; and Viele, G. W. (eds.), *The geology of North America, the Appalachian–Ouachita orogen in the United States*: Geological Society of America, v. F-2, p. 621–634.
- Arkansas Oil and Gas Commission (AOGC), 1967a, Order reference #6-67 Waveland Field Rules: available in the public record at AOGC office, El Dorado and Fort Smith, Arkansas.
- \_\_\_\_\_, 1967b, Order reference #97-67 Waveland Field Rules: available in the public record at AOGC offices, El Dorado and Fort Smith, Arkansas.
- \_\_\_\_\_, 1968, Order reference #11-68 Waveland Field Rules: available in the public record at AOGC offices, El Dorado and Fort Smith, Arkansas.
- \_\_\_\_\_, 2003, Order Reference #20-2003-02 Waveland Field Rules, order and public exhibits by Southwestern Energy: available in the public record at AOGC offices, El Dorado and Fort Smith, Arkansas.
- \_\_\_\_\_, 2004, Order reference #86-2004-07 Waveland Field Rules, order and exhibits by Southwestern Energy: avail-

- able in the public record at AOGC offices, El Dorado and Fort Smith, Arkansas.
- Blythe, A. E.; Suga, Arnon; and Phipps, S. P., 1988, Structural profiles of Ouachita Mountains, Western Arkansas: American Association of Petroleum Geologists Bulletin, v. 72, p. 810–819.
- Bouma, A. H.; Sprague, R. A.; and Khan, A. M., 2002, Geological reservoir characteristics of fine-grained turbidite systems: Gulf Coast Association of Geological Societies Transactions, v. 52, p. 59–64.
- Coalson, E. B.; Hartmann, D. J.; and Thomas, J. B., 1990, Applied petrophysics in exploration and exploitation: notes from short course sponsored by University of Colorado–Denver, var. pages.
- Cohon, R. R.; and Vere, V. K., 1988, Blue Mountain Dam and Magazine Mountain, Arkansas, *in* G. T. Hayward (ed.), Centennial Field Guide—South Central Section: Geological Society of America, v. 4, p. 243–248.
- Delery, A. M.; and Bouma, A. H., 2003, Aspect ratios in coarse-grained and fine-grained submarine fan channels: Gulf Coast Association of Geological Sciences/Gulf Coast Society of SEPM, v. 53, p. 170–182.
- Denison, R. E., 1989, Foreland structure adjacent to the Ouachita foldbelt, *in* Hatcher, R. D., Jr.; Thomas, W. A.; and Viele, G. W. (eds.), The geology of North America, the Appalachian-Ouachita orogen in the United States: Geological Society of America, v. F-2, p. 681–688.
- Elmore, R. D.; Sutherland, P. K.; and White, P. B., 1990, Middle Pennsylvanian recurrent uplift of the Ouachita fold belt and basin subsidence in the Arkoma Basin, Oklahoma: Geology, v. 18, p. 906–909.
- Hartman, D. J.; Beaumont, E. A.; and Coalson, Edward, 2000, Predicting sandstone reservoir system quality and example of petrophysical evaluation: Search and Discovery article #40005, <http://www.searchanddiscovery.net/documents/beatmont/index.htm>
- Lillie, R. J.; Nelson, R. D.; De Voogd, Beatrice; Brewer, J. A.; Oliver, J. E.; Brown, L. D.; Kaufmann, Sidney; and Viele, G. W., 1983, Crustal structure of Ouachita Mountains, Arkansas: a model based on integration of COCORP reflection profiles and regional geophysical data: American Association of Petroleum Geologists Bulletin, v. 67, p. 907–931.
- Link, M. H.; and Roberts, M. T., 1986, Pennsylvanian paleogeography for the Ozarks, Arkoma, and Ouachita Basins in east-central Arkansas: Arkansas Geological Commission Guidebook 86-3, p. 37–60.
- PI/Dwights Plus on CD, 2004, Louisiana and Arkansas production data: IHS Energy, v. 14, no. 9.
- Rohde, R. A., 2004, GeoWhen database: <http://www.stratigraphy.org/geowhen>
- Saltzman, M. R., 2003, Late Paleozoic ice age: oceanic gateway or pCO<sub>2</sub>? Geology, v. 31, p. 151–154.
- Scheffler, Kay; Hoernes, Stephan; and Schwark, Lorenz, 2003, Global changes during Carboniferous-Permian glaciation of Gondwana: linking polar and equatorial climate evolution by geochemical proxies: Geology, v. 31, p. 605–608.
- Smith, L. B.; and Reed, J. F., 2000, Rapid onset of Late Paleozoic glaciation on Gondwana: evidence from Upper Mississippian strata of the Midcontinent, United States: Geology, v. 28, p. 279–282.
- Sutherland, P. K., 1988, Late Mississippian and Pennsylvanian depositional history in the Arkoma Basin, Oklahoma and Arkansas: Geological Society of America Bulletin, v. 100, p. 1787–1802.
- U.S. Geological Survey, 2004, The national map seamless data distribution system, EROS Data Center, USGS, projection: UTM (Ft) NAD 1927. <http://seamless.usgs.gov>
- Vail, P. R.; and Wornardt, Walter, Jr., 1991, An integrated approach to exploration and development in the 90s: well log-seismic sequence stratigraphy analysis: Transactions—Gulf Coast Association of Geological Sciences, v. XLI, p. 630–650.
- Van Wagoner, J. C.; Mitchum, R. M.; Campion, K. M.; and Rahmanian, V. D., 1990, Siliciclastic sequence stratigraphy in well logs, cores, and outcrops: concepts for high-resolution correlation of time and facies: American Association of Petroleum Geologists, Methods in Exploration Series, no. 7, 55 p.

# Outcrop Fracture Characterization of Pennsylvanian Jackfork Group Sandstones, Ouachita Mountains, Southeastern Oklahoma

***Kevin J. Smart***

Southwest Research Institute®  
San Antonio, Texas

***Seth Busetti***

University of Oklahoma  
Norman, Oklahoma

***Kimberly Scott***

Chesapeake Energy Corporation  
Oklahoma City, Oklahoma

***Roger M. Slatt***

University of Oklahoma  
Norman, Oklahoma

**ABSTRACT**—The Ouachita Mountains Fold–Thrust Belt in Oklahoma and Arkansas represents the exposed portion of a >2,000-km-long (>1200-mi-long) orogenic system that includes the Marathon Thrust Belt in Texas and the Appalachian orogenic system. The majority of the Oklahoma Ouachitas consists of Mississippian to Pennsylvanian clastic rocks of the central Ouachitas that are deformed into broad, open synclines separated by tight (thrust-cored) anticlines. The Pennsylvanian Jackfork Group, a deepwater turbidite deposit, is a major exposed stratigraphic interval in the central Ouachitas and plays an important role in Oklahoma as a tight-gas reservoir (e.g., the Potato Hills Field). Outcrop fracture characterization was undertaken as part of a larger structural and stratigraphic study. The goals were to collect and synthesize fracture data from surface exposures and to formulate relationships that could be used as predictive tools for subsurface exploration.

Fractured bedding pavements on the Lynn Mountain and Rich Mountain Synclines were analyzed to assess the relationship between stratigraphic and structural fracture controls. Linear scanlines were used to collect orientation and intensity data, along with stratigraphic and mechanical bed thicknesses from 31 sandstone beds. Two orthogonal, bed-normal fracture sets were identified. The first set is parallel to bedding strike and has tracelengths ranging from 20 to 500 cm (8 to 197 in.) with a median length of 66 cm (26 in.). The second set is parallel to bedding dip, typically have a shorter median tracelength (39 cm [15 in.]), and terminates against the first set approximately 80% of the time. Average spacing for Set 1 fractures is approximately 30 cm (12 in.) whereas the average spacing for Set 2 fractures is slightly more than 40 cm (16 in.). Set 1 fractures show a moderate positive correlation between spacing and layer thickness and are characterized by spacing-to-layer thickness ratios of 0.4 to 4.5 (mean is 1.3). Set 2 fractures have a weaker but still positive correlation between spacing and thickness, and spacing-to-layer thickness ratios that range from 0.3 to 3.5 (mean is 1.1).

The bedding-normal orientation of both fracture sets suggests that they developed prior to or during development of the Lynn Mountain and Rich Mountain Synclines. The longer tracelength of the Set 1 fractures, coupled with the high percentage of Set 2 fractures abutting against Set 1 fractures, may indicate that the Set 1 fractures developed somewhat earlier than the Set 2 fractures. Estimation of average fracture spacing based on layer thickness is likely to be an effective predictive tool for Jackfork sandstone beds in similar structural positions in the Ouachitas.

## INTRODUCTION

The Ouachita Mountains in Oklahoma and Arkansas represent a portion of the late Paleozoic orogenic belt that extends from Alabama, through Mississippi, Arkansas, and Oklahoma, into southwestern Texas (Viele, 1989). Similar to the Appalachians, this orogenic belt marks the final assembly of Pangea following collision of Laurasia and Gondwana in the late Paleozoic (Arbenz, 1989a; Thomas, 1989; Viele, 1989; Viele and Thomas, 1989). Although the Ouachitas share a somewhat similar tectonic history with the Appalachians, the Ouachitas are different in that they are a clastic-dominated system. Unlike the Appalachians, the Ouachitas lack a thick carbonate strut in the older part of the stratigraphy. In fact, the Ouachitas are somewhat unique in that the lower portion is dominated by weak shales whereas the upper part contains a greater percentage of strong sandstones (Arbenz, 1989b). Thus, the mechanical framework of the Ouachitas is significantly different from most other fold-thrust systems (Couzens and Wiltschko, 1996).

The Oklahoma Ouachitas (Fig. 1) have typically been divided into three regions on the basis of stratigraphy and structural style (Suneson and others, 1990). The relatively narrow frontal zone marks the transition from the foreland Arkoma Basin to the Ouachita Mountains proper and is characterized by imbricated and tightly folded Early Pennsylvanian clastic rocks. The mapped trace of the Choctaw Fault forms the northern and western boundary whereas the Windingstair Fault separates the frontal zone from the central Ouachitas (Arbenz, 1989a). The central Ouachitas, a wide zone dominated by Mississippian to Early Pennsylvanian clastic rocks, is characterized by northwest-vergent thrust faults and open synclines. The Potato Hills are a roughly elliptical exposure of middle Ordovician through Early Mississippian rocks within the otherwise younger stratigraphy (Arbenz, 1989a). The Broken Bow Uplift is the most structurally complex province in the Oklahoma Ouachitas and consists of weakly metamorphosed Early Ordovician to Early Mississippian rocks. These rocks exhibit tight to isoclinal folds that are south-vergent and record at least two episodes of deformation (Feenstra and Wickham, 1975; Nielsen and others, 1989).

The Pennsylvanian Jackfork Group is a major exposed interval in the central Ouachitas and is recognized as a deepwater turbidite deposit (e.g., Cline, 1970; Morris, 1989; Pauli, 1994; Montgomery, 1996a,b; Slatt and others, 2000; Tillman, 2000). Sandstone beds in the Jackfork Group play an important role in Oklahoma as a tight-gas reservoir (e.g., the frontal zone and the

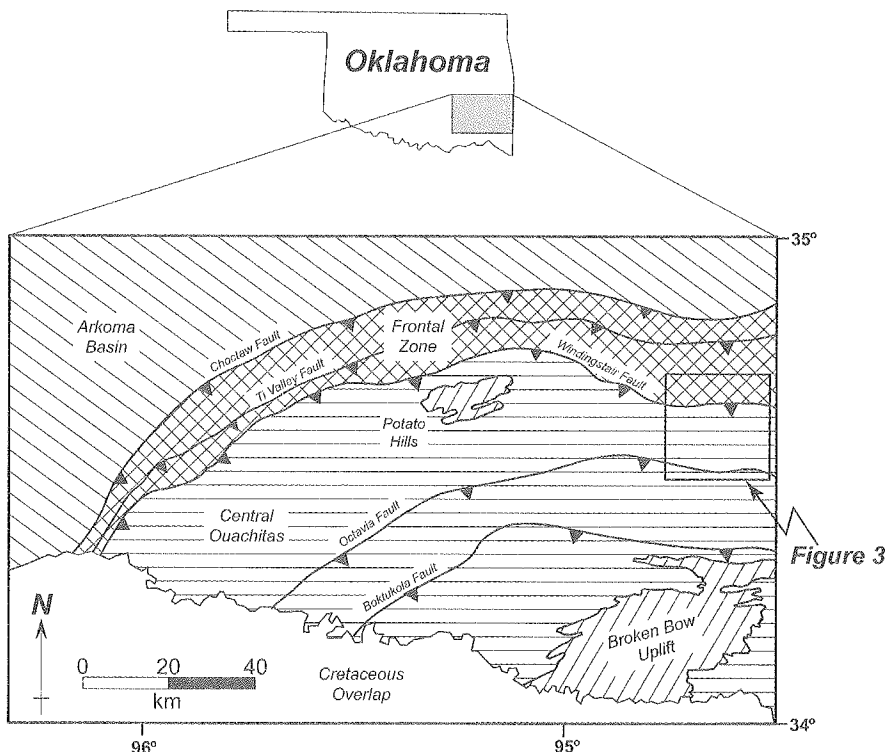


**Figure 1.** Map showing general tectonic-structural setting of Ouachitas including the study area.

Potato Hills Field) with much of the focus on exploitation of fractured channel sandstones (Montgomery, 1996a). The Jackfork Group (Fig. 2) is divided into five major formations, which are, in order of deposition, the Wildhorse Mountain, Prairie Mountain, Markham Hill, Wesley, and Game Refuge (Legg and others, 1990; Montgomery, 1996a; Tillman, 2000). The lowermost Wildhorse Mountain Formation consists of 800–975 m (2,700–3,200 ft) of fine- to coarse-grained sandstone with intervals of silty shale. A 0.6-m-thick (2-ft-thick) siliceous shale generally separates the Wildhorse Mountain Formation from the 450-m-thick (1,500-ft-thick) Prairie Mountain Formation, which is essentially compositionally indistinct from the Wildhorse Mountain Formation. The Markham Hill Formation contains 90–140 m (300–450 ft) of interbedded sandstone and shale. The Wesley Formation consists of 45–120 m (150–400 ft) of shale, chert, and fine-grained sandstone. As much as 150 m (500 ft) of shale and sandstone in the Game Refuge Formation separates the Jackfork Group from the overlying Pennsylvanian Johns Valley Shale.

### Project Rationale

Although the stratigraphic architecture of the Jackfork Group in the Ouachitas has been well studied and the macroscale structural style is reasonably well understood, little detailed work has been published on smaller-scale geologic structures such as fractures. The increased interest in exploration of Jackfork reservoirs, together with recognition that fractures play an important role in

PENNSYLVANIAN	Atoka	Atoka Formation	
		Johns Valley Shale	
	Morrowan	Jackfork Group	Game Refuge Formation
			Wesley Formation
			Markham Hill Formation
			Prairie Mountain Formation
			Wildhorse Mountain Formation
MISSISSIPPIAN	Meramecian and Chesterian	Stanley Group	

**Figure 2.** Simplified stratigraphic column for Jackfork Group (modified from Legg and others, 1990; Pauli, 1994).

the reservoir dynamics of these sandstone intervals, provided the impetus for our study.

Although a general correlation of fracture intensity and lithology (i.e., stronger rock equals greater intensity) has been accepted for some time (e.g., Price, 1966; Stearns and Friedman, 1972; Ladeira and Price, 1981; Narr and Currie, 1982), the full extent of this parameter has not been fully assessed and some disagreement exists (e.g., Narr, 1991; Narr and Suppe, 1991). Several years of field study in south-central Arkansas (see summary in Slatt and others, 2000) support the causal relationship between lithology and fractures. Clean, quartz-cemented sandstones appear to be more prone to fracturing than are sandstones with a muddy matrix. Both sandstone types are common in the Jackfork and owe their primary depositional, and subsequent diagenetic, characteristics to different parts of a turbidite succession. Specifically, well-sorted clean sandstones are the product of high-energy, turbidity-current deposition. Muddy sandstones are the product of lower-energy turbidity currents or sandy debris-flow deposition. Upon burial, clean sandstones become tightly cemented by

quartz, because there are no silt or clay particles to prevent nucleation of quartz cement onto quartz grains (Al-Siyabi, 1998).

An often-quoted observation in structural geology is that fracture spacing in layered (i.e., sedimentary) rocks is nearly equal to the thickness of the stratigraphic beds (e.g., Price, 1966; Huang and Angelier, 1989; Narr and Suppe, 1991; Gross, 1993; Ji and Saruwatari, 1998), which is recognized by a fracture-spacing to layer-thickness (S/T) ratio of nearly 1. In a recent article, Bai and Pollard (2000) summarized data from numerous published sources that showed that this rule holds for many examples, but that exceptions do occur (e.g., Ladeira and Price, 1981; Narr and Suppe, 1991).

Outcrop fracture characterization was undertaken as part of a larger structural and stratigraphic study. The goals were to collect and synthesize fracture data from surface exposures and to formulate relationships that could be used as predictive tools for subsurface exploration. In particular, we wanted to investigate the extent to which layer thickness in well-cemented Jackfork sandstone beds could be used as a predictive tool for subsurface fracture characteristics, especially fracture intensity.

### Study Location

The study area (Figs. 1, 3) is located within the Lynn Mountain and Rich Mountain Synclines in Le Flore County, Oklahoma. Three outcrops that included 11 bedding surfaces in the northern limb of the Lynn Mountain Syncline along U.S. Highway 259 (secs. 26, 27, and 34, T. 2 N., R. 25 E.) were studied in detail. An additional location with seven bedding surfaces on the south limb, but near the nose of the Lynn Mountain Syncline (secs. 8 and 9, T. 2 N., R. 25 E.), was also examined. Outcrop measurements were conducted on 13 sandstone beds in the north limb of the Rich Mountain Syncline along the Talimena Drive scenic road (sec. 36, T. 3 N., R. 25 E.; sec. 1, T. 2 N., R. 25 E.; sec. 6, T. 2 N., R. 26 E.).

The study outcrops (Fig. 4A) contain excellent exposures of sandstone and shale beds that are primarily within the Wildhorse Mountain Formation (i.e., the lower Jackfork Group). Two distinct sandstone lithologies are present (Pauli, 1994; Omatsola, 2003). One lithology consists of well-cemented sandstones that generally occur as planar, continuous beds ranging from centimeters to hundreds of centimeters (several inches to several feet) thick. The second type of sandstone bed is poorly cemented and essentially unconsolidated. The fracture analyses presented here focused on the well-cemented sandstone beds, as fracture preservation is poor in the unconsolidated beds.

### METHODOLOGY

Standard linear-scanline techniques (Fig. 4B) were employed for this study to collect systematic measurements of fractures from 33 Jackfork sandstone beds (Priest and Hudson, 1981; LaPointe



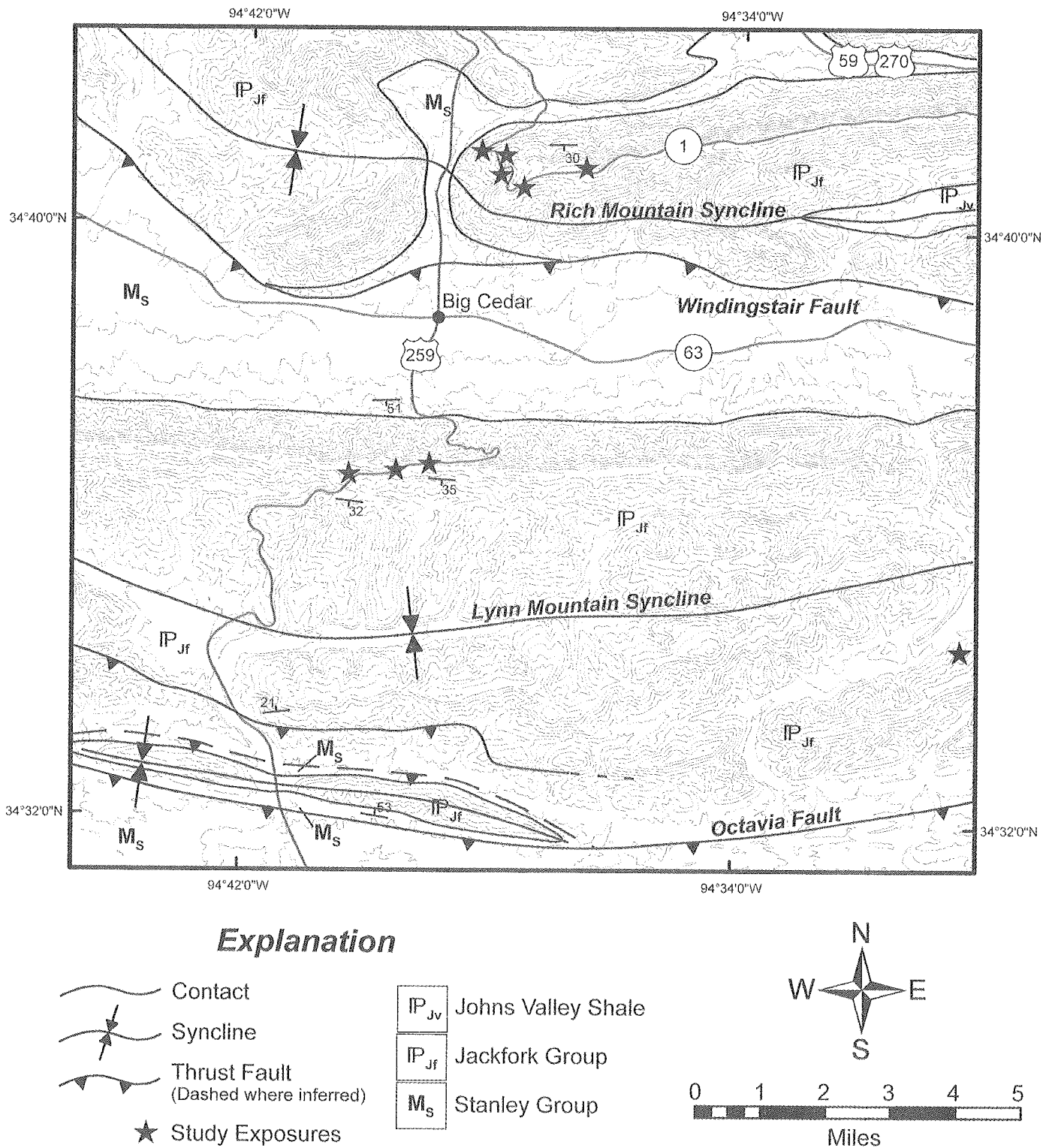


**Figure 3.** Simplified geologic map of the study area showing Jackfork Group exposures with respect to the folds and faults, as well as major roads. Geologic contacts and structures are compiled from Miser (1954), Hart (1963), Seely (1963), and Briggs (1973). Contours are from USGS 1:100,000 topographic maps.

and Hudson, 1985; Priest, 1993). This approach is advantageous because it allows a large quantity of data to be collected relatively quickly. The orientation (i.e., strike and dip) of each bed was recorded along with the stratigraphic layer thickness. The thickness and lithology (i.e., sandstone versus shale) of surrounding beds was also documented. For a limited number of Jackfork layers, fractures were observed to cross more than one sandstone bed in the absence of an intervening shale layer. For this situation, an additional measurement of mechanical layer thickness (sum of stratigraphic bed thicknesses) was recorded. Observations were made on the fracture-termination type. Termination types were classified into one of three categories: abutting fractures terminated against another fracture, blind fractures ended within the rock volume, and covered fractures extended beyond the visible exposure. For each sampled sandstone bed, a 100-m (300-ft) measuring tape was deployed across the exposure. The orientation of the

scanline was recorded with respect to the bedding orientation. For scanlines that are not oriented orthogonal to fractures, the scanline orientation was used to correct fracture-spacing measurements and provide the true spacing (Terzaghi, 1965).

Data collection focused on orientation, spacing, and trace length for each fracture that intersected the scanline. Initial observations of the Jackfork exposures revealed an orthogonal fracture pattern that suggested the presence of two primary bedding-perpendicular fracture sets defined by orientation—one set approximately parallel to bedding strike and one set perpendicular to bedding strike. Once quantitative measurements confirmed this qualitative observation, measured fractures were further categorized into sets.

## RESULTS

Jackfork Group exposures in the Ouachitas of southeastern Oklahoma consist of interbedded sandstone and shale, with layers ranging from centimeters to hundreds of centimeters (tens of inches to several feet) in thickness. The average bedding orientation for all outcrops in the study area is N.89°W., 33°SW (Fig. 5A). The sandstone beds can be divided into two primary types on the basis of their cementation characteristics and morphology (Slatt and others, 2000; Omatsola, 2003; Romero, 2004). The well-cemented sandstones typically occur as laterally continuous tabular bodies that have been interpreted to represent distal sheet-sand deposition. The poorly cemented sandstones are commonly thick-bedded lenticular bodies that are inferred to represent channel-fill deposits.

Initial observations revealed a blocky, orthogonal fracture pattern formed by two prominent fracture orientations or sets. A pilot study was conducted by Combs-Scott and Smart (2002) using eight sandstone beds from two outcrop exposures on the north limb of the Lynn Mountain Syncline. This study demonstrated that the orthogonal pattern is formed by two bedding-perpendicular fracture sets. The first set is oriented nearly parallel to bedding strike, whereas the second is parallel to bedding dip. Further, the fractures in the sandstone beds are strata-bound in that they are typically confined to a single stratigraphic layer, rather than crossing intervening shale layers. A more comprehensive study was undertaken by Busetti (2003) and forms the basis for most of the material presented here.

Busetti (2003) confirmed the presence of the two primary fracture sets (Figs. 5A, 5B). The Set 1 fractures have an average orientation of N.81°W., 58°NE. The Set 2 fractures have an average orientation of N.14°E., 87°SE. Both sets are well developed on all sandstone beds on the north limb of the Lynn Mountain Syncline. Set 2 fractures were also well developed on nearly all bedding surfaces in the Rich Mountain Syncline. Interestingly, Set 1 fractures were observed only sporadically on approximately two-thirds of the Rich Mountain sandstone beds. Busetti (2003) also noted two poorly developed secondary fractures sets that were

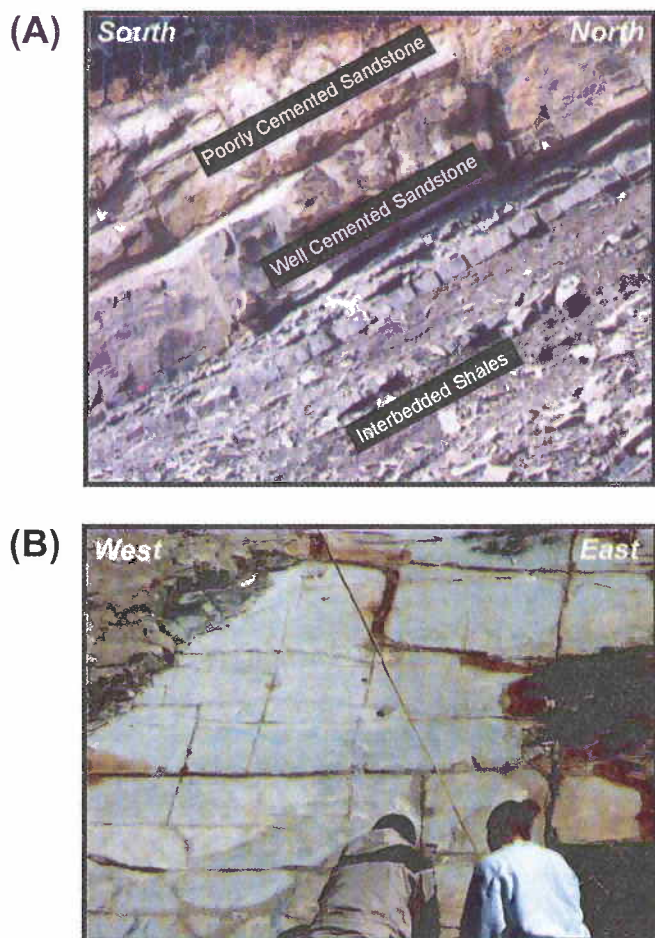


**Figure 4.** Outcrop photographs of Jackfork Group exposures on the north limb of the Lynn Mountain Syncline. (A) Comparison of well-cemented versus “punky” sandstone beds. The well-cemented sandstone in the photograph is approximately 1.2 m (4 ft) thick. (B) Illustration of scanline technique. View is toward the north looking down onto the bedding pavement.

present at only selected exposures. One set was oriented approximately N.35°W whereas the other trended approximately N.55°E. Neither set was abundant enough for detailed characterization.

Detailed measurements show that fracture spacings in the Jackfork Group are quite variable (Table 1). The median spacing for Set 1 fractures was approximately 30 cm (12 in.), although individual measurements ranged from 6 to 72 cm (2 to 28 in.). The average spacing for Set 2 fractures was approximately 40 cm with a slightly larger range of 8 to 97 cm (3 to 38 in.). For any individual sandstone bed, the ratio of Set 2 to Set 1 spacing averaged approximately 1.5, although the ratio ranged from as little as 0.8 to as much as 2.8.

Qualitative observations (Figs. 6A, 6B) suggested that the strike-parallel fractures (i.e., Set 1) were longer than the dip-parallel (Set 2) fractures; this was confirmed by the scanline measurements. The distribution of fracture tracelengths, however, is

rather skewed, with greater than two-thirds of the fractures having tracelengths of less than 100 cm (39 in.) but some exceeding 500 cm (197 in.) in length (Fig. 7). The median tracelength for Set 1 fractures is 66 cm (26 in.) whereas the median for Set 2 fractures is approximately 39 cm (15 in.).

As discussed in the Methodology section, the termination of each fracture was categorized as abutting, blind, or not exposed. Overall, nearly two-thirds (65%) of the Set 1 fractures abut against other fractures. The remaining one-third is dominated by blind fractures (Fig. 8A). In contrast, 4 out of 5 (80%) Set 2 fractures abut against other fractures (Fig. 8B). Again, the remainder is dominantly blind.

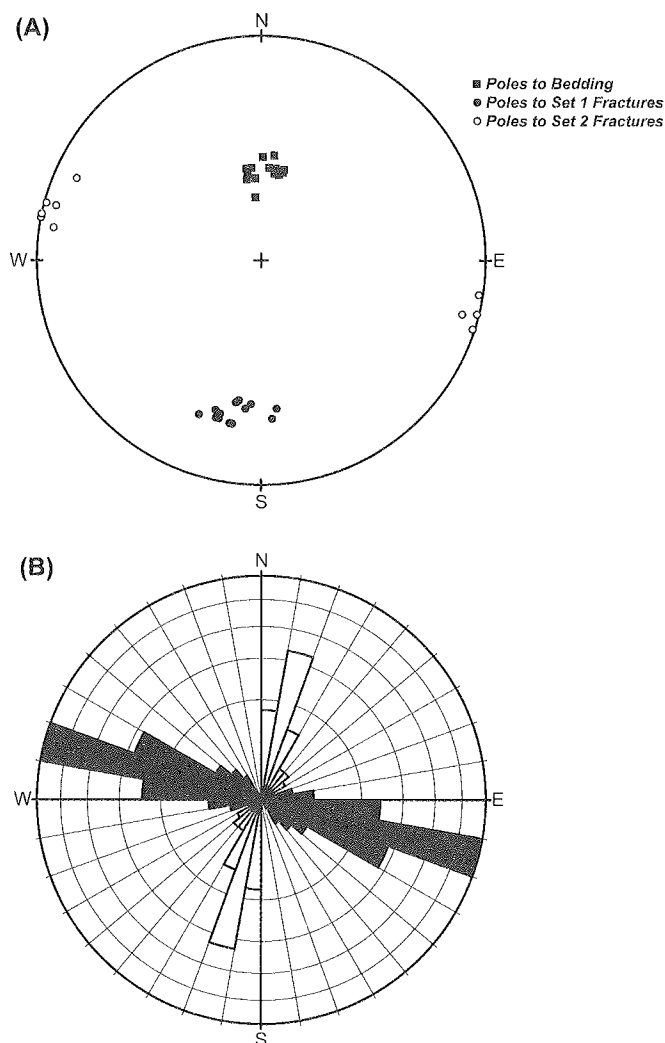
## DISCUSSION

Based on bedding-normal orientation, both fracture sets could have formed prior to or during development of the Lynn Mountain and Rich Mountain Synclines. Relative timing of fracture formation is not simple and straightforward. The overall termination pattern suggests that Set 1 fractures slightly predate Set 2 fractures because 80% of Set 2 fractures abut against other fractures, although local exceptions were observed in which Set 1 fractures terminated against Set 2 fractures (Fig. 6B). This interpretation of relative timing is also supported by the tracelength data which show that Set 1 fractures are approximately 1.7 times longer than the Set 2 fractures.

The fracture data demonstrate that a moderate positive correlation exists between spacing and layer thickness in the Jackfork Group exposures that were examined (Fig. 9A). As previously noted, the S/T ratio has been used to quantify the relationship between fracture spacing and sedimentary layer thickness. The S/T ratio for Set 1 ranges from 0.4 to 4.5 and has a mean value of 1.3 (Table 1). Set 2 S/T ratios range from 0.3 to 3.5 with a mean value of 1.1. Many of the Jackfork sandstone beds have fracture spacings that are roughly equal to the layer thickness (i.e., an S/T ratio near 1), but exceptions occur. The S/T ratios are most variable for the thinner beds, with the very thinnest beds displaying the largest ratios (Fig. 9B). In contrast, the thicker beds are characterized by a smaller range with values generally close to or slightly less than 1. Based on this data set, it appears that predictions of fracture spacing as a function of layer thickness is most appropriate for Jackfork sandstone beds that are at least 30 to 40 cm (12 to 16 in.) thick.

## CONCLUSIONS

Jackfork Group sandstone beds exposed in the Lynn Mountain and Rich Mountain Synclines in southeastern Oklahoma display two well-developed fracture sets that are oriented perpendicular to bedding and appear to have formed prior to or during syncline development. The first set is approximately parallel to bedding strike with a mean orientation of N.81°W, 58°NE.,



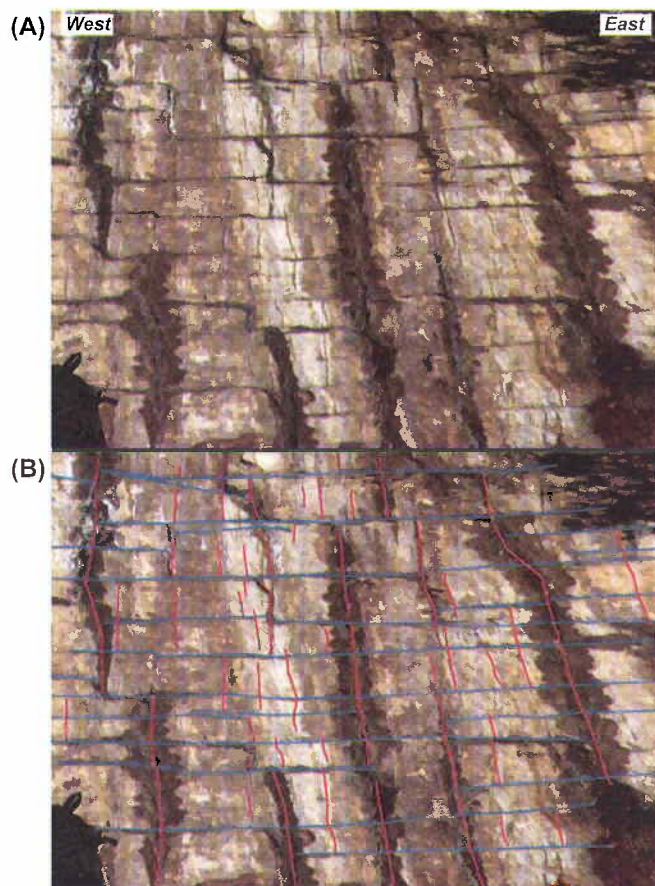
**Figure 5.** Summary of fracture-orientation data. (A) Equal-area stereonet plot of poles to bedding and fractures. (B) Rose diagram of fracture orientations (Set 1 with black petals, Set 2 with white petals).

TABLE 1.— Summary of Data on Layer Thickness, Fracture Spacing, and Spacing-to-Thickness Ratio.

Location	#	Layer		Set 1 Fractures			Set 2 Fractures		
		Thickness (cm)		Spacing (cm)		Spacing-to-Thickness Ratio	Spacing (cm)		Spacing-to-Thickness Ratio
		Stratigraphic	Mechanical	Stratigraphic	Mechanical		Stratigraphic	Mechanical	
Lynn Mountain	1	13	13	8	0.6	0.6	13	1.0	1.0
	2	93	106	33	0.4	0.3	59	0.6	0.6
	3	44	78	26	0.6	0.3	51	1.2	0.7
	4	79	103	72	0.9	0.7	97	1.2	0.9
	5	33	33	17	0.5	0.5	48	1.5	1.5
	6	17	25	24	1.4	1.0	60	3.5	2.4
	7	20	52	40	2.0	0.8	31	1.6	0.6
	8	20	52	37	1.9	0.7	30	1.5	0.6
	9	12	12	6	0.5	0.5	n.a.*	n.a.	n.a.
	10	12	12	7	0.6	0.6	n.a.	n.a.	n.a.
	11	17	17	10	0.6	0.6	n.a.	n.a.	n.a.
	12	30	30	28	0.9	0.9	n.a.	n.a.	n.a.
	13	32	32	42	1.3	1.3	n.a.	n.a.	n.a.
	14	51	51	61	1.2	1.2	n.a.	n.a.	n.a.
	15	15	15	19	1.3	1.3	n.a.	n.a.	n.a.
	16	18	18	48	2.7	2.7	n.a.	n.a.	n.a.
	17	2	2	9	4.5	4.5	n.a.	n.a.	n.a.
	18	9	9	13	1.4	1.4	n.a.	n.a.	n.a.
Rich Mountain	1	35	35	27	0.8	0.8	36	1.0	1.0
	2	26	26	20	0.8	0.8	40	1.5	1.5
	3	64	64	57	0.9	0.9	45	0.7	0.7
	4	17	17	n.a.	n.a.	n.a.	8	0.5	0.5
	5	15	15	n.a.	n.a.	n.a.	11	0.7	0.7
	6	40	40	n.a.	n.a.	n.a.	32	0.8	0.8
	7	30	30	n.a.	n.a.	n.a.	31	1.0	1.0
	8	116	116	n.a.	n.a.	n.a.	40	0.3	0.3
	9	97	97	n.a.	n.a.	n.a.	48	0.5	0.5
	10	61	61	n.a.	n.a.	n.a.	39	0.6	0.6
	11	74	74	n.a.	n.a.	n.a.	28	0.4	0.4
	12	26	26	45	1.7	1.7	61	2.3	2.3
	13	32	32	44	1.4	1.4	34	1.1	1.1

\*Indicates bedding surface with insufficient fractures of a given set for measurement.





**Figure 6.** Photograph of Jackfork bedding surface. View is toward the north-northeast. Width of photograph is approximately 2 m (7 ft). (A) Uninterpreted photograph. (B) Interpreted photograph showing Set 1 fractures (blue) and Set 2 fractures (red).

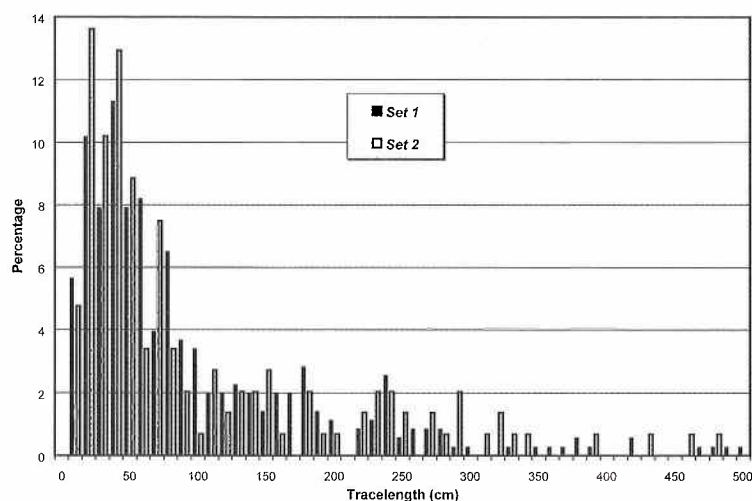


**Figure 7.** Frequency histogram of fracture tracelength data for Set 1 and Set 2 fractures.

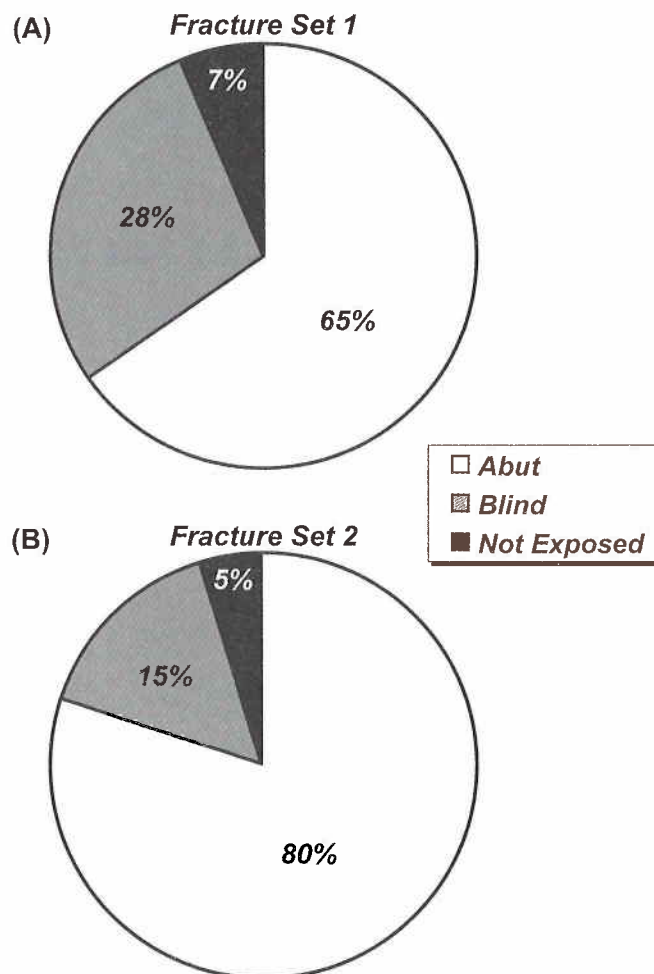


**Figure 8.** Summary of termination types for (A) Set 1 fractures and (B) Set 2 fractures.

whereas the second set is dip-parallel with an average orientation of N.14°E., 87°SE. The longer average tracelength of the Set 1 fractures, coupled with the observation that 80% of Set 2 fractures abut against Set 1 fractures, suggests that the Set 1 fractures developed somewhat earlier than the Set 2 fractures. Although measured fracture spacings show considerable variability from one sandstone layer to another, a positive correlation was found between layer thickness and fracture spacing. The majority of sandstone beds yielded S/T ratios near 1, indicating that a reasonable prediction of average fracture spacing can be obtained from estimates of layer thickness. Further, the predictions are most appropriate for layers more than approximately 30 cm in thickness.

## ACKNOWLEDGMENTS

The study presented here represents portions of an M.S. thesis by Buseti (2003) and an undergraduate thesis

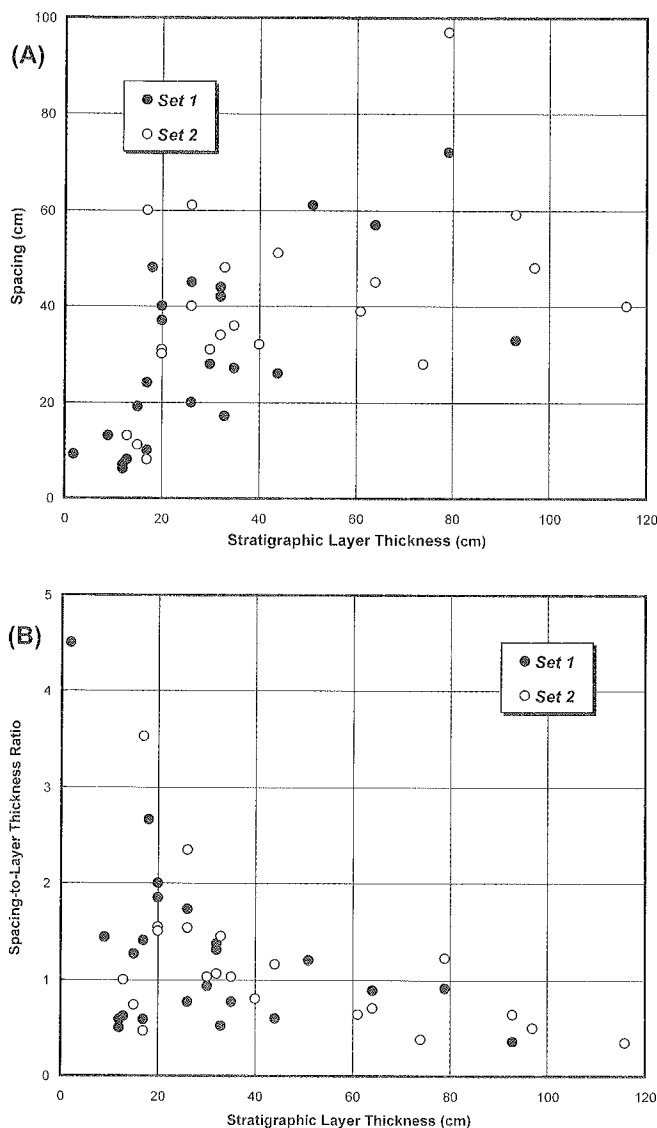


**Figure 9.** Summary of fracture spacing and layer thickness data showing plots of layer thickness versus (A) fracture spacing and (B) S/T ratio.

by Scott (Combs-Scott and Smart, 2002) at the University of Oklahoma (OU). Partial financial support was provided by a Geological Society of America South-Central Section undergraduate research grant (K. Scott), an OU junior faculty research grant (K.J. Smart), and the School of Geology and Geophysics at OU. Acknowledgment is also made to the donors of the Petroleum Research Fund, administered by the American Chemical Society (grant ACS-PRF# 37022-AC2 to K.J. Smart and R.M. Slatt) for support of this research. Thorough and critical reviews by Danielle Wyrick, David Ferrill, and Neil Suneson greatly improved this manuscript.

## REFERENCES CITED

Al-Siyabi, H. A., 1998, Sedimentology and stratigraphy of the Early Pennsylvanian upper Jackfork interval in the Caddo

Valley quadrangle, Clark and Hot Springs Counties, Arkansas: Colorado School of Mines, unpublished Ph.D. dissertation, 272 p.

Arbenz, J. K., 1989a, The Ouachita System, in Bally, A. W.; and Palmer, A. R. (eds.), *The Geology of North America—an overview*: Geological Society of America, Boulder, Colorado, *The Geology of North America*, v. A, p. 371–396.

—, 1989b, Ouachita thrust belt and Arkoma Basin, in Hatcher, R. D., Jr.; Thomas, W. A.; and Viele, G. W. (eds.), *The Appalachian–Ouachita orogen in the United States*: Geological Society of America, Boulder, Colorado, *The Geology of North America*, v. F-2, p. 621–634.

Bai, Taixu; and Pollard, D. D., 2000, Fracture spacing in layered rocks: a new explanation based on the stress transition: *Journal of Structural Geology*, v. 22, p. 43–57.

Briggs, Garrett, 1973, *Geology of the eastern part of Lynn Mountain Syncline, Le Flore County, Oklahoma*: Oklahoma Geological Survey Circular 75, 34 p.

Busetti, S. A., 2003, *Fracture characterization and analysis of the Pennsylvanian Jackfork Group, Ouachita Mountains, southeastern Oklahoma*: University of Oklahoma, Norman, unpublished M.S. thesis, 96 p.

Cline, L. M., 1970, Sedimentary features of the late Paleozoic flysch, Ouachita Mountains, Oklahoma, in Lajoie, Jean (ed.), *Flysch sedimentology in North America*: Geological Association of Canada Special Paper 7, p. 85–101.

Combs-Scott, K. D.; and Smart, K. J., 2002, Surface fracture characterization of Jackfork Group turbidite sandstones in the Ouachita Mountains, Oklahoma: *Shale Shaker*, v. 53, p. 71–78.

Couzens, B. A.; and Wiltschko, D. V., 1996, The control of mechanical stratigraphy on the formation of triangle zones: *Bulletin of Canadian Petroleum Geology*, v. 44, p. 165–179.

Feenstra, Roger; and Wickham, John, 1975, Evolution of folds around Broken Bow Uplift, Ouachita Mountains, southeastern Oklahoma: *American Association of Petroleum Geologists Bulletin*, v. 59, p. 974–985.

Gross, M. R., 1993, The origin and spacing of cross joints: examples from the Monterey Formation, Santa Barbara coastline, California: *Journal of Structural Geology*, v. 15, p. 737–751.

Hart, O. D., 1963, *Geology of the eastern part of Windingstair Range, Le Flore County, Oklahoma*: Oklahoma Geological Survey Bulletin 103, 87 p.

Huang, Qin; and Angelier, Jacques, 1989, Fracture spacing and its relation to bed thickness: *Geological Magazine*, v. 126, p. 355–362.

Ji, Shaocheng; and Saruwatari, Kazuko, 1998, A revised model for the relationship between joint spacing and layer thickness: *Journal of Structural Geology*, v. 20, p. 1495–1508.

Ladeira, F. L.; and Price, N. J., 1981, Relationship between fracture spacing and bed thickness: *Journal of Structural Geology*, v. 2, p. 179–183.



- LaPointe, P. R.; and Hudson, J. A., 1985, Characterization and interpretation of rock mass joint patterns: Geological Society of America Special Paper 199, 37 p.
- Legg, T. E.; Leander, M. H.; and Krancer, A. E., 1990, Exploration case study: Atoka and Jackfork section, Lynn Mountain Syncline, Le Flore and Pushmataha Counties, Oklahoma, *in* Suneson, N. H.; Campbell, J. A.; and Tilford, M. J. (eds.), *Geology and resources of the frontal belt of the western Ouachita Mountains*: Oklahoma Geological Survey Special Publication 90-1, p. 131–144.
- Miser, H. D., 1954, Geologic map of Oklahoma: Oklahoma Geological Survey, scale 1:500,000, 2 sheets.
- Montgomery, S. L., 1996a, Jackfork Group: Ouachita Mountains: *Petroleum Frontiers*, v. 13, 57 p.
- \_\_\_\_\_, 1996b, Jackfork Group, southeastern Oklahoma: new gas play in the Ouachita overthrust: *American Association of Petroleum Geologists Bulletin*, v. 80, p. 1695–1709.
- Morris, R. C., 1989, Stratigraphy and sedimentary history of post-Arkansas Novaculite Carboniferous rocks of the Ouachita Mountains, *in* Hatcher, R. D., Jr.; Thomas, W. A.; and Viele, G. W. (eds.), *The Appalachian-Ouachita orogen in the United States*: Geological Society of America, Boulder, Colorado, *The Geology of North America*, v. F-2, p. 591–602.
- Narr, Wayne, 1991, Fracture density in the deep subsurface: techniques with application to Point Areguella Oil Field: *American Association of Petroleum Geologists Bulletin*, v. 75, p. 1300–1323.
- Narr, Wayne; and Currie, J. B., 1982, Origin of fracture porosity—example from Altamont Field, Utah: *American Association of Petroleum Geologists Bulletin*, v. 68, p. 637–648.
- Narr, Wayne; and Suppe, John, 1991, Joint spacing in sedimentary rocks: *Journal of Structural Geology*, v. 13, p. 1037–1048.
- Nielsen, K. C.; Viele, G. W.; and Zimmerman, Jay, Jr., 1989, Structural setting of the Benton–Broken Bow Uplifts, *in* Hatcher, R. D., Jr.; Thomas, W. A.; and Viele, G. W. (eds.), *The Appalachian–Ouachita orogen in the United States*: Geological Society of America, Boulder, Colorado, *The Geology of North America*, v. F-2, p. 635–660.
- Omatsala, Botosan, 2003, Origin and distribution of friable and cemented sandstones in outcrops of the Pennsylvanian Jackfork Group, southeast Oklahoma: University of Oklahoma, unpublished M.S. thesis, 227 p.
- Pauli, D. A., 1994, Friable submarine channel sandstones in the Jackfork Group, Lynn Mountain Syncline, Pushmataha and Le Flore Counties, Oklahoma, *in* Suneson, N. H.; and Hemish, L. A. (eds.), *Geology and resources of the eastern Ouachita Mountains frontal belt and southeastern Arkoma Basin*, Oklahoma: Oklahoma Geological Survey Guidebook 29, p. 179–202.
- Price, N. J., 1966, *Fault and joint development*: Pergamon Press, Oxford, 176 p.
- Priest, S. D., 1993, *Discontinuity analysis for rock engineering*: Chapman and Hall, New York, 473 p.
- Priest, S. D.; and Hudson, J. A., 1981, Estimation of discontinuity spacing and trace length using scanline surveys: *International Journal of Rock Mechanics and Mining Sciences and Geomechanics Abstracts*, v. 18, p. 183–197.
- Romero, G. A., 2004, Identification of architectural elements of turbidite deposits, Jackfork Group, Potato Hills, eastern Oklahoma: University of Oklahoma, unpublished M.S. thesis, 238 p.
- Seely, D. R., 1963, Structure and stratigraphy of Rich Mountain area, Oklahoma and Arkansas: *Oklahoma Geological Survey Bulletin* 101, 173 p.
- Slatt, R. M.; Stone, C. G.; and Weimer, Paul, 2000, Characterization of slope and basin facies tracts, Jackfork Group, Arkansas, with applications to deepwater (turbidite) reservoir management: Gulf Coast Section, Society of Sedimentary Geology 20th Annual Reservoir Conference, Deep Water Reservoirs of the World, Houston, p. 940–980.
- Suneson, N. H.; Campbell, J. A.; and Tilford, M. J., 1990, *Geology and resources of the frontal belt of the western Ouachita Mountains*, Oklahoma: Oklahoma Geological Survey Special Publication 90-1, 196 p.
- Stearns, D. W.; and Friedman, Melvin, 1972, Reservoirs in fractured rock, *in* King, R. E. (ed.), *Stratigraphic oil and gas fields*: American Association of Petroleum Geologists Memoir 16, p. 82–106.
- Terzaghi, R. D., 1965, Sources of error in joint surveys: *Geotechnique*, v. 15, p. 287–304.
- Tillman, R. W., 2000, Sedimentology and sequence stratigraphy of Jackfork Group, U.S. Highway 259, Le Flore County, Oklahoma, *in* Johnson, K. S. (ed.), *Marine clastics in the southern Midcontinent*, 1997 symposium: Oklahoma Geological Survey Circular 103, p. 65–85.
- Thomas, W. A., 1989, The Appalachian–Ouachita orogen beneath the Gulf Coastal Plain between the outcrops in the Appalachian and Ouachita Mountains, *in* Hatcher, R. D., Jr.; Thomas, W. A.; and Viele, G. W. (eds.), *The Appalachian–Ouachita orogen in the United States*: Geological Society of America, Boulder, Colorado, *The Geology of North America*, v. F-2, p. 537–553.
- Viele, G. W., 1989, The Ouachita orogenic belt, *in* Hatcher, R. D., Jr.; Thomas, W. A.; and Viele, G. W. (eds.), *The Appalachian–Ouachita orogen in the United States*: Geological Society of America, Boulder, Colorado, *The Geology of North America*, v. F-2, p. 555–561.
- Viele, G. W., and Thomas, W. A., 1989, Tectonic synthesis of the Ouachita orogenic belt, *in* Hatcher, R.D. Jr.; Thomas, W. A.; and Viele, G. W. (eds.), *The Appalachian–Ouachita orogen in the United States*: Geological Society of America, Boulder, Colorado, *The Geology of North America*, v. F-2, p. 695–728.

# Lower Atoka Highstand Systems Tract: Delineating the Lower Atoka in the Arkoma Basin, Oklahoma

*Azzeldeen A. Saleh*

Geology Department, Faculty of Science,  
University of Tanta, Egypt

**ABSTRACT**—The lower Atoka lithostratigraphic interval is poorly defined in Oklahoma's Arkoma Basin. Several authors acknowledge the presence of a lower Atoka section in Oklahoma, but no clear definition or boundaries have been drawn for this interval. Moreover, this name is frequently used as synonymous with the Spiro sandstone.

The lower Atoka interval has a characteristic conductivity-log pattern that allows tracking the lateral and shelf-to-basin distribution of this unit, and defining its boundaries in terms of sequence stratigraphy. Accordingly, this interval represents the highstand systems tract (HST) of a third-order sequence underlying the middle Atoka turbidites. This framework helps to decipher relationships, in terms of relative age and depositional setting, for several lithostratigraphic sandstone units that have been reported in different parts of the shelf area of the basin in Oklahoma.

Based on this work, the majority of sandstones on the shelf in the northern and western parts of the basin belong to the lower Atoka HST. The lower Atoka sandstones carry the Arkansas nomenclature such as Dunn (A through C), Jenkins, and Sells in the northeastern part of the basin. These lithostratigraphic units are time-equivalent to the deltaic sandstones of the Dutcher and the majority of Gilcrease sandstones in the northern and western parts of the Arkoma Basin in Oklahoma.

## INTRODUCTION

The Atoka Formation (Middle Pennsylvanian) in the Arkoma Basin is divided informally into lower, middle, and upper units (Stone, 1968; McGee, 1979; Sutherland and Manger, 1979; Lonsinger, 1980; Houseknecht and Kacena, 1983; Zachry, 1983). Many studies have referred to these divisions, yet the bases for such divisions and their boundaries are not well defined in the Oklahoma part of the Arkoma Basin. The vague understanding of the stratigraphy of the lower Atoka section may be because most of the studies conducted on the Atoka Formation in Oklahoma were on outcrops of the frontal Ouachitas, where the lower Atoka section is relatively thin and shaly. This is in contrast to the Arkansas part of the Arkoma Basin, where the lower Atoka sandstones crop out.

Zachry (1983) mentioned that the lower Atoka section in the Arkansas part of the Arkoma Basin is composed of 7–8 sandstone units separated by intervals of shale. These units are relatively thin and persistent throughout the northern and

central parts of the Arkoma Basin in Arkansas. In outcrops, the thin sandstone beds grade upward into intervals of medium- to thick-bedded sandstones that suggest progradational sequences. To the south, these sandstone units above the basal Spiro sandstone become thinner and are replaced by shale. Zachry (1983) distinguished the lower and middle Atoka sections using the thickness change across growth faults (Fig. 1) and occurrence of metamorphic rock fragments in the middle Atoka sandstones. Johnson and others (1989) mentioned that the lower Atoka sandstones above the Spiro in the Arkansas part of the Arkoma Basin are replaced by shale westward in Oklahoma. Houseknecht (1987) stated that typically 100- to 200-m-thick dark shale immediately overlies the Spiro throughout the basin. He interpreted this shale section as the stratal equivalent of expanded sections on the downthrown side of major faults. Visser (1996) mentioned that lower Atoka strata are not present on the Oklahoma Platform. Several authors acknowledge the presence of a lower Atoka section in

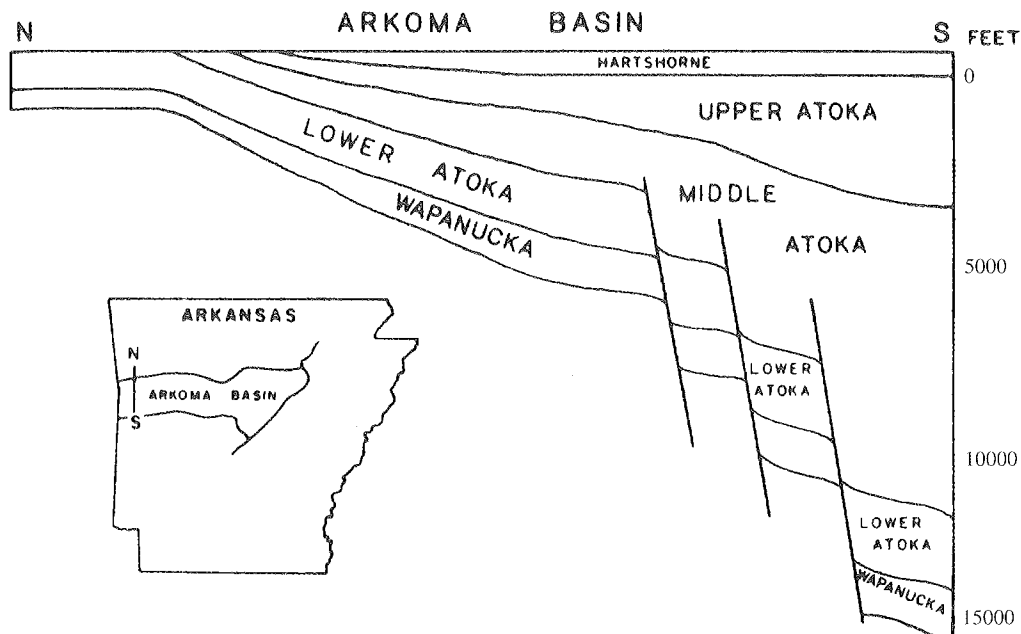


**Figure 1.** North-south section across the Arkoma Basin in Arkansas depicting the Atoka sedimentary section and adjacent strata. Changes in thickness across syndepositional faults and sandstone distribution were used to define the divisions of the Atoka Formation into lower, middle, and upper units (modified after Johnson and others, 1989).

Oklahoma, but the name is frequently used as synonymous with the Spiro sandstone.

The purpose of this work is to identify the stratigraphic interval between the basal Atoka (which includes the Spiro sandstone) and the overlying middle Atoka turbidites. Delineation of this poorly defined section required covering the entire Arkoma Basin in Oklahoma using detailed well-log correlations. The study area is about 7,000 mi<sup>2</sup>, covering more than 200 townships (Fig. 2). The main data source for this study was the huge accumulation of both conductivity and gamma ray (GR) logs for thousands of wells drilled in the basin.

### LOWER ATOKA HST LOG PATTERN AND BOUNDARIES

Zachry and Sutherland (1984) stated that in the absence of correlatable sandstone units above the Spiro in Oklahoma, the upper boundary of the lower Atoka interval occurs within a shale succession and is poorly defined. This demonstrates that using lithostratigraphic sandstone units as a basis for regional correlations is inadequate because of the discontinuous nature of these units. The system tracts in a sequence stratigraphic hierarchy, however, can be uniquely defined by the nature of the bounding surfaces and the geometry of the parasequence stacking patterns within them. Each tract may be composed

of one or more parasequence sets. The stacking pattern and geometry of a parasequence set is dependent on the ratio of sediment-supply rate to accommodation rate ( $S/A$  ratio) (Van Wagoner and others, 1988). A transgressive systems tract is characterized by retrogradational parasequence sets ( $S/A < 1$ ). A HST is characterized by both progradational ( $S/A > 1$ ) and aggradational ( $S/A = 1$ ) parasequence sets (Fig. 3). In a prograding setting, an overall coarsening upward is observed.

The lower Atoka shale has a very characteristic conductivity-log pattern that can be tracked throughout the Arkoma Basin. Figure 4 shows a stacking pattern of decreasing conductivity values from base to top of the lower Atoka section in five wells drilled in different parts of the Arkoma Basin in Oklahoma. Within this overall decreasing-conductivity pattern, which is clearly shown in the Waycott #1-3 and Graham #1 wells, low-conductivity sandstone units are stacked in a series of parasequences in the Brown #1 and the Skinner-Davis #1 wells (Fig. 4). Each parasequence starts with relatively high conductivity-log values that decrease upward toward the deltaic sandy facies at the top of the parasequence, with older parasequences generally having higher conductivity-log patterns than younger ones.

The GR-log response shows no clear change corresponding to the gradual vertical decrease of the conductivity values in the lower Atoka section except where sandstone units occur

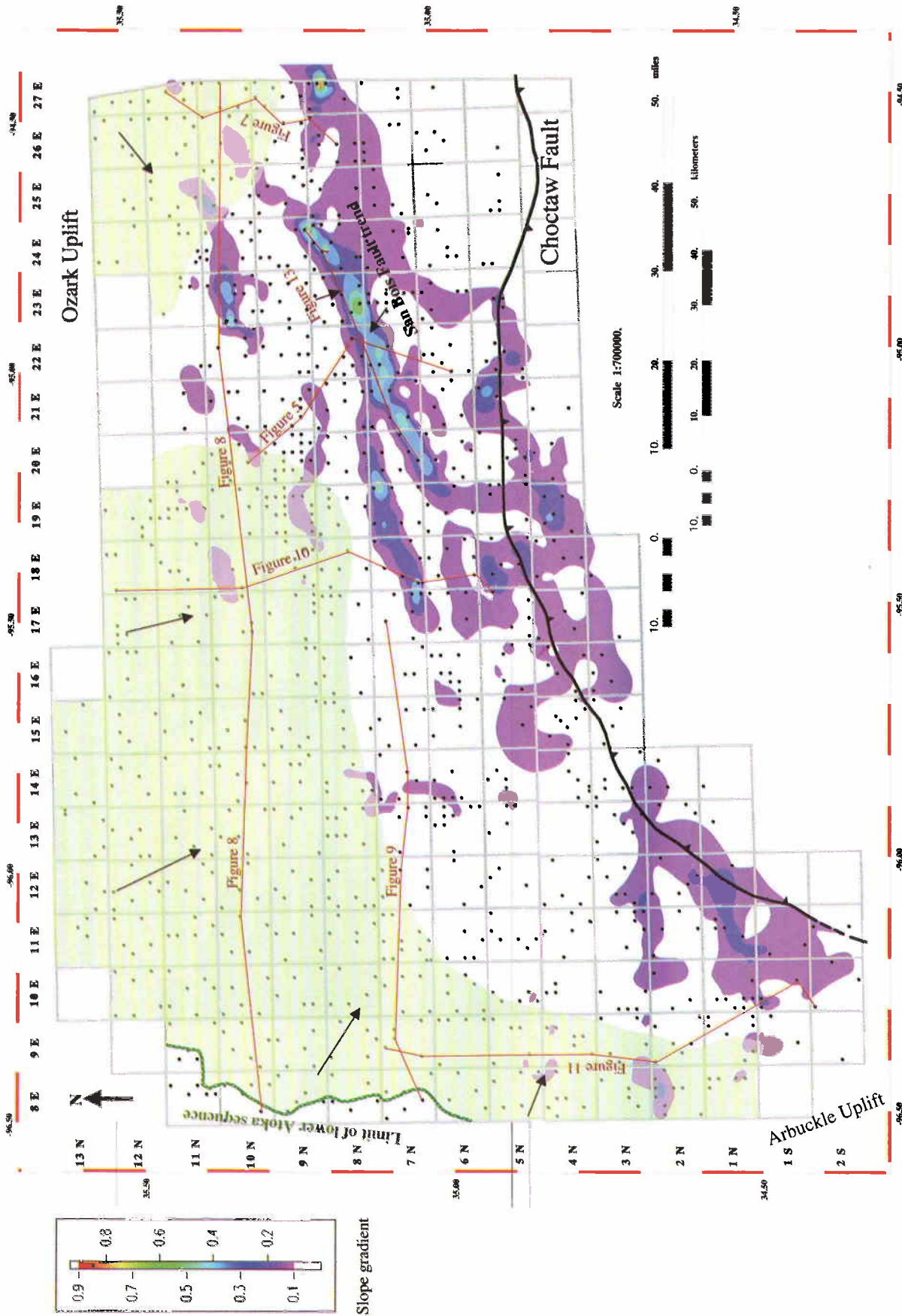


**Figure 2.** Map showing the locations of the wells studied in this work. It also shows the first derivative of the structure on the top of the lower Atoka sequence indicating the San Bois Fault trend. The slope gradient is color-coded on the top left corner of the map. The map also shows areas where delta-front sandstones may occur within the lower Atoka HST (green-shaded areas). The green line is the limit of the lower Atoka sequence. Deltas prograded from northeast, northwest, and west in the shelf areas of the Arkoma Basin (black arrows). To the south of these areas, the section is predominantly composed of prodelta shale. The map also shows the location of the cross sections presented in this work.



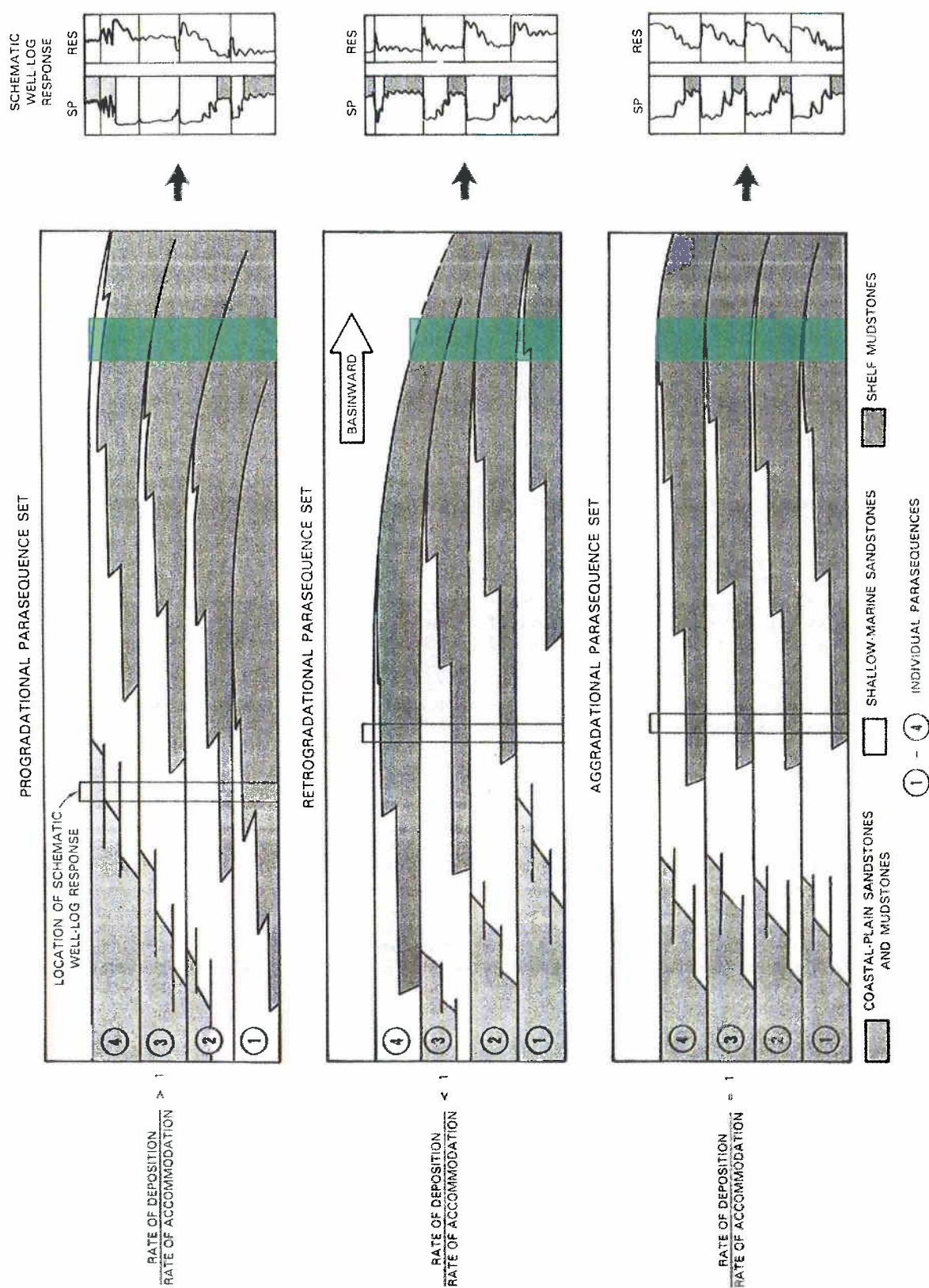


**Figure 3.** Stacking patterns of parasequence sets are progradational, retrogradational, or aggradational depending on the ratio of deposition rate (sediment supply) to accommodation rate. Parasequences can still be detected using the conductivity log even when they become shaly (green-shaded areas; modified after Van Wagoner and others, 1988). Abbreviations: SP = spontaneous potential log; RES = resistivity log.



(Zehnder #1 and Fudge #1–28 wells in Fig. 5). This could be attributed to the conductivity log's high sensitivity to changes in the grain size of clastics, which should increase upward in a prograding delta (coarsening-upward pattern; Fig. 3). Textural variations play an important role in conductivity (or resistivity) log measurements (Brie and others, 1985; Schoch, 1989). Such variations may include changes in grain size of the quartz in shale intervals, pore size, packing of the quartz fraction, and consequently the interconnection between pores, which affect the electric-current path. On the other hand, the GR log is merely a measure of radioactivity level in sedimentary rocks and consequently does not detect changes in the grain size, as shown in the Kent Unit #2 well in Figure 5.

The lower Atoka interval is underlain by the basal Atoka, which consists of both lowstand and transgressive systems tracts (LST, TST). The lower bounding surface of the lower Atoka interval is the top of the basal Atoka transgressive systems tract (Fig. 5). This surface is the top of the Cecil and Pope Chapel sandstones on the northeastern and northern shelf of the basin, respectively. Elsewhere in the basin, this surface is distinguished by a condensed section on the GR log or the low-conductivity pattern that is characteristic of the shale in the basal Atoka TST (Fig. 5).

The parasequences within the lower Atoka section exhibit either truncation or thinning in different areas of the Arkoma Basin. As an example of thinning, most of the lower Atoka parasequences in the Brown #1 well (in the northeast part of the basin) exist in the Skinner-Davis #1 well (in the west part of the basin) with total thickness more than 2,500 ft in the first well and less than 750 ft in the latter, respectively. Truncation is indicated by abrupt absence, for a distance, of one or more parasequences. The interpretation of truncation as a result of subaerial or submarine erosion would be in the context of the place where truncation occurs in the basin, whether on the shelf or in the deep part of the basin, and whether the overlying systems tract is transgressive or lowstand.

The upper bounding surface is an unconformity marked by an abrupt change in the conductivity pattern. In the deep parts of the Arkoma Basin, relatively thin lower Atoka prodelta shale is overlain by middle Atoka turbidites. Non-deposition and/or submarine erosion may have contributed to the absence of several parasequences (Short Unit #1 and Graham #1 wells in Fig. 4). On the shelf where the middle Atoka turbidites are absent, the unconformity is marked by:

1. Extensive truncation as several parasequences are abruptly absent, with no indication of thinning of parasequences in nearby wells. This can be demonstrated by correlating the lower Atoka parasequences in both the Zehnder #1 and McCafferty Unit #2 wells in Figure

5, which could be indicative of subaerial erosion in the latter well.

2. The presence of the basal transgressive sandy facies of the upper Atoka section (McCafferty Unit #2, Zehnder #1, and Fudge #1–28 wells in Fig. 5).

In terms of sequence stratigraphy, this lower Atoka interval represents a HST bounded by a TST at its base and an unconformity at its top. The stratal pattern of a HST setting, in a landward direction, will usually show aggradation as the space between the sea floor and the base level is filled, whereas the basinward limit of progradation is a function of sediment supply and basin-margin geometry (Posamentier and Vail, 1988). Figure 6 shows that in several areas on the shelf, the vertical stacking pattern of some sandstone intervals changes to a retrogradational pattern within the overall progradation or coarsening-upward pattern characteristic of the lower Atoka delta system. This can be attributed to changes in the S/A ratio along the shelf of the Arkoma Basin, implying autocyclic factors or higher-order relative sea-level cyclicity.

### REGIONAL SETTING OF THE LOWER ATOKA HST DELTAS AND DELINEATING THE LOWER ATOKA SANDSTONES

The regional setting for the lower Atoka HST in the Oklahoma part of the Arkoma Basin is illustrated by a series of regional cross sections (Figs. 7–11). These figures demonstrate the facies changes from shale in the south (prodelta facies) to the development of aggrading and prograding sandstones in the north and west (delta-front facies). These sandstones carry different lithostratigraphic nomenclatures and have been placed in different positions within the Atoka stratigraphic section.

The thickest lower Atoka sandstones occur in a delta system in the northeastern part of Arkoma Basin that grades to prodelta shale to the south and west (Figs. 7 and 8, respectively). Figure 8 shows that along the northern edge of the Arkoma Basin, different sandstone units appear farther to the west, indicating the development of another thin and broad delta system. Along the northwestern edge of the Arkoma Basin, the lower Atoka section is completely absent where the upper Atoka strata overlie the Union Valley shale (Rife-Reed Trust #1 well in Fig. 8 and Phillips #1 well in Fig. 9).

Figure 9 is an east–west cross section in the west-central part of the Arkoma Basin showing that the sandy intervals of the lower Atoka delta grade eastward to prodelta shale toward the center of the basin. The same pattern is observed in a north–south direction across the central and western parts of the Arkoma Basin (Figs. 10 and 11, respectively). The deltaic sandstones in the north and west grade into prodelta shale to

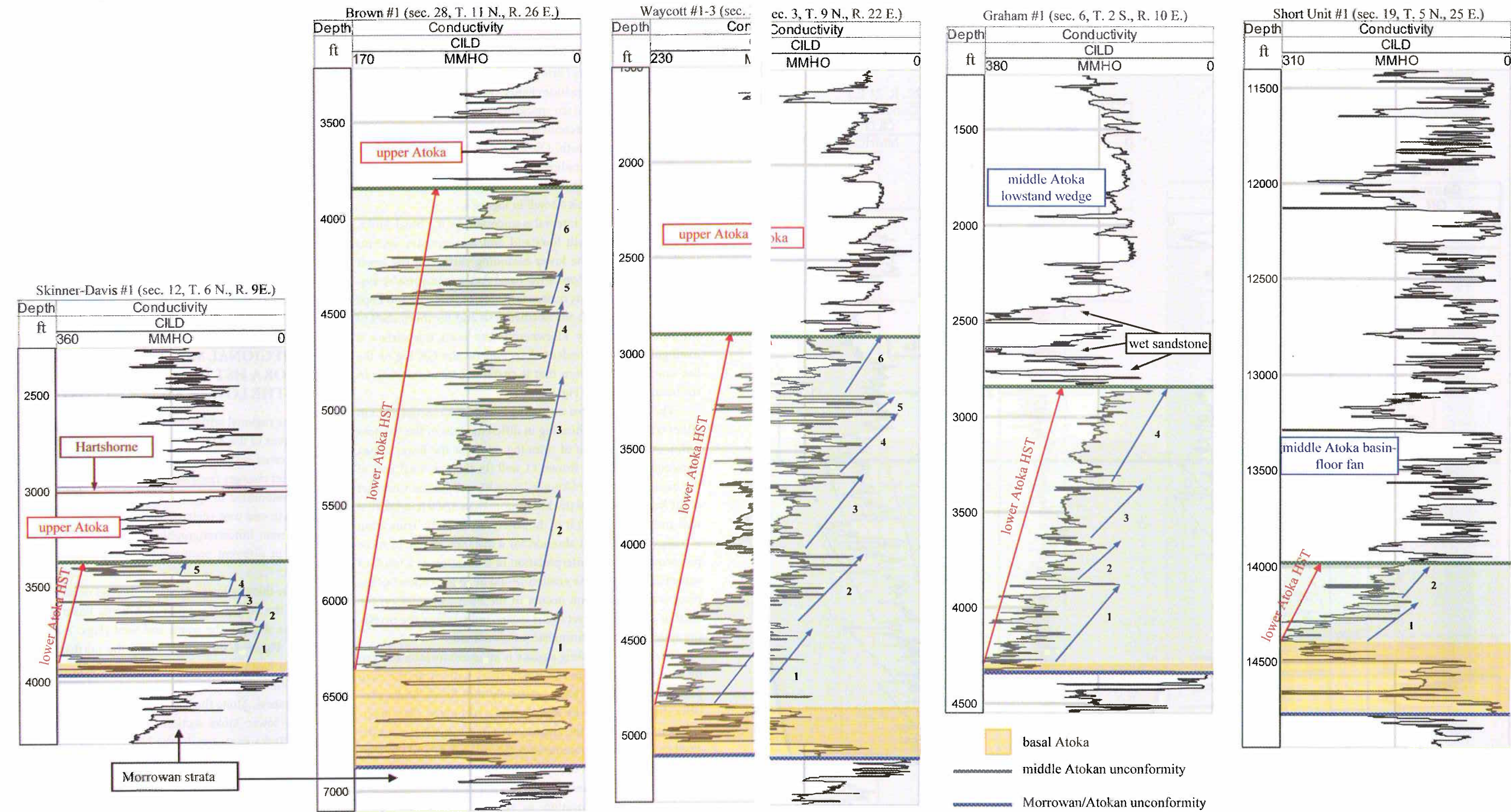


**Figure 4.** Examples from wells drilled in different parts of the Arkoma Basin in Oklahoma showing the characteristic decreasing-conductivity pattern of the lower Atoka interval (compare with the progradational parasequences in Figure 3). The section in the two wells on the right is composed of prodelta shale, with indications of unconformity as several lower Atoka parasequences are absent, and middle Atoka basin-floor fans and lowstand wedges overlie the prodelta shale. The lower Atoka interval in the two

wells on the left shows two different delta fronts composed of several parasequences (blue arrows). Each parasequence starts with relatively high conductivity-log values that decrease upward as they approach sandy facies at the top of the parasequence. Abbreviations: CILD = conductivity log in MMHO units.



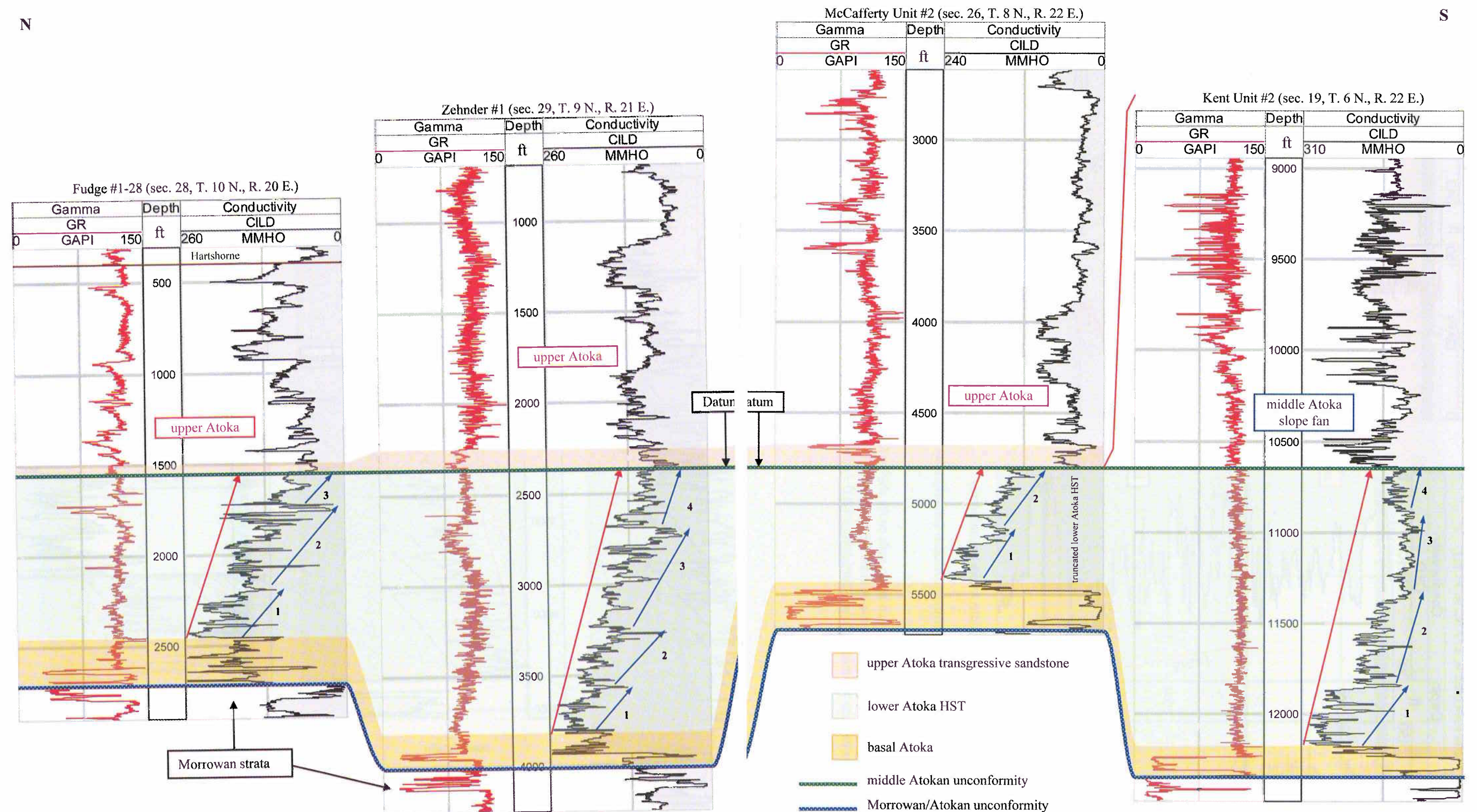


**Figure 5.** North-south cross section using gamma ray (GR) and conductivity logs. The GR log shows no clear change corresponding to the gradual vertical decrease of conductivity values in the lower Atoka interval except where sandstone units occur. This can be attributed to the high sensitivity of the conductivity log to changes in clastics grain size, which should increase upward in a prograding delta (coarsening-upward pattern). The unconformity surface at the top of lower Atoka is marked by the

middle Atoka turbidites in the deep part of Arkoma Basin (Kent Unit #2 well), truncation of the lower Atoka section, and deposition of the upper Atoka basal transgressive sandstone on the shelf. The cross section datum is the middle Atokan unconformity. Horizontal scale is equal spacing. For location, see Figure 2. Abbreviations: CILD = conductivity log in MMHO units; GR = gamma ray log in GAPI units.



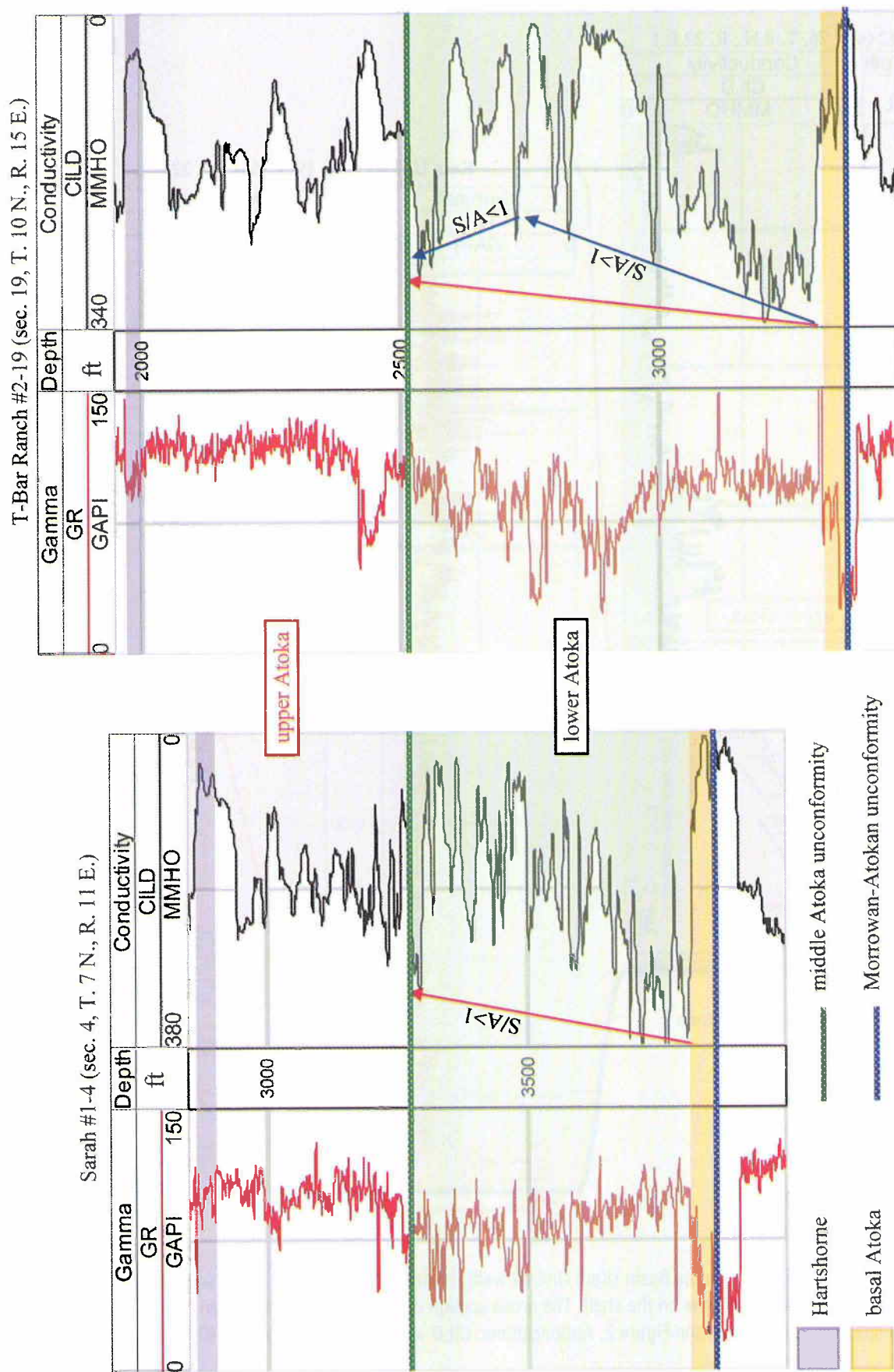


**Figure 6.** The decreasing-conductivity pattern is shown in two wells on the shelf of Arkoma Basin. Within this overall pattern, changes in sediment supply to accommodation rate ( $S/A$ ) led to higher cyclicity as shown in the T-Bar Ranch #2-19 well (right), where delta-front clean sandstones in the middle of the lower Atoka HST are overlain by shaly sandstones and marine shales. Abbreviations: CILD = conductivity log in MMHO units; GR = gamma ray log in GAPI units.

the south where sandstone intervals of the middle Atoka LST unconformably overlie the lower Atoka HST.

The lower Atoka HST is characterized by substantial development of deltas in the shelf areas of the Arkoma Basin. Delta systems prograded from the northeast, northwest, and west, across the shelf whereas prodelta shale extended well into the southern parts of the basin (Fig. 2). Sandstone intervals occur at the top of each parasequence within the lower Atoka HST in the northeastern part of the Arkoma Basin in Oklahoma, which may represent part of a major delta system centered in western Arkansas (Fig. 7 and Brown #1 well in Fig. 4). These sandstones carry the Arkansas nomenclature such as Dunn (A, B, and C), Jenkins, and Sells. These lithostratigraphic units are time-equivalent to the deltaic sandstones of the Dutcher, and the majority of the Gilcrease sandstones in the northern and western parts of the Arkoma Basin (Fig. 8). This interpretation is different from that of Suneson and Hemish (1994) and Visher (1996). Suneson and Hemish (1994) included all Gilcrease sandstones within the upper Atoka section. Visher (1996) included both Gilcrease and Dutcher sandstones in the middle and upper Atoka sections.

Estimates for the time span of the Atokan series differ, but they are generally between 3 and 6 million years (Salvador, 1985; Spotl and others, 1993; Visher, 1996). This time frame implies that the Atoka sediments were deposited within a third-order cyclic hierarchy, or the sequence/composite sequence time range of 1–10 million years. Both of the basal Atoka (LST and TST) and lower Atoka (HST) systems tracts compose a third-order sequence referred to in this work as the lower Atoka sequence. This sequence is bounded by the Morrowan–Atokan unconformity at its base and by the middle Atokan unconformity at its top. An isopach map for this sequence shows an axis trending northeast-southwest for the thickest part of the sequence (Fig. 12). The maximum thickness (more than 3,000 ft) occurs in the northeastern part of the Arkoma Basin, where the sandstones in both the TST and HST are best developed. In the central parts of the basin, the thickness of the lower Atoka sequence is between 1,500 and 2,000 ft. The lower Atoka thins dramatically to the northwest as the basinal accommodation space becomes less available, and it is completely absent in the extreme northwestern part of the basin, probably due to the lack of accommodation space and/or sediment supply (Fig. 12). Non-deposition or submarine erosion along the unconformity surface on the top of the sequence may have contributed to thinning of the sequence in the southern area of the Arkoma Basin where middle Atoka turbidites were later deposited.

An interesting feature in the isopach map is an anomalous and abrupt thinning close to the southern margin of the Arkoma Basin (Fig. 12). This feature supports the existence of a regional unconformity. It coincides with the northeast-southwest trend of the San Bois Fault, which is inferred from the first derivative structural map on the top of the sequence (Fig. 2). A cross section trending northeast-southwest shows that most of the lower Atoka HST is truncated along this trend, with more than 1,000 ft of section having been eroded in some wells (Fig. 13). The only remaining HST parasequences are the oldest ones, characterized by relatively high conductivity-log patterns. There is no indication of thinning of individual younger parasequences along or to the north of this feature. The truncated section is on the upthrown side of the San Bois syndepositional fault, which was active during middle Atokan time. This part of the basin may represent an area of subaerial erosion on the shelf during that time. On the downthrown side of this fault, thick middle Atoka turbidites were deposited to the south where several middle Atoka sandstone reservoirs have been discovered. Figure 2 shows all cross section locations and the important features previously discussed.

## CONCLUSIONS

The lower Atoka stratigraphic interval in Oklahoma represents a HST. It provides a sequence stratigraphic link between the transgressive, basal Atoka sandstones and the lowstand, middle Atoka turbidites. The lower Atoka HST has a characteristic conductivity-log pattern that can be tracked throughout the basin. It is bounded at the base by the basal Atoka TST and at the top by the middle Atokan unconformity. The middle Atoka turbidites overlie the lower Atoka prodelta shales in the deeper parts of the Arkoma Basin. The upper Atoka stratigraphic interval overlies the lower Atoka delta-front facies on the shelf of the Arkoma Basin in Oklahoma.

The lower Atoka systems tract is the highstand portion of a third-order sequence referred to in this work as the lower Atoka sequence. This sequence is bounded by the Morrowan–Atokan unconformity at its base and by the middle Atokan unconformity at its top. It is composed of both the basal Atoka LST and TST and the lower Atoka HST.

Several highstand deltas extend along the shelf area where sandstones were deposited in a series of parasequences. The bounding surfaces for each parasequence represent a powerful tool to correlate and define individual sandstones for gas prospecting on the shelf area of the Arkoma Basin.



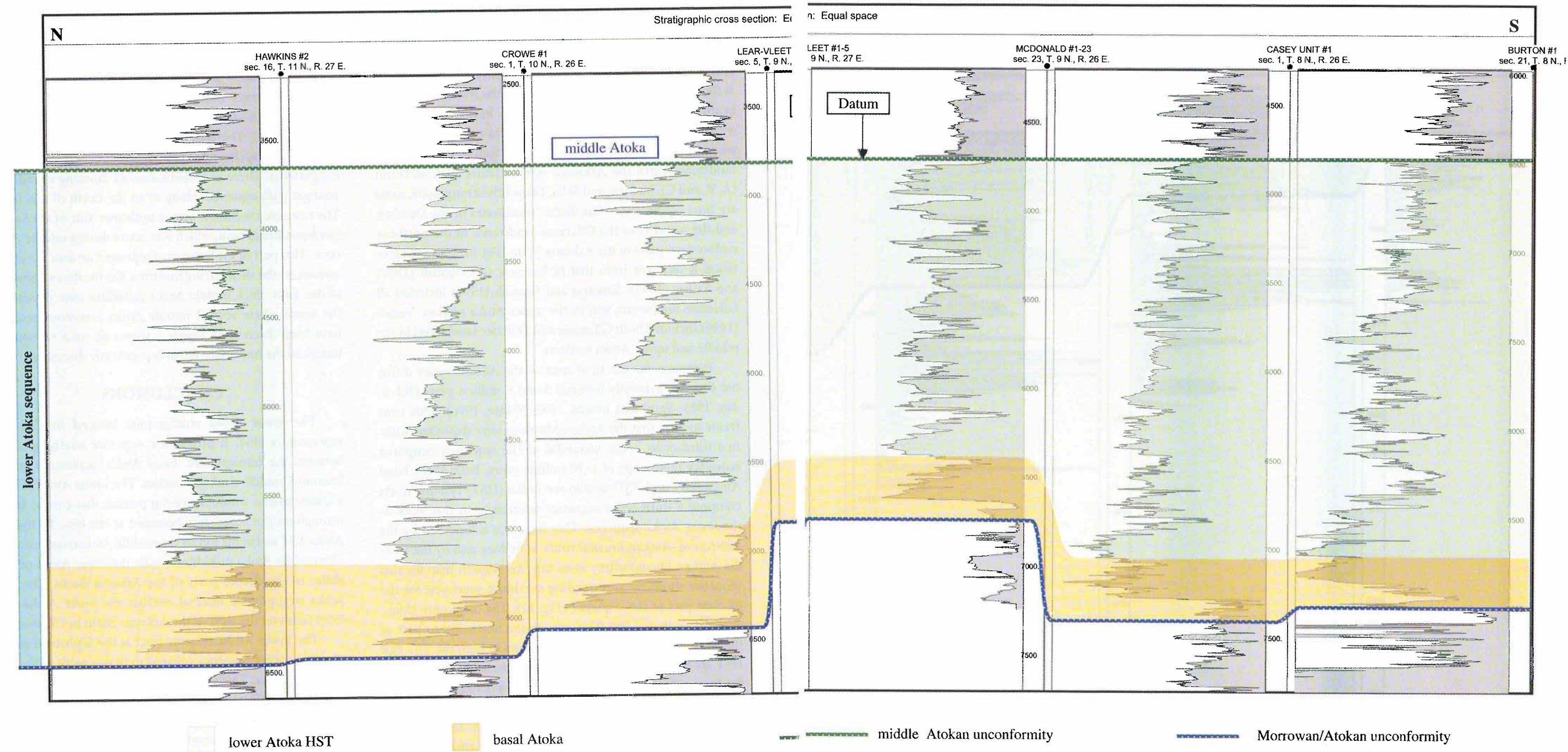


**Figure 7.** North-south regional stratigraphic cross section in the eastern part of the Arkoma Basin using conductivity logs. The

thickest delta system in the lower Atoka HST occurs in this part of the basin. In the north, the section is composed of several

parasequences stacked with delta-front sandstones which grade to prodelta shale toward the south. The lower Atoka HST is

unconformably overlain by the middle Atoka turbidites in this part of the basin. The cross section datum is the middle Atoka

unconformity. For location, see Figure 2.



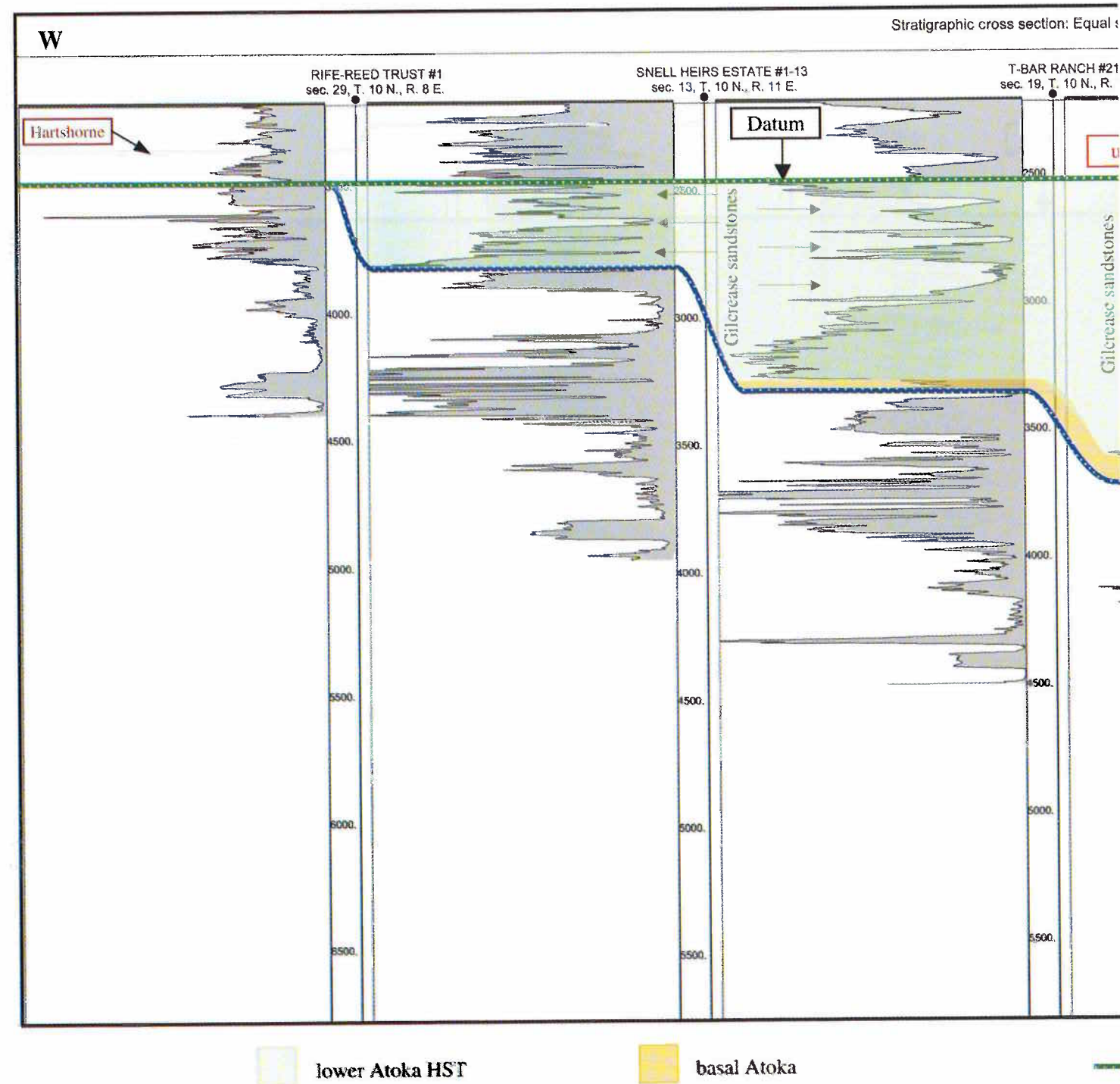
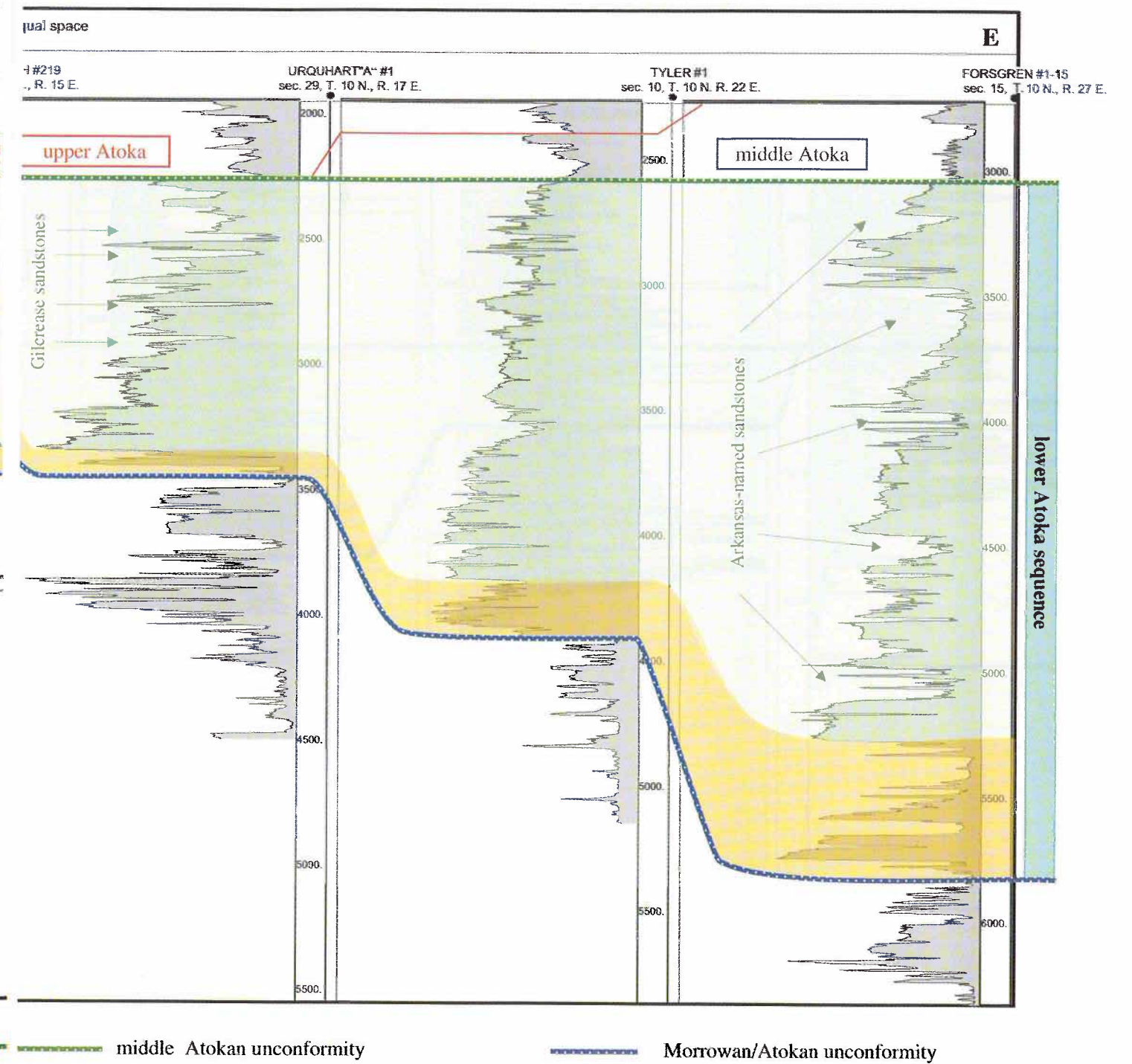


**Figure 8.** East-west regional stratigraphic cross section in the northern part of the Arkoma Basin using conductivity logs. Along the basin shelf, the eastern sandstone-topped parasequences of the lower Atoka delta front grade to shale to the west (Tyler #1 well); then another delta-front sandstone appears farther west. The lithostratigraphic sandstone units in the east carry Arkansas nomenclature. They are, however, time-equivalent to the Dutcher and most of the Gilcrease sandstones in the western part of the



Arkoma Basin. The lower Atoka section is absent in the Rife-Reed Trust #1 well in the extreme northwestern part of the basin where the upper Atoka strata overlie the Union Valley shale. The cross section datum is the middle Atokan unconformity. For location, see Figure 2.



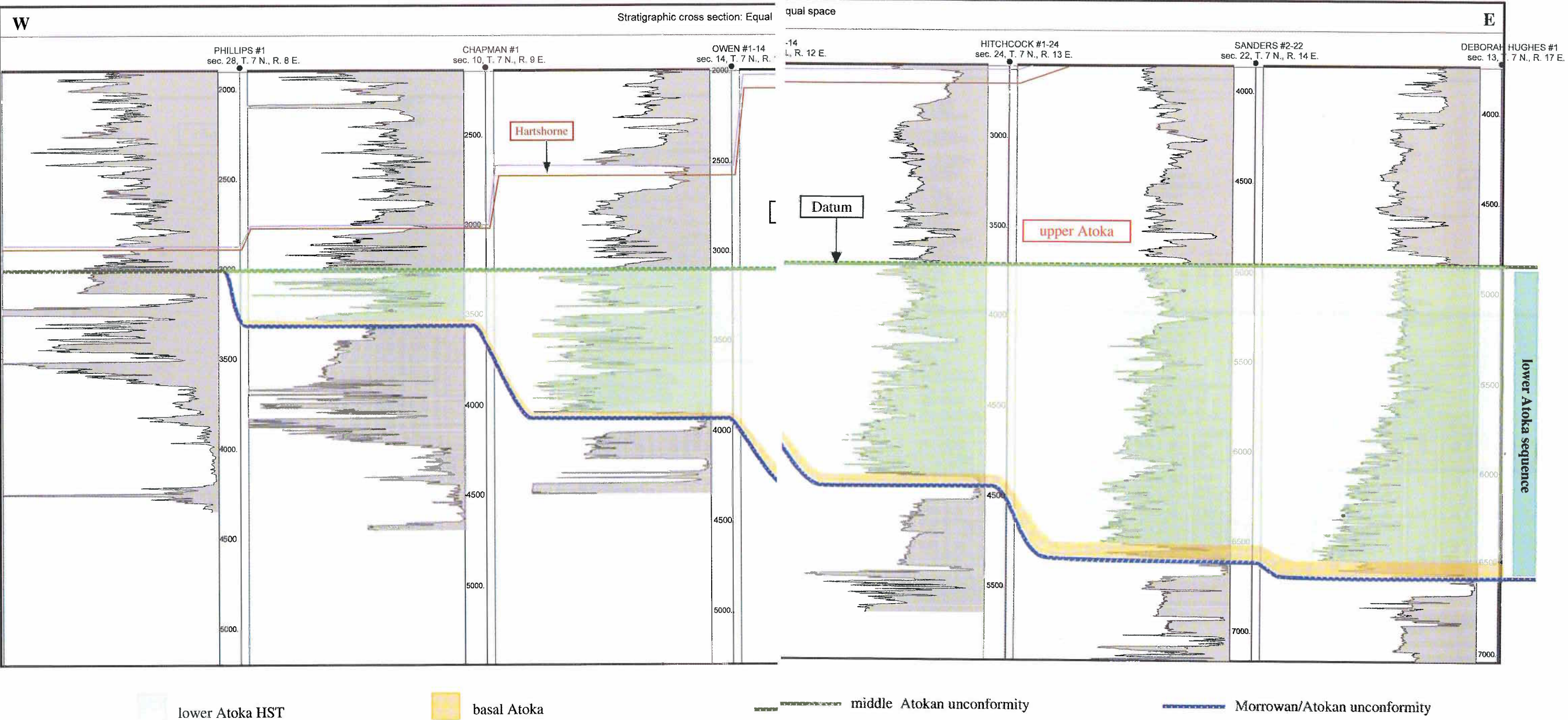


**Figure 9.** East–west regional stratigraphic cross section in the west-central part of the Arkoma Basin using conductivity logs. The figure shows that western deltaic sandstones of the lower Atoka grading to prodelta shale in the east. Note the thinning of the

section to the west; it becomes completely absent in Phillips #1 well where the upper Atoka strata overlie the Union Valley shale. The cross section datum is the middle Atokan unconformity. For location, see Figure 2.



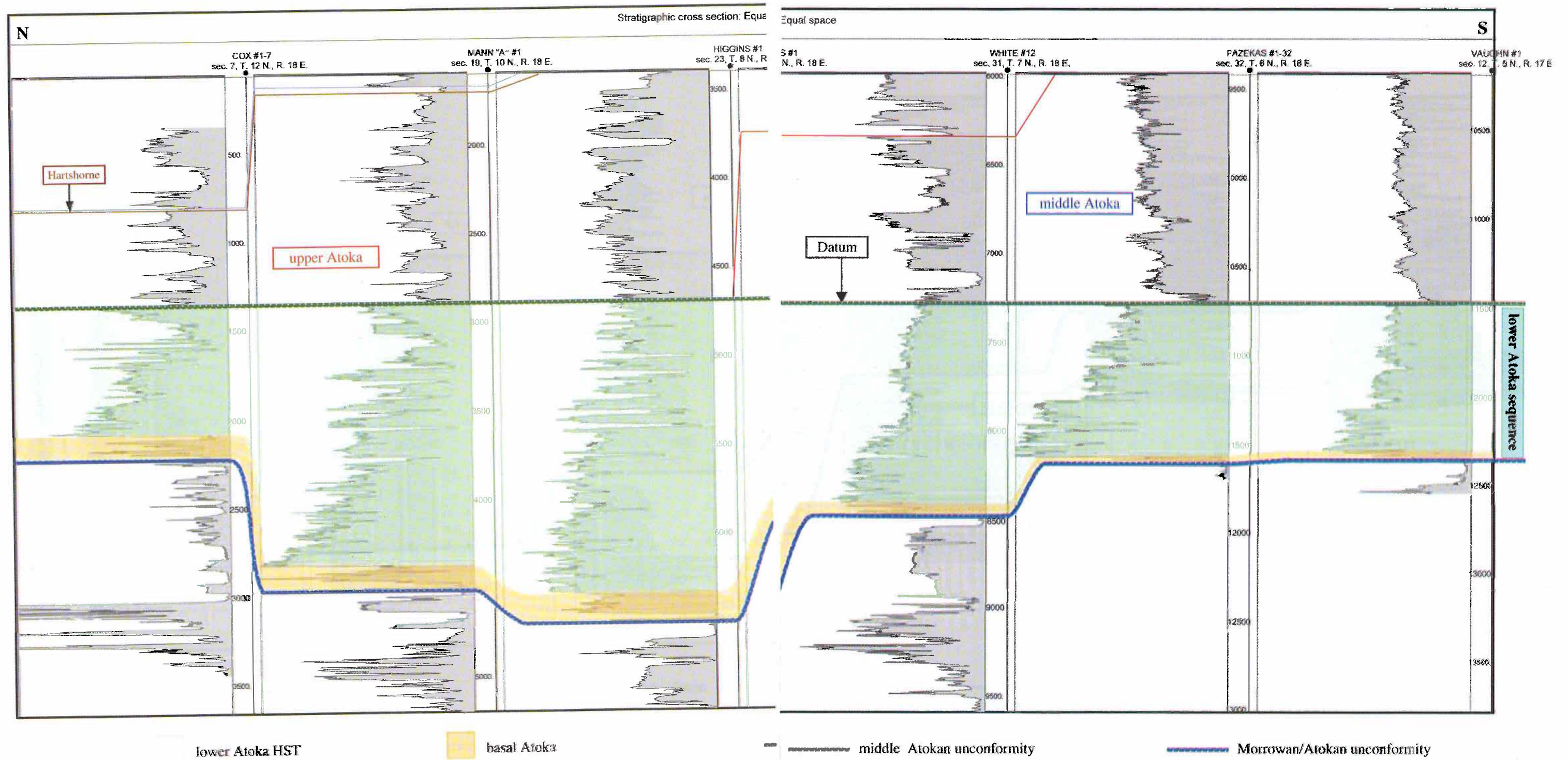


**Figure 10.** North-south regional stratigraphic cross section in the central part of the Arkoma Basin using conductivity logs. Thick lower Atoka HST occurs in the central part of the basin. To the south the section thins (probably because of non-depositional and/or submarine erosion), and sandstones of the middle Atoka turbidites unconformably overlie the lower Atoka prodelta shale. To the

north the lower Atoka HST section thins with occurrence of delta-front sandstones; it is unconformably overlain by the upper Atoka section. The cross section datum is the middle Atokan unconformity. For location, see Figure 2.



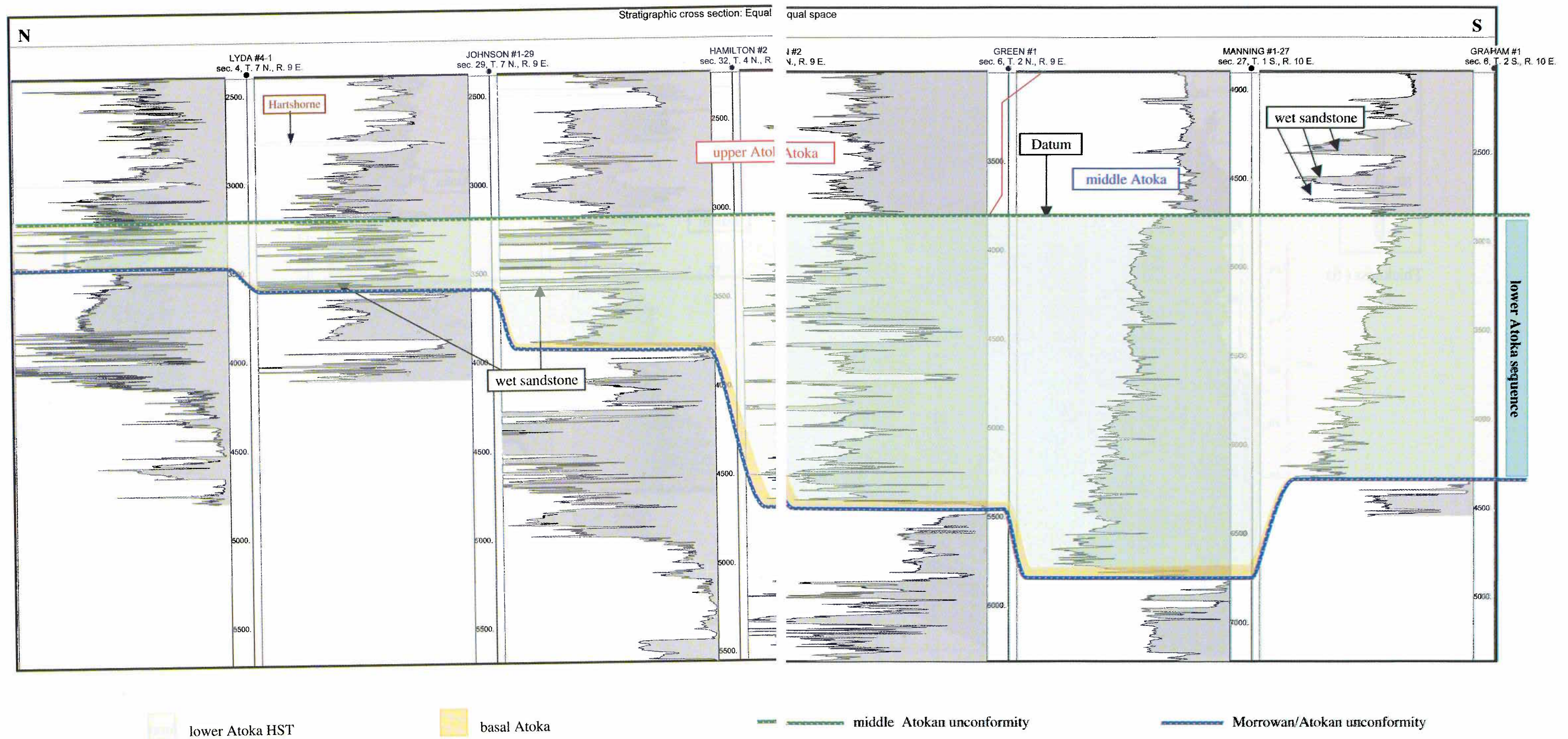


**Figure 11.** North-south regional stratigraphic cross section in the southwestern part of the Arkoma Basin using conductivity logs. Lower Atoka deltaic sandstones are stacked along the western margin of the basin. These deltaic sandstones grade into shale

toward the south and east. The cross section datum is the middle Atokan unconformity. For location, see Figure 2.



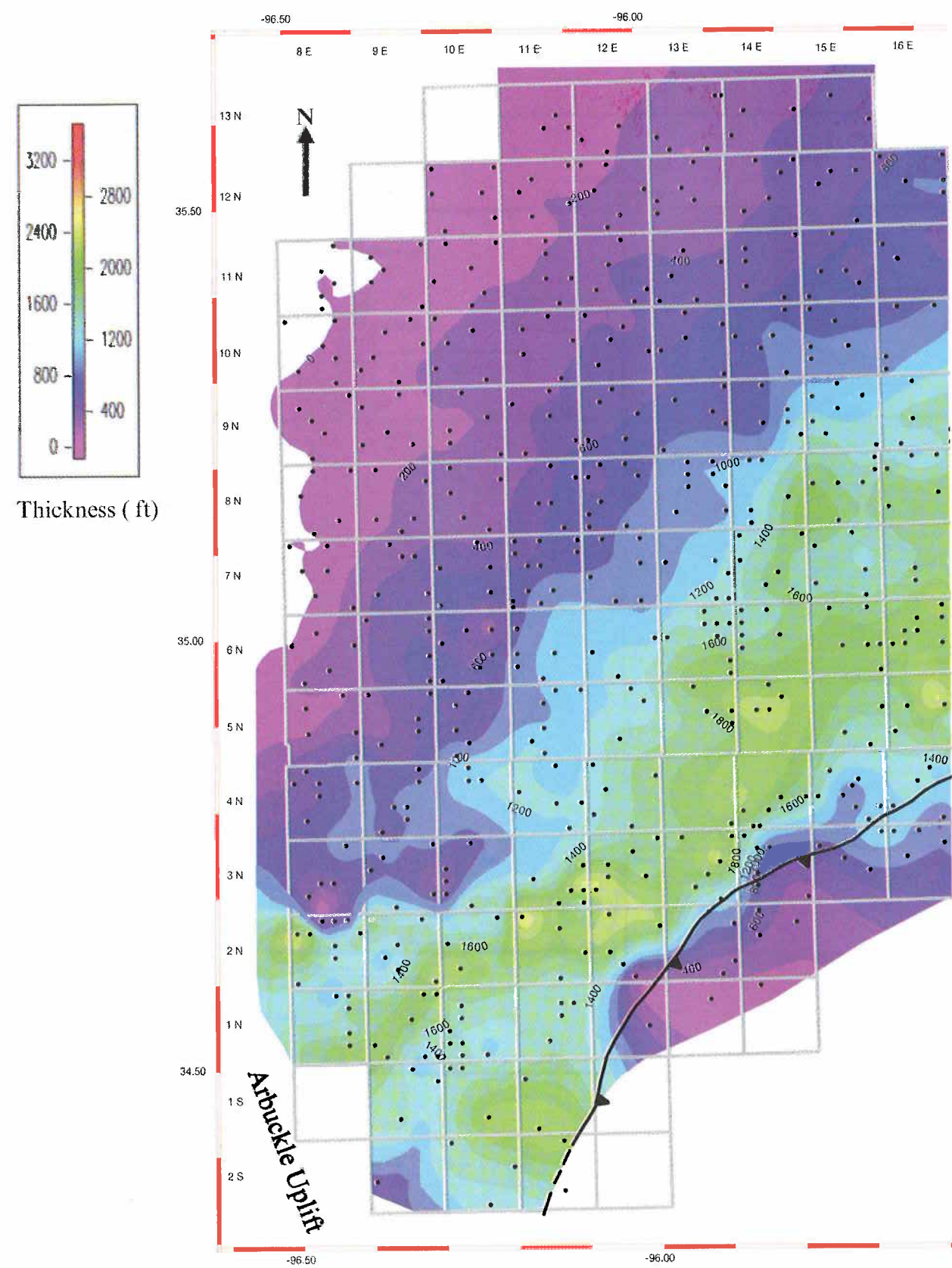
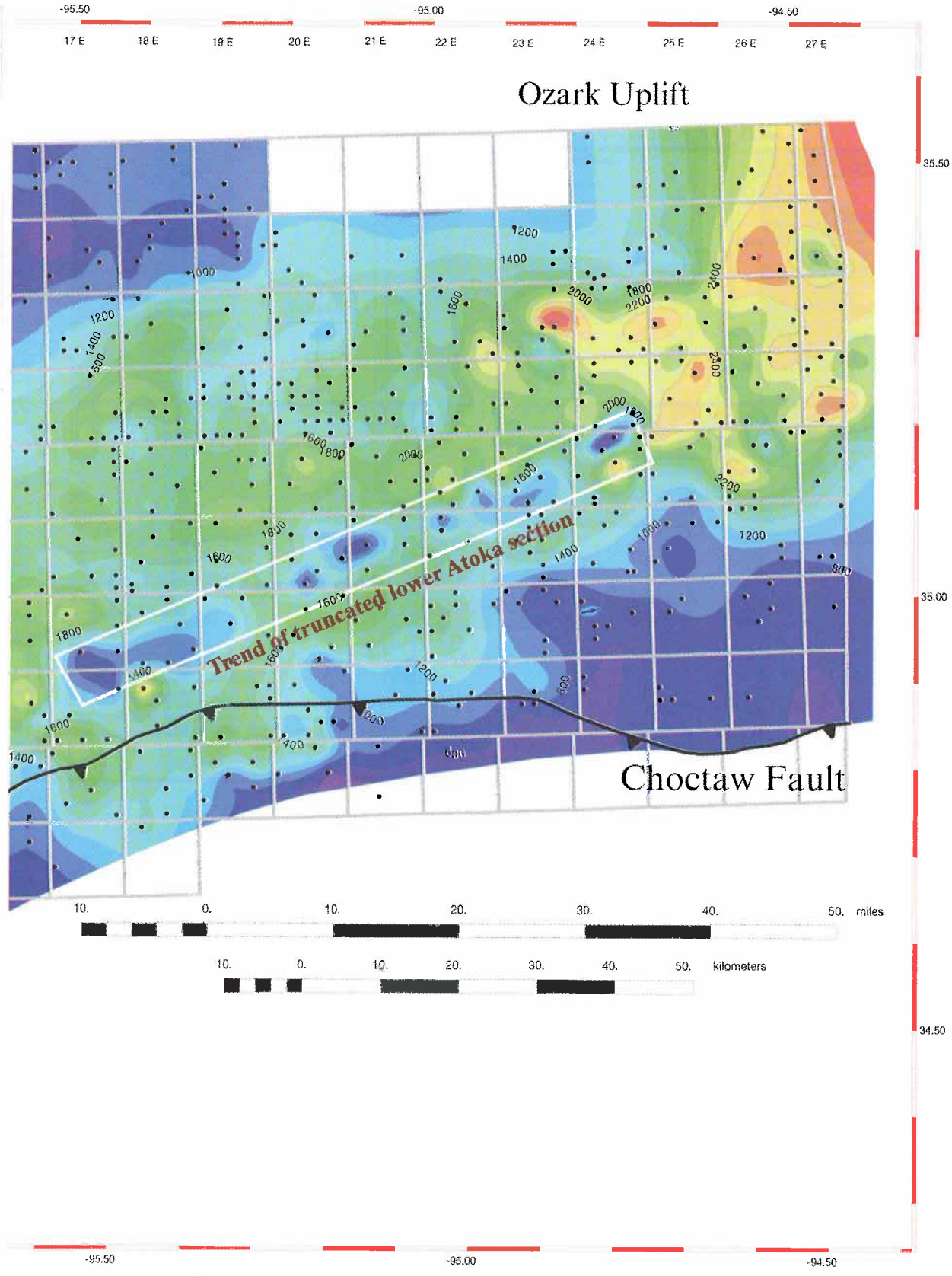


**Figure 12.** Isopach map of the lower Atoka sequence (basal Atoka LST and TST, and lower Atoka HST). The map shows an axis trending northeast-southwest for the thickest part of the lower Atoka sequence. The sequence thins to the north and south and is



completely absent in the extreme northwestern corner of the Arkoma Basin. An area of abrupt and anomalous thinning (white box) coincides with the northeast-southwest trend of the San Bois Fault indicated in Figure 2. Colored contour interval = 200 ft.



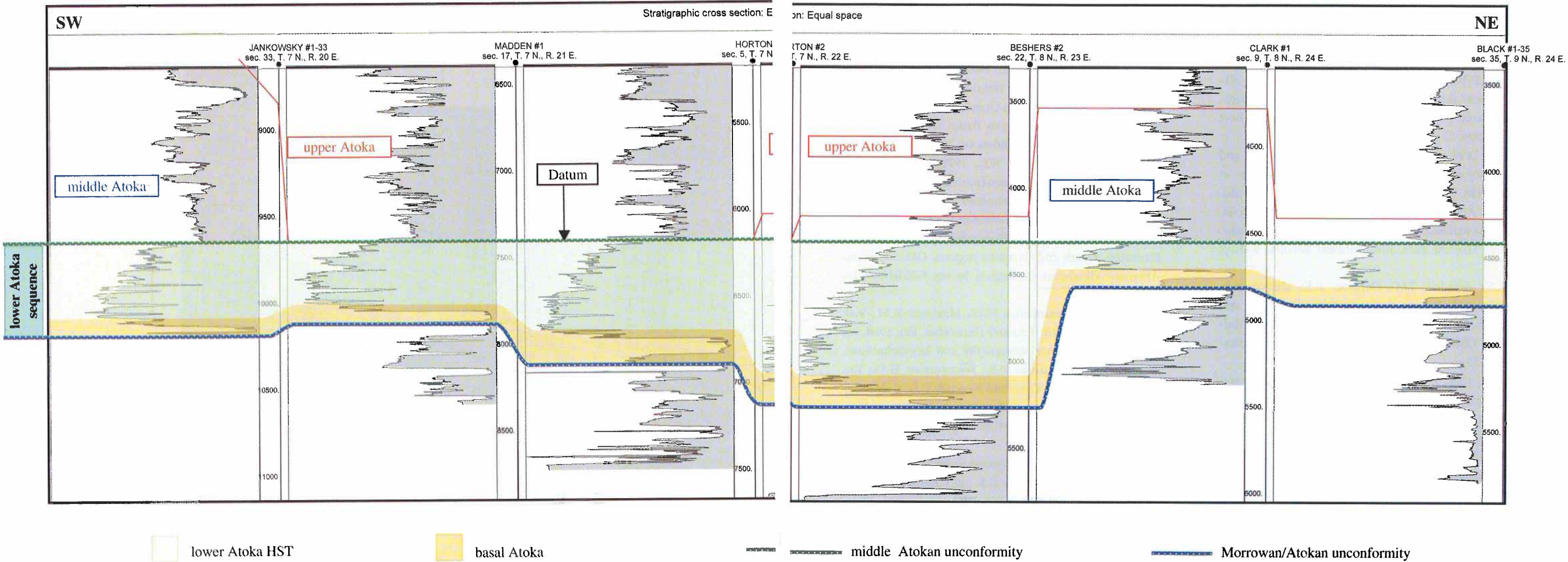


**Figure 13.** Northeast-southwest detailed stratigraphic cross section along the upthrown side of the San Bois Fault in the southern part of the Arkoma Basin. The figure shows that the lower Atoka HST is abruptly truncated at different levels, with more than 1,000 ft of section that may have been eroded in the Clark #1 and Black #1-35 wells. The only remaining lower Atoka HST parasequences

are the oldest ones, characterized by relatively high conductivity-log patterns. For pattern recognition, see Figure 4. The upthrown side of this syndepositional fault was probably an exposed shelf area during middle Atokan time. South of this fault thick middle Atoka turbidites were deposited. The cross section datum is the middle Atokan unconformity. For location, see Figure 2.

## REFERENCES CITED

- Brie, Alain; Johnson, D.L.; and Nurmi, R.D., 1985, Effect of spherical pores on sonic and resistivity measurements: Society of Professional Well Log Analysts, 26th Annual Logging Symposium, v. 1, paper W.
- Houseknecht, D.W., 1987, The Atoka Formation of the Arkoma Basin: tectonics, sedimentology, thermal maturity, sandstone petrology: Tulsa Geological Society Short Course Notes, 72 p.
- Houseknecht, D.W.; and Kacena, J.A., 1983, Tectonic and sedimentary evolution of the Arkoma foreland basin, *in* Houseknecht, D. W. (ed.), Tectonic-sedimentary evolution of the Arkoma Basin and guidebook to deltaic facies, Hartshorne sandstone: Society of Economic Paleontologists and Mineralogists, Midcontinent Section, v. 1, p. 3-33.
- Johnson, K.S.; Amsden, T.W.; Denison, R.E.; Dutton, S.P.; Goldstein, A.G.; Rascoe, Bailey, Jr.; Sutherland, P.K.; and Thompson, D.M., 1989, Geology of the southern Midcontinent: Oklahoma Geological Survey Special Publication 89-2, 53 p.
- Lonsinger, L.P., 1980, Lithostratigraphy and depositional systems of Pennsylvanian sandstones in the Arkoma Basin: University of Arkansas, Fayetteville, unpublished M.S. thesis, 97 p.
- McGee, K.R., 1979, Lithostratigraphy and depositional systems of upper Bloyd and lower Atoka strata in western Arkansas and eastern Oklahoma: University of Arkansas, Fayetteville, unpublished M.S. thesis, 131 p.
- Posamentier, H.W.; and Vail, P.R., 1988, Eustatic controls on clastic deposition II—sequence and systems tract models, *in* Wilgus, C.K.; Hastings, B.K.; Posamentier, H.W.; Van Wagoner, J.C.; Ross, C.A.; and Kendall, C.G. (eds.), Sea level changes: an integrated approach: Society of Economic Paleontologists and Mineralogists Special Publication, no. 42, p. 125-154.
- Salvador, Amos, 1985, Chronostratigraphic and geochronometric scales in COSUNA stratigraphic correlation charts of the United States: American Association of Petroleum Geologists Bulletin, v. 69, p. 181-189.
- Schoch, R.M., 1989, Stratigraphy: Principles and methods: Van Nostrand Reinhold, New York, 375 p.
- Spötl, Christoph; Houseknecht, D.W.; and Jaques, R.C., 1993, Clay mineralogy and illite crystallinity of the Atoka Formation, Arkoma Basin, and frontal Ouachita Mountains: The Clay Minerals Society, Clays and Clay Minerals, v. 41, p. 745-754.
- Stone, C.G., 1968, The Atoka Formation in north-central Arkansas: Arkansas Geological Commission, 11 p.
- Suneson, N.H.; and Hemish, L.A., 1994, Red Oak-Norris gas field, *in* Suneson, N.H.; and Hemish, L.A. (eds.), Geology and resources of the eastern Ouachita Mountains frontal belt and southeastern Arkoma Basin, Oklahoma: Oklahoma Geological Survey Guidebook 29, p. 49-53.
- Sutherland, P.K.; and Manger, W.L., 1979, Comparison of Ozark shelf and Ouachita Basin facies for upper Mississippian and lower Pennsylvanian series in eastern Oklahoma and western Arkansas, *in* Sutherland, P.K.; and Manger, W.L. (eds.), Mississippian-Pennsylvanian shelf-to-basin transition, Ozark and Ouachita regions, Oklahoma and Arkansas: Oklahoma Geological Survey Guidebook 19, 81 p.
- Van Wagoner, J.C.; Posamentier, H.W.; Mitchum, R.M.; Vail, P.R.; Sarg, J.F.; Loutit, T.S.; and Hardenbol, Jan, 1988, An overview of sequence stratigraphy and key definitions, *in* Wilgus, C.K.; Hastings, B.K.; Posamentier, H.W.; Van Wagoner, J.C.; Ross, C.A.; and Kendall, C.G. (eds.), Sea level changes: an integrated approach: Society of Economic Paleontologists and Mineralogists Special Publication, no. 42, p. 39-45.
- Visher, G.S., 1996, A history of Pennsylvanian deltaic sequences in Oklahoma, *in* Johnson, K.S. (ed.), Deltaic reservoirs in the southern Midcontinent, 1993 symposium: Oklahoma Geological Survey Circular 98, p. 18-31.
- Zachry, D.L., 1983, Sedimentary framework of the Atoka Formation, Arkoma Basin, Arkansas, *in* Houseknecht, D.W. (ed.), Tectonic-sedimentary evolution of the Arkoma Basin and guidebook to deltaic facies, Hartshorne sandstone: Society of Economic Paleontologists and Mineralogists, Midcontinent Section, v. 1, p. 34-52.
- Zachry, D.L.; and Sutherland, P.K., 1984, Stratigraphy and depositional framework of the Atoka Formation (Pennsylvanian), Arkoma Basin of Arkansas and Oklahoma, *in* Sutherland, P.K.; and Manger, W.L. (eds.), The Atokan Series (Pennsylvanian) and its boundaries—a symposium: Oklahoma Geological Survey Bulletin 136, p. 9-17.

# Middle Atoka Lowstand Systems Tract: Delineating the Middle Atoka in the Arkoma Basin, Oklahoma

*Azzeldeen A. Saleh*

Geology Department, Faculty of Science,  
University of Tanta, Egypt

**ABSTRACT**—The middle Atoka is the thickest stratigraphic interval within the Arkoma Basin in Oklahoma and is mainly confined to the southern and eastern parts of the basin. Its thickness changes dramatically (within a distance of 30 mi) from a few hundred feet close to the shelf area to about 10,000 ft north of the Choctaw Fault in the southeastern part of the basin. This interval is a lowstand systems tract (LST) and is mainly composed of turbidites deposited in a basin with significant structural relief associated with syndepositional faults.

The lower and upper bounding surfaces of the middle Atoka LST were correlated in hundreds of wells drilled in more than 200 townships throughout the Arkoma Basin in Oklahoma. The lower bounding surface is a sequence boundary marked by an unconformity on the top of the lower Atoka sequence. The upper bounding surface is a transgressive surface marking the rise of relative sea level during late Atokan time.

Several gas fields, such as the Red Oak, Kinta, and Wilburton Fields, have produced large amounts of gas from the sandstones within the middle Atoka LST in the Arkoma Basin in Oklahoma. The application of sequence stratigraphy provides tools for regionally and locally correlating and defining the stratigraphic position of the numerous sandstones within the thick shale-dominated LST. The lithostratigraphically defined sandstones that occur within the middle Atoka LST can be arranged as follows (from bottom to top): basin-floor sandstones, such as the Shay sandstone; slope-fan sandstones deposited in several channel-levee complexes, such as the Brazil, Diamond, Panola, and Red Oak sandstones; and lowstand wedge sandstones, such as the Fanshawe sandstone.

## INTRODUCTION

Several lithostratigraphic sandstone units occur in the Atoka Formation south of the San Bois and Kinta Faults in the Oklahoma part of the Arkoma Basin. Based on the informal subdivision of the Atoka Formation into lower, middle, and upper intervals (Houseknecht and Kacena, 1983; Zachry, 1983), these sandstones have been assigned to the middle Atoka, primarily based on their position in the middle of the thick Atoka shale section south of the major faults. These sandstones, such as the Red Oak, Brazil, and Panola, have been interpreted as deep-water sediments (turbidites) driven by gravity flows (Vedros and Visser, 1978; Wanslow, 1985; Johnson and others, 1989; Houseknecht and Ross, 1992; Visser, 1996).

Sequence stratigraphic concepts provide powerful tools for analyzing the evolutionary history of sedimentary basins (Nummedal and Swift, 1987). In a Type 1 sequence, the LST is dominated by turbidites. It is deposited during a time of rapid fall followed by a slow rise of relative sea level, and is followed by a transgressive systems tract (TST) deposited during a rapid rise in relative sea level (Van Wagoner and others, 1988).

These systems tracts are bounded by key surfaces that can be utilized to delineate the thick shale-dominated middle Atoka turbidites throughout the Arkoma Basin in Oklahoma. The bounding surfaces include unconformities, first transgressive (marine flooding) surfaces, and maximum flooding surfaces (Fig. 1). These sequence stratigraphic tools provide a framework for correlating, mapping, and conse-

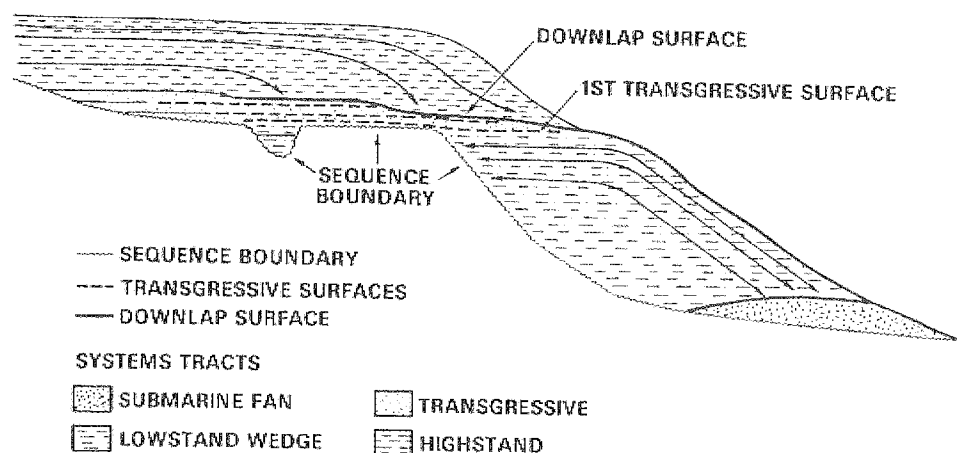


**Figure 1.** Schematic diagram showing the stratigraphic relationship of key correlation surfaces within a sequence. These surfaces are: sequence boundary (unconformity), first transgressive surface, and downlap surface (maximum flooding surface marked by condensed sections on the gamma ray log) (modified after Loutit and others, 1988).

quently delineating depositional trends on the shelf or in the deep parts of the basin.

### THE BOUNDING SURFACES OF THE MIDDLE ATOKA LST

The middle Atoka interval overlies the lower Atoka sequence (Saleh, this volume). Their bounding surface can be identified by an abrupt change in the conductivity pattern characteristic of the highstand systems tract (HST) of the lower Atoka sequence (Figs. 2 and 3). This surface in the deep parts of the Arkoma Basin is marked by thick sandstones (basin-floor fan) or thin sand and thick shale (slope fan), overlying the thin, lower Atoka prodelta shale (Figs. 2 and 3). On the shelf, this surface represents an unconformity and is marked by three characteristics:

1. Truncation of the lower Atoka HST, especially on the upthrown side of the San Bois Fault (Saleh, this volume);
2. Absence of the thick, middle Atoka shale that contains turbidite sandstones such as Red Oak and Brazil (Fig. 3);
3. Presence of the basal transgressive sandstone–shale of the upper Atoka interval directly overlying the lower Atoka HST in the shelf areas (Fig. 3).

This unconformity surface is a sequence boundary between the lower Atoka sequence and the overlying upper Atoka interval, and is termed the “middle Atokan unconformity.”

The first transgressive surface is produced during a transgression of high-energy near-shore environments across the shelf area of a basin (Loutit and others, 1988). Thus, the sur-

face forms a boundary between the LST, generally confined to the fore-deep of a basin, and the overlying transgressive sediments. The upper bounding surface of the middle Atoka interval is a transgressive surface between the middle Atoka and the upper Atoka intervals, and extends across the shelf areas of the Arkoma Basin (Fig. 3). A relatively high conductivity signature at the top of the middle Atoka LST marks this surface (Fig. 4). In areas where the basal upper Atoka sandstone becomes shaly, a condensed section occurs at its top (Fig. 3). This condensed section is widespread in the southern parts of the Arkoma Basin, making it easy to track the transgressive surface

beneath (Fig. 4).

The lower and upper bounding surfaces of the middle Atoka interval were correlated in hundreds of wells drilled in more than 200 townships throughout the Arkoma Basin in Oklahoma. An isopach map reveals that this interval is mainly confined to the southern and eastern parts of the basin (Fig. 5). It is completely absent in the north-northwest parts of the Arkoma Basin, which may represent parts of the shelf area during the deposition of the middle Atoka turbidites in the south. The thickness of the middle Atoka interval changes dramatically (within a distance of 30 mi) from a few hundred feet close to the shelf area to about 10,000 ft north just of the Choctaw Fault in the southeastern part of the basin, which is the thickest stratigraphic interval in the Arkoma Basin in Oklahoma (Fig. 5).

This interval represents a LST that was deposited during the falling stage and early slow rise of the relative sea level, as indicated by the shift of the depocenter to the southern parts of the Arkoma Basin (compared to the lower Atoka HST) and the occurrence of an unconformity on the shelf. This thick LST contains several sandstones that are confined to the deep parts of the basin and are interpreted as turbidites by several authors.

Different nomenclatures are used to define the units within a LST. Vail (1987) and Van Wagoner and others (1987) defined a basin-floor fan, slope fan, and prograding complex as separate depositional units within the LST. Posamentier and Vail (1988) and Posamentier and others (1991) divided the LST into a lowstand fan (basin-floor fan) and a lowstand wedge. The lowstand wedge has two components: early lowstand (slope fan) and late lowstand (prograding complex).



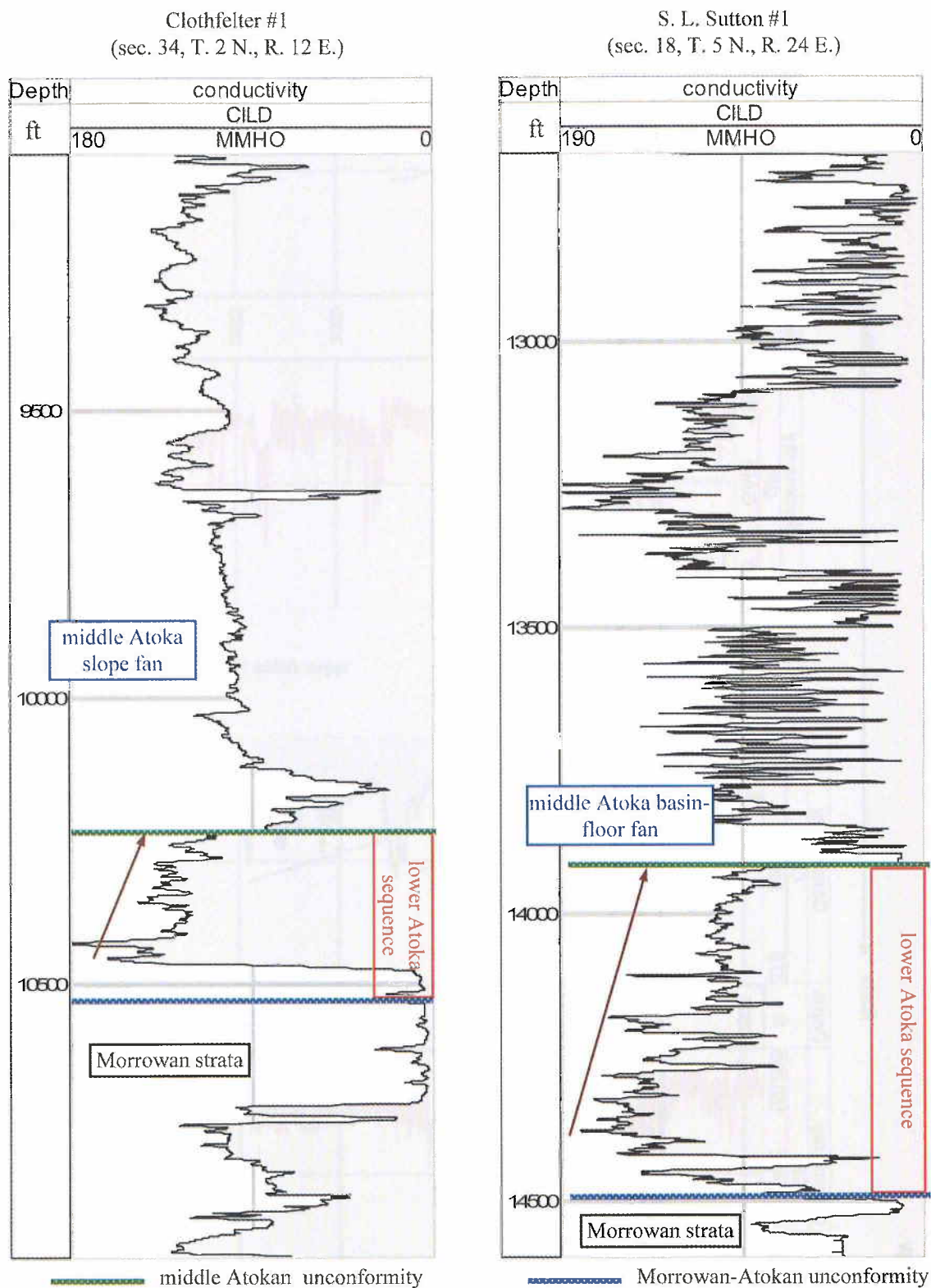


**Figure 2.** Two wells in the east and west within the southern depocenter of the Arkoma Basin showing the remaining section of the lower Atoka sequence unconformably overlain by a middle Atoka basin-floor fan (right) and middle Atoka slope fan (left). Note the decreasing conductivity-log pattern that is characteristic of lower Atoka HST (brown arrows). The prodelta shale of the lower Atoka HST in both wells is very thin compared to more than 3,000 ft of the lower Atoka section in the northeastern Arkoma Basin (Saleh, this volume).

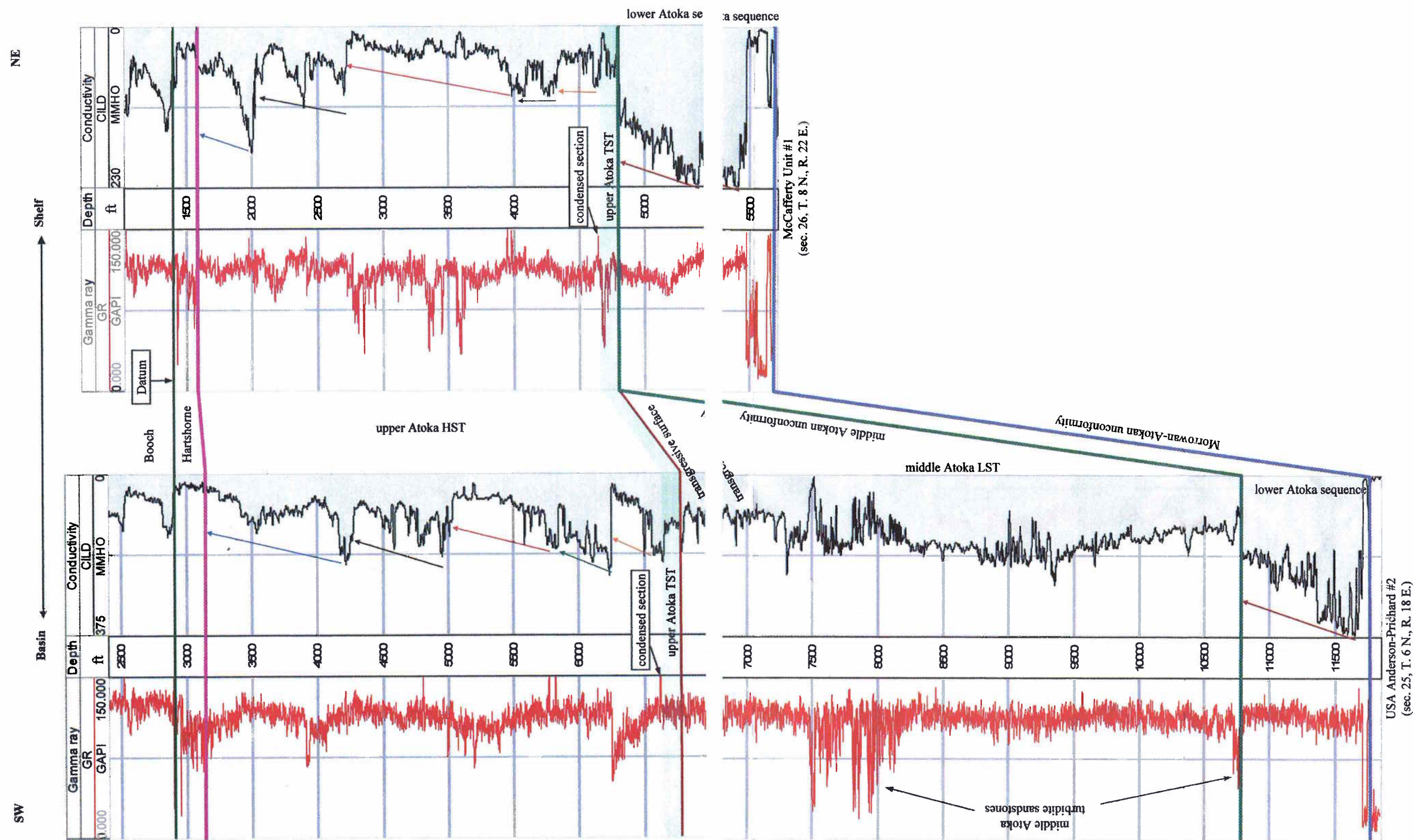


**Figure 3.** The bounding surfaces for the middle Atoka LST. The lower surface is identified by an abrupt change in the conductivity pattern characteristic of the HST of the lower Atoka sequence. On the shelf, this surface represents an unconformity and is marked by: (1) truncation of the lower Atoka HST, especially on the upthrown side of the San Bois Fault; (2) the absence of the thick, middle Atoka shale that contains turbidite sandstones such as Red Oak and Brazil; and (3) the presence of the basal transgressive sandstone–

shale of the upper Atoka interval directly overlying the lower Atoka HST in shelf areas. This surface is termed the middle Atokan unconformity. The middle Atoka upper bounding surface is a transgressive surface that extends across shelf areas of the Arkoma Basin. In areas where the basal upper Atoka sandstone becomes shaly, a widespread condensed section occurs at its top.



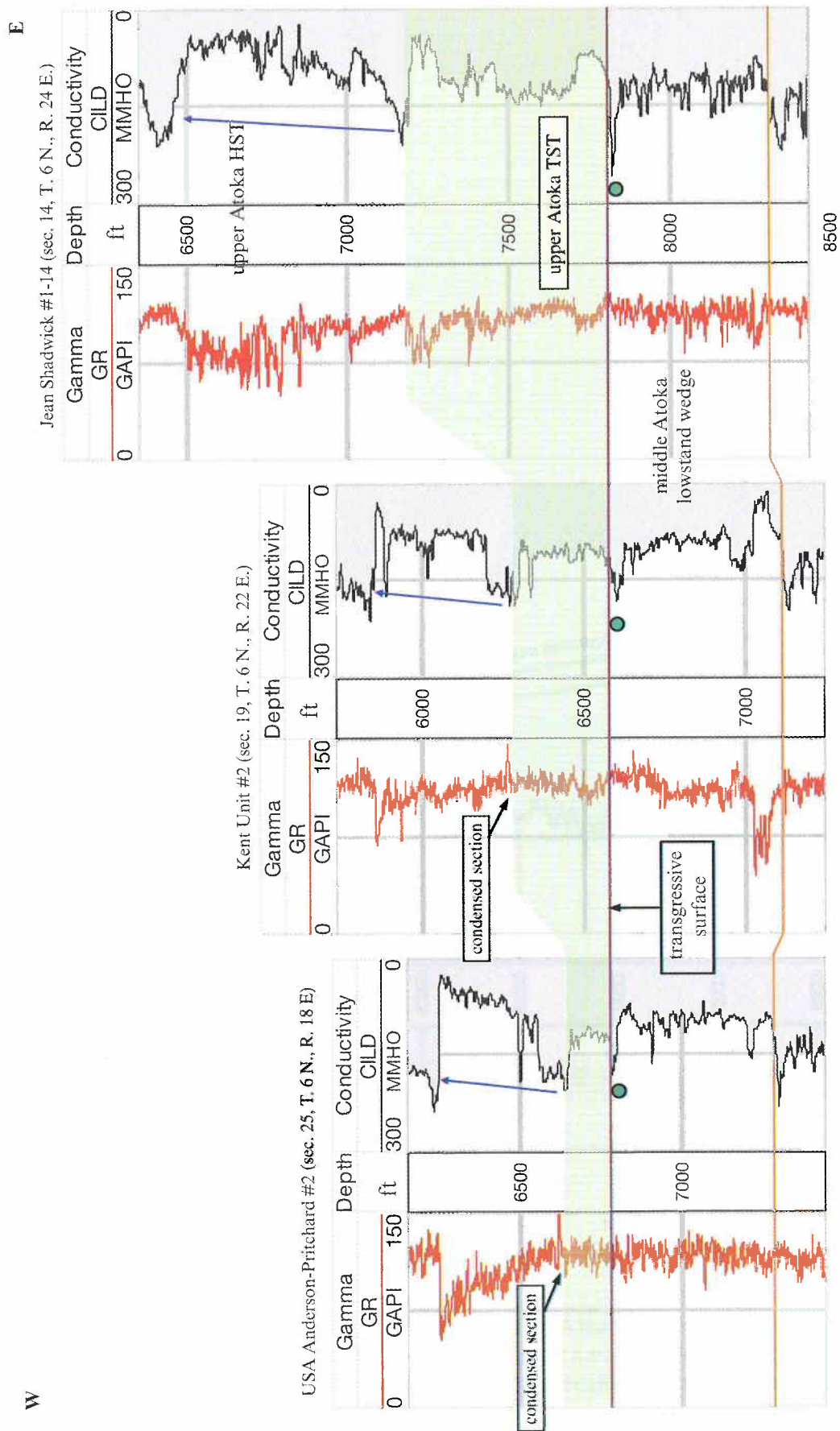


**Figure 4.** East-west detailed cross section using gamma ray and conductivity logs. A relatively high conductivity signature (green circle) marks the transgressive surface between the middle Atoka LST and upper Atoka TST. In areas where the upper Atoka TST becomes shaly, a condensed section occurs at its top, which facilitates tracking the transgressive surface beneath. Datum is the upper Atoka transgressive surface. Horizontal scale is equal spacing. For location, see Figure 5.

This work follows Van Wagoner and others' (1988) terminology of dividing the LST into basin-floor fan, slope fan, and lowstand wedge (Fig. 6).

### THE BASIN-FLOOR FAN

Generally, basin-floor fans tend to be best developed on a third-order sequence boundary (Mitchum and Van Wagoner, 1991). The middle Atoka basin-floor fan overlies the lower Atoka third-order sequence and is generally limited to the southeastern depocenter of the Arkoma Basin. It is composed of interbedded sandstone and shale intervals with common occurrence of thick sandstone intervals (S.L. Sutton #1 well in Fig. 2). Its thickness is more than 3,000 ft in the Short Unit #1 well (Fig. 6). Houseknecht (1986, 1987) and Houseknecht and McGilvery (1990) described an axial fan system in the foredeep of the Arkoma Basin in Oklahoma, implying a single-point source for sediment dispersal from the east. McGilvery and Houseknecht (2000), in a study that included outcrops in the Ouachita Mountains, acknowledged the multiple, coeval sediment-dispersal systems with primary sediment input from the east and southeastern margins of the basin. Based on this interpretation, the authors defined the basin-floor fan as an apron complex.

On scout tickets, the sandstones within this basin-floor fan are called the Cecil or Shay sandstones. The name "Cecil" was used for the first sandstone units occurring above the Spiro sandstone in Arkansas and the eastern part of the Arkoma Basin in Oklahoma. The Cecil sandstone belongs to the lower Atoka sequence (Saleh, this volume). Thus, it should not be confused with sandstones of the basin-floor fan deposited unconformably on the top of the lower Atoka prodelta shale in the deep parts of the Arkoma Basin.

### THE SLOPE FAN

The basin-floor fan is overlain by a thick shale interval with thin sandstone beds. This interval is interpreted as a mud-rich slope fan that extends along the southern margin of the Arkoma Basin. This is shown in two east-west and north-south cross sections (Figs. 6 and 7, respectively). The maximum thickness of the slope fan lies to the south of both the San Bois and Kinta Fault trends, where it is more than 5,000 ft thick in some locations. The huge thickness of the slope fan indicates that, despite the rapid sediment influx, the fault-controlled basin was subsiding at such a rapid rate that slope or basinal water depths were maintained. Several sandstone intervals occur within the channel-levee complexes of the mud-rich slope fan. These sandstones have been interpreted as deep-water sediments driven by gravity flows (Vedros and Visser, 1978; Wanslow, 1985; Johnson and others, 1989; Houseknecht and Ross, 1992; Visser, 1996). They

were deposited in slope-channel complexes (Houseknecht and Ross, 1992; McGilvery and Houseknecht, 2000).

The vertically stacked channel-levee complexes can be grouped as a fourth-order cycle. The Brazil sandstone is the oldest of these complexes within the slope fan of the third-order sequence. The base of the Brazil channel-levee complex can be considered a fourth-order sequence boundary because of its relatively widespread occurrence south of the San Bois and Kinta Fault trends. Also, it separates the deeper slope-fan shale, overlying the basin-floor fan, from the stacked channel-levee complexes above it (Figs. 6 and 7).

Several sandstone intervals within the channel-levee complexes occur south of the San Bois Fault trend. Adopting the classification of Galloway (1998), the sediment feeder system for these complexes within the Arkoma Basin may have changed from a line-source (shelf-fed) along the San Bois Fault in the east, to a point-source feeder (channel or canyon) in the west (Fig. 8). This is shown in three cross sections across the Arkoma deep basinal areas (Figs 9, 10 and 11). Figure 9 shows several channel-levee complexes within the slope fan without a clear indication of a point source such as a canyon or thick channel. Detailed correlations indicate that the sandstones within these complexes were funneled from north to south through notches, forming pod-like geometries overlain by shales with few thin-bedded sandstones within a specific stratigraphic zone (Fig. 12). The line-source interpretation for the turbidites south of the San Bois Fault is supported by the presence of a wide area of extensive erosion of the lower Atoka HST section along the upthrown side of the fault (Saleh, this volume). Farther west, better indication of a long channel with sourcing from the north can be observed in Figures 10 and 11. For example, the thick sandstone interval at 6,235–6,564 ft in the George Peden #2 well in Figure 11 is correlates to the deeper sandstone at 6,675–7,210 ft at the Lewis #4–12 well about 10 mi to the south where the slope-fan section thickens. In the southwestern part of the Arkoma Basin the shaly slope fan gradually becomes thin and several fining-upward parasequences dominate the middle Atoka LST.

Despite the general north-south trend of the channel-levee complexes (Figs. 9–12), the sandstones within some complexes show an easterly or westerly component to the north-south trend, indicating changes in the source direction or in the availability of accommodation space. Based on paleocurrent measurements from Atoka turbidite outcrops in the frontal Ouachitas, Ferguson and Suneson (1988) concluded that sediments were distributed by at least two spatially distinct, coeval, oppositely directed fan systems; some sourced from the east and others from the west (Fig. 13). In my view, the idea of predominant eastern sourcing for the turbidites in the Arkoma Basin is incorrect and is mainly in-



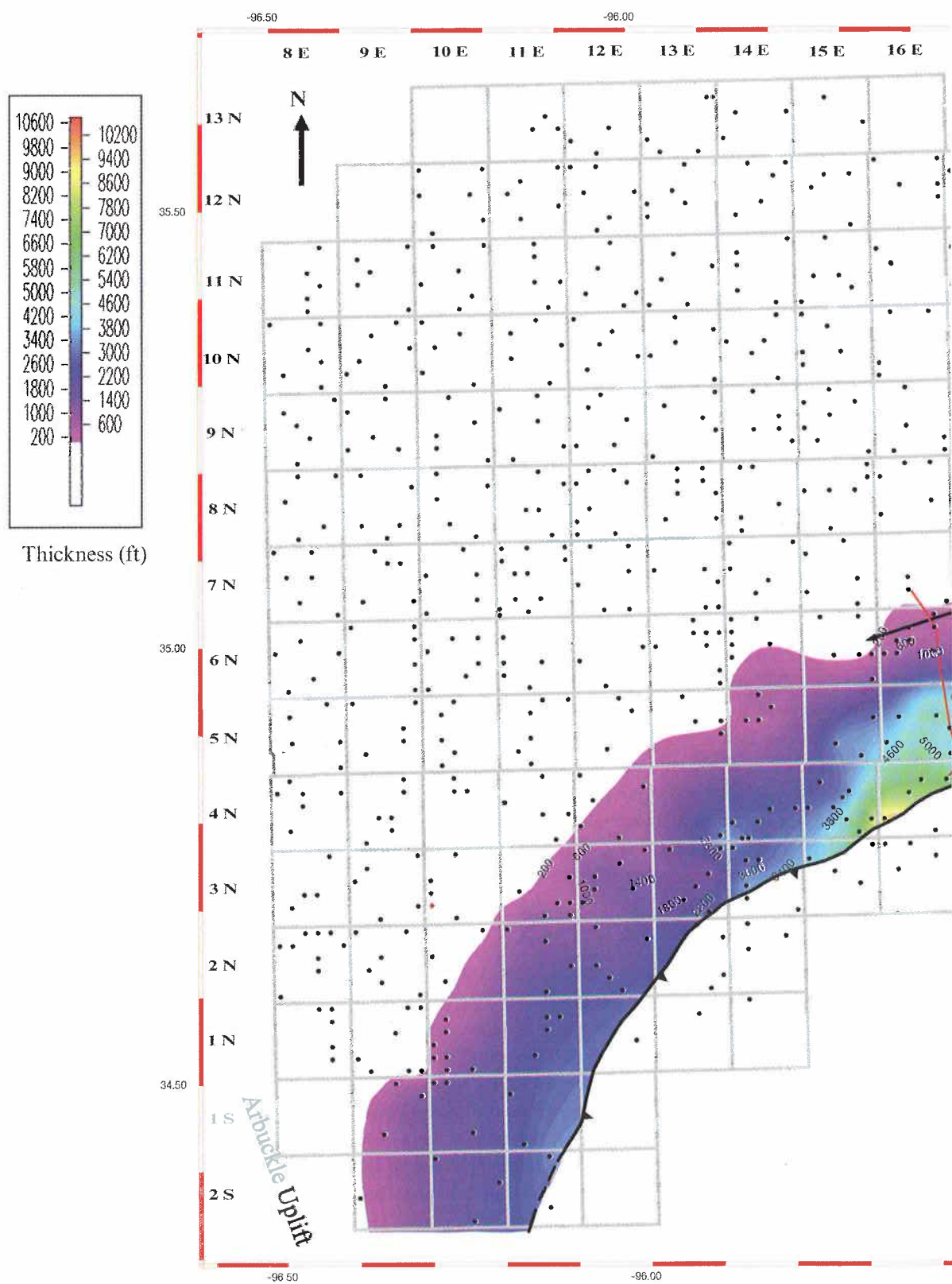
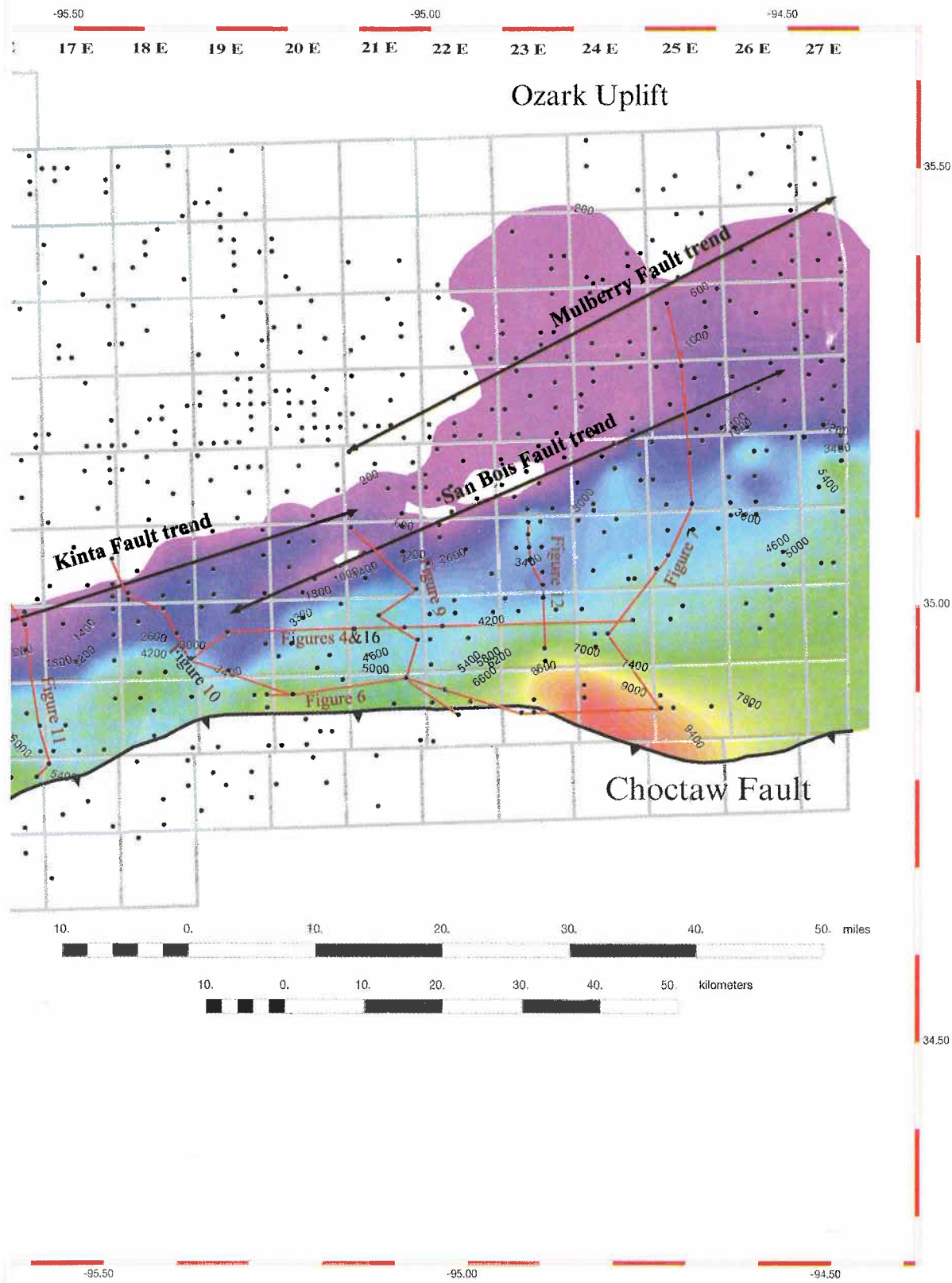


**Figure 5.** Isopach map of the middle Atoka LST showing its areal extent in relation to major syndepositional fault trends. The growth faults provided a huge accommodation space for deposition of basin-floor and slope fans, which abruptly thicken on the downthrown side of both the San Bois and Kinta Fault trends. The downthrown side of the Mulberry Fault provided accommodation space for more



widespread accumulation of a thick, lowstand wedge that extended farther northeast beyond the limit of the San Bois Fault trend. A platform extending to the north and northwest of these faults may have been part of the shelf area with no turbidite sedimentation during middle Atokan time. The map also shows the location of all cross sections. Colored contour interval = 200 ft.



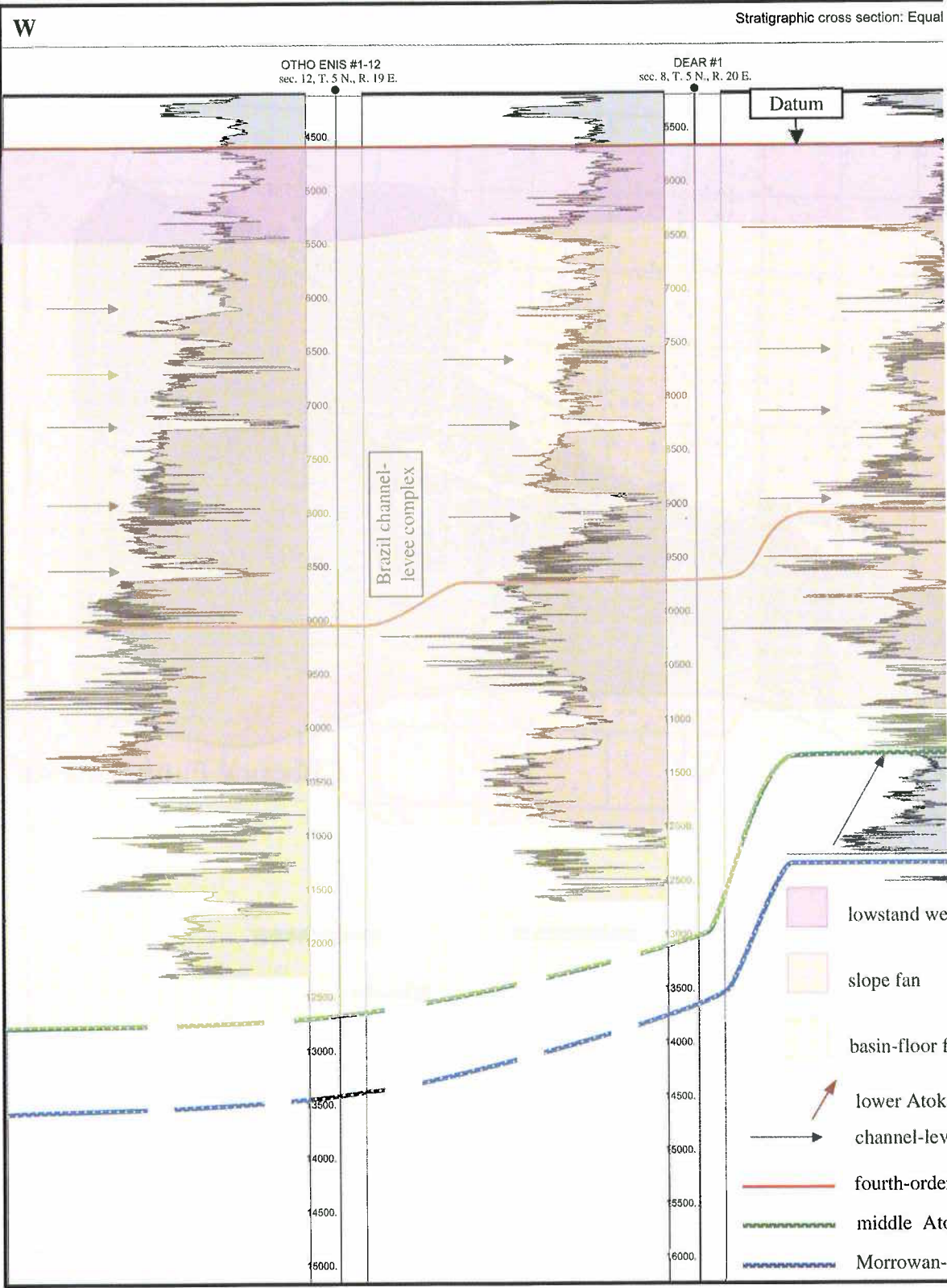
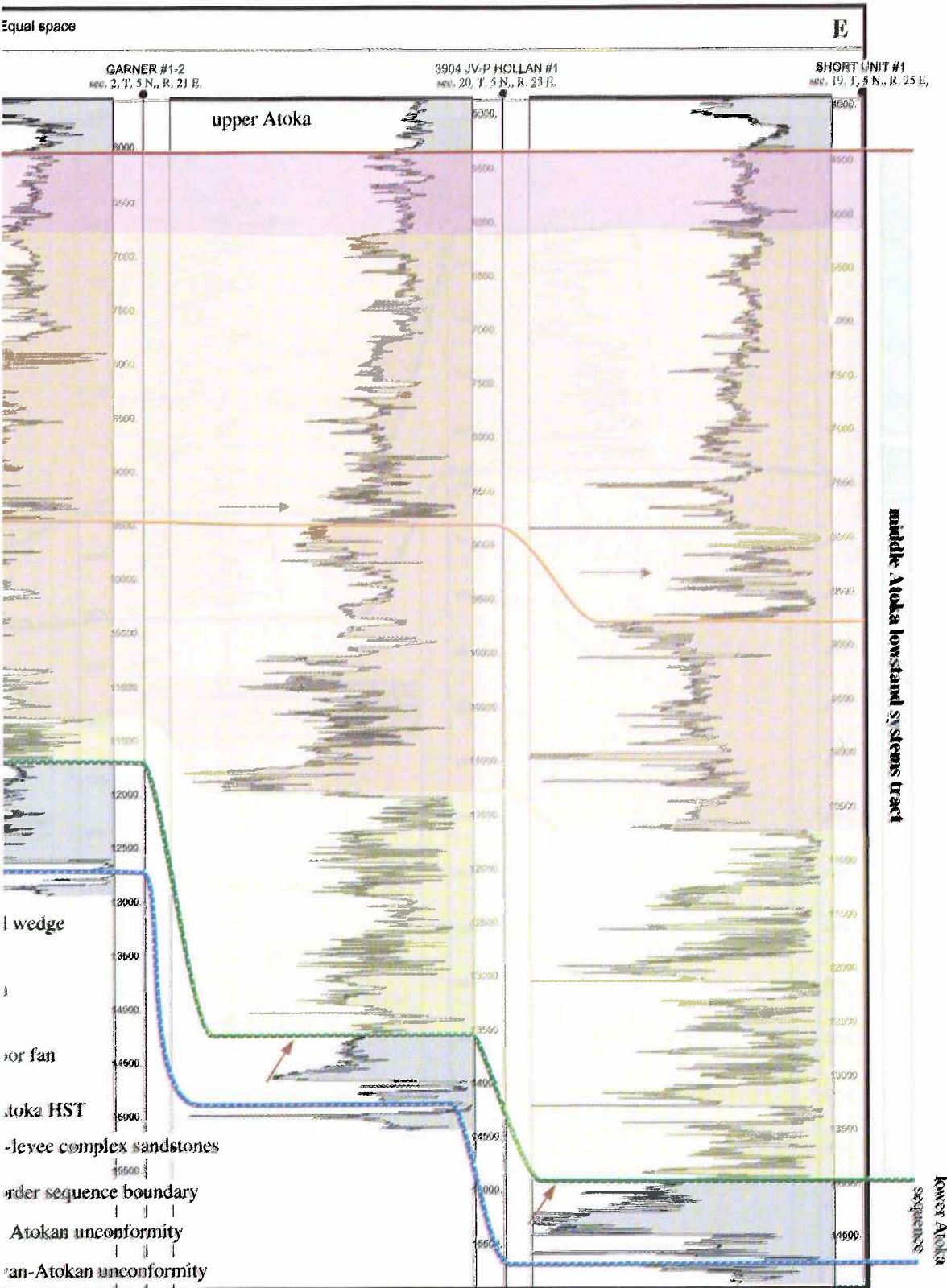


**Figure 6.** East-west stratigraphic cross section in the southwest margin of the Arkoma Basin where the thickest middle Atoka LST section occurs. The section is composed of a basin-floor fan, a slope fan, and a lowstand wedge. The sandstones within the basin-floor fan are mistakenly called Cecil sandstones, which were deposited within the lower Atoka sequence. The channel-levee



complexes may represent a fourth-order cycle within the third-order mud-rich slope fan. The Brazil channel-levee complex is considered to be the base of this fourth-order sequence because of its widespread occurrence overlying an older, thick shaly slope fan. The cross-section datum is the upper Atoka transgressive surface. For location, see Figure 5.



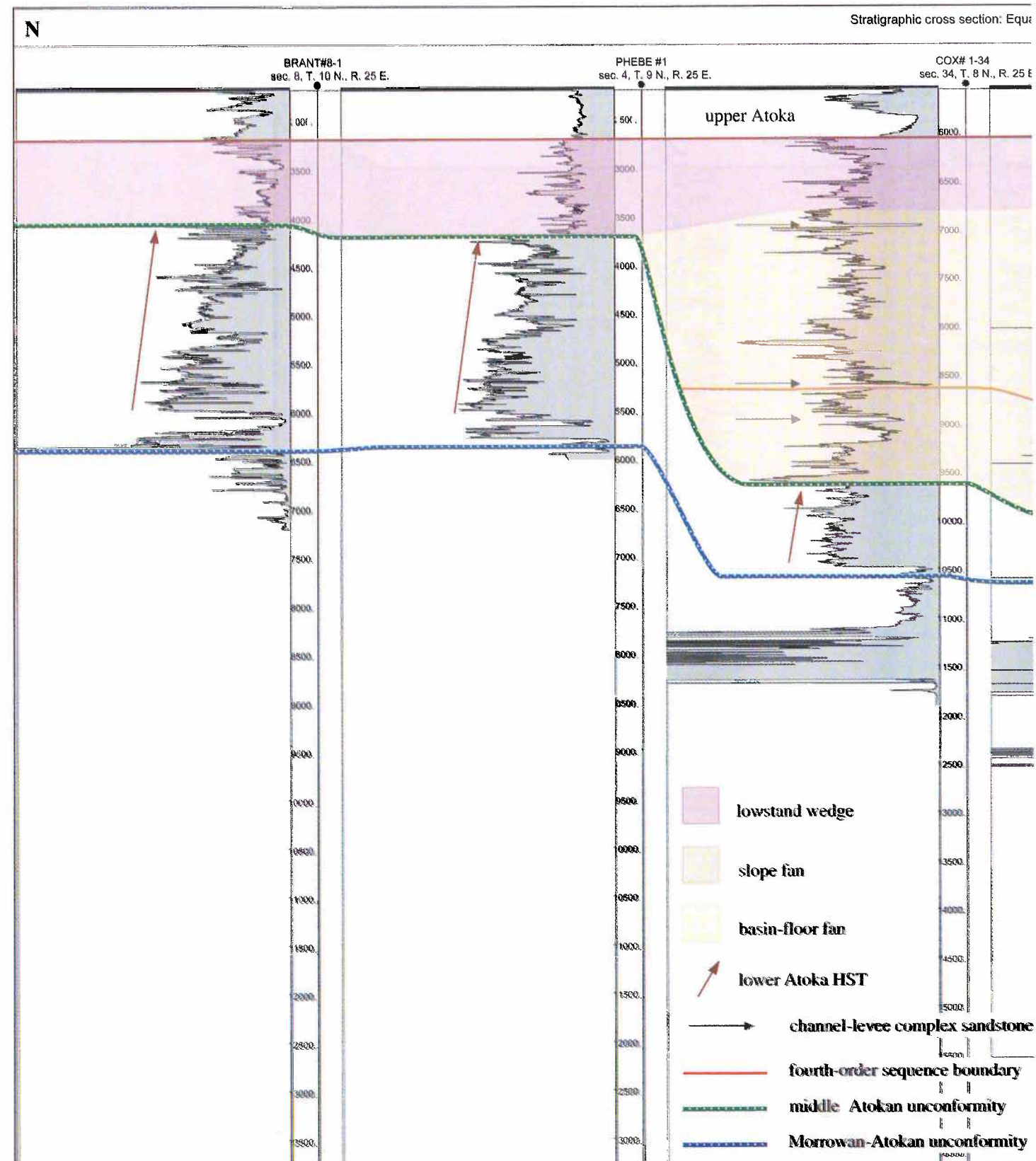
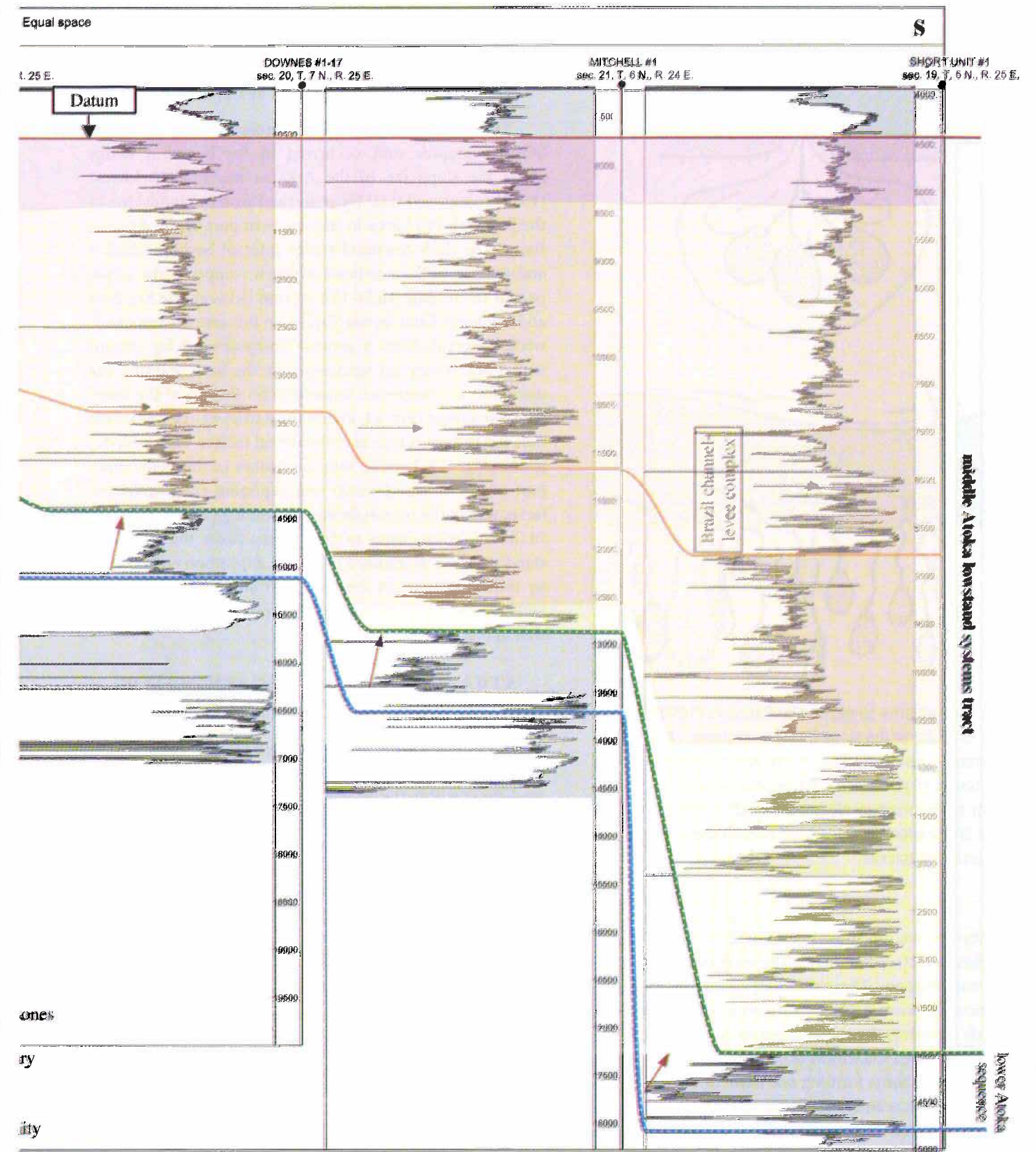


**Figure 7.** North-south stratigraphic cross section across the eastern part of the Arkoma Basin where the farthest northward extension of the middle Atoka LST section occurs. Thickness of the section changes from a few hundred feet to nearly 10,000 ft within a distance of less than 30 mi. Growth faults in the south provided huge accommodation space for deposition of the basin-



floor fan and the thick, mud-rich slope fan. Both fans are mainly confined to these growth faults but the lowstand wedge extends farther north, as shown in the Phebe #1 and Brant #8-1 wells. The cross-section datum is the upper Atoka transgressive surface. For location, see Figure 5.

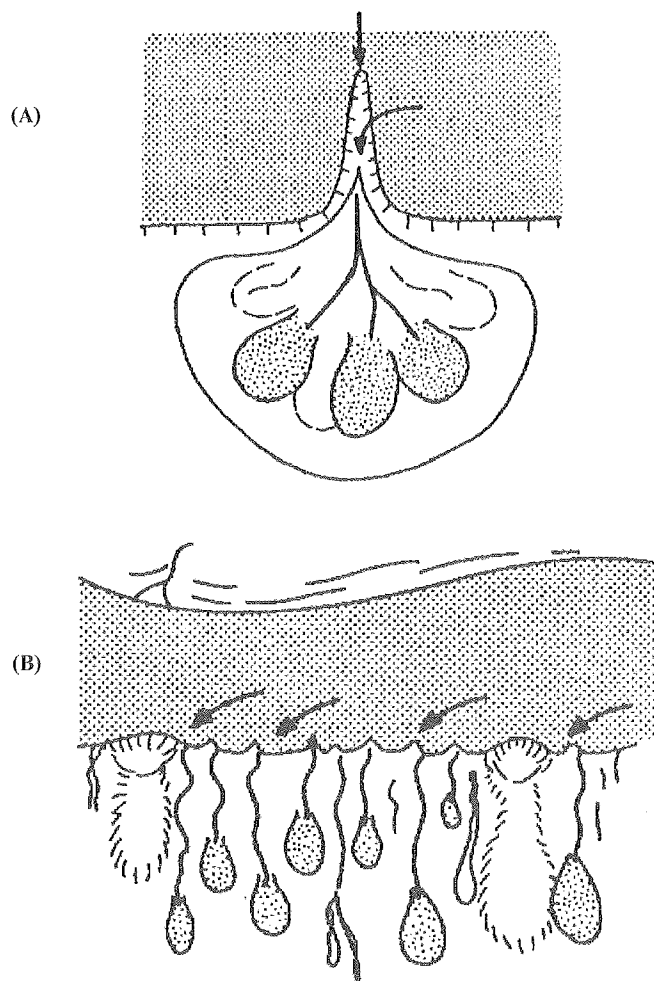


**Figure 8.** Two patterns suggested by Galloway (1998) for sediment sourcing of the slope turbidite systems. (A) Point-source through submarine canyon, basin-floor channel, or tectonic trough. (B) Sediments are locally funneled through notches or small erosional channels that shift frequently, creating a line-source along the shelf margin with several channel-levee complexes.

fluenced by the outcrop studies conducted in the Ouachitas. In describing a tectonic model for the evolution of the Ouachita system, Viele and Thomas (1989) stated that growth of an accretionary prism probably formed a submarine ridge, imperfectly dividing the closing ocean into two primary basins: the southern Ouachitas of Arkansas and the central Ouachitas of Oklahoma forming one basin in the south, and the frontal Ouachitas and Arkoma Basin developing another basin to the north. If this model is valid, we should not extend the eastern sourcing observed in the Ouachitas to the Arkoma Basin, especially with the knowledge that turbidite sequences from southern parts of the Ouachita system were

thrust northward to their present position close to the southern margin of the Arkoma Basin.

### THE LOWSTAND WEDGE

The Fanshawe sandstone represents the uppermost lithostratigraphic unit occurring in the lowstand wedge above the slope fan in the Arkoma Basin. Houseknecht (1987) recognized tidal facies in the Fanshawe sandstone in the Red Oak Field area in the southern part of the Arkoma Basin. The shaly lowstand-wedge interval becomes thicker and sandier to the northeast where it comprises the major part of the middle Atoka LST section between the San Bois and Mulberry Fault trends (Fig. 5). In this area the lowstand-wedge interval shows a general fining-upward log pattern with thick, valley-fill sandstones at the base marking the unconformity (sequence boundary) on the top of the lower Atoka sequence (Fig. 14, except the Battles #1–19 well). This well-log pattern is typical of the fluvial incised-valley-fill deposits (Fig. 15). Locally, thin sandstones in the shaly upper part of the lowstand wedge may represent splay-overbank facies within the overall fining-upward log pattern (Fig. 14). In the southwest corner of the Arkoma Basin, the thick lowstand wedge is dominated by fluvial deposition as indicated by thin sandstones at the base of fining-upward intervals, with no indication of valley-fill deposition (Battles #1–19 well in Fig. 14).

### STRATIGRAPHIC IMPLICATIONS FOR DEFINING THE MIDDLE ATOKA LST

Several gas fields, such as the Red Oak, Kinta, and Wilburton Fields, have produced large amounts of gas from sandstones within the middle Atoka slope fan in the Arkoma Basin in Oklahoma. It is important to recognize a stratigraphic datum for correlating the channel-levee complexes within this slope fan. Without such a datum, it is easy to miscorrelate the sandstones within these complexes because of their laterally discontinuous nature and vertical multiple occurrences within a thick shale section (Fig. 16). The transgressive surface at the base of the overlying upper Atoka TST is considered the proper datum because of its continuous nature above the middle Atoka LST and the presence of the overlying, condensed-section "hot shale" marker (Fig. 16). It is somewhat confusing to obtain the correct order of lithostratigraphic nomenclature of these sandstones from scout tickets or the literature. In many instances, scout tickets reported by drilling companies refer to such sandstones merely as middle Atoka sandstones or upper and lower sandstones. Based on detailed correlations, the vertical succession of these sandstones is as follows (from top to bottom): Red Oak, Panola, Diamond, and Brazil sandstones, which is in



agreement with Suneson and Hemish (1994). Some of these sandstones disappear and reappear but do so within a specific stratigraphic zone that has a characteristic conductivity-log pattern (Fig. 16).

There is inconsistency regarding the age of the turbidites section in the Arkoma Basin and frontal Ouachitas. In Coal County, Oklahoma, along the southwestern edge of the Arkoma Basin, Sutherland and Manger (1984) reported middle Atokan fusulinids from outcrops typical of the Atoka Formation approximately 400 ft above its base. In a study conducted on conodonts in outcrops in the same county, Grayson (1984) reported that the basal Atoka above the Wapanucka Limestone is middle Atokan (that is, no early Atokan section). On the other hand, workers such as Sprague (1985) considered the turbidite deposits in the frontal Ouachitas to be lower Atoka. Meanwhile, Visher (1996) assumed that the turbidites in the Arkoma Basin and frontal Ouachitas span both the early and middle Atokan ages.

Figure 2 shows examples from two wells in the eastern and the western parts of the southern depocenter of the Arkoma Basin. The prodelta shale of the lower Atoka HST in both wells is very thin compared to more than 3,000 ft of the lower Atoka section in the northeastern part of the Arkoma Basin. The remaining section of the lower Atoka sequence is a few hundred feet thick and is unconformably overlain by either the basin-floor or slope fans of the middle Atoka turbidites (Fig. 2). It is likely that the thin lower Atoka section, such that shown in Figure 2, was completely eroded in areas within the frontal Ouachitas, resulting in the merging of two unconformities: the Atokan-Morrowan unconformity, at the base of the lower Atoka sequence (Saleh, this volume); and the middle Atokan unconformity at its top. The merging of these two unconformities would represent one major unconformity that likely spans the late Morrowan through early Atokan. The merging of the two unconformities, coupled with the inability to identify the thin, shaly lower Atoka interval partially preserved updip in the Arkoma Basin (such as in the wells in Figure 2), may have mistakenly led some workers to consider the middle Atoka turbidites to be early Atokan in age.

## CONCLUSIONS

The middle Atoka interval in the Arkoma Basin is a LST deposited during a falling phase and slow rise of relative sea level. It represents the thickest stratigraphic interval in the Oklahoma part of the Arkoma Basin. Its lower bounding surface is a sequence boundary on top of the lower Atoka third-order sequence. This boundary, on the shelf of the Arkoma Basin, is an unconformity between the lower Atoka sequence and the upper Atoka interval. The upper bounding surface is

a transgressive surface that can be identified throughout the Arkoma Basin.

From bottom to top, the middle Atoka LST is composed of a basin-floor fan, slope fan, and lowstand wedge. The basin-floor fan is confined to the deepest part of the Arkoma Basin. The middle Atoka slope fan is a very thick, mud-rich fan with several channel-levee complexes generally sourced from the north. The overlying lowstand wedge is thinner than both the basin-floor and slope fan. This thin, shaly interval in the south becomes thicker to the north with the deposition of fluvial-tidal sandstones.

The San Bois, Mulberry, and Kinta syndepositional faults controlled to great extent the deposition of the middle Atoka LST in Oklahoma. The distribution of this LST illustrates the complex interaction of sedimentation and tectonic evolution in this basin. The growth faults provided significant accommodation space for the deposition of basin-floor and slope fans, which abruptly thicken on the downthrown side of both the San Bois and Kinta Fault trends. The basin-floor fan extends in an east-to-west direction parallel to the major syndepositional faults. The slope-fan feeder system switched from line-sourcing along the San Bois Fault to point-sourcing away from the fault farther west. The downthrown side of the Mulberry Fault provided accommodation space for more widespread accumulation of a thick, lowstand wedge that extended farther northeast beyond the limit of the San Bois Fault trend. A platform to the north and northwest of these faults may have been part of the shelf area, with no turbidite sedimentation during the middle Atoka.

## REFERENCES CITED

- Browne, G.H.; and Slatt, R.M., 1997, Thin-bedded slope fan (channel-levee) deposits from New Zealand: an outcrop analog for reservoirs in the Gulf of Mexico: *Gulf Association of Geological Societies Transactions* v. XLVII, p. 75-86.
- Ferguson, C.A.; and Suneson, N.H., 1988, Tectonic implications of early Pennsylvanian paleocurrents from flysch in the Ouachita Mountains frontal belt, southeast Oklahoma, in Johnson, K.S. (ed.), *Shelf-to-basin geology and resources of Pennsylvanian strata in the Arkoma Basin and frontal Ouachita Mountains of Oklahoma*: Oklahoma Geological Survey Guidebook 25, p. 49-60.
- Galloway, W.E., 1998, Siliciclastic slope and base-of-slope depositional systems: component facies, stratigraphic architecture, and classification: *American Association of Petroleum Geologists Bulletin*, v. 82, p. 569-595.
- Grayson, R.C., Jr., 1984, Morrowan and Atokan (Pennsylvanian) conodonts from the northeast margin of the Arbuckle Mountains, southern Oklahoma, in Sutherland, P.K.; and Manger, W.L. (eds.), *The Atokan Series and its*

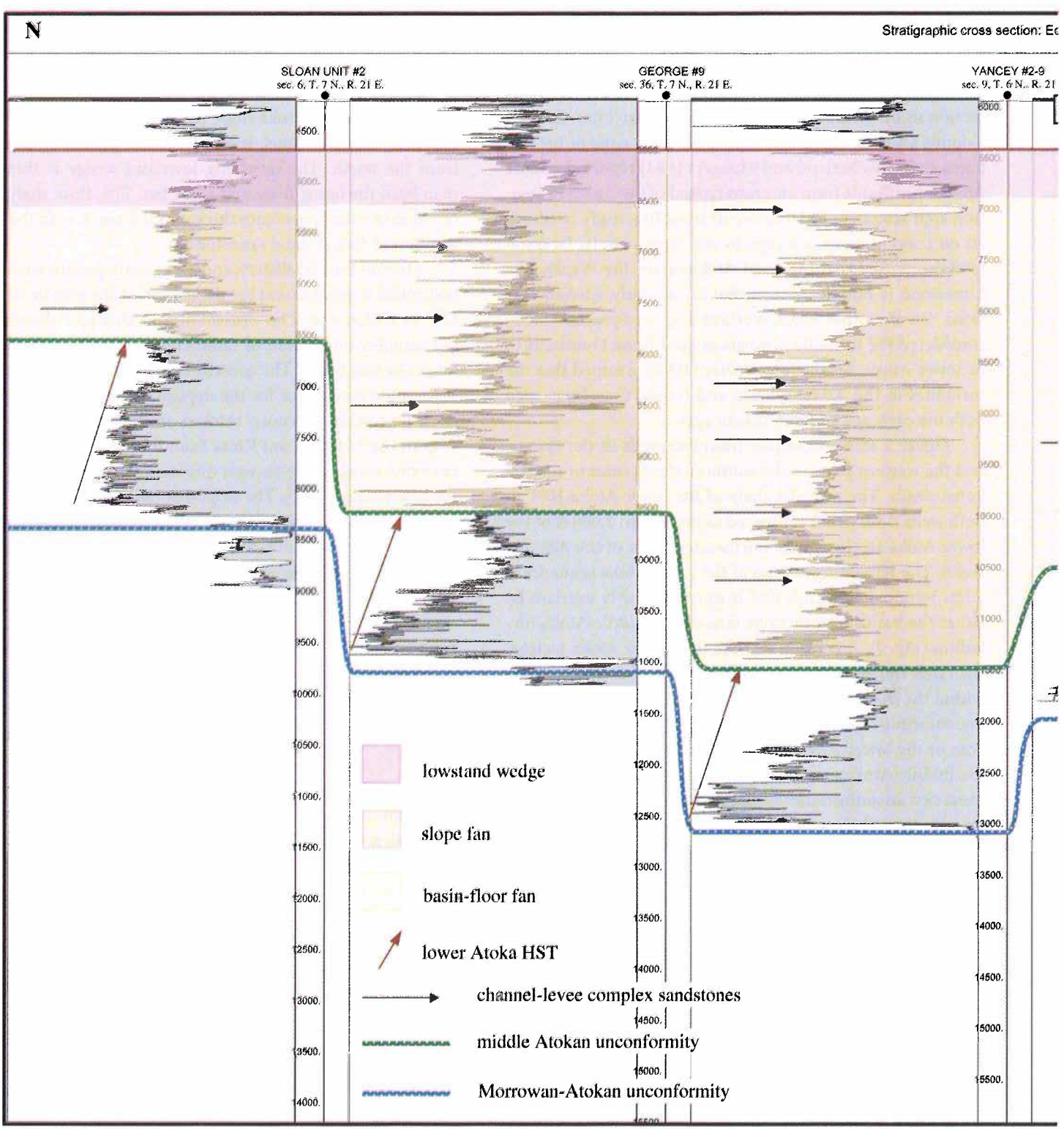
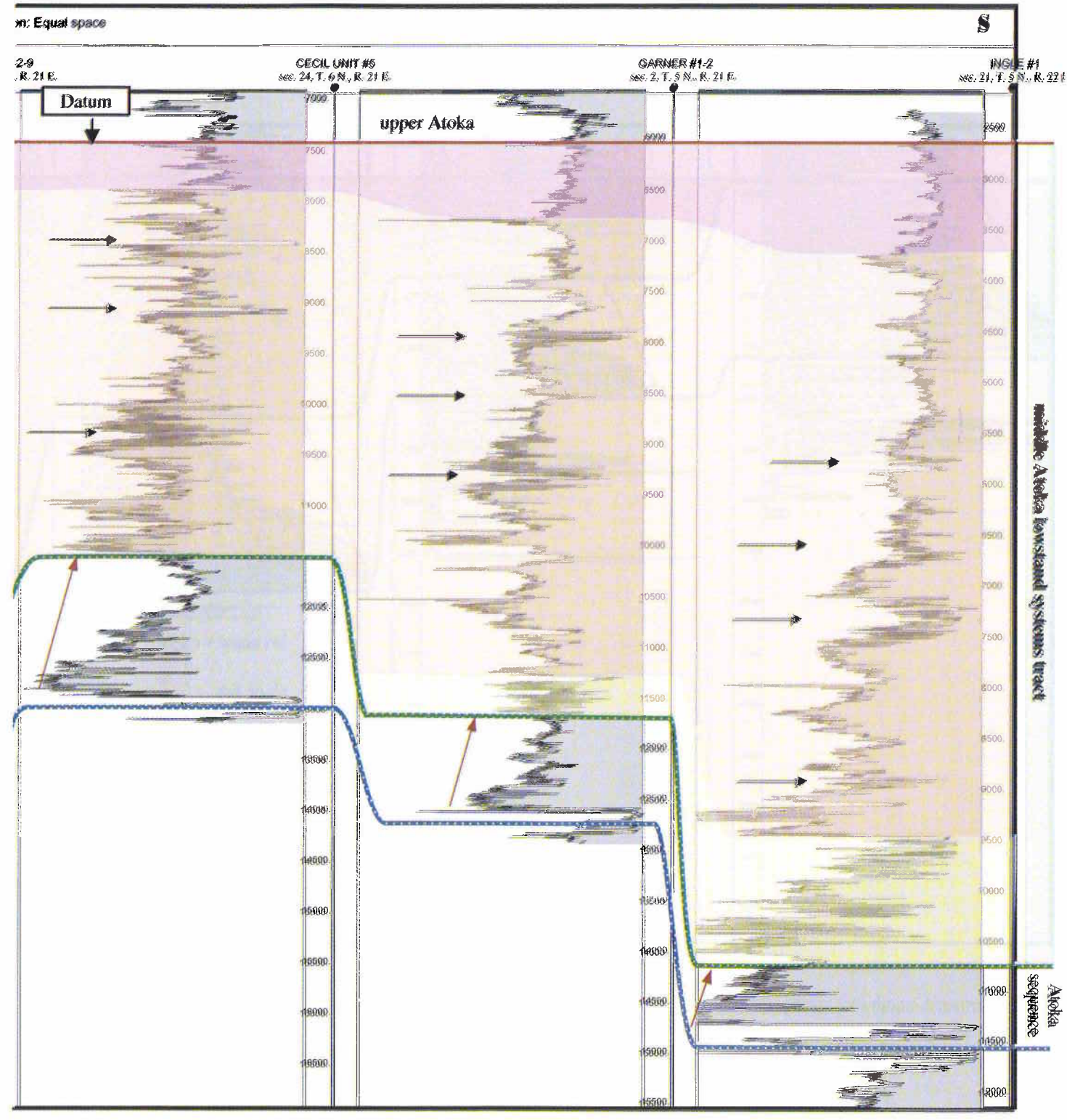


**Figure 9.** North-south stratigraphic cross section across the San Bois Fault trend shown in Figure 5. Several sandstones of the channel-levee complexes, comprising the slope fan, occur south of the San Bois Fault trend. Many of these sandstones



occur without a clear indication of a point-source such as a canyon or long, thick channel. This suggests a line-source for these sediments. The cross-section datum is the upper Atoka transgressive surface. For location, see Figure 5.



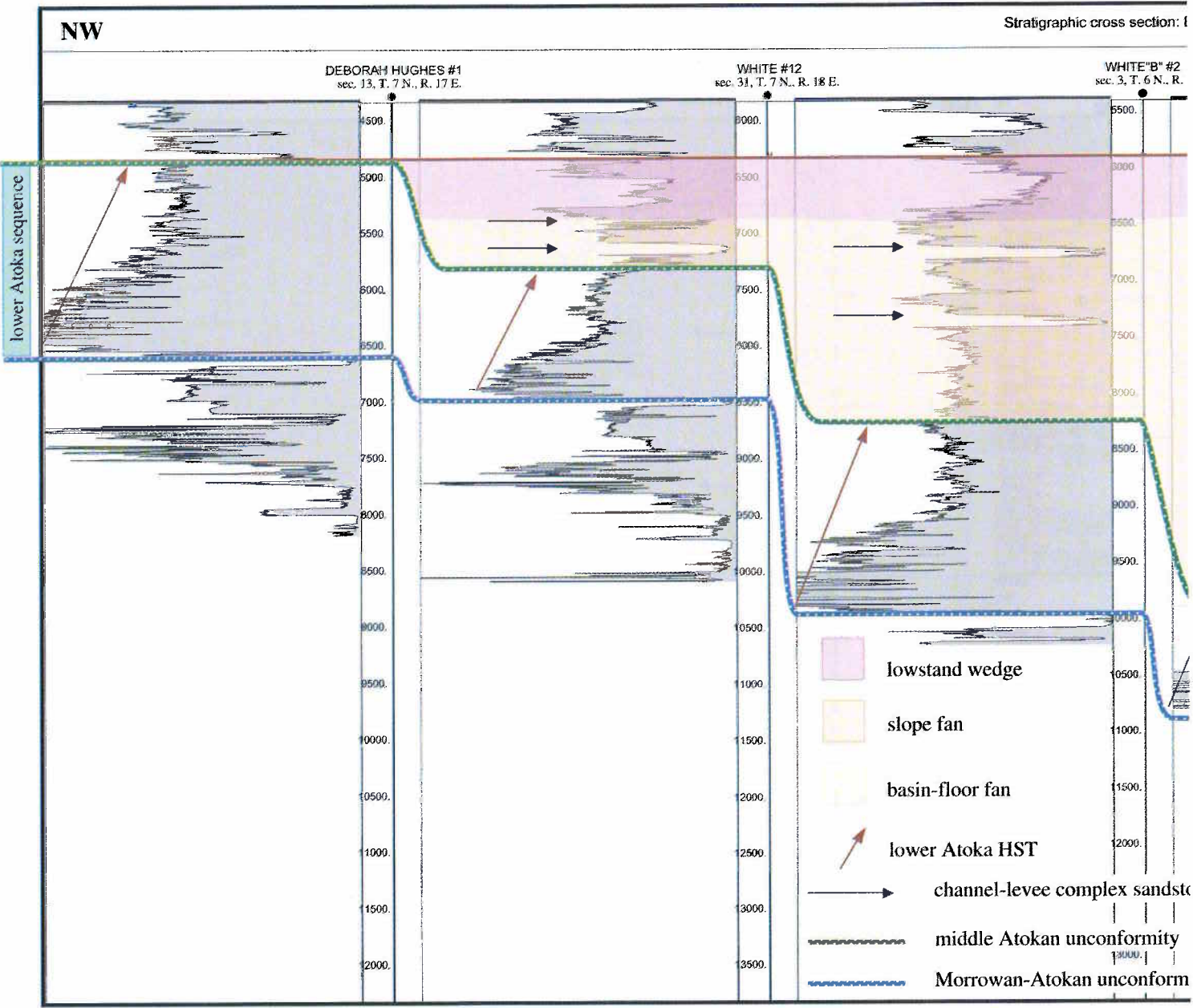
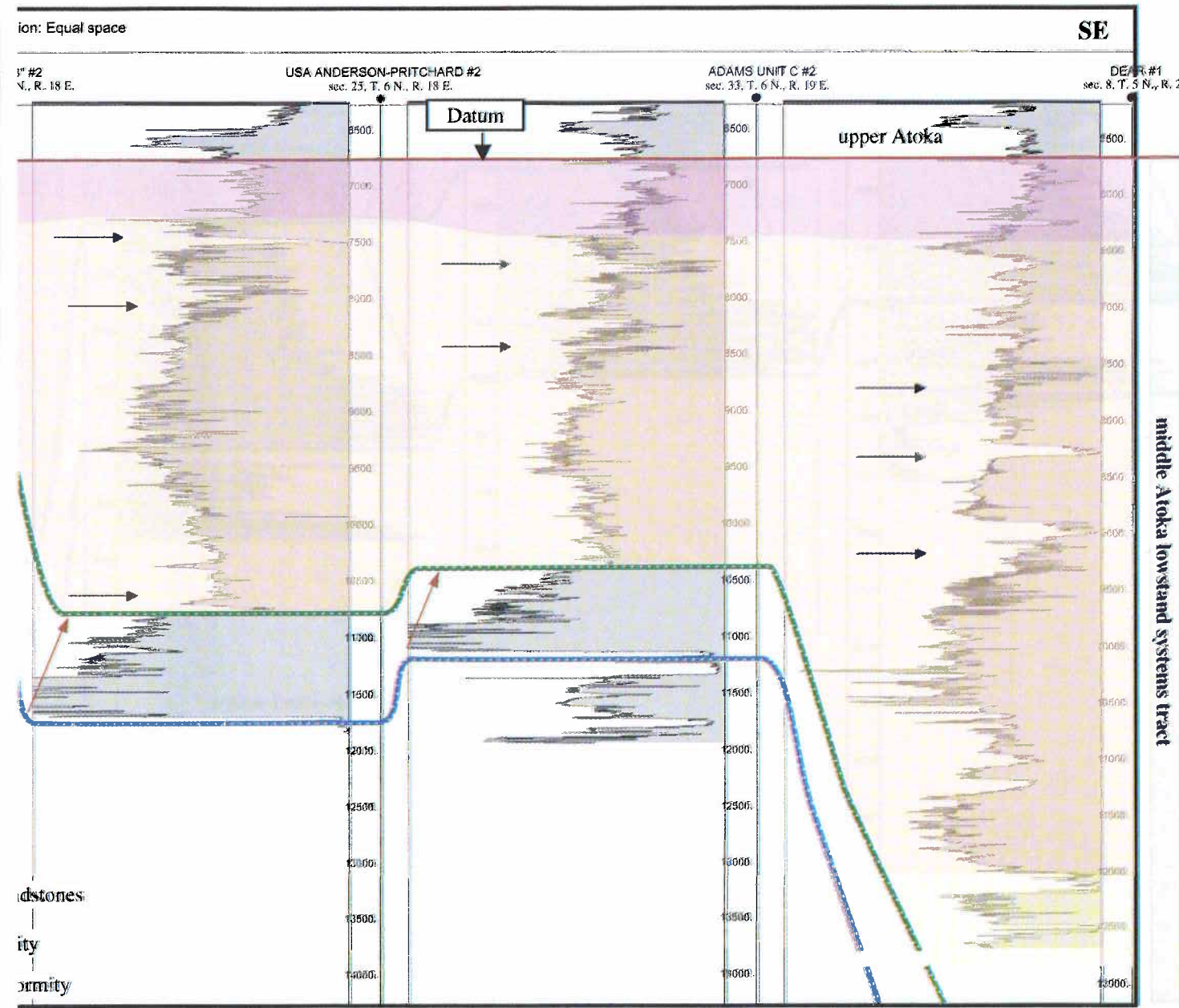


**Figure 10.** Northeast-southwest stratigraphic cross section just west of the San Bois Fault trend and across the Kinta Fault trend shown in Figure 5. Thick sandstones occur within the slope fan close to the shelf area of the Arkoma Basin indicating deposition within a canyon or long channel that can be tracked for an extended distance. Adopting the Galloway (1998) classification, this



pattern may suggest a point-source for these sediments. The cross-section datum is the upper Atoka transgressive surface. For location, see Figure 5.



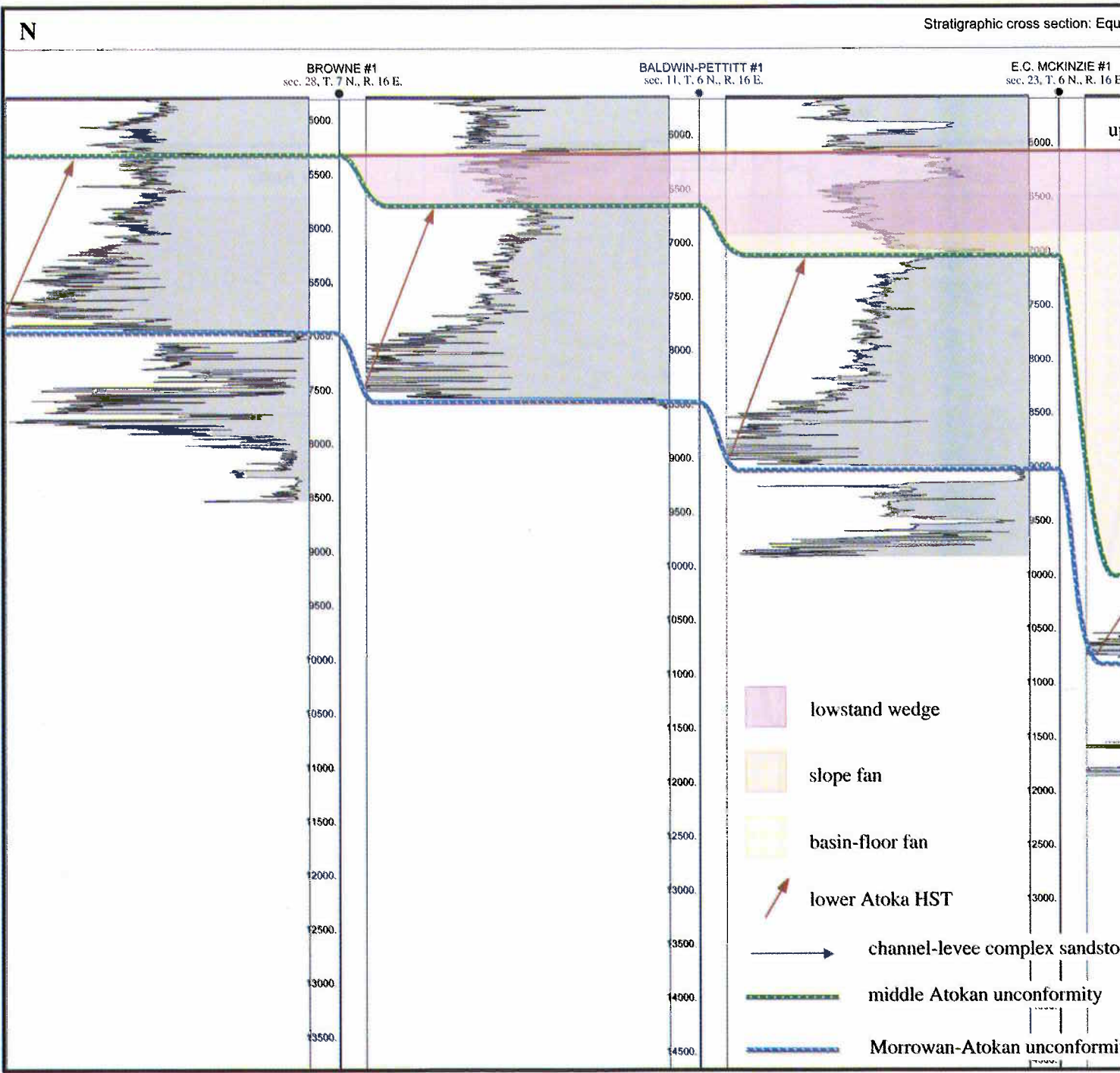
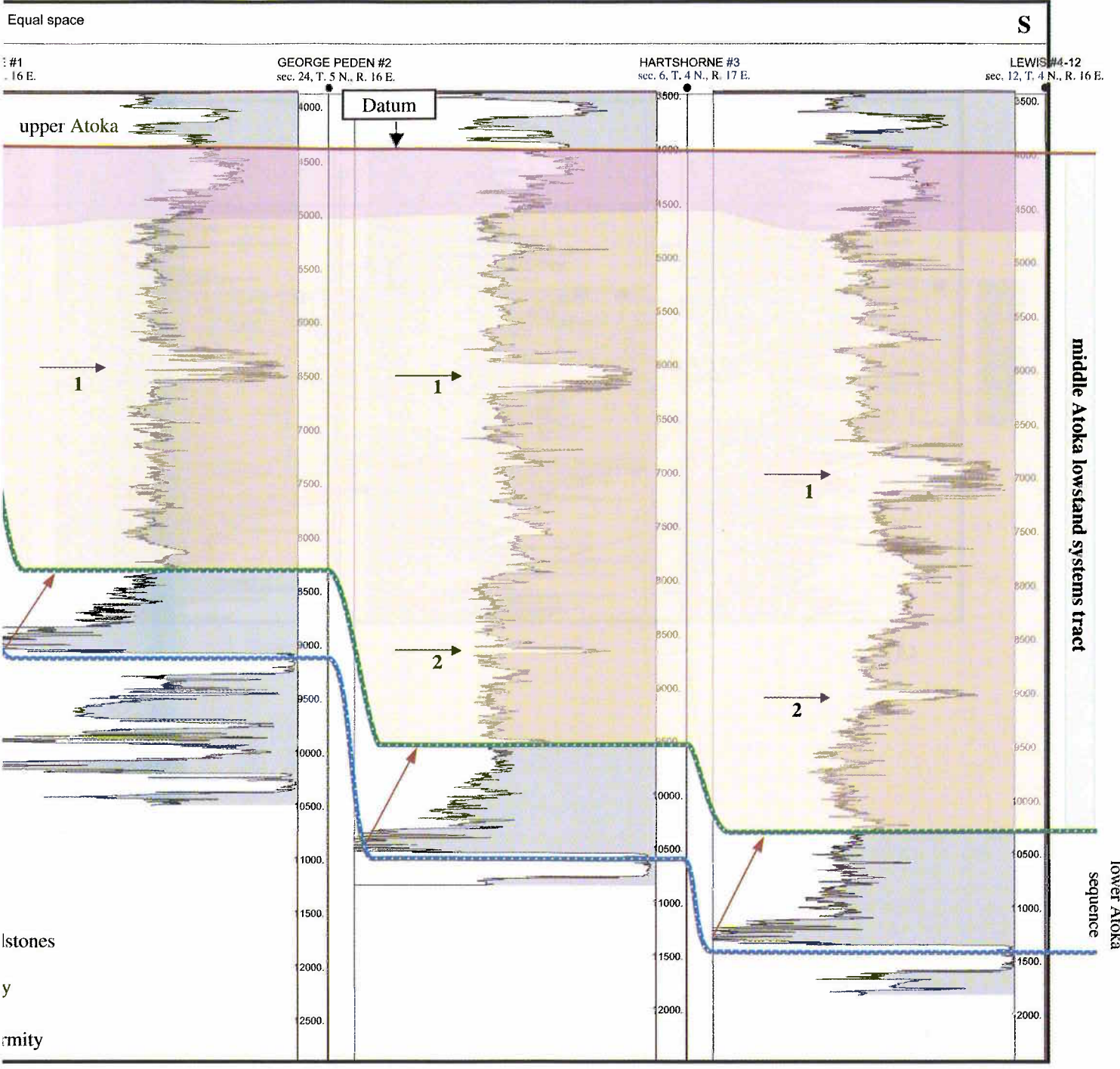


**Figure 11.** North-south stratigraphic cross section across the Kinta Fault trend shown in Figure 5. A thick sandstone channel occurs within the slope fan of the middle Atoka LST, clearly indicating a point-source for sediment supply at this area of the



Arkoma Basin. The cross-section datum is the upper Atoka transgressive surface. For location, see Figure 5.



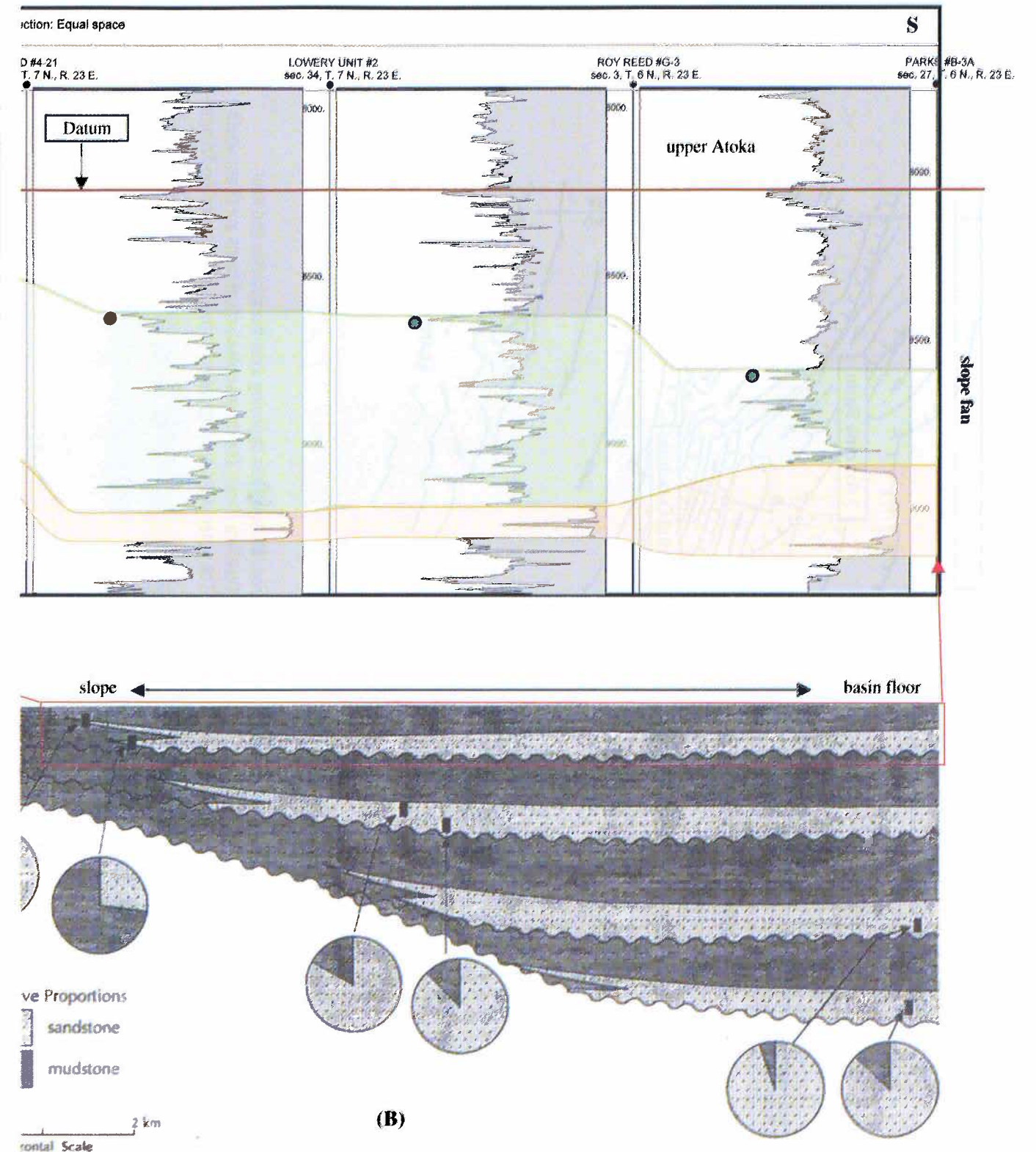
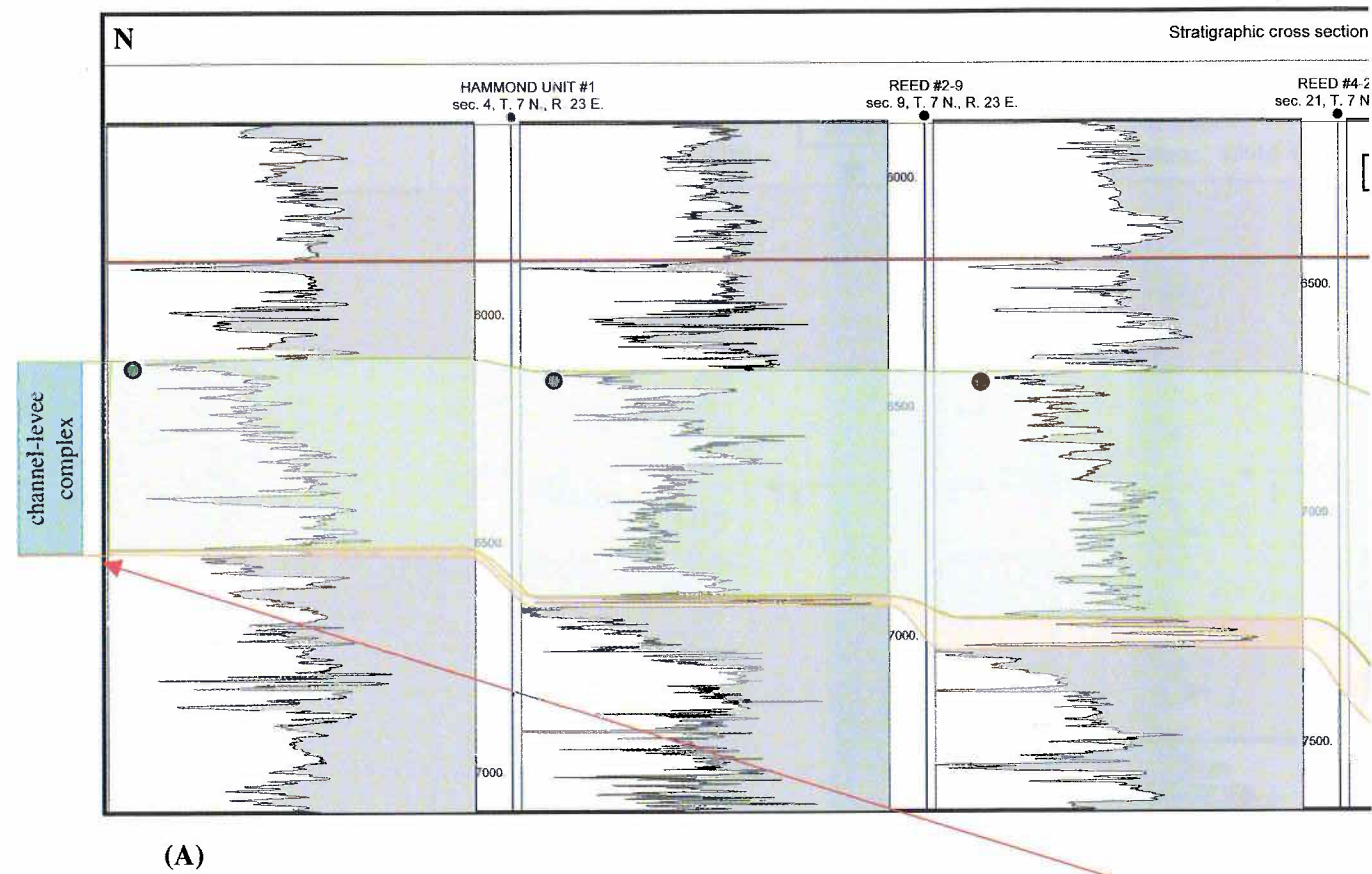


**Figure 12.** (A) North-south detailed stratigraphic cross section showing channel-levee complex at the top part of the middle Atoka slope fan. A 10-mi-long sandstone interval at the base of the complex (light brown) dips from north to south, contrary to the east-west direction suggested by other workers for turbidite channels in the Arkoma Basin. This sandstone body is funneled through a notch and overlain by shale with occasional thin-bedded sandstones within a specific channel-levee complex zone. The top of this complex is

defined by a conductivity marker (green circle). The cross-section datum is the upper Atoka transgressive surface. For location, see Figure 5. Several of these complexes occur south of the San Bois Fault trend. They are stacked both vertically and laterally. (B) A depiction for a series of channel-levee complexes of slope-fan outcrops in the Mt. Messenger Formation, New Zealand (after Browne and Slatt, 1997). This depiction may serve as an analogue for the stacking of channel-levee complexes in the Arkoma Basin.

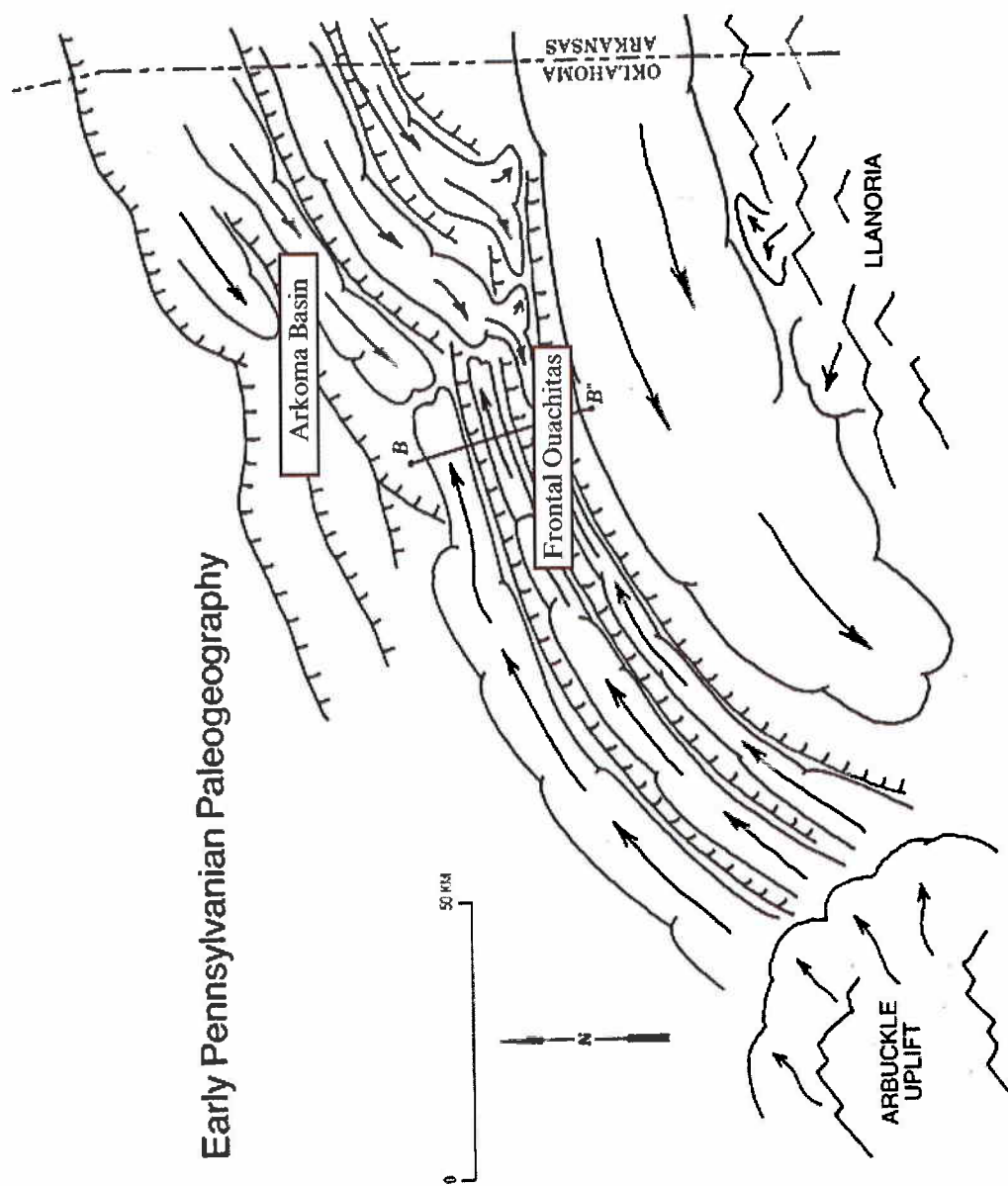
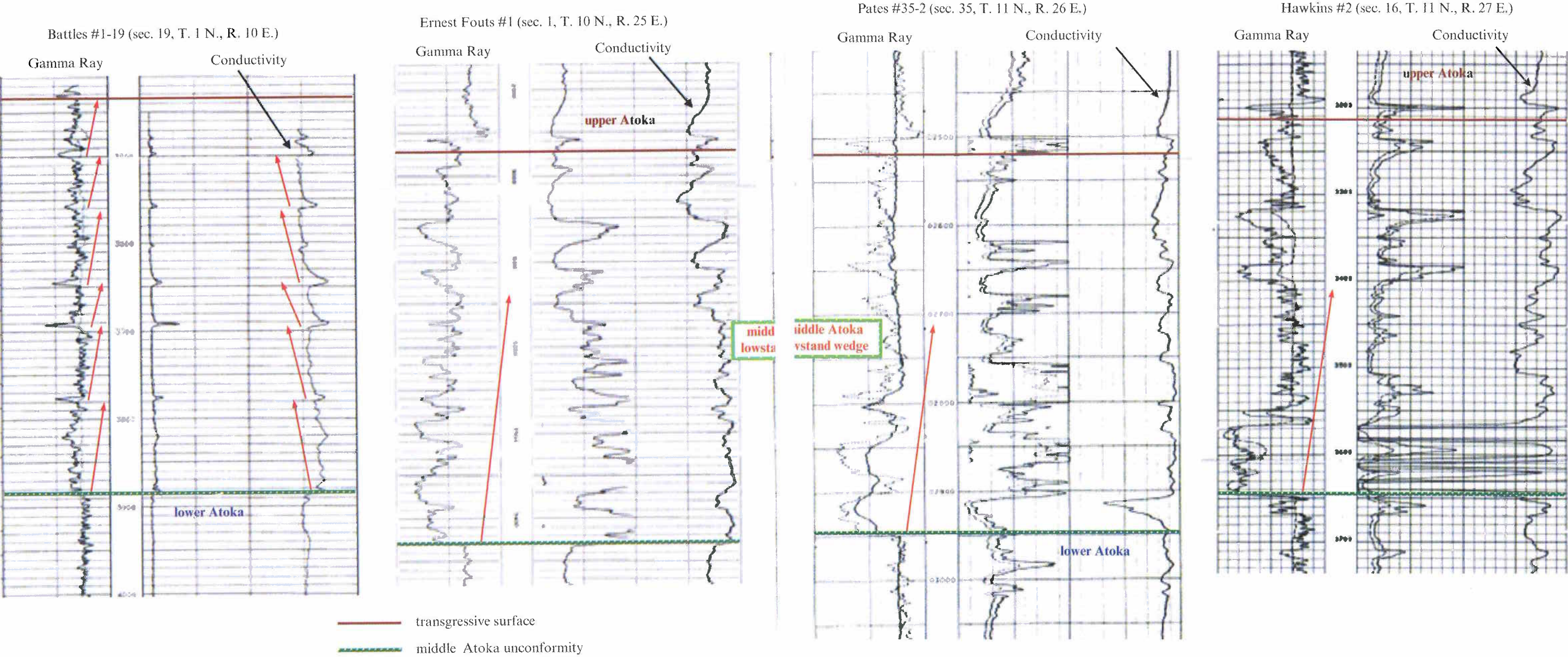


**Figure 13.** Early Pennsylvanian paleogeography of the Ouachita region, showing two opposing axial-fan systems and their relationship to growth-fault troughs along the northern edge of the Ouachita Basin. The three southernmost faults are (from south to north): the Ti Valley, the Pine Mountain, and the Choctaw Faults. The other faults are recognized in the subsurface of the Arkoma Basin (modified after Ferguson and Suneson, 1988).



- boundaries: Oklahoma Geological Survey Bulletin 136, p. 41–63.
- Houseknecht, D.W., 1986, Evolution from passive margin to foreland basin: the Atoka Formation of the Arkoma Basin, south-central U.S.A., in Allen, P.A.; and Homewood, Peter (eds.), *Foreland basins*: International Association of Sedimentologists, Special Publication 8, p. 327–345.
- 1987, The Atoka Formation of the Arkoma Basin: Tectonics, sedimentology, thermal maturity, sandstone petrology: Tulsa Geological Society Short Course Notes, 72 p.
- Houseknecht, D.W.; and Kacena, J.A., 1983, Tectonic and sedimentary evolution of the Arkoma foreland basin, in Houseknecht, D.W. (ed.), *Tectonic–sedimentary evolution of the Arkoma Basin and guidebook to deltaic facies, Hartshorne sandstone*: Society of Economic Paleontologists and Mineralogists, Midcontinent Section, v. 1, p. 3–33.
- Houseknecht, D.W.; and McGilvery, T.A., 1990, Red Oak Field, in Beaumont, E.A.; and Foster, N.H. (eds.), *Structural traps II, traps associated with tectonic faulting*: American Association of Petroleum Geologists, *Treatise of Petroleum Geology, Atlas of oil and gas fields*, p. 201–225.
- Houseknecht D.W.; and Ross, L.M., 1992, Clay minerals in the Atokan deep-water sandstone facies, Arkoma Basin: origins and influence on diagenesis and reservoir quality, in Houseknecht, D.W.; and Pittman, E.D. (eds.), *Origin, diagenesis, and petrophysics of clay minerals in sandstones*: Society of Economic Paleontologists and Mineralogists Special Publication 47, p. 227–240.
- Johnson, K.S.; Amsden, T.W.; Denison, R.E.; Dutton, S.P.; Goldstein, A.G.; Rascoe, Bailey, Jr.; Sutherland, P.K.; and Thompson, D.M., 1989, *Geology of the southern Midcontinent*: Oklahoma Geological Survey Special Publication 89-2, 53 p.
- Krystinik, L.F.; and Blakeney, B.A., 1990, Sedimentology of the upper Morrow Formation in eastern Colorado and western Kansas, in Sonnenberg, S.A.; Shannon, L.T.; Rader, Kathleen; Von Drehle, W.F.; and Martin, G.W. (eds.), *Morrow sandstones of southeast Colorado and adjacent areas*: The Rocky Mountain Association of Geologists, Denver, p. 37–50.
- Loutit, T.S.; Hardenbol, Jan; Vail, P.R.; and Baum, G.R., 1988, Condensed sections: The key to age dating and correlation of continental margin sequences, in Wilgus, C.K.; Hastings, B.K.; Posamentier, H.W.; Van Wagoner, J.C.; Ross, C.A.; and Kendall, C.G. (eds.), *Sea level changes: an integrated approach*: Society of Economic Paleontologists and Mineralogists Special Publication 42, p. 183–213.
- McGilvery, T.A.; and Houseknecht, D.W., 2000, Depositional systems and diagenesis of slope and basin facies, Atoka Formation, Arkoma Basin: Oklahoma Geological Survey Circular 103, p. 129–140.
- Mitchum, R.M., Jr.; and Van Wagoner, J.C., 1991, High-frequency sequences and their stacking patterns: sequence-stratigraphic evidence of high-frequency eustatic cycles: *Sedimentary Geology*, v. 70, p. 131–160.
- Nummedal, Dag; and Swift, D. J. P., 1987, Transgressive stratigraphy at sequence-bounding unconformities: some principles derived from Holocene and Cretaceous examples: *Society of Economic Paleontologists and Mineralogists Special Publication 41*, p. 241–260.
- Posamentier, H.W.; Erskine, R.D.; and Mitchum, R.M., 1991, Models for submarine-fan deposition within a sequence-stratigraphic framework, in Weimer, Paul; and Link, M.H. (eds.), *Seismic facies and sedimentary processes of submarine fans and turbidite systems*: Springer-Verlag, New York, p. 127–136.
- Posamentier, H.W.; and Vail, P.R., 1988, Eustatic controls on clastic deposition II—sequence and systems tract models, in Wilgus C.K.; Hastings, B.K.; Posamentier, H.W.; Van Wagoner, J.C.; Ross, C.A.; and Kendall, C.G. (eds.), *Sea level changes: an integrated approach*: Society of Economic Paleontologists and Mineralogists Special Publication 42, p. 125–154.
- Sprague, A.R.G., 1985, Depositional environment and petrology of the lower member of the Pennsylvanian Atoka Formation, Ouachita Mountains, Arkansas and Oklahoma: University of Texas–Dallas, unpublished Ph.D. dissertation, 553 p.
- Suneson, N.H.; and Hemish, L.A., 1994, Red Oak–Norris gas field, in Suneson, N.H.; and Hemish, L.A. (eds.), *Geology and resources of the eastern Ouachita Mountains frontal belt and southeastern Arkoma Basin, Oklahoma*: Oklahoma Geological Survey Guidebook 29, p. 49–53.
- Sutherland, P.K.; and Manger, W.L., 1984, The Atokan Series: an interval in search of a name, in Sutherland, P.K.; and Manger, W.L. (eds.), *The Atokan Series and its boundaries*: Oklahoma Geological Survey Bulletin 136, p. 1–8.
- Vail, P.R., 1987, Seismic stratigraphy interpretation using sequence stratigraphy, part 1: seismic stratigraphy interpretation procedure, in Bally, A.W. (ed.), *Atlas of seismic stratigraphy*: American Association of Petroleum Geologists Studies in Geology 27, v. 1, p. 1–10.
- Van Wagoner, J.C., Mitchum, R.M., Jr.; Posamentier, H.W.; and Vail, P.R., 1987, Seismic stratigraphy interpretation using sequence stratigraphy, part 2: key definitions of sequence stratigraphy, in Bally, A.W. (ed.), *Atlas of seismic stratigraphy*: American Association of Petroleum Geologists Studies in Geology 27, v. 1, p. 11–14.



overall fining-upward log pattern shown in the three northeastern wells (right). Meanwhile, the lowstand wedge is dominated by fining-upward parasequences deposited in a fluvial environment in the southwestern part of the Arkoma Basin (Battles #1-19 well). The lithostratigraphic name of Fanshawe is assigned to these sandstones.



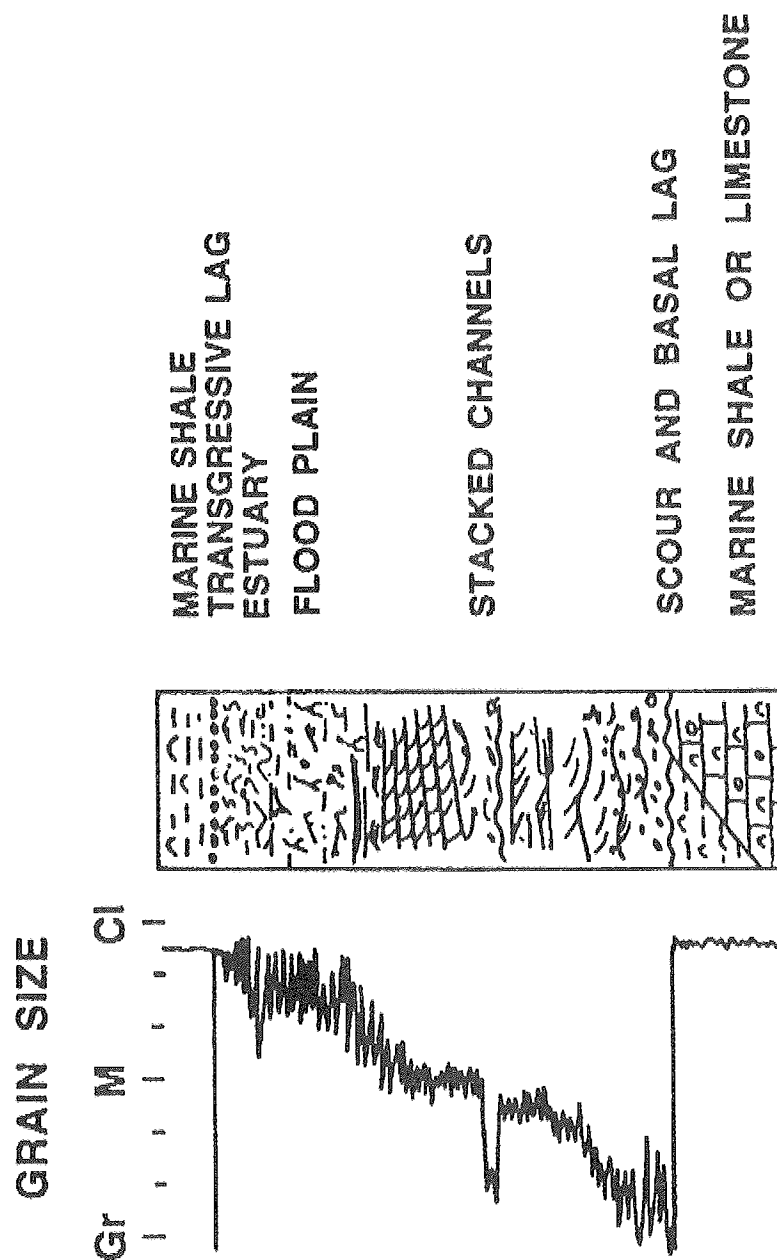


**Figure 15.** Typical vertical profile through a valley-fill deposit (after Krystinik and Blakeney, 1990). This fining-upward stacking pattern compares to that of the lowstand wedge in Figure 14.

- Van Wagoner, J.C.; Posamentier, H.W.; Mitchum, R.M.; Vail, P.R.; Sarg, J.F.; Loutit, T.S.; and Hardenbol, Jan, 1988, An overview of sequence stratigraphy and key definitions, *in* Wilgus C.K.; Hastings, B.K.; Posamentier, H.W.; Van Wagoner, J.C.; Ross, C.A.; and Kendall, C.G. (eds.), *Sea level changes: an integrated approach*: Society of Economic Paleontologists and Mineralogists Special Publication 42, p. 39–45.
- Vedros, S.G.; and Visher, G.S., 1978, The Red Oak sandstone: a hydrocarbon-producing submarine fan deposit, *in* Stanley, D.J.; and Kelling, Gilbert (eds.), *Sedimentation in submarine canyons, fans, and trenches*: Dowden, Hutchinson, and Ross, Inc., Stroudsburg, Pennsylvania, p. 292–308.
- Viele G.W.; and Thomas W.A., 1989, Tectonic synthesis of the Ouachita orogenic belt, *in* Hatcher, R.D., Jr.; Thomas, W.A.; and Viele, G.W. (eds.), *The Appalachian–Ouachita Orogen in the United States*: The Geological Society of America, *The Geology of North America*, v. F-2, p. 695–728.
- Visher, G.S., 1996, A history of Pennsylvanian deltaic sequences *in* Oklahoma, *in* Johnson, K.S. (ed.), *Deltaic reservoirs in the southern Midcontinent*, 1993 symposium: Oklahoma Geological Survey Circular 98, p. 18–31.
- Wanslow, J.L., 1985, Stratigraphy and depositional framework of the Red Oak sandstone, Atoka Formation, *in* the Arkoma Basin of Oklahoma: University of Arkansas, Fayetteville, unpublished M.S. thesis, 81 p.
- Zachry, D.L., 1983, Sedimentary framework of the Atoka Formation, Arkoma Basin, Arkansas, *in* Houseknecht, D.W. (ed.), *Tectonic–sedimentary evolution of the Arkoma Basin and guidebook to deltaic facies*, Hartshorne sandstone: Society of Economic Paleontologists and Mineralogists, Midcontinent Section, v. 1, p. 34–52.

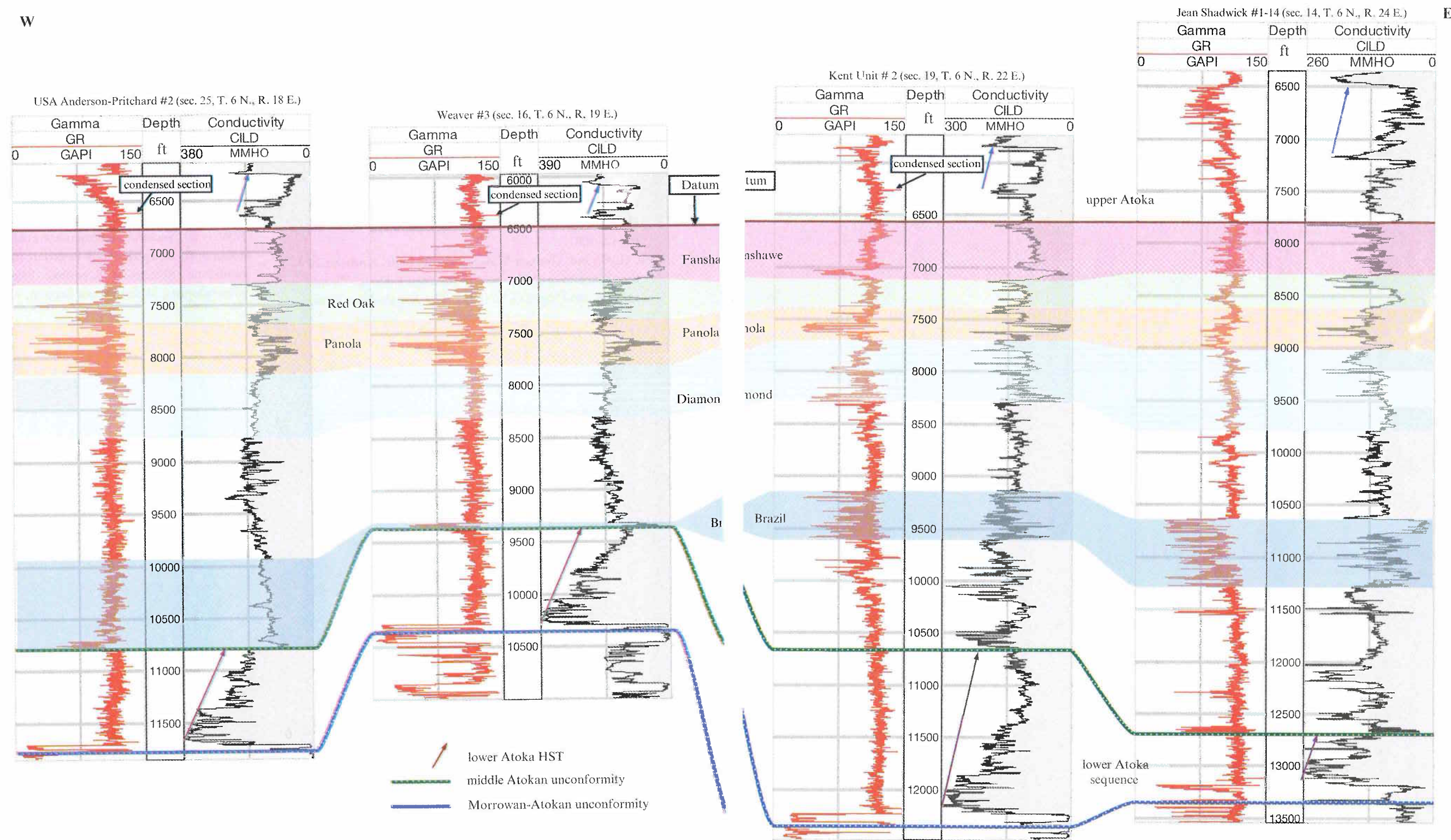


**Figure 16.** East-west stratigraphic cross section south of the San Bois Fault trend. It shows the importance of recognizing a proper datum for correlating the sandstones within the channel-levee complexes. This is because of the laterally discontinuous nature of these sandstones and their vertical multiple occurrence within a thick shale section. The transgressive surface at the

base of the upper Atoka section provides the proper datum for correlation because of its continuous nature and the presence of a condensed section "hot shale" above it. Horizontal scale is equal spacing. For location, see Figure 5.





# Upper Atoka Transgressive and Highstand Systems Tracts: Delineating the Upper Atoka in the Arkoma Basin, Oklahoma

*Azzeldeen A. Saleh*

Geology Department, Faculty of Science,  
University of Tanta, Egypt

**ABSTRACT**—A sequence stratigraphic study has been conducted using the logs of hundreds of wells to delineate the upper Atoka interval in the Arkoma Basin in Oklahoma. The characteristic patterns displayed in conductivity logs were utilized to correlate this stratigraphic interval in the basin. In addition, condensed sections identified on the gamma-ray (GR) logs were also used.

The upper Atoka section consists of several distinctive parasequences comprising transgressive and highstand systems tracts (TST, HST). These parasequences extend across the major syndepositional faults present in the southeastern part of the Arkoma Basin. The lower boundary of the upper Atoka section is a transgressive surface that overlies both the middle Atoka lowstand systems tract (LST) in the southern and eastern parts of the Arkoma Basin, and the middle Atokan unconformity at the top of the lower Atoka sequence on the basin shelf.

A regional unconformity exists between the upper Atoka HST and the Desmoinesian Hartshorne Formation and is termed the Atokan–Desmoinesian unconformity. The middle Atoka LST, and the upper Atoka TST and HST represent a single third-order sequence. This middle–upper Atoka sequence is bounded by the middle Atokan unconformity at its base and the Atokan–Desmoinesian unconformity at its top.

## INTRODUCTION

The upper Atoka stratigraphic interval represents the youngest unit of the thick Atoka section in the Arkoma Basin in Oklahoma and is overlain by the Desmoinesian Hartshorne Formation. Zachry (1983) stated that the upper Atoka sandstone succession in the Arkansas part of the Arkoma Basin accumulated in delta systems that prograded southward after faulting had ceased. Interpreting and differentiating the upper Atoka section from the underlying middle Atoka turbidites could not be achieved on a regional scale in the Oklahoma portion of the Arkoma Basin by correlating lithostratigraphic sandstone units or simply using GR logs for correlation. This is because of the discontinuous nature of these sandstones on a regional scale and the dominance of shale lithology throughout the Atoka section. Instead, a sequence stratigraphic approach was used.

Sequence stratigraphy represents a definitive approach to stratigraphic interpretations. It integrates a predictive model in which a series of systems tracts forming a sequence are deposited in response to the cyclic fall and rise of relative sea

level. A depositional systems tract is a three-dimensional assemblage of lithofacies deposited at a predictable position in a basin during a specific phase of the relative sea-level cycle. A LST is deposited during a time of rapid fall followed by a slow rise in relative sea level. A TST is deposited during a rapid rise in relative sea level. A HST is deposited during the late part of a relative sea-level rise, stillstand, and the early part of relative sea-level fall (Van Wagoner and others, 1988).

Depositional sequences are bounded by unconformities and their correlative surfaces. An unconformity is a surface separating younger strata from older ones. Along this surface there is evidence of absent strata, subaerial exposure, erosional truncation or time hiatus, and, in some areas, submarine erosion. The other two major surfaces that divide the depositional sequence into systems tracts are the first transgressive and the downlap surfaces (Van Wagoner and others, 1988). The first transgressive surface is produced during a transgression of high-energy nearshore environments across the shelf area of a basin (Loutit and others, 1988). Thus, the surface forms a boundary between the LST and the overlying TST. The down-

lap surface is a starvation surface developed during a regional transgression of sea level. This surface is also called a maximum flooding surface (MFS) and is usually associated with the occurrence of condensed sections. A condensed section can be readily recognized on well logs because of its characteristic pattern of abnormally high GR readings ("hot shale").

### UPPER ATOKA TST AND HST LOG PATTERNS AND BOUNDARIES

The upper Atoka section consists of several distinctive parasequences forming TSTs and HSTs that can be identified on the conductivity logs for many wells drilled in the Arkoma Basin in Oklahoma. These parasequences extend across the major syndepositional faults present in the southeast part of the Arkoma Basin (Fig. 1). The lower boundary of the upper Atoka section is a transgressive surface that overlies the middle Atoka section in the southern and eastern parts of the Arkoma Basin and the unconformity at the top of the lower Atoka sequence on the basin shelf (Fig. 1). Overlying this surface, a thick interval is well developed in the eastern part of the Arkoma Basin (Figs. 2 and 3). This interval includes widespread sandstones at the base of the upper Atoka section and extends onto the Arkoma Basin shelf, forming the TST (Fig. 1). The sandstones within this interval are well developed in the eastern part of the Arkoma Basin (Goodwin #1 and Hoffman Unit #1 wells in Fig. 2) where they are parallel to the trend of the San Bois Fault (Frederick #4–33 well in Fig. 2), and in the northern shelf area of the Arkoma Basin. To the south and west these sandstones become thin and shaly (Davis Kemp #1 well in Fig. 2).

The upper boundary of this TST is a downlap surface usually marked by a condensed section recognized as hot shale on GR logs (Figs. 1 and 2). The Alma sandstone is the basal interval in the upper Atokan section in Arkansas where it is composed of single or multiple sandstone units (Zachry, 1983). The same nomenclature can be used for sandstones in this interval in the eastern part of the Arkoma Basin in Oklahoma.

The upper Atoka TST and HST are best developed in the eastern part of the Arkoma Basin, with well-defined and thick parasequences to the southeast (Figs. 3 and 4). In this area the upper Atoka HST is composed of at least five thick aggradational parasequences with sandstone intervals at their tops. Along the southern margin of the Arkoma Basin the upper Atoka HST parasequences remain thick but become less defined and shaly to the west, indicating a prodelta marine environment (Fig. 5). Close to the Arbuckle Uplift in the extreme southwestern corner of Arkoma Basin, the upper Atoka section is composed of fining-upward parasequences developed in a fluvial environment (Riley #2–3 well in Fig. 5). High

GR spikes (condensed sections) occur at the base of several highstand parasequences as they become thin and shaly in the central part of the Arkoma Basin (Fig. 6). This indicates a prodelta marine environment with less sediment supply in that area. An east–west cross section in the northern part of the Arkoma Basin shows that the thickness of the upper Atoka section changes significantly (Fig. 7). The thick highstand parasequences, with several sandstone intervals in the east, become very thin and merge, forming a shaly interval marked at its base by the upper Atoka TST. This TST commonly includes thin sandstone that unconformably overlies the lower Atoka sequence or Morrowan strata in the northwestern part of the Arkoma Basin (T-bar Ranch #2–19 well in Fig. 6; McKee #3 and Cook #1–33 wells in Fig. 7). This thin sandstone represents the uppermost sandstone of the lithostratigraphic Gilcrease sandstones in the northwestern part of the basin (T-bar Ranch #2–19 well in Fig. 6).

The Desmoinesian Hartshorne Formation overlies the upper Atoka section. Several interpretations have been proposed for the nature of the upper boundary of the upper Atoka section. In the eastern part of the Arkoma Basin, several drilling operators mistakenly put the top of the upper Atoka section at the base of one of the highstand parasequences, confusing it with the base of Hartshorne Formation. In their study on the boundaries of the Atoka Formation in the Arkoma Basin, Sutherland and Manger (1984) mentioned that biostratigraphic information is extremely limited for the upper part of the formation. Zachry and Sutherland (1984) stated that a pre-Desmoinesian unconformity truncates the Atoka strata adjacent to the Arbuckle Mountains west of the Arkoma Basin and along the western margin of the Ozark Uplift in northeastern Oklahoma. Some workers supported the unconformable relationship between the upper Atoka and Hartshorne (Haley, 1961; Visher, 1996; Storm, 1998). Others interpreted this contact as conformable to disconformable in different parts of the Arkoma Basin (Hemish and Suneson, 1997; Andrews, 1998).

Houseknecht and others (1983) concluded that the Atoka–Hartshorne contact is regionally conformable based on the argument that the uppermost Atokan shales are prodelta facies deposited in the Hartshorne delta system. Donica (1978) identified two thin coal beds in the upper part of the Atoka Formation in the Arkoma Basin in southeastern Oklahoma. He suggested that this Atokan section represents intertributary-bay deposits. Williams (1978) suggested that the upper part of the Atoka Formation consists of delta-front or delta-fringe clastics grading upward to delta-plain marsh and swamp deposits.

Two criteria were used in this work to define the nature of the upper Atoka–Hartshorne contact:



1. The presence of a conductivity marker that represents the base of the major upper parasequence of the upper Atoka HST (Fig. 8);
2. The characteristic fining-upward pattern of the Hartshorne incised-channel deposits in the southern part of the Arkoma Basin (Fig. 9).

Based on these two criteria, a regional unconformity is identified between the upper Atoka HST and the Hartshorne LST; this is termed the Atokan–Desmoinesian unconformity. Figure 8 shows that the Hartshorne channel incises into the upper Atoka HST at different levels with respect to the underlying conductivity marker. This may explain the different interpretations of the depositional environment of the upper Atoka at the base of the Hartshorne Formation. In areas where the incision is deepest, the Hartshorne is underlain by prodelta facies (McCafferty Unit #2 well in Fig. 8). In other areas where the incision is shallower, the Hartshorne Formation is underlain by shallow marine or delta-plain marsh–swamp deposits (USA Anderson–Pritchard #2 and Owens #E–1 wells in Fig. 8, also see Fig. 9). Accordingly, the Atokan–Desmoinesian contact should be cautiously defined by identifying the top-most parasequence of the upper Atoka HST to avoid including its prograding sandy facies into the Hartshorne Formation (Fig. 9).

### OVERALL PICTURE: THE UPPER ATOKA TST AND HST IN THE ARKOMA BASIN IN OKLAHOMA

An isopach map of the upper Atoka TST and HST in the Arkoma Basin in Oklahoma shows a general thickening south of the major normal faults in the basin, with more than 4,000 ft of upper Atoka sediments deposited south of the San Bois Fault trend (Fig. 10). Interesting features can also be observed on a structural contour map of the transgressive surface at the base of the upper Atoka TST (Fig. 11). A series of synclines are aligned in a zone trending east-northeast–west-southwest and clearly show the downthrown side of the San Bois and Kinta Faults. If the plate collision during the Ouachita orogeny—which is responsible for the formation of the Arkoma Basin—was from the southeast, with the main compressional vector in that direction, this en echelon pattern of folds is aligned in a shear zone (Riedel antithetic shear zone, R'; Fig. 11). These synclines or small pull-apart sub-basins coincide with the thickening trend observed in the upper Atoka TST and HST isopach map and may have helped provide accommodation space for both systems tracts. This indicates that during late Atokan time the Arkoma Basin was still subsiding south of the major syndepositional faults.

The parasequence pattern of both the TST and HST of the upper Atoka section indicates that the source for sediment

supply was generally from the east where the parasequences not only thicken but are also topped by delta-front sandy facies (coarsening-upward pattern). The availability of substantial accommodation space, provided by the tectonic subsidence south of the syndepositional faults and the formation of synclinal areas in the southeastern part of the Arkoma Basin, allowed the development of thick, well-defined parasequences. In contrast, the northwestern part of the basin was dominated by thin marine shale indicative of insufficient sediment supply and accommodation space.

The fundamental unit of sequence stratigraphy is the sequence, which is a relatively conformable succession of genetically related strata bounded by unconformities and their correlative conformities. A sequence is divided into three depositional systems tracts deposited in response to the cyclic fall and rise of relative sea level: the LST, the TST, and the HST. Thus, in terms of sequence stratigraphy, both the middle Atoka LST and the upper Atoka section (TST and HST) can be interpreted as a single third-order sequence. This middle–upper Atoka sequence is bounded by the middle Atokan unconformity at its base and the Atokan–Desmoinesian unconformity at its top.

### CONCLUSIONS

The upper Atoka section consists of several distinctive parasequences forming transgressive and highstand systems tracts. These parasequences extend across the major syndepositional faults present in the southeastern part of the Arkoma Basin. The lower boundary of the upper Atoka section is a transgressive surface that overlies the middle Atoka LST in the southern and eastern parts of the Arkoma Basin, and the middle Atokan unconformity at the top of the lower Atoka sequence on the basin shelf.

The upper Atoka TST and HST are best developed in the eastern part of the Arkoma Basin, with well-defined and thick parasequences in the southeast. The highstand parasequences (with several sandstone intervals in the east) become very thin and merge, forming a shaly interval marked at its base by the upper Atoka TST. This TST usually includes thin sandstone that unconformably overlies either the lower Atoka sequence or Morrowan strata in the northwestern part of the Arkoma Basin.

Two criteria were used in this work to define the nature of the upper Atoka–Hartshorne contact:

1. The presence of a conductivity marker that represents the base of the major upper parasequence of the upper Atoka HST;
2. The characteristic fining-upward pattern of the Hartshorne incised-channel deposits in the southern part of the Arkoma Basin.

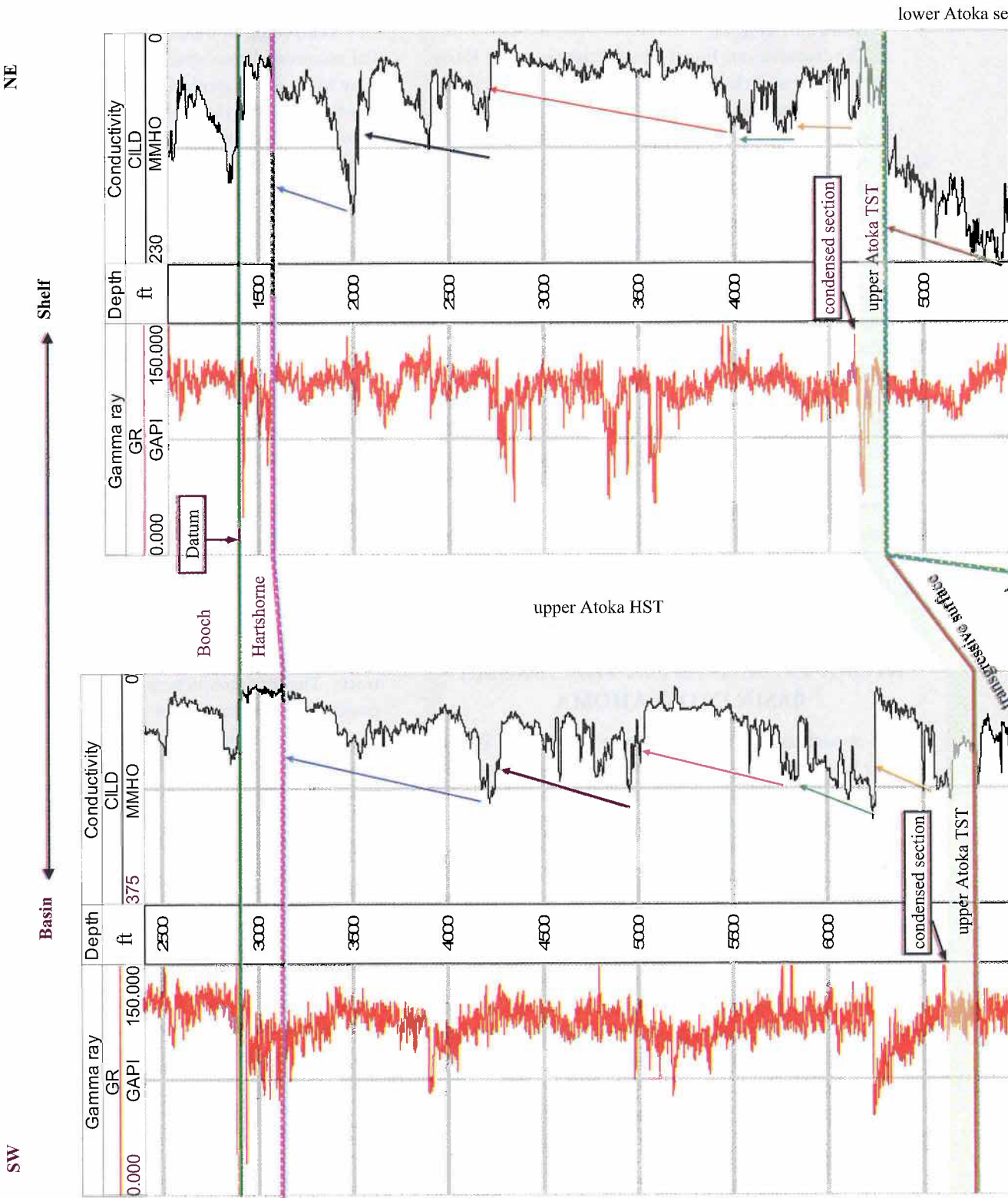
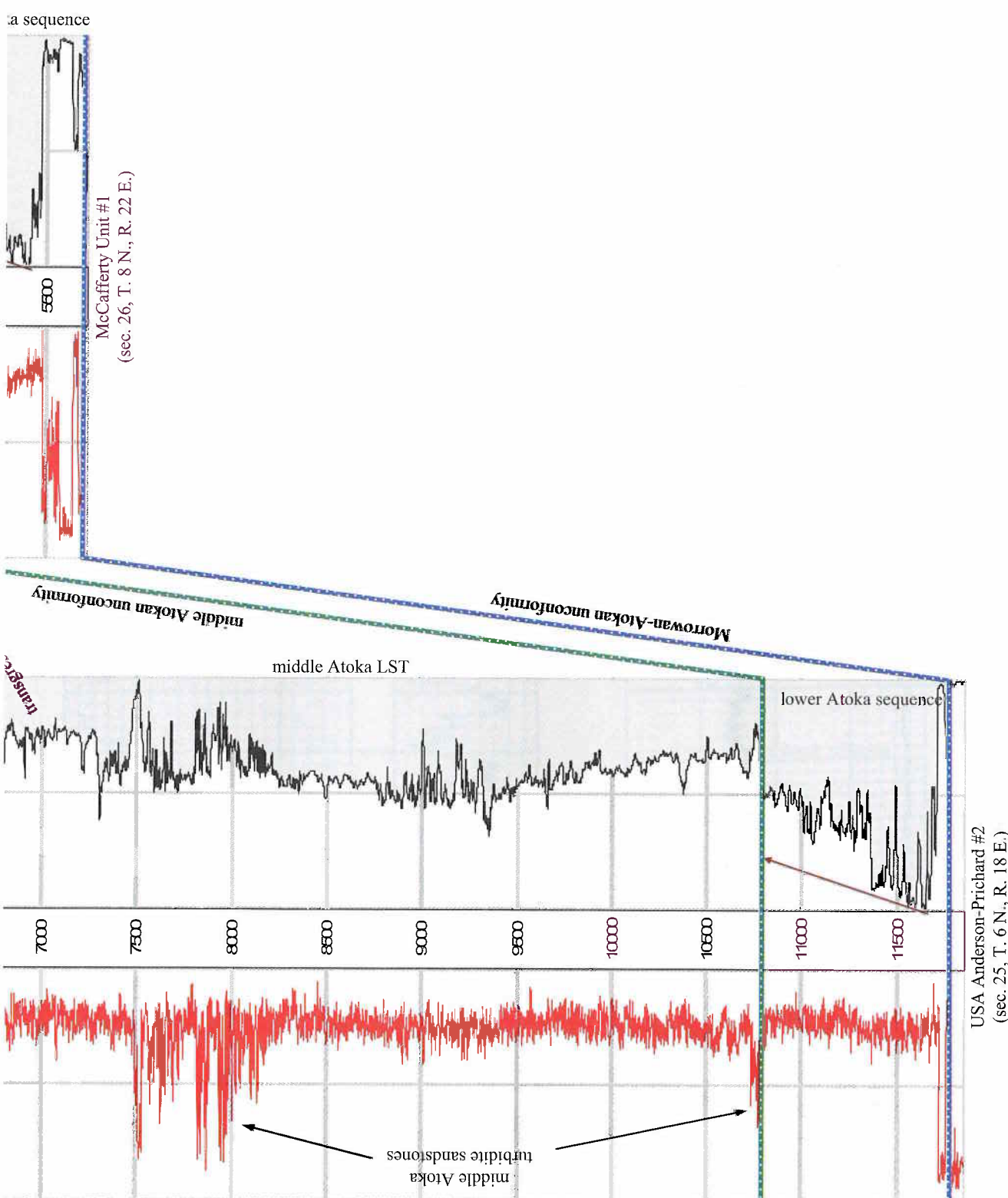


**Figure 1.** The upper Atoka section consists of several distinctive parasequences comprising transgressive and highstand system tracts. These parasequences extend across the major syndepositional faults where middle Atoka turbidites are present in the deep Arkoma Basin. The lower boundary of the upper Atoka section is a transgressive surface that overlies the middle Atoka LST in the



southern and eastern parts of the Arkoma Basin, and the unconformity at the top of the lower Atoka sequence on the basin shelf. A widespread condensed section at the top of the upper Atoka TST marks its boundary with the overlying upper Atoka HST.



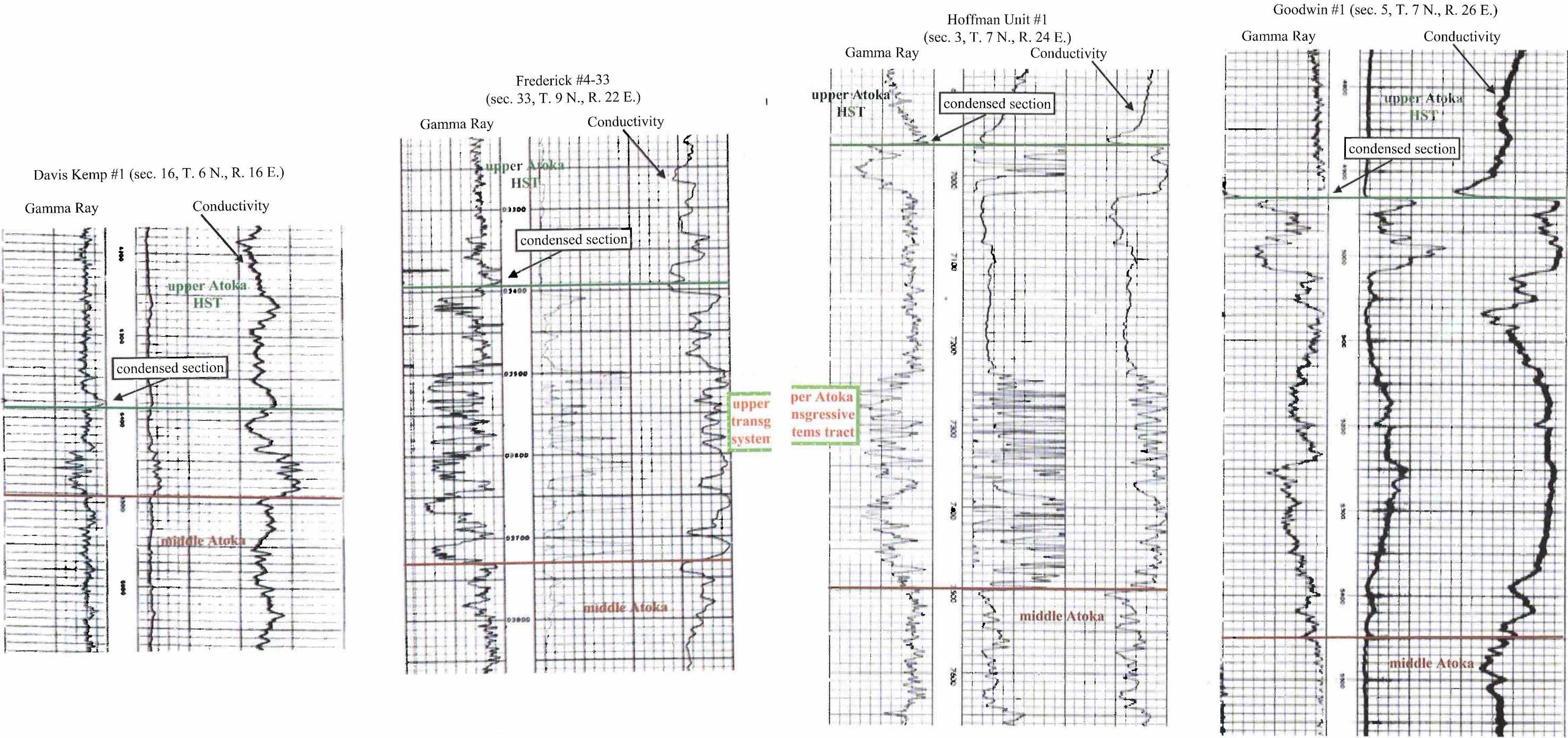


**Figure 2.** The TST of the upper Atoka section overlies the middle Atoka LST as shown in four wells in the Arkoma Basin in Oklahoma. This TST is composed of several sandstones with blocky and coarsening-upward stacking patterns in the eastern part of the Arkoma Basin (three wells on the right). To the south and west, the upper Atoka TST becomes thin and shaly (Davis Kemp

#1 well on the left). A condensed section usually marks the top of this interval. The lithostratigraphic name assigned to these sandstones is Alma.



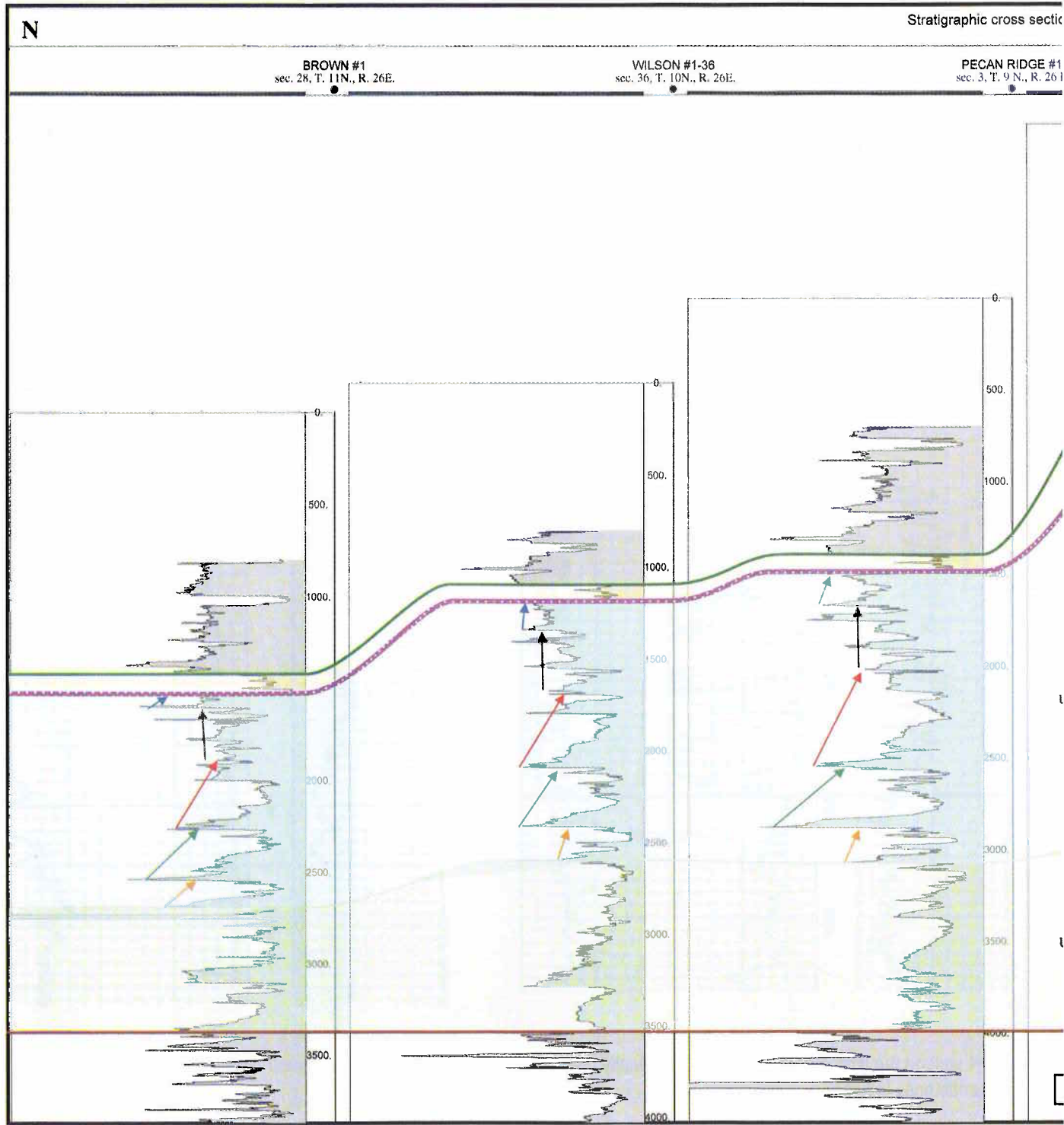
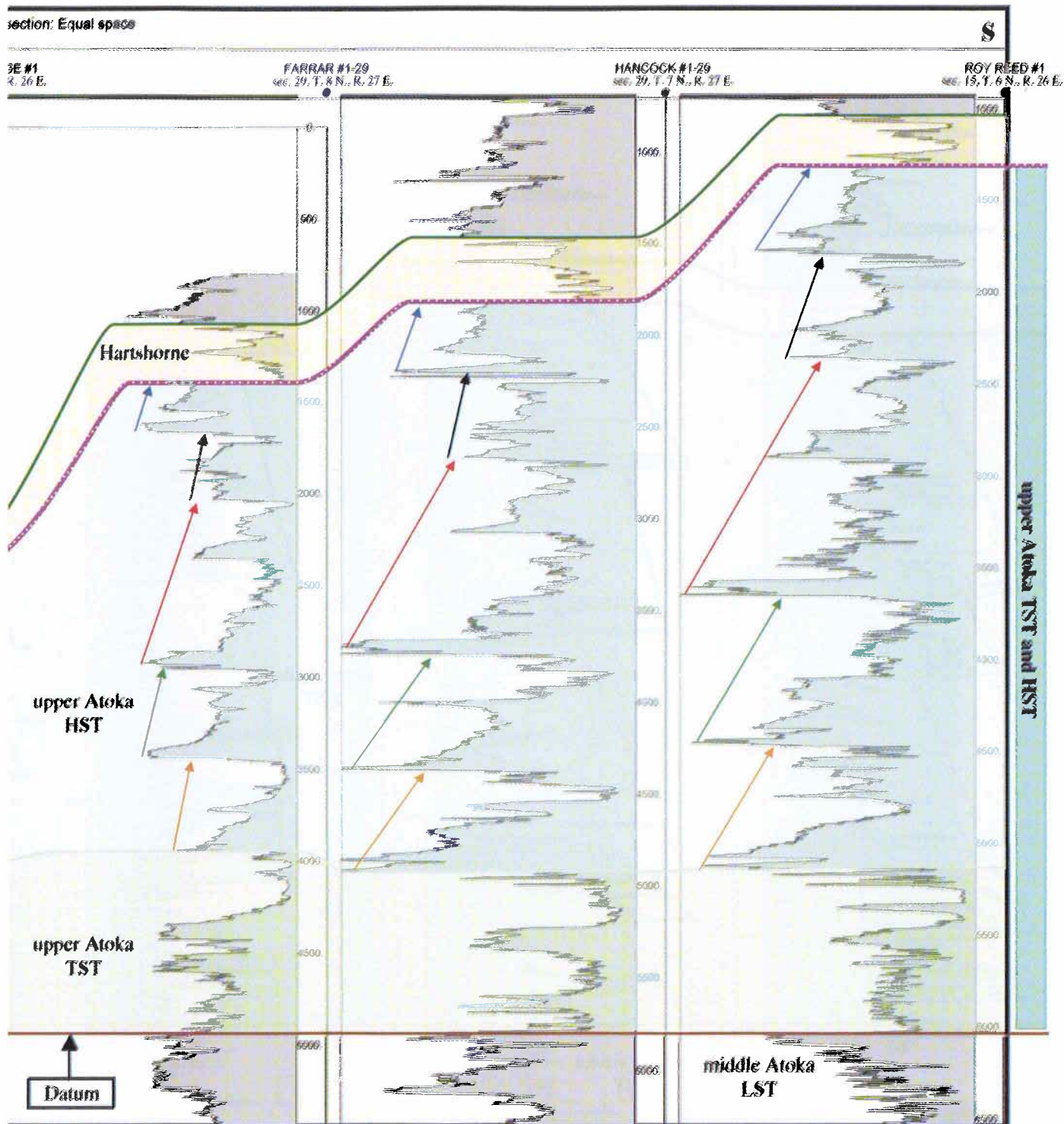


**Figure 3.** A north–south regional stratigraphic cross section across the eastern part of the Arkoma Basin. The figure shows that the upper Atoka TST is well developed and thick in this part of the basin. In the south part of the cross section the upper Atoka HST is composed of at least five thick aggradational parasequences. These parasequences thin to the north but remain distinguishable,



with sandstone intervals at the top of several of them. The cross-section datum is the upper Atoka transgressive surface. For location, see Figure 10.



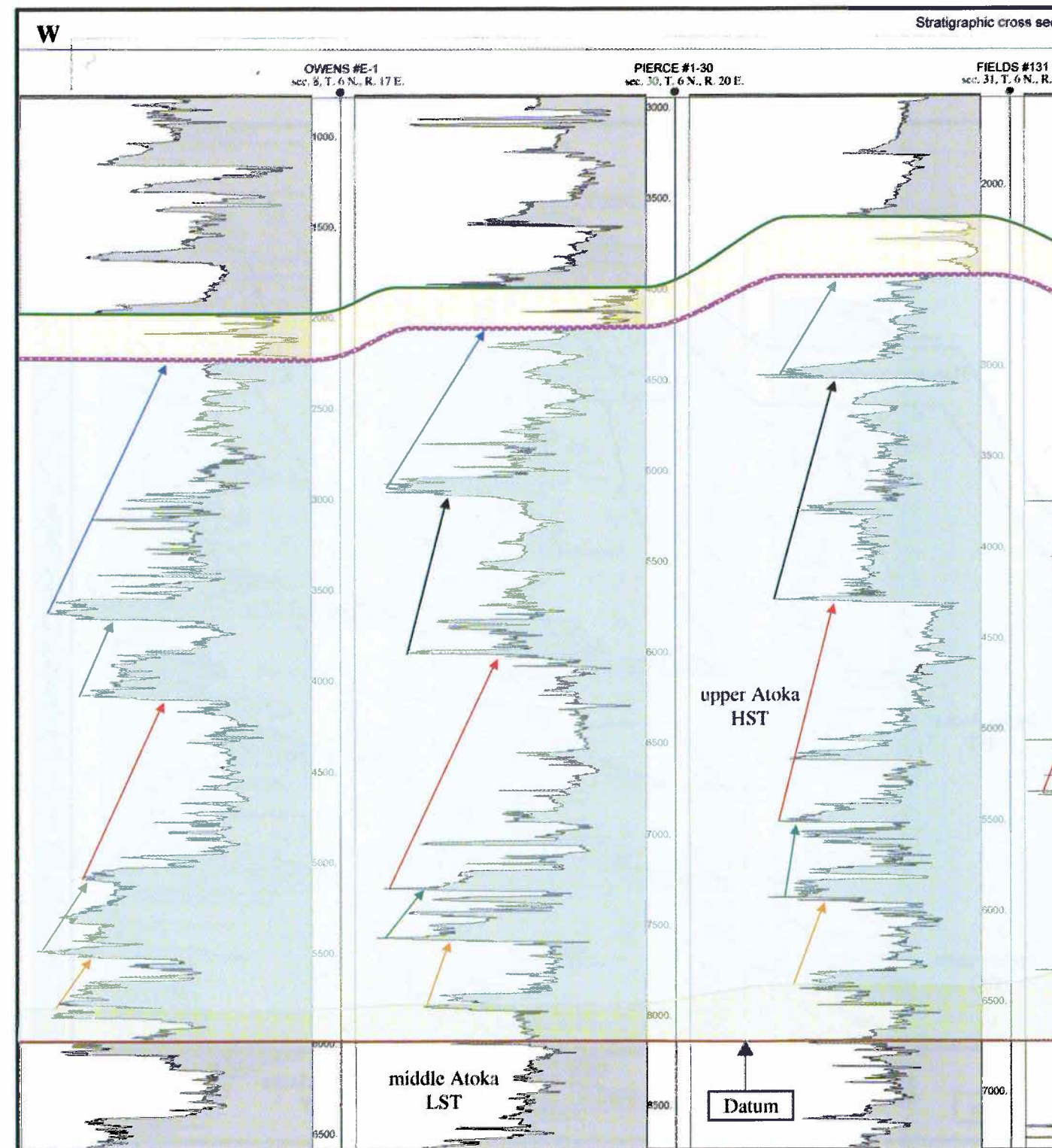
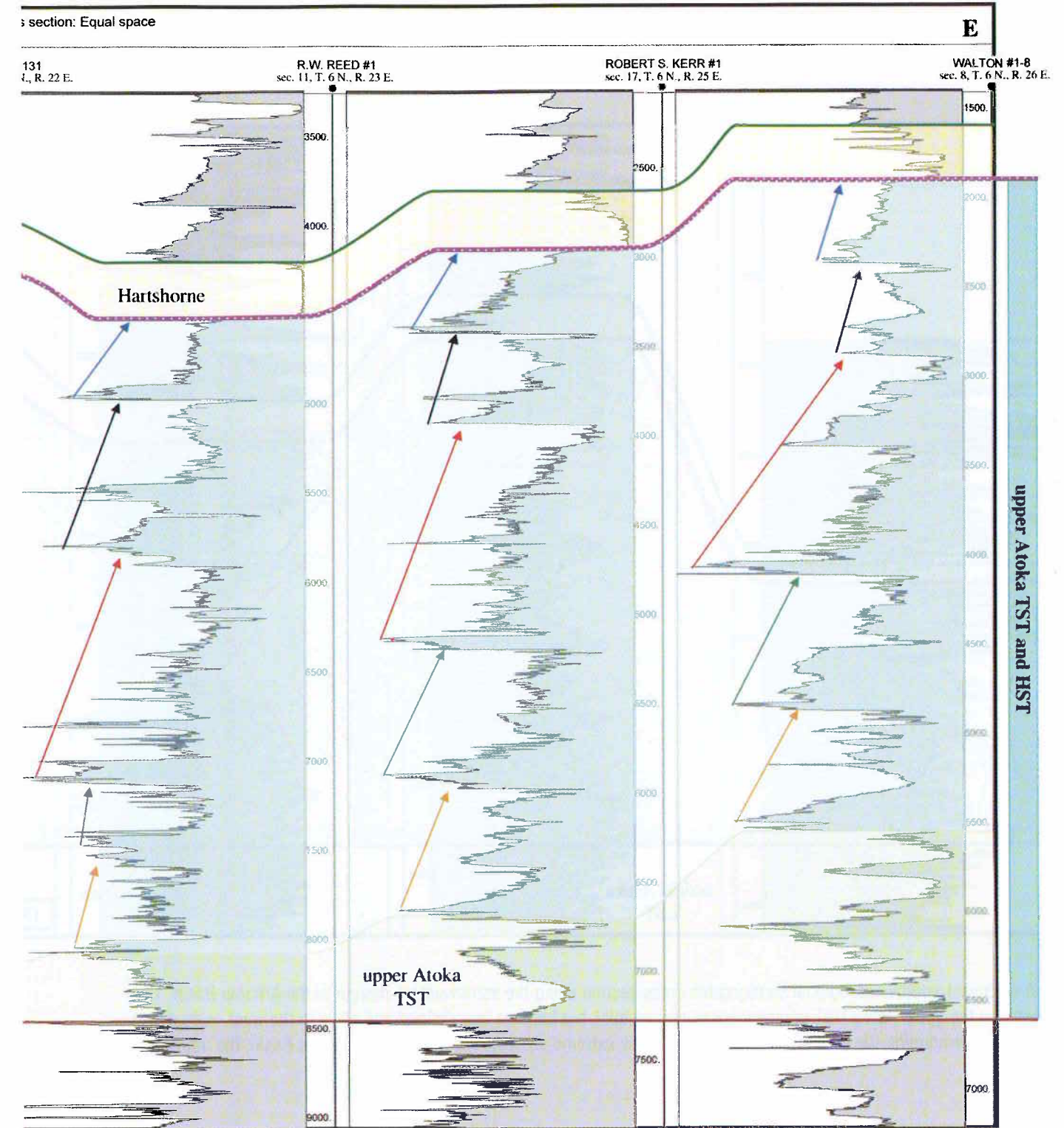


**Figure 4.** An east-west regional stratigraphic cross section in the southeastern part of the Arkoma Basin. The figure shows that the upper Atoka TST becomes thicker toward the east (more than 1,000 ft in the Walton #1-8 well). This TST thins significantly and become shaly to the west, where it is capped by a condensed section marking the maximum flooding surface. The upper Atoka



HST is best developed in this part of the Arkoma Basin, where it is composed of well-defined and thick parasequences that extend for long distances along the southern margin of the basin (the cross-section length is more than 50 mi). The cross-section datum is the upper Atoka transgressive surface. For location, see Figure 10.



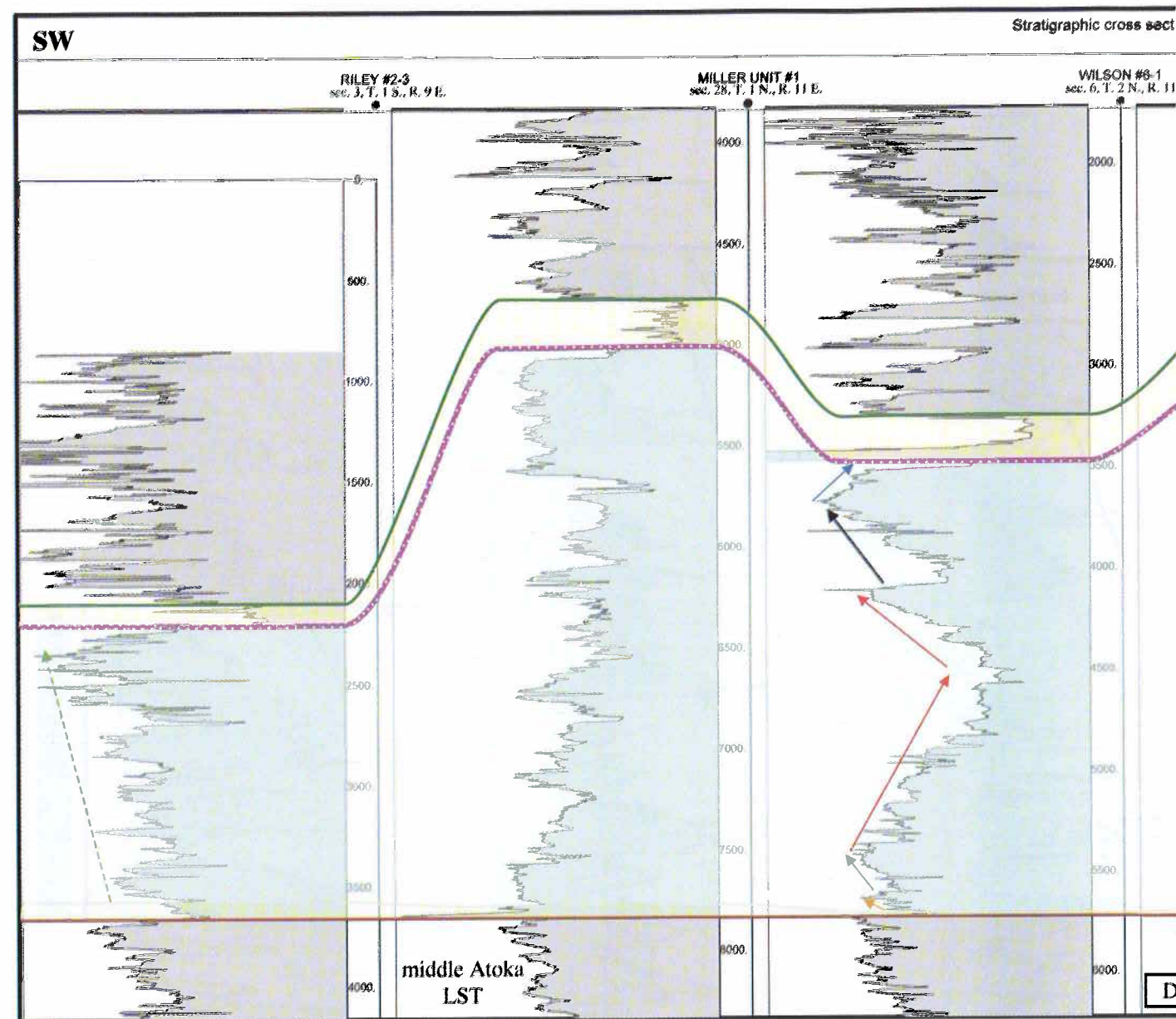
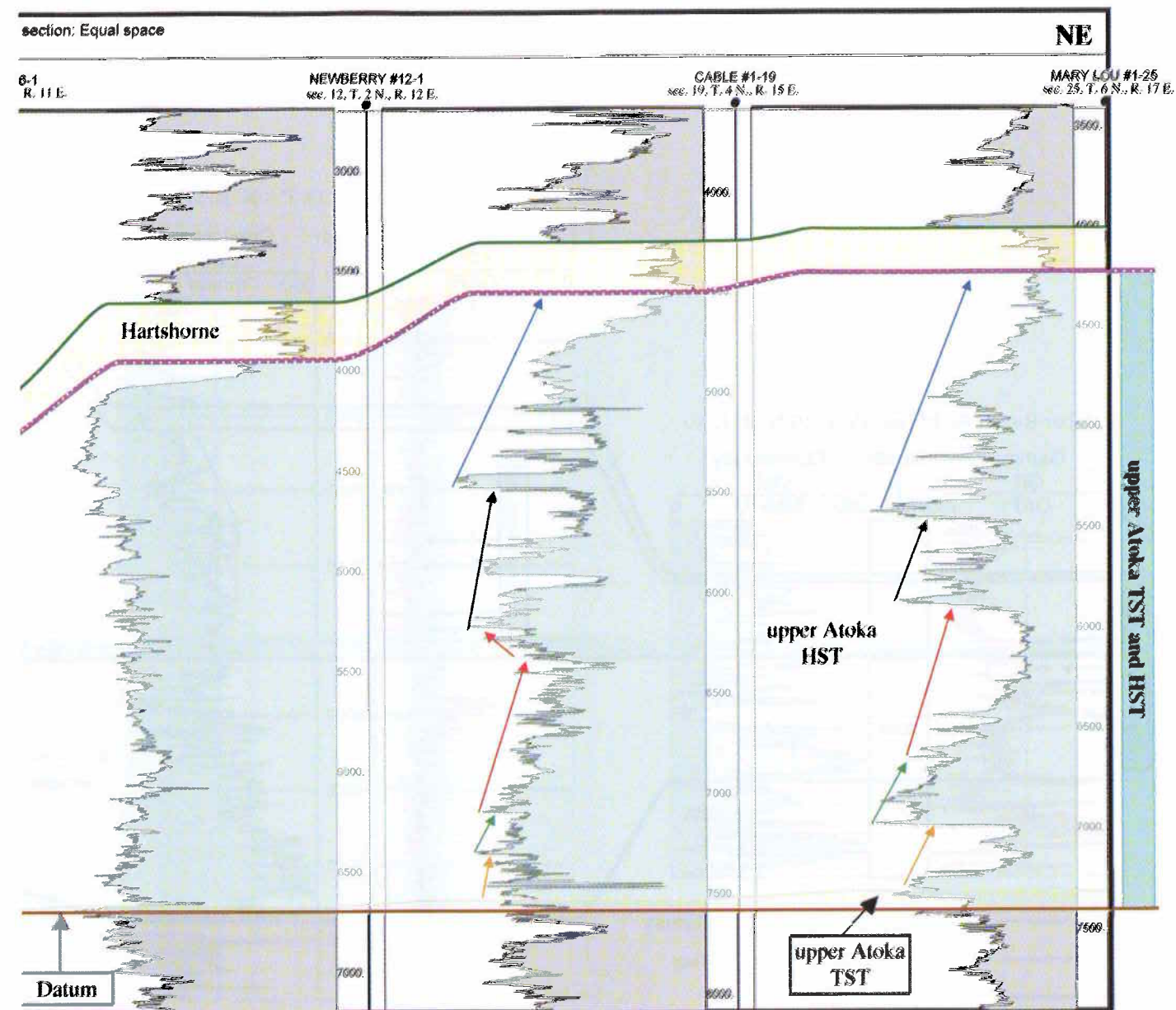


**Figure 5.** A northeast-southwest regional stratigraphic cross section along the southwestern margin of the Arkoma Basin. The figure shows that the upper Atoka HST parasequences remain thick but become less defined and shaly to the west, indicating a prodelta marine environment. Close to the Arbuckle Uplift in the extreme southwest corner of the Arkoma Basin, the upper Atoka



section is composed of fining-upward parasequences developed in a fluvial environment (Riley #2-3 well). The cross-section datum is the upper Atoka transgressive surface. For location, see Figure 10.



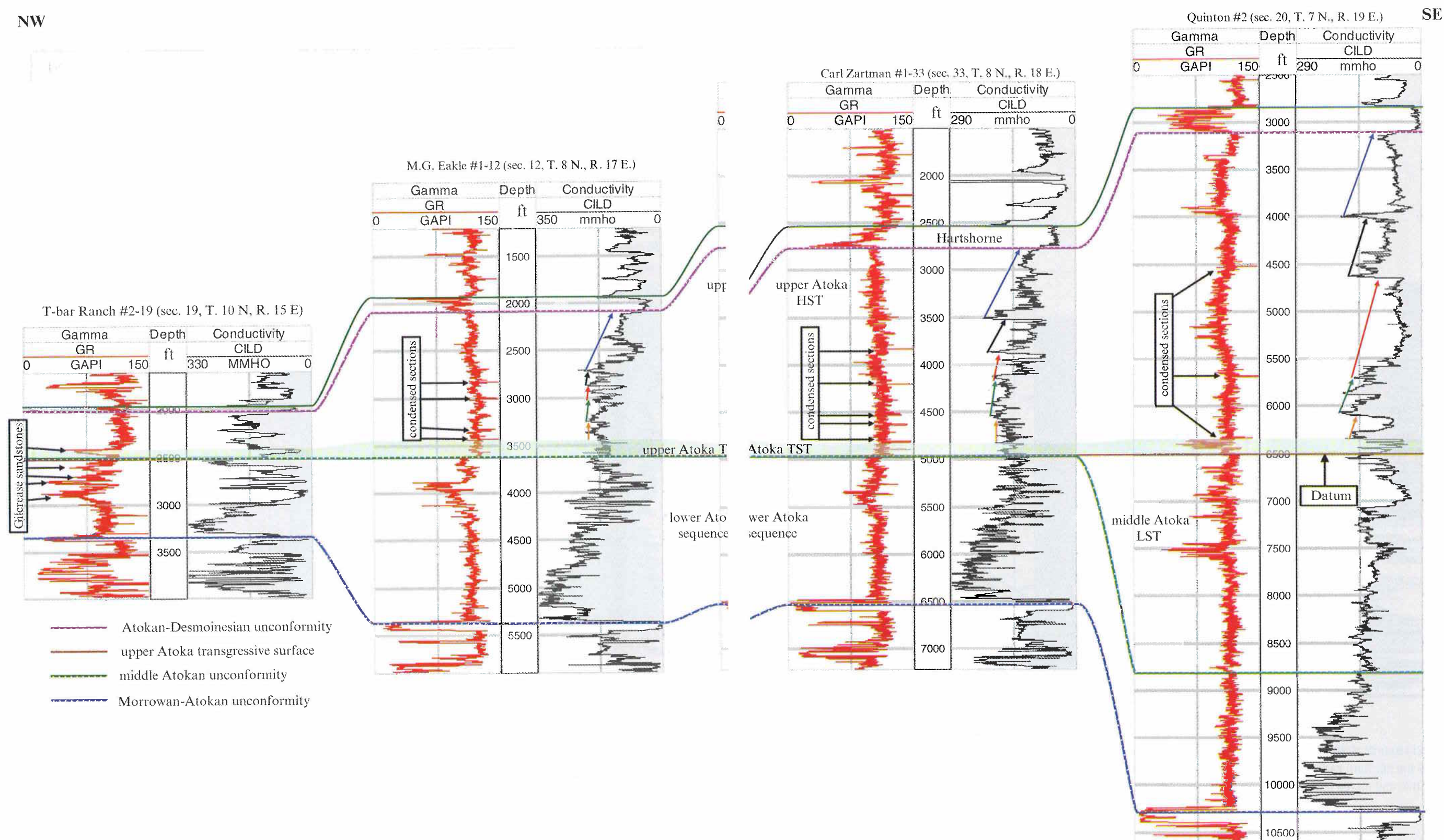


**Figure 6.** A northwest-southeast stratigraphic cross section across the central part of the Arkoma Basin. The figure shows that high GR spikes (condensed sections) occur at the base of several highstand parasequences where they become thin and shaly. This indicates a prodelta marine environment with less sediment supply in that part of the Arkoma Basin. Note the development

of sandstone within the upper Atoka TST in both the southeastern and the northwestern parts of the basin. This thin sandstone represents the uppermost sandstone of the lithostratigraphic Gilcrease sandstones. Horizontal scale is equal spacing. The cross-section datum is the upper Atoka transgressive surface. For location, see Figure 10.



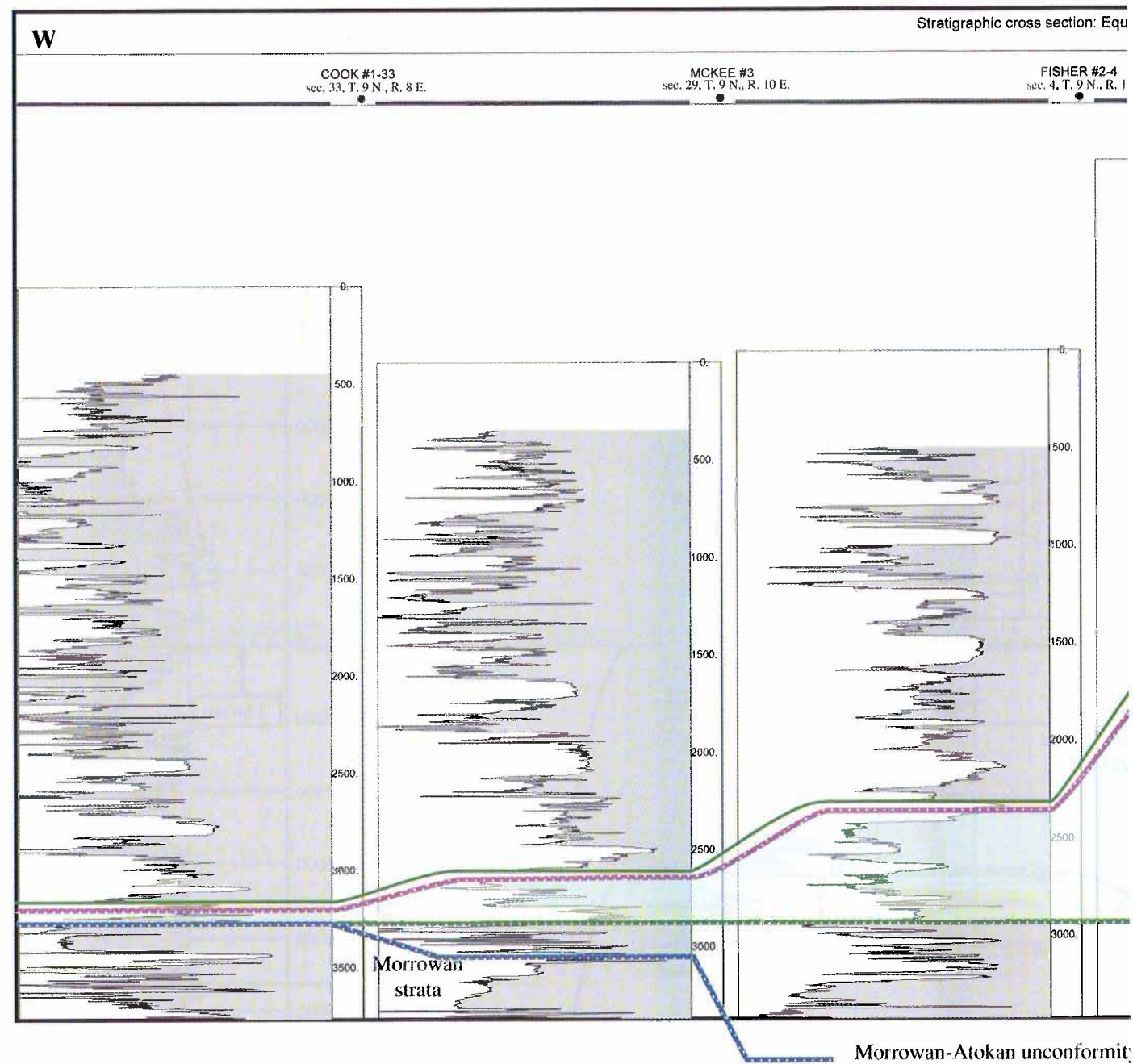
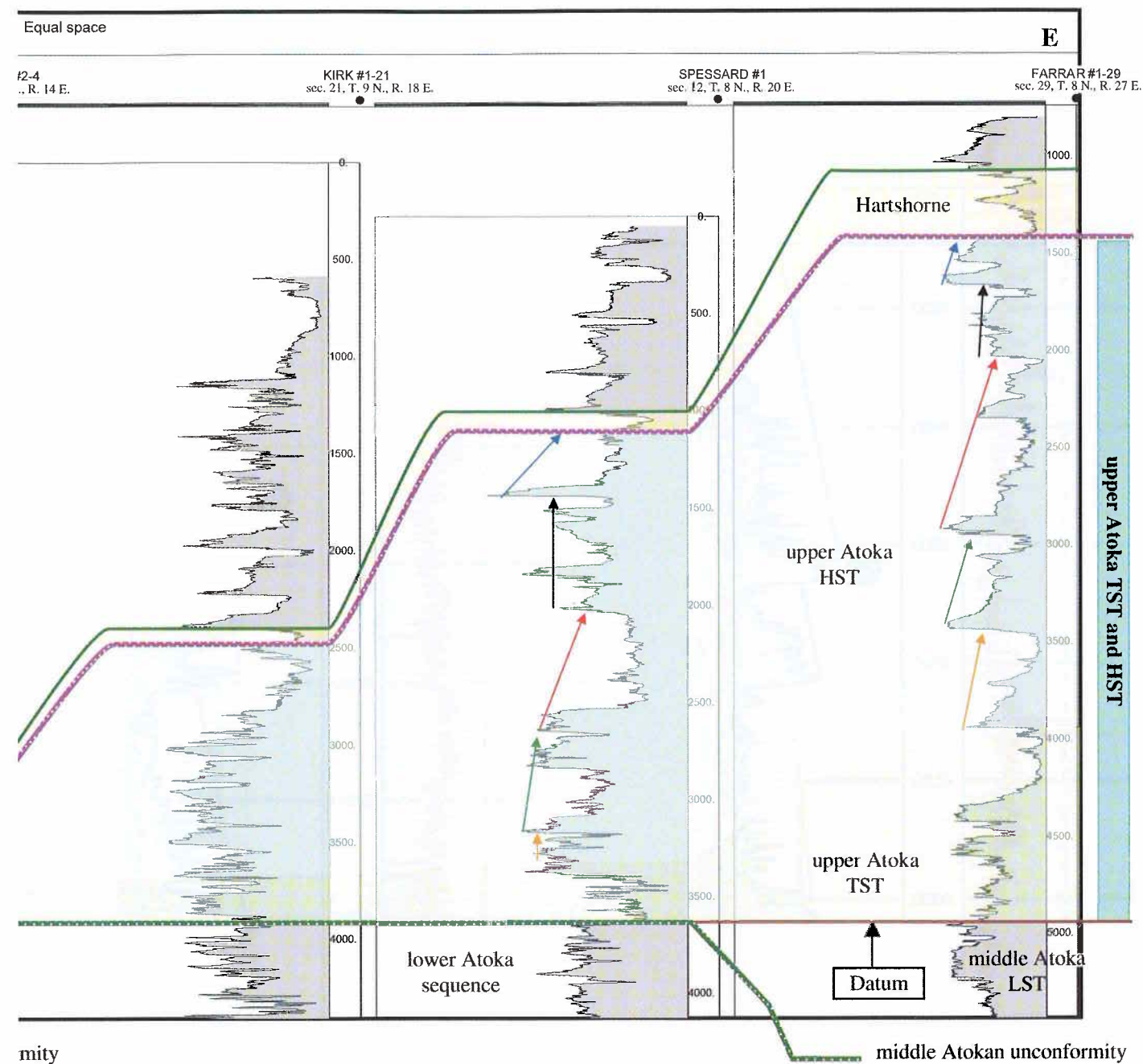


**Figure 7.** East-west regional stratigraphic cross section. The figure shows that the thickness of the upper Atoka section changes significantly across the northern part of the Arkoma Basin. The highstand parasequences, with several sandstone intervals in the east, become very thin and merge together forming a shaly interval marked at its base by the upper Atoka TST. This TST usually



mity

includes thin sandstones that unconformably overlie the lower Atoka sequence (McKee #3 well) and the Morrowan strata (Cook #1-33 well) in the northwestern part of the Arkoma Basin. The cross-section datum is the upper Atoka transgressive surface. For location, see Figure 10.



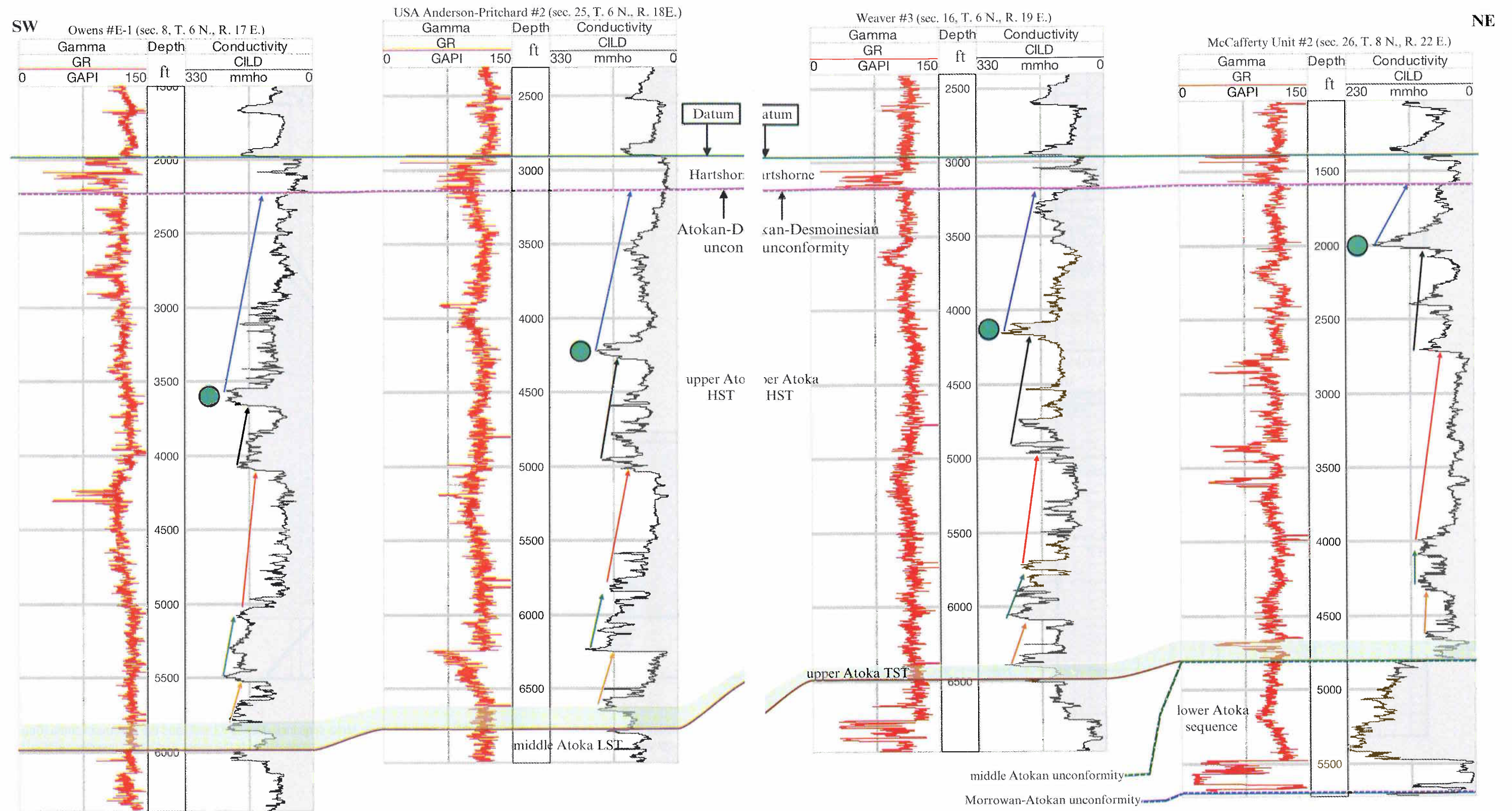


**Figure 8.** A northeast-southwest stratigraphic cross section in the southern part of the Arkoma Basin. Tracking the conductivity marker at the base of the topmost parasequence of the upper Atoka HST (green circle) helps in defining the nature of the upper Atoka-Hartshorne contact as an unconformity surface. It shows how the Hartshorne channel incises the upper Atoka HST at different levels with respect to the underlying conductivity marker. Where the incision is deepest the Hartshorne is underlain by

prodelta facies (McCafferty Unit #2 well). Where the incision becomes shallower the Hartshorne is underlain by shallow-marine or delta-plain marsh-swamp deposits (USA Anderson-Pritchard #2 and Owens #E-1 wells). The cross-section datum is the top of the Hartshorne Formation. Horizontal scale is equal spacing. For location, see Figure 10.



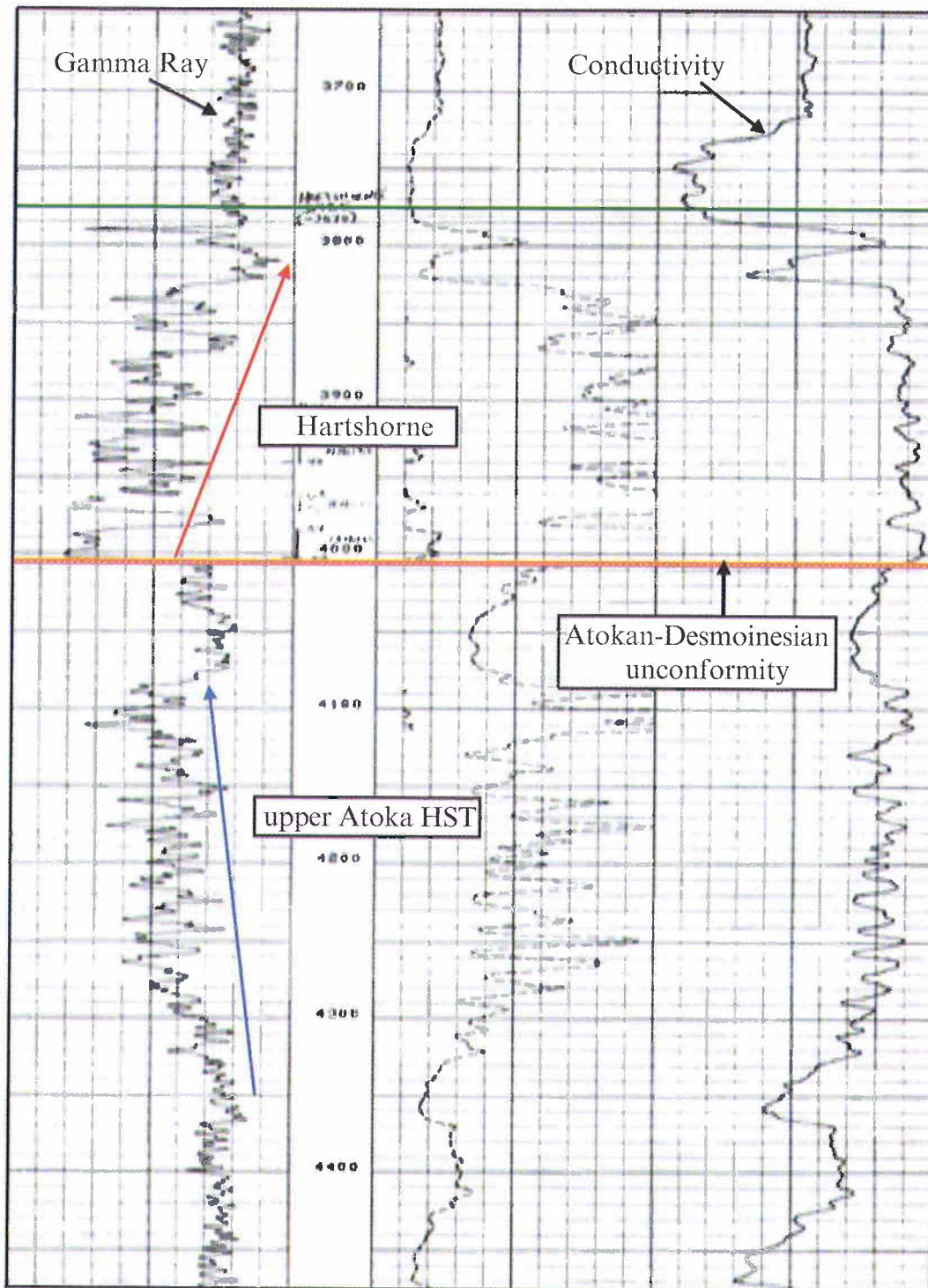


**Figure 9.** An example from the Rouse #1 well (sec. 23, T. 6 N, R. 15 E). The figure shows the clear distinction between the top parasequence of the upper Atoka HST and the Hartshorne Formation. The upper Atoka parasequence shows a coarsening-upward pattern (blue arrow), whereas the Hartshorne Formation shows a fining-upward pattern (red arrow). In wells where the Hartshorne channels incise deeply into the upper Atoka HST, the sandy facies of the upper Atoka parasequence were mistakenly included with the Hartshorne Formation. The boundary between the upper Atoka HST and Hartshorne Formation is an unconformity termed the Atokan–Desmoinesian unconformity.

Based on these two criteria, a regional unconformity between the upper Atoka HST and the Hartshorne Formation is identified where the channels of the latter incised into the upper Atoka HST at different levels. In this work this unconformity is termed the Atokan-Desmoinesian unconformity.

The middle Atoka LST and the upper Atoka TST and HST represent a single third-order sequence. This middle-upper Atoka sequence is bounded by the middle Atokan unconformity at its base and the Atokan-Desmoinesian unconformity at its top.

## REFERENCES CITED

- Andrews, R.D., 1998, Part I—Overview of the Hartshorne play in Oklahoma, *in* Andrews, R.D., The Hartshorne play in southeastern Oklahoma: regional and detailed sandstone reservoir analysis and coalbed-methane resources: Oklahoma Geological Survey Special Publication 98-7, p. 1–40.
- Davis, G.H.; and Reynolds, S.J., 1996, Structural geology of rocks and regions: John Wiley and Sons, New York, 776 p.
- Donica, D.B., 1978, The geology of the Hartshorne coals (Desmoinesian) in parts of the Heavener 15' Quadrangle, Le Flore County, Oklahoma: University of Oklahoma, unpublished M.S. thesis, 128 p.
- Haley, B.R., 1961, Thickness trends in the Hartshorne sandstone and the McAlester Formation in northwestern Arkansas, U.S. Geological Survey Professional Paper 424 C-D, p. C80–C81.
- Hemish, L.A.; and Suneson, N.H., 1997, Stratigraphy and resources of the Krebs Group (Desmoinesian), south-central Arkoma Basin, Oklahoma: Oklahoma Geological Survey Guidebook 30, 83 p.
- Houseknecht D.W.; Zaengle, J.F.; Steyaert, D.J.; Matteo, A.P., Jr.; and Kuhn, M.A., 1983, Facies and depositional environments of the Desmoinesian Hartshorne sandstone, Arkoma Basin, *in* Houseknecht, D.W. (ed.), Tectonic-sedimentary evolution of the Arkoma Basin and guidebook to deltaic facies, Hartshorne sandstone: Society of Economic Paleontologists and Mineralogists, Midcontinent Section, v. 1, p. 3–33.
- Loutit, T.S.; Hardenbol, Jan; Vail, P.R.; and Baum, G.R., 1988, Condensed sections: the key to age dating and correlation of continental margin sequences, *in* Wilgus, C.K.; Hastings, B.K.; Posamentier, H.W.; Van Wagoner, J.C.; Ross, C.A.; and Kendall, C.G. (eds.), Sea level changes: an integrated approach: Society of Economic Paleontologists and Mineralogists Special Publication 42, p. 183–213.
- Storm, Taylor, 1998, Part III—the Hartshorne Formation of Arkansas, *in* Andrews, R.D., The Hartshorne play in southeastern Oklahoma: regional and detailed sandstone reservoir analysis and coalbed-methane resources: Oklahoma Geological Survey Special Publication 98-7, p. 63–68.
- Sultan, M.N.; and Halim, M.A., 1988, Tectonic framework of Northern Western Desert, Egypt, and its effects on hydrocarbon accumulations: Egyptian General Petroleum Corporation, Ninth Exploration Seminar, Cairo, 22 p.
- Sutherland, P.K.; and Manger, W.L., 1984, The Atokan Series: an interval in search of a name, *in* Sutherland, P.K.; and Manger, W.L. (eds.), The Atokan Series and its boundaries: Oklahoma Geological Survey Bulletin 136, p. 1–8.
- Van Wagoner, J.C.; Posamentier, H.W.; Mitchum, R.M.; Vail, P.R.; Sarg, J.F.; Loutit, T.S.; and Hardenbol, Jan, 1988, An overview of sequence stratigraphy and key definitions, *in* Wilgus, C.K.; Hastings, B.K.; Posamentier, H.W.; Van Wagoner, J.C.; Ross, C.A.; and Kendall, C.G. (eds.), Sea level changes: an integrated approach: Society of Economic Paleontologists and Mineralogists Special Publication 42, p. 39–45.
- Visher, G.S., 1996, A history of Pennsylvanian deltaic sequences in Oklahoma, *in* Johnson, K.S. (ed.), Deltaic reservoirs in the southern Midcontinent, 1993 symposium: Oklahoma Geological Survey Circular 98, p. 18–31.
- Williams, C.E., 1978, The economic potential of the lower Hartshorne coal on Pine Mountain, Heavener, Oklahoma: Oklahoma State University, unpublished M.S., 109 p.
- Zachry, D.L., 1983, Sedimentary framework of the Atoka Formation, Arkoma Basin, Arkansas, *in* Houseknecht, D.W. (ed.), Tectonic-sedimentary evolution of the Arkoma Basin and guidebook to deltaic facies, Hartshorne sandstone: Society of Economic Paleontologists and Mineralogists, Midcontinent Section, v. 1, p. 34–52.
- Zachry, D.L.; and Sutherland, P.K., 1984, Stratigraphy and depositional framework of the Atoka Formation (Pennsylvanian), Arkoma Basin of Arkansas and Oklahoma, *in* Sutherland, P.K.; and Manger, W.L. (eds.), The Atokan Series (Pennsylvanian) and its boundaries—a symposium: Oklahoma Geological Survey Bulletin 136, p. 9–17.



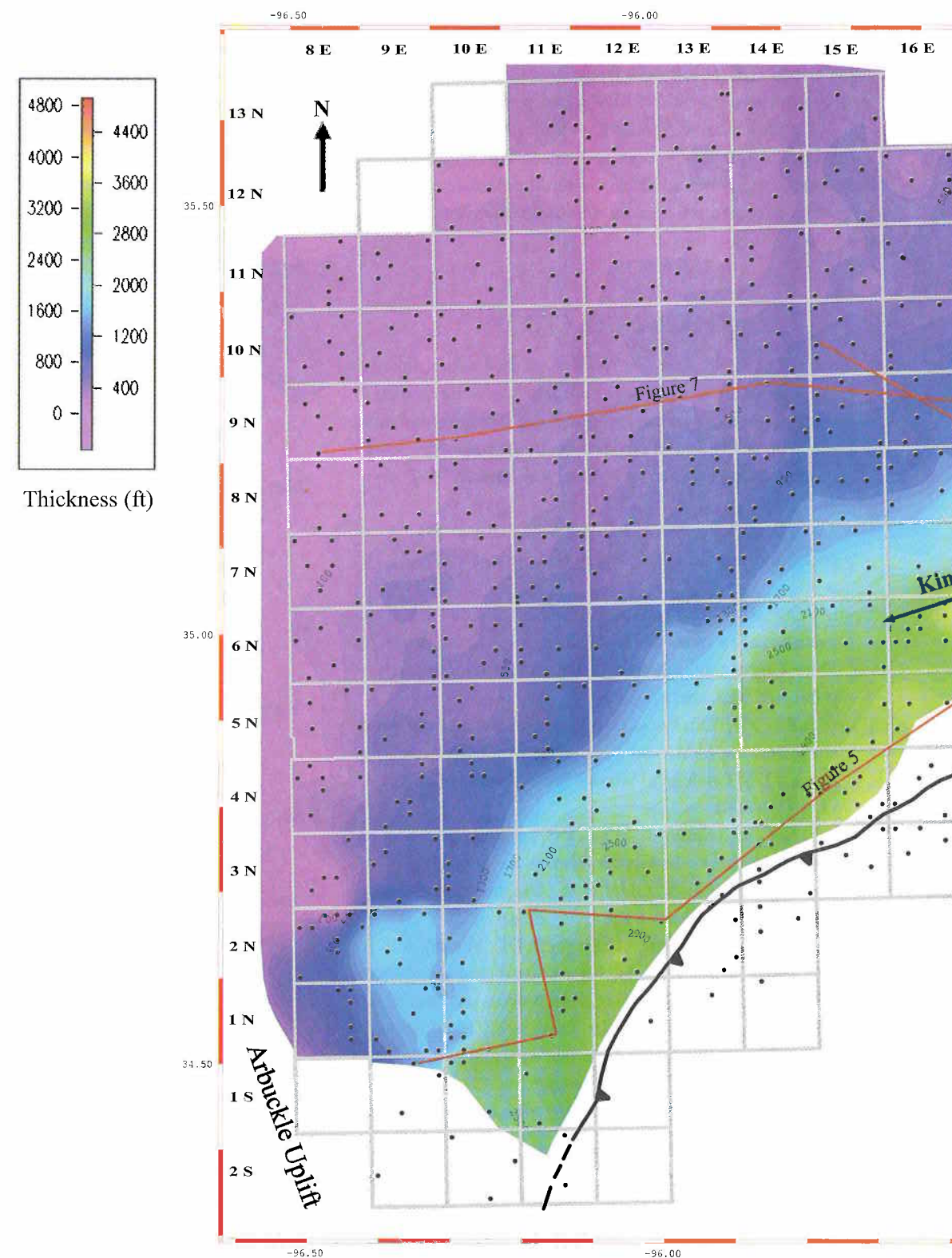
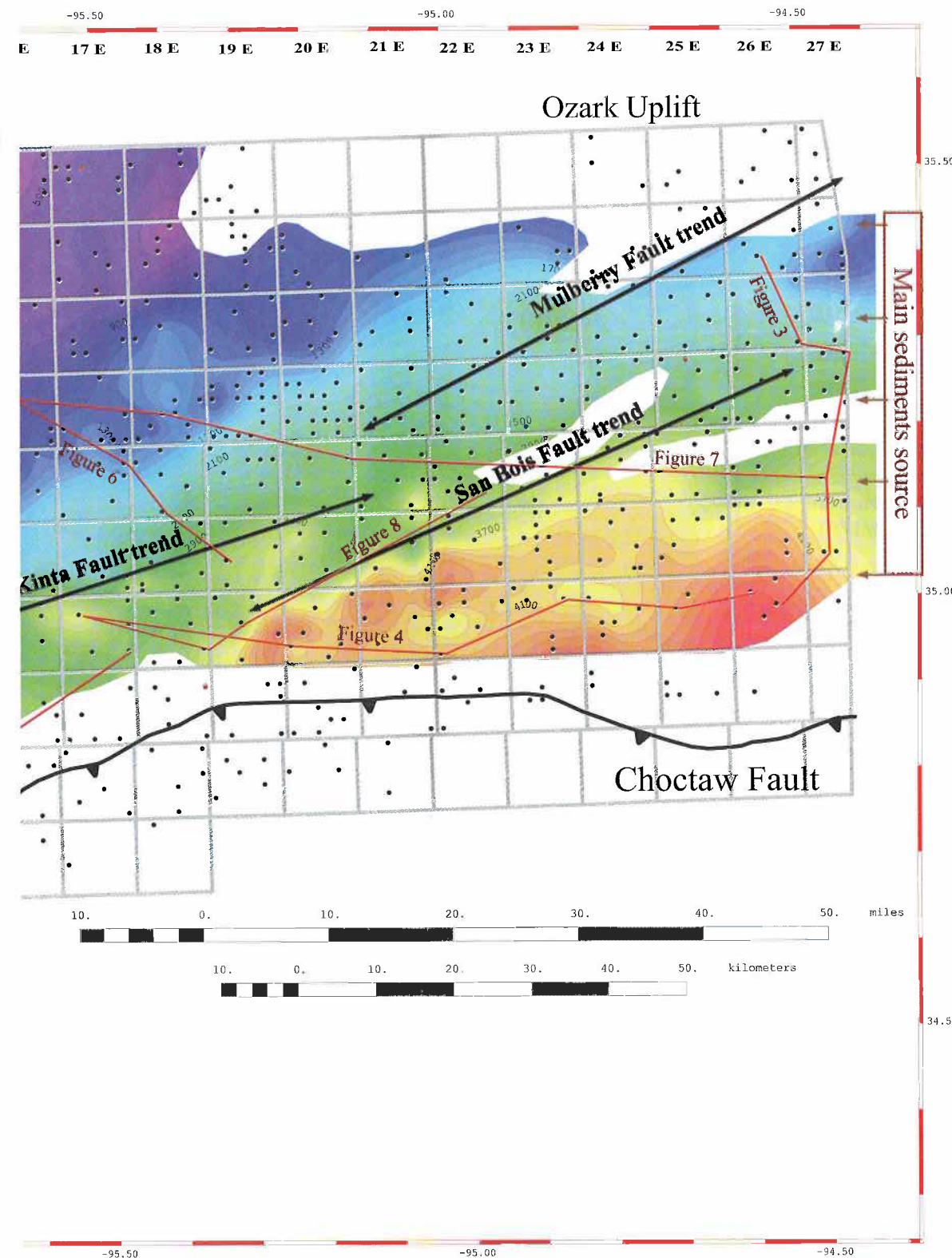


**Figure 10.** Isopach map of the upper Atoka TST and HST in the Arkoma Basin in Oklahoma. The figure shows a general thickening to the south. More than 4,000 ft of sediment was deposited south of the San Bois Fault trend with the main sediment source from the east. The map also shows the location of all cross sections presented in this paper. The map limit is where the upper Atoka



HST crops out (indicated by wells that do not penetrate the top of the upper Atoka HST) and the outcrop belt of the overlying Hartshorne Formation from Andrews (1998). Colored contour interval = 100 ft.



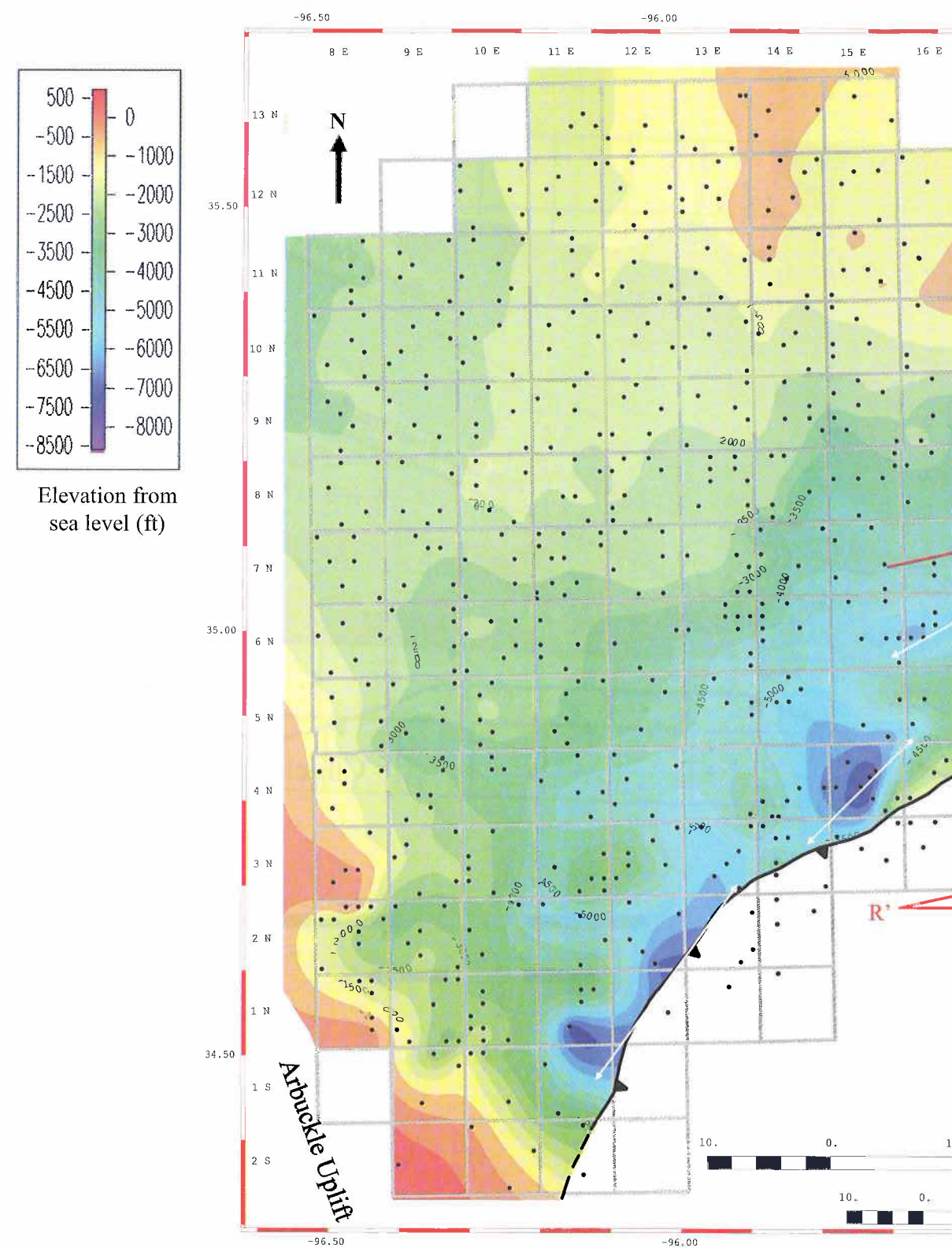
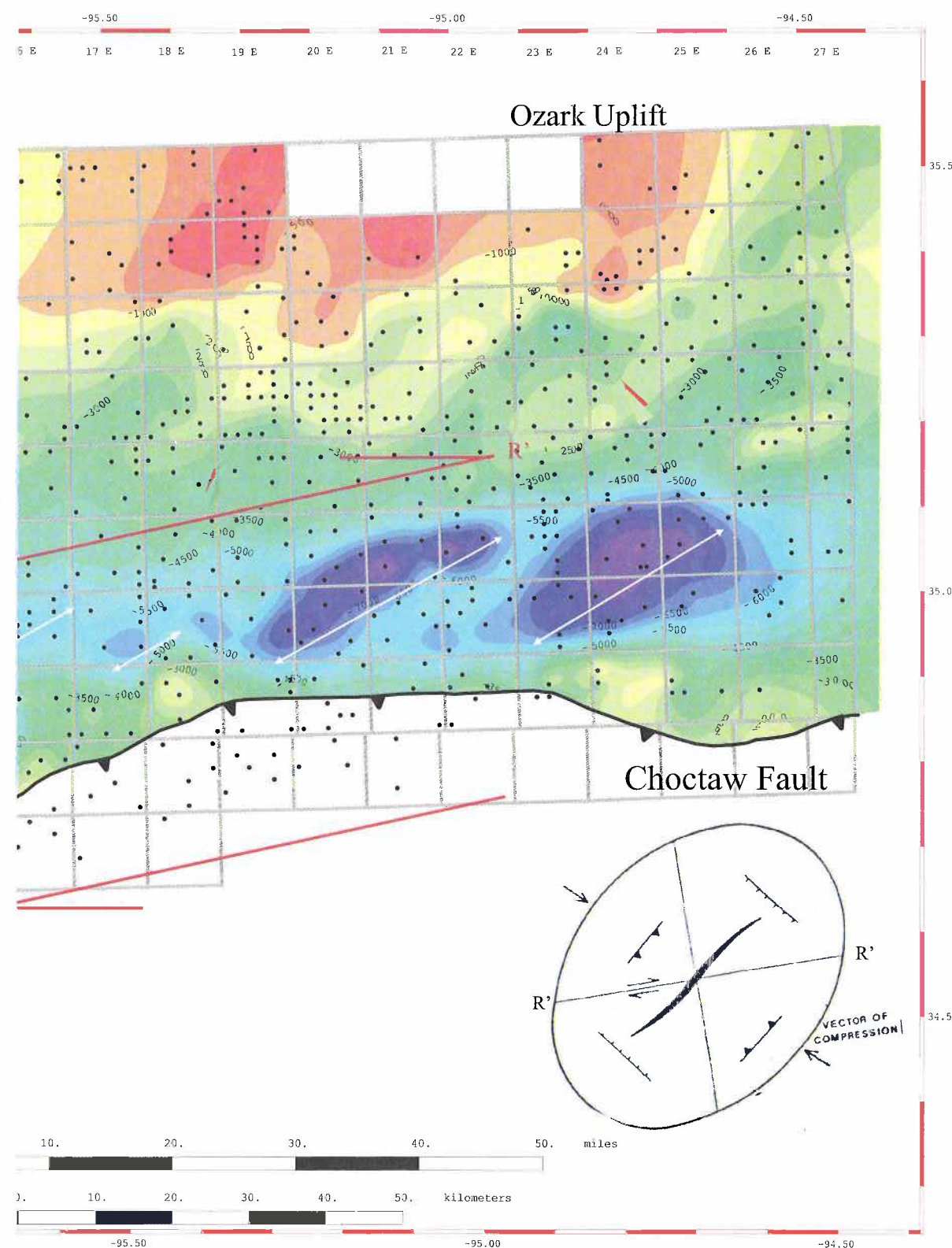


**Figure 11.** Structure contour map on the base of upper Atoka TST. A series of synclines (dark blue areas) are aligned in a zone trending east-northeast–west-southwest (light blue areas). They are located on the downthrown side of the San Bois and Kinta syndepositional fault trends, shown in Figure 10. If the plate collision during the Ouachita orogeny was from the southeast with the main compressional vector in that direction, then this en echelon pattern of folds is aligned in a shear zone (Riedel antithetic shear



zone, R'). The Riedel shear ellipse (bottom right) is modified from Sultan and Halim (1988) and Davis and Reynolds (1996). The synclines or small pull-apart sub-basins were the depocenter sites for the overlying upper Atoka systems tracts. Colored contour interval = 500 ft.



# Exploration Discipline Matrix: A Key to Reestablishing a Vibrant Exploration Industry in the Midcontinent and Other Mature Provinces

*Lyle F. Baie and John J. Gallagher, Jr.*

Creative Energy Investments  
Tulsa, Oklahoma

(*Editor's note:* The figures in this paper are part of a powerpoint presentation and reflect the images used by the authors to develop the concept behind their exploration discipline matrix. They have been accepted as submitted and without editorial changes because the editor believes that the ideas expressed in the paper should be presented to the wider oil and gas audience.)

**ABSTRACT**—A recent *Oil & Gas Journal* article (Tippee, 2004) reported that the leading issue restricting the domestic U.S. petroleum industry is the lack of high-quality prospects in the lower 48 states. This tells us that the status of our domestic energy industry and its future as an employment source is tenuous at best. Without a new strategy that yields high-quality prospects, the U.S. domestic oil and gas industry will be unsustainable for even a few more years. Operations will be limited to infill drilling and offsetting known fields.

In this report, we plan to attack the lack of high-quality domestic prospects head-on by promulgating a set of new exploration disciplines. These are laid out in matrix form. The exploration discipline matrix reflects the explorationist's level of experience, and codifies the actual exploration idea-generating process and its various approaches into a new and powerful tool for reinvigorating the petroleum industry. Using this matrix as a guide, both experienced and novice explorationists can access and organize the combined knowledge and experience of those who have gone before as well as modern information and technology. This will stimulate a more continuous flow of exploration ideas, eventually leading to quality prospects.<sup>1</sup>

This paper is the first of a series expounding on one of 12 different approaches that can be used for developing exploration targets in the mature basins of North America. The initial discipline, termed *translocation*, takes an idea related to vertical hydrocarbon migration in Nevada (Chamberlain, 2003), and applies it to the southeastern extension of the Ardmore Basin, where an underexplored volume of rock plunges beneath the Ouachita Thrust Belt. The vertical migration idea is used to explain the enigmatic Isom Springs Oil Field in Marshall County, Oklahoma, and could help define an exploration fairway for oil and gas within the allochthonous thrust sheets as well as within the underlying autochthon.

## INTRODUCTION

The shortage of high-quality domestic exploration ideas, which is well documented, is negatively affecting the domestic petroleum industry and its future, as well as limiting energy availability from domestic sources in the United States. In addition, for geoscientists and engineers, the movement away from a robust domestic oil and gas industry is having

negative repercussions on employment. The ways that organizations and individuals generate ideas have been studied and discussed for years (Wantland, 1992; Beaumont and Foster, 1999; Tucker, 2003). Tucker summarized the problem and offered some generic solutions. His key conclusions were that most ideas are "happy accidents" stumbled onto by freelancing groups operating without hands-on direction, and that most organizations are not satisfied with their results when creating new ideas. Tucker proposed a seven-step methodology, but none of the processes were earthshaking or likely to produce

---

<sup>1</sup>We designed this paper to highlight a process only, and do not mean to develop a complete exploration project, although the process we describe can be used to that end.



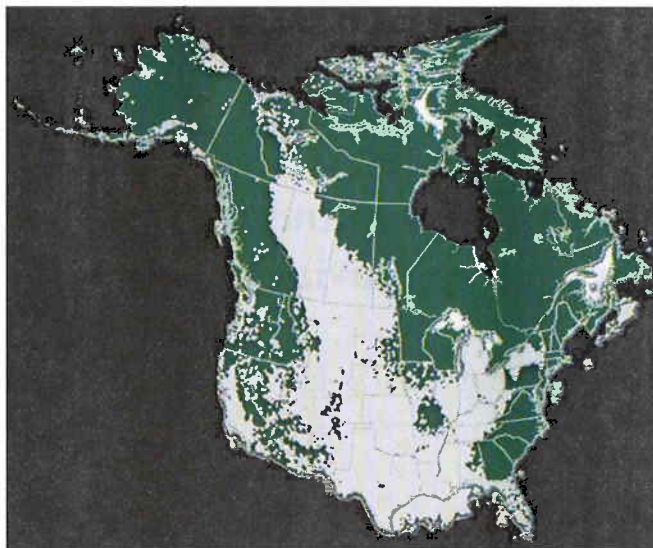


**Figure 1.** The distribution of the 3.5 million wells (white areas) drilled in the United States and Canada.

desired results in an exploration environment. It is against this background that we explored the industry situation of today.

The reasons for current circumstances are many and varied and include industry restructuring, demographics, and the loss of corporate memory. The most critical cause, however, is the lack of a formalized process for generating new exploration. Some may argue that no great exploration opportunities remain in the lower 48 states (Fig. 1). We can look at this image of the surface locations of the 3.5 million wells drilled on the North American continent in two ways. We can say that, from an exploration perspective, everything has been done. Or, we can posit that robust data exist for our use in exploring the mature basins of North America. Recent, significant domestic successes would argue for the latter position, but the frequency of these successes is not high enough to support a vigorous level of industry activity.

In 2003, the Tulsa Geological Society hosted American Association of Petroleum Geologists (AAPG) Midcontinent Section meeting technical program focused on bringing new ideas to geoscientists to help reinvigorate exploration activity in the area. This meeting, along with an ongoing series of discussions with exploration managers, led us to develop the exploration discipline matrix concept. This model is designed to formalize the many different processes of exploration by drawing on new technology and concepts—as well as

our combined historical experience—to establish methods for creating new opportunities or identifying unexplored locations. This process should help recapture some of the lost corporate memory and provide ways for both experienced and novice explorationists to develop new target areas for in-depth analysis. These methods are each slightly different and require a unique series of steps to reach the end game, which is an exploration target area not currently being pursued by industry.

## THE EXPLORATION DISCIPLINE MATRIX

Figure 2 illustrates the 12-box matrix, organized from left to right, with experienced explorationists being most comfortable working on the left. Novice explorationists will normally be at ease beginning on the right side, as these disciplines are more data- and technology-oriented and therefore require less literature review and/or hands-on experience gained from successes and failures. For example, Arco in Indonesia and Kerr McGee in China used the “migration path exploration” discipline successfully to find oil fields downdip from either shows or production. By accessing the 3.5 million oil and gas wells drilled in North America and using some of the currently

ENHANCING E&P IDEA GENERATION PROCESSES/DISCIPLINES		
TRANSLOCATIONAL	OUT-OF-THE-BOX POSSIBILITIES	DATA MINING
DATA ACCESS	NEW TECHNOLOGY	MIGRATION PATH EXPLORATION
TRANSFORMATIONAL	VISUALIZATION OF COMPLEX GEOLOGICAL RELATIONSHIPS	RECALIBRATED DATA
NEW APPLICATIONS OVERLYING OLD “SHOWS”	“READING” THE LITERATURE	NEW ECONOMIC CONDITIONS

**Figure 2.** Exploration discipline matrix organized from extensive experience and in-depth knowledge on the left to less experience, less knowledge, and more cutting-edge technology on the right. The matrix highlights 12 separate approaches to developing exploration ideas.

available computer data-mining technologies, the “data-mining” discipline has already turned up some interesting leads in the Rocky Mountain region. The “data-access” discipline can be illustrated by new land and data availability on the King

Ranch in southern Texas. Recent major discoveries in the Maverick Basin of western Texas and the significant reserve additions at Lake Washington salt dome in Louisiana are the result of the “new applications overlying old shows” discipline, and so on.

Here, we focus on the “translocation” discipline, whereby an exploration idea either proposed or found to be applicable in one basin is moved, or translocated, to another basin and validated by local data. This allows unexplored or underdeveloped play concepts to be explored in the new locality. The recognition that this model or discipline is in play usually begins with an anomaly of some sort in the target basin. In this case study, a “remigration of hydrocarbon” model (proposed by Alan Chamberlain for the Grant Canyon Field in Nevada) is used to help explain oil found in the Isom Springs Field in Marshall County, Oklahoma.

At Isom Springs, oil is found trapped within the Ouachita Thrust Belt folds in an allochthonous position. The lower Paleozoic reservoir rocks have been moved from a deep-water depositional environment and thrust over Paleozoic shelf and platform deposits. The mystery arises from the fact that the source rock for these oils seems to be the shelf and platform rocks underlying the thrust sheets.

Once such a translocation candidate is recognized, the first step is to review the literature on the Isom Springs Field. A scan of the literature reveals that some interesting geologic relationships that need explanation are occurring in the vicinity.

Figure 3 shows the Bouguer gravity map of northeastern Texas, southeastern Oklahoma, and southwestern Arkansas. The Ardmore Basin is clearly defined by the gravity and delimited by the Washita Valley Fault on the north and the

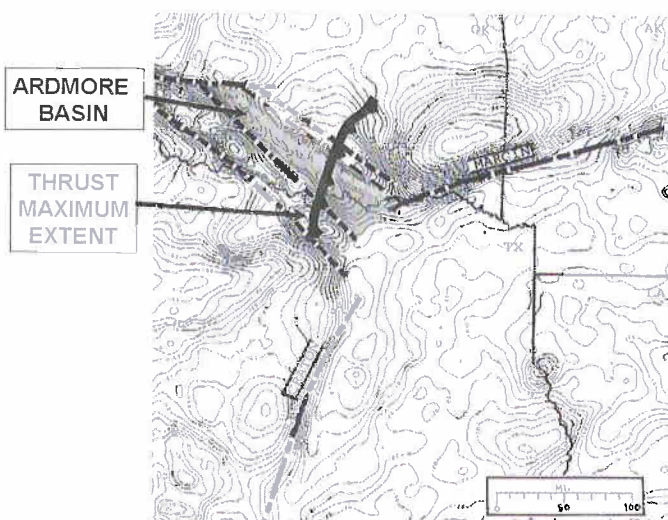


**Figure 3.** Basement structure overprinted on the Bouguer gravity map of Oklahoma, showing the Ardmore Basin, its controlling faults (dashed lines), and fault extension beneath the maximum extent (solid lines) of Ouachita thrusting (modified from McBee, 1995).

Criner Fault on the south. It appears that this area was a Precambrian triple junction and the Ardmore Basin was the failed arm. Even more interesting is the fact that the Ardmore Basin and its bounding faults clearly extend beneath the current, as well as the maximum extent of the low-angle Ouachita thrust faults for a distance of as much as 50 mi.

The fact that the Ardmore Basin portion not covered by the current Ouachita thrusts is highly productive for oil and gas leads to speculation about the prospectivity of the Ardmore Basin portion underlying the current Ouachita thrust front (often called the Choctaw Fault). Figure 4 offers a closer view of the structural situation in the area around the Ardmore Basin. The westernmost thrust fault shown is the maximum extent of thrusting published in the literature. The second, more eastern, thrust fault is the current surface expression of

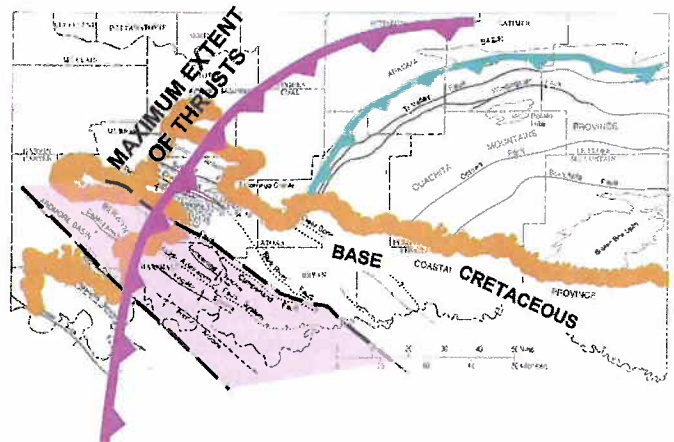


**Figure 4.** Current structural context of southern Oklahoma (modified from Huffman and others, 1987).

the thrusting that occurred across the Ouachita Mountains province (the Choctaw Fault) before it was covered by Cretaceous sediments in southern Oklahoma. The figure also shows other proposed subsurface structural trends.

Figure 5 gives a closer view of the Ardmore Basin structures and the adjacent Tishomingo basement uplift. The difference in surface orientations and positions of the westernmost extent of thrusting (now eroded away) and the current subcrop of the leading thrust fault reflects the post-thrusting erosion and relative uplift across the area. This pattern demonstrates the reasons for the hydrocarbon distribution seen in Figure 6. The map clearly illustrates that the Ardmore Basin steps down across several parallel basin-edge faults, with the northerly one being the Bryan Fault. Current hydrocarbon-producing fields lie along features known as rails that border the deep Ardmore Basin. These rails appear to separate oil-prone production from gas-prone production in the deeper basin.



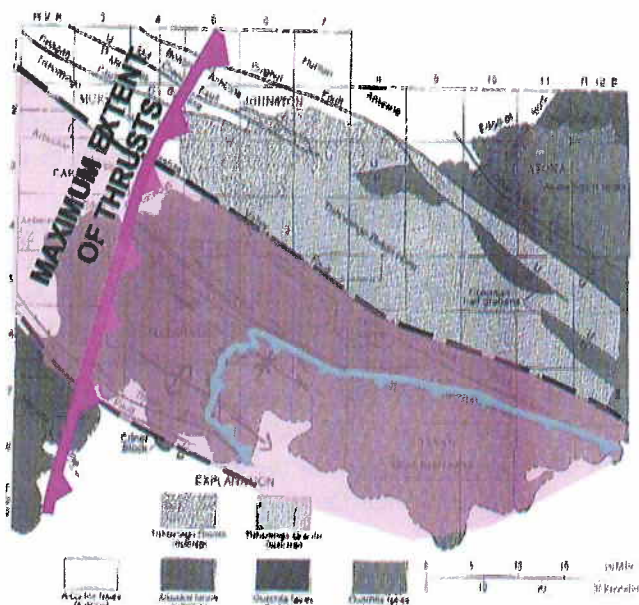


**Figure 5.** Close-up of current structural context of southern Oklahoma, including the extension of structural elements beneath the Choctaw Thrust Faults (modified from Huffman and others, 1987).

The stratigraphic relationships observed in the field (Fig. 6) indicate that the thrusting was post-Pennsylvanian Dornick Hills/Deese (Desmoinesian). These relationships are illustrated in Figure 7. The connection between the time of maximum thrusting and the later Viola critical moment is important because it confirms that the thrust-fold structural style was in place when the potential source rocks were generating hydrocarbons.

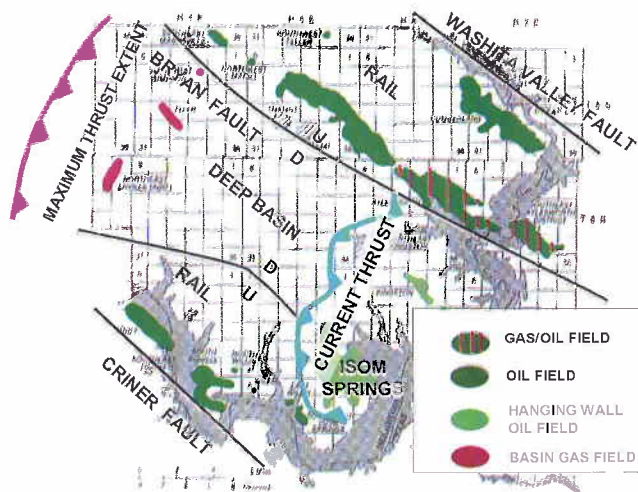


**Figure 6.** Distribution of hydrocarbon fields in the Ardmore Basin, showing the basin boundary faults, the parallel "rail" faults, and the maximum and current Choctaw Thrust Fault (modified from Huffman and others, 1987).

Figure 8 summarizes the Ardmore Basin geology and hydrocarbon distribution at the time of maximum thrusting. Many of the fields discovered to date were clearly in a sub-thrust position at the time of hydrocarbon migration. Little or no exploration has occurred below the current thrust sheets for similarly positioned traps (i.e., beneath the Choctaw Fault).

## GEOCHEMISTRY

Key elements in this and other potential plays in the area are the nature, timing of maturation, and tectonic history of the source rocks. Oil characterization and oil-source correlation techniques have become more sophisticated during the last 20 years. Weber (1994) summarizes a comprehensive study of the Ouachita Mountains province oils and nearby areas bordering the current tectonic front as defined by the Choctaw Fault.

Regionally, the rocks of the Ouachita Mountains province (the allochthon) were transported along low-angle thrust faults from a deep-water depositional environment (shales, cherts, and novaculites), from the south and the east. Most often the source rocks in this transported section contain Type III, gas-prone kerogen (Curiale, 1992 and personal communication, 2004). The foreland, over which the deep-water sediments were thrust, is composed of nearshore, shelf, and platform sedimentary rocks (sandstones, shales, and carbonates) that contain Type II, oil-prone kerogen in two well-known source sections: the Devonian Woodford Shale and the Ordovician Viola-Simpson (Wang and Philp, 1997).

A review of the pertinent literature and our personal communications with geochemists have confirmed the probable source rocks for many of the hydrocarbons trapped in the southeast portion of the Ardmore Basin as the Viola-Simpson petroleum system (Viola) Type D and G oils (Wavrek, 1992). These trapped oils have the chemical characteristics of a carbonate source rock as opposed to the Devonian Woodford Shale source rocks. Type D and G oils have the unique chemical signatures associated with Middle and Lower Ordovician *Gloeocapsomorpha prisca* (Figs. 9, 10, and 11; Wavrek and others, 1997). From this correlation, we can draw an interesting conclusion: that fields such as North Madill in northern Marshall County, Oklahoma, were sourced from the Viola system while that trap and its reservoir rocks were positioned under the thrust sheets (Weber, 1994). Relative uplift and erosion later removed the remnants of the thrust material, leaving the fields in their current geometric position. But the relationship of these traps to the thrust sheets at the time of filling with hydrocarbons is important.

Isom Springs oils that are contained within the thrust sheets themselves are nearly identical to those currently found in front of the Choctaw thrust sheets in fields such as North Madill (Weber, 1994). This implies that Isom Springs oils were trapped in a highly complicated thrust-sheet package of a



A				B	
PER.	SERIES	ARDMORE BASIN	EASTERN OKLA.	OUACHITA PROVINCE	OROGENIC EVENTS
CRET.	32. PKE-CRET.				
PERM.	31. VERMILION	MONITOR			
	30. MISSOURIAN	NOXON			
PENN.	29. U. DESMOINESIAN		KARMATOR		
	28. U. DESMOINESIAN	DEESE	KREBS		
	24. ATOKAN	U. DORNIC HILLS			
	21. MORROWAN	U. DORNIC HILLS	MORROW	JOHN VALLEY	
MISS.	20. CHESTERTON	CHERTON	CHESTER	STANLEY	
	19. MERAMECIAN	CANEY	MERAMEC		
	18. USAGEAN	STAMPA	DEAN	ARKANSAS	
	17. KINDERHOOKIAN	WOODFORD		NOVACULITE	
DEV.		16. "UPPER" HUNTON		ISOM SPRINGS	
SIL.		15. "LOWER" HUNTON		MISSOURI MTH	
				BIATUCK	
ORD.	UPPER	14. VIOLA		POLK CREEK	
	MIDDLE	13. SIMPSON		WOMBLE	
CAMB.	LOWER	12. U. CANADIAN		MAZAP	
		11. L. CANADIAN		CRYSTAL MIN.	
		10. TRIMPTONIAN		COLLIER SHALE	
		9. FRANCONIAN		?	
PROT.		8. ORESBACHIAN		?	

**Figure 7.** Index of stratigraphic names used in Oklahoma tectonic provinces with significant geologic times highlighted (Viola and Woodford source intervals, the time of the maximum extent of Ouachita thrusting, and Viola's critical moment resulting in generation of hydrocarbons; modified from McBee, 1995).

deep-water affinity within the fractured Arkansas Novaculite (Siluro-Devonian and Mississippian age) and were sourced from below the basal thrust by the Viola. Recalling that the most common kerogen type in the allochthonous, thrust sediments was gas-prone Type III, and that the oils entrapped

within the thrusts are very similar to Viola-sourced oils, it seems likely that the oils in Isom Springs Field and other thrust-belt oils to the north and east (Fig. 12; Weber, 1994), have leaked upward into the allochthon from source rocks and/or traps below the thrusts.

The case for oil and gas entrapment below the thrusts is supported by a number of fields (located north and west of the current Choctaw leading thrust fault) that would have been in a subthrust position at the end of the Desmoinesian, when the thrusts extended farther north and west; these fields also share the Viola source affinity. Figure 12 (Wavrek and others, 1997) describes the maturity level of the Viola across the Ardmore Basin, extending to the current surface location of the Choctaw Fault. The presence of the Viola below the thrust is implied by the nature of the oils trapped above the thrust faults in the Isom Springs Field. Figure 13 shows support for structuring beneath the thrust

sheets (Wavrek and others, 1997). The figure shows that the anticlines of the Ardmore Basin also extend up to the current surface location of the Choctaw Fault.

Applying the concept of translocation to upward migration of oil across thrust faults demonstrates the possibility

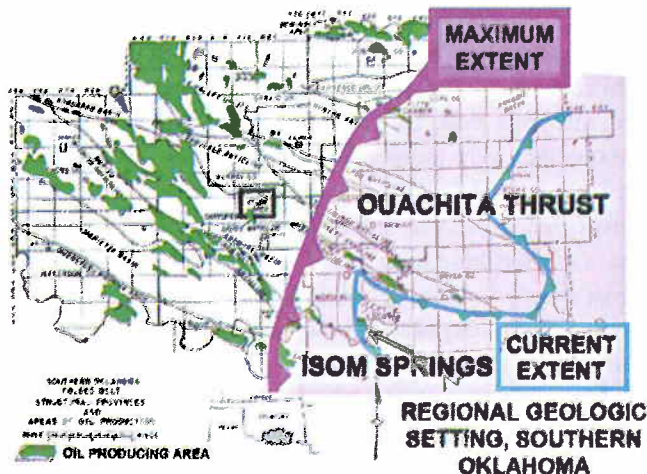


**Figure 8.** Regional geologic setting of southern Oklahoma showing peri- and subthrust hydrocarbon fields, maximum and current extents of the Choctaw thrusting, and the key Isom Springs Field (modified from Garvey and others, 1993).

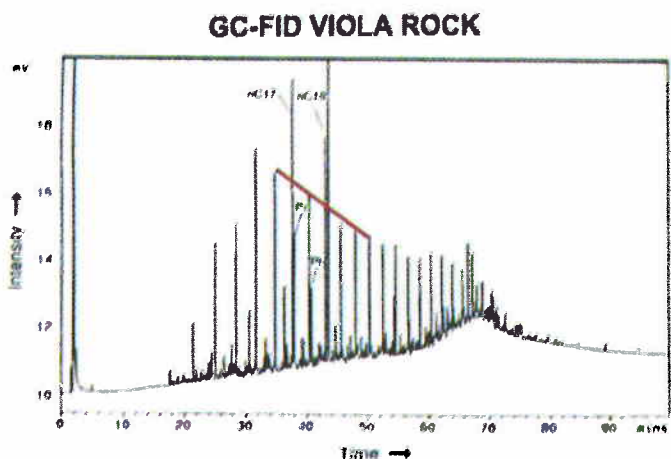


**Figure 9.** Gas chromatography-flame ionization detector (GC-FID) profile of a typical Viola source rock. Note the nC17 and nC19 peak heights represented. (Figure modified from Wavrek and others, 1997.)

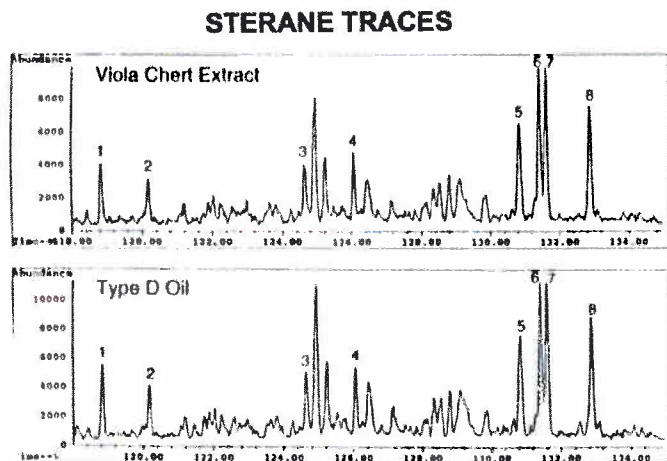


**Figure 10.** Sterane biomarkers of a Viola source-rock extract and a representative Viola oil (Type D) establishing their positive correlation (modified from Wavrek and others, 1997).

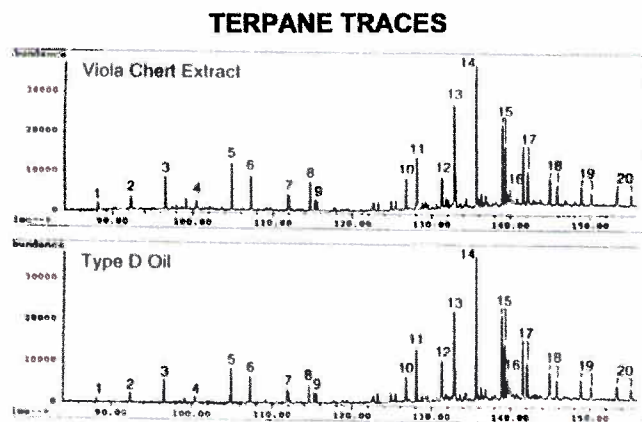


**Figure 11.** Terpane biomarkers of a Viola source-rock extract and a representative Viola oil (Type D) establishing their positive correlation (modified from Wavrek and others, 1997).

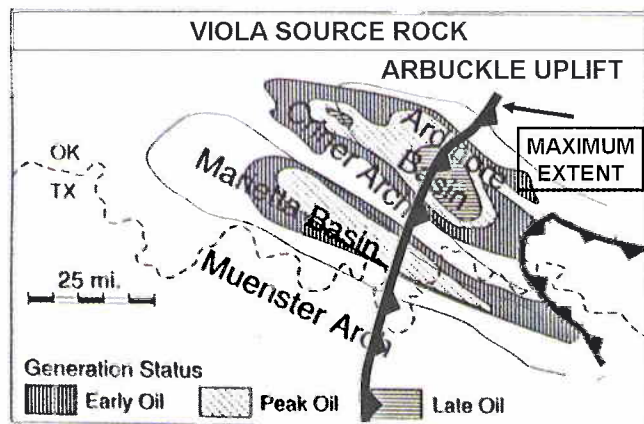


**Figure 12.** Maturity level of Viola petroleum-system source rock in southern Oklahoma, showing the generative status of Viola extending beneath the maximum extent of Choctaw thrusting and up to the current thrust front (modified from Wavrek and others, 1997).

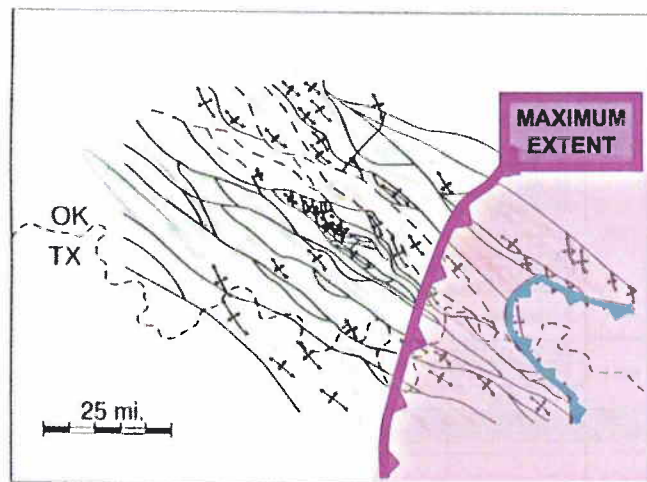


**Figure 13.** Distribution of known anticlines in the Ardmore Basin extending beneath the maximum extent of Choctaw thrusting and up to the current thrust front (modified from Wavrek and others, 1997).

of new fields in the southeastern portion of Oklahoma's Ardmore Basin. To verify the concept and develop exploration leads, explorationists can now apply a methodology such as that published by Coleman and others (1997) to the area. Such research could result not only in a significant exploration play in the Ardmore Basin, but also one extending to the north and east along the Ouachita Mountains province, where other Viola-affinity oils have been found within the thrust sheets (Fig. 12; Weber, 1994).

## SUMMARY

Using the translocation discipline—one of 12 approaches shown in the exploration discipline matrix (Fig. 2)—we have demonstrated how the exploration industry in the Midcontinent could be revitalized. Specifically, we showed that an active, subthrust Viola petroleum system has generated hydrocarbons that were trapped both below (new targets beneath the Isom Springs Oil Field) and within pre-existing Ouachita Thrust Belt structures in the Ardmore Basin. Farther to the east, Viola oils have been found trapped within the Ouachita thrust sheets, leading to speculation that undiscovered, subthrust oil traps may exist there as well. It is now up to explorationists to find them.

## REFERENCES CITED

- Beaumont, E.A.; and Foster, N.H. (eds.), 1999, Exploring for oil and gas traps, *Treatise of Petroleum Geology, Handbook of Petroleum Geology: American Association of Petroleum Geologists*, Tulsa, Oklahoma, unpaginated.

- Chamberlain, A.K., 2003, Tectonic controls on the remigration of hydrocarbons: looking beyond Nevada's commercial oil seep play (abs.): American Association of Petroleum Geologists Midcontinent Section Meeting, <http://www.search-anddiscovery.net/documents/abstracts/2003midcont/abs/chamberlain.pdf>, retrieved February 13, 2008.
- Coleman, J.L.; Cook, J.A.; Davis, M.H.; Eggers, L.D.; and Tasker, D.R., 1997, Overview of exploration and exploitation risks in thrust belts and foreland basins, *in* Bishop, R.S.; Martell-Andrade, Bernardo; and Sánchez-Montes de Oca, Rafael (eds.), Oil and gas exploration and production in fold and thrust belts: Second Joint American Association of Petroleum Geologists/Asociación Mexicana Geólogos Petroleros Hedberg Research Symposium, Veracruz, Mexico, p. 4.
- Curiale, J.A., 1992, Petroleum geochemistry of Texas and Oklahoma oils along the Marathon-Ouachita fold-thrust belt, south-central U.S.A.: *Geochemical Geology*, v. 98, p. 151–173.
- Garvey, D.J.; Potts, M.C.; Forgothson, J.M., Jr.; and Knapp, R.M., 1993, Characterization and simulation of the fractured Sycamore Limestone reservoir within the Springer Field, Carter County, Oklahoma, *in* Johnson, K.S.; and Campbell, J.A. (eds.), Petroleum-reservoir geology in the Midcontinent, 1991 symposium: Oklahoma Geological Survey Circular 95, p. 52–59.
- Huffman, G.G.; Bridges, K.F.; Ganser, R.W.; Holtzman, A.M., Jr., and Merritt, M.L., 1987, Geology and mineral resources of Marshall County: Oklahoma Geological Survey Bulletin 142, 126 p.
- McBee, William, Jr., 1995, Tectonic and stratigraphic synthesis of events in the region of the intersection of the Arbuckle and Ouachita structural systems, Oklahoma, *in* Johnson, K.S. (ed.), Structural styles in the southern Midcontinent, 1992 symposium: Oklahoma Geological Survey Circular 97, p. 45–81.
- Tippee, Bob, 2004, What 126 managers think: *Oil & Gas Journal*, v. 102, issue 19, p. 13.
- Tucker, R.B., 2003, Seven strategies for generating ideas: *The Futurist*, v. 32, no. 2, p. 20–25.
- Wang, H.D.; and Philp, R.P., 1997, A geochemical study of Viola source rocks and associated crude oils in the Anadarko Basin, Oklahoma, *in* Johnson, K.S. (ed.), Simpson and Viola Groups in the southern Midcontinent, 1994 symposium: Oklahoma Geological Survey Circular 99, p. 87–101.
- Wantland, K.F., 1992, Building creative environments and leading creative people, *in* Steinmetz, Richard (ed.), The business of petroleum exploration: American Association of Petroleum Geologists, Tulsa, Oklahoma, p. 205–214.
- Wavrek, D.A., 1992, Characterization of oil types in the Ardmore and Marietta Basins, Southern Oklahoma Aulacogen, *in* Johnson, K.S.; and Cardott, B.J. (eds.), Source rocks in the southern Midcontinent, 1990 symposium: Oklahoma Geological Survey Circular 93, p. 185–195.
- Wavrek, D.A.; Garcia, M.A.; and Ferebee, C.D., 1997, The Viola Group as a petroleum system: implications for horizontal-drilling prospects, *in* Johnson, K.S. (ed.), Simpson and Viola Groups in the southern Midcontinent, 1994 symposium: Oklahoma Geological Survey Circular 99, p. 78–86.
- Weber, J. L., 1994, A geochemical study of crude oils and possible source rocks in the Ouachita tectonic province and nearby areas, southeast Oklahoma: Oklahoma Geological Survey Special Publication 94-2, 32 p.